

**TOLUENE DEGRADATION BY AN UNSATURATED
BIOFILM: THE IMPACT OF ENVIRONMENTAL
PARAMETERS ON THE CARBON END-POINTS IN
BIOFILTRATION**

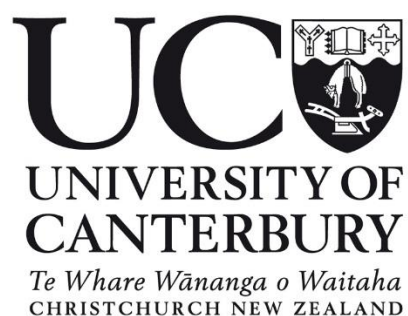
A thesis submitted in the partial fulfilment of the requirement for the degree of
DOCTOR OF PHILOSOPHY IN CHEMICAL AND PROCESS ENGINEERING

at the

UNIVERSITY OF CANTERBURY

By

ACHINTA BORDOLOI



2016

Abstract

The ultimate fate of the degraded pollutants in biofiltration is not understood conclusively. Simple hydrocarbons such as toluene are often assumed to be completely mineralized to carbon dioxide especially in systems without supplemental nutrient addition. However many reports indicate this is not correct. The key focus of this work was to explicitly track and quantify toluene degradation to various carbon end-points and product ratios using soil as the active biofiltration matrix.

Each carbon end-point was measured independently, as compared to determining one by difference, using gas chromatography and total carbon analysis of the solid and liquid phases. A differential biofiltration system was used which exposes the biofilm to uniform set of conditions at any given point in time. This allows interpreting the parameter driven response of the system in a more precise way as opposed to conventional biofilters where conditions change in space and time. The system was operated as a non-growth system to track the degraded carbon components in various phases.

The average carbon balance closure was quantified to 90 % {85; 95} at ($\alpha=0.05$) level of significance over 16 separate biofiltration experiments. Considering the experimental uncertainties and a robust statistical approach to propagating error estimates associated with combining independent sources, all the carbon can be considered to have been accounted for. The carbon endpoints were tracked as CO₂ in the gas phase and the non-mineralized fractions cumulatively accumulated within the solid and liquid fractions of the system. The variation in CO₂ recovery versus the non-mineralized fractions as a function of multiple environmental parameters was further investigated to elucidate the driving phenomena for the variations in carbon end-points.

A factorial design approach was used to explore potential interactions and the main effects between three critical parameters (temperature, matric potential and substrate concentration) over a wide range chosen as categorical factors. A 3x3 factorial design

matrix of temperature (20 °C, 30 °C, 40 °C) and toluene concentration (75 ppm, 120 ppm, 193 ppm) evaluated through a 2-way ANOVA indicated significant interactions resulting in CO₂ recovery from toluene degradation varying from 54-90%. These results showed that mineralization is not always coupled with temperature because at the higher toluene concentration of 193 ppm, CO₂ recovery was not statistically different (*p-value* < 0.05) across the temperature range unlike at lower inlet feeds. A 2x3 factorial design matrix evaluating temperature (20 °C, 40 °C) and matric potentials (-10 cm_{H₂O}, -20 cm_{H₂O}, -100 cm_{H₂O}) illustrated the significant main effect between the parameters without any significant interaction. CO₂ recovery decreased at 20 °C from 71% at -10 cm_{H₂O} to 35% at -100 cm_{H₂O}.

The corresponding elimination capacity of the system was influenced by significant interaction between all the studied parameters. Operations at 40 °C resulted in a 2-fold higher elimination capacities compared to 30 °C and 20 °C whereas elimination capacities decreased over operations at lower matric potentials. For operations at 40°C, elimination capacity decreased by almost ~30% with lower matric potential from -10 cm_{H₂O} to -100 cm_{H₂O}. Results from the start-up condition experiments with a lower initial feed concentration to subsequently higher feeds resulted in a two-three-fold increase in EC at the higher toluene concentration, compared to constant feeds starting at the higher concentration. An EC_{max} of $127 \pm 2 \text{ g.m}^{-3}.\text{h}^{-1}$ was achieved going from 75-193 ppm feed before coming to a steady state EC of $38 \pm 3 \text{ g.m}^{-3}.\text{h}^{-1}$. This can have significant practical implications in terms of acclimatization protocols. This experiment was investigated at 40 °C and -10 cm_{H₂O}.

The trends observed for CO₂ recovery and *EC*, in particular start-up conditions, were also seen with the pure culture study with *Pseudomonas putida*. Microscopy work with lectin binding stain WGA-647 corroborated the findings of carbon end-points as the fate of non-mineralized carbon accumulating as EPS and other storage polymers.

To summarize, this multivariable investigation into the fate of carbon end-points associated with toluene degradation provided potential insight on the impact on metabolic pathways and community structure from the quantified carbon fractions. However future work will be required to determine the relative importance of these

two potential causes for shifting ratios of carbon endpoints. These results also provided a good framework to help bridge the connection between achieving better process efficacy through knowledge pertaining to the physiological response. This can be beneficial in deciding operational parameters, especially in regards to averting practical problems such as clogging and degradation stability.

THIS THESIS IS DEDICATED TO MAA AND DEUTA

Acknowledgements

As I sat down to write this final words to what has been a unique journey that has transformed, fascinated, despised and strengthened me in many ways. I thought of what kept me going, what kept motivating me and a wave of thoughts splashed upon me with memories abound. I guess it was all worth it and I am really thankful to everyone for the support.

At the very outset I would like to thank my Supervisor Dr Peter A. Gostomski (Pete) for his generous support and guidance throughout this project. In Pete I've had the good fortune of having a very compassionate and an inquisitive advisor that helped me explore and learn numerous things which helped be grow as a researcher. PS: Very few can match his wit and sense of humour.

I would also thank my co-supervisor Dr Daniel Gapes for this unique ideas and directions that was immensely helpful throughout this project even though he was based in Rotorua.

I am really grateful to all the people in our electrical and mechanical workshop for helping me to keep things up and running, no matter what. Tim Moore, Frank, Leigh, Stephen, Michael you guys are amazing. A special thanks to Stephen Hood for pulling off the lab shifting adequately to minimize the time loss in the final year. Special thanks to Tony for all the IT related help, hope you are enjoying your retired life to the fullest. I would also like to extend my appreciation to Manfred Ingerfeld and Dr David Collins for their help and inputs for carrying out the confocal microscopy work. Dr Kerry Swanson and Mike Flaws for helping with the scanning electron microscopy work. I would also like to thank Dr Elena Moltchanova and Dr Daniel Gerhard for their immensely helpful discussions regarding the statistical design and analysis of the data.

However this journey would not have been as fruitful without the many wonderful people I've had the pleasure to know and became friends with. To my office mates for those engaging discussions over tea, and the great bunch of students I met during my time with the post grad association. To my friends who helped settle me into the scheme of things when I arrived, swami, sandipan. However my world here would not have been as fruitful and fun without my bunch of these awesome people, Mimi, Amol and Arvind, thanks for the support.

Finally, all of these wouldn't have been possible without my family, mom, dad and kanku thanks for bearing those extended length of time without me. Without your pillar of support this would not have been possible. A special thanks to my mother for motivating me in pursuing this career path as a researcher.

Table of Contents

ABSTRACT.....	II
ACKNOWLEDGEMENTS.....	VI
LIST OF FIGURES.....	XIII
LIST OF TABLES.....	XVII
NOMENCLATURE & ABBREVIATIONS	XVIII
CHAPTER 1	1
1.1 Background: Motivation for the current research.....	1
1.2 Research Objectives:.....	2
1.3 Thesis layout	4
CHAPTER 2	5
2.1 Biofiltration: Towards effective abatement of air pollution	5
2.1.1 Types and sources of air pollutants.....	5
2.1.2 Environmental and health hazards of VOCs	6
2.2 Process overview.....	7
2.2.1 Types of waste gas treatment techniques	8
2.3 Environmental parameters impacting biofiltration.....	9
2.3.1 Microbiological aspects for biofiltration	9
2.3.3 Temperature	11
2.3.4 Water content.....	12
2.3.4.1 Packing materials	13
CHAPTER 3	14
3.1 Differential biofilter.....	14
3.1.1 Components and configuration.....	14
3.2 Experimental set-up.....	16
3.2.1 Pollutant feed generation.....	17
3.2.1.1 Diffusion system.....	17
3.2.2 Temperature control.....	19
3.2.3 Matric potential control	20

3.2.4 Soil characteristics.....	20
3.3 Analytical procedures	20
3.3.1 Gas Analysis	20
3.3.1.2 CO ₂ analysis.....	21
3.4 Biofilter loading and start-up	22
3.5 Biofilm reactor.....	22
3.5.1 Culture regeneration and cell plating	22
3.5.2 Biofilm Reactor loading and inoculation.....	23
3.5.3 Biofilm dry biomass measurements	24
3.5.4 Carbon quantification of the biofilm	24
3.6 Microscopic analysis	24
3.6.1 Confocal scanning laser microscopy (CLSM).....	24
3.6.1.1 Polysaccharide staining	24
3.6.1.2 Live dead staining.....	25
3.6.2 Scanning electron microscopy (SEM).....	25
CHAPTER 4	26
4.1 Carbon balance and fate of pollutants	26
4.1.2 Gas phase end-points.....	29
4.1.3 Solid Phase end-points.....	31
4.1.4 Liquid phase end-points.....	33
4.2 Results and Discussion.....	38
4.2.1 Differential Biofilter	38
4.2.2 Carbon balance model for the differential biofilter	39
4.2.4 Carbon flux tracking in various phases.....	43
4.2.4.1 Gas phase carbon end-points quantification	43
4.4 Solid phase carbon end-points quantification	47
4.4.1 Control soil sampling	47
4.4.2 Biofilter soil sampling.....	49
4.5 Liquid phase carbon end-points quantification	51
4.5.1 Soluble carbon fractions in soil.....	51

4.5.2 Implications of soluble carbon flux in the liquid phase	52
4.6 Carbon end-points quantification: Carbon balance.....	54
4.6.1 Carbon balance: Data analysis and error propagation.....	55
4.7 Conclusions.....	56
CHAPTER 5	58
5.1. Introduction.....	58
5.2 Impact of temperature on the fate of transformed carbon	59
5.2.1 Temperature mediated response on substrate utilization	59
5.2.2 Link between temperature and community to degradation products.....	60
5.3 Water potential in unsaturated media	61
5.3.1 Transient water content dynamics in biofiltration	62
5.3.2 Microbial response to water stress	62
5.3.3 Effect of matric potential on carbon recovery	64
5.4 Results and Discussion.....	65
5.4.1 Influence of environmental parameters on the CO ₂ recovery	65
5.4.2 Interaction of temperature and substrate concentration	67
5.4.3 Effect of inlet feed and temperature on residual toluene concentration....	69
5.4.4 Implications of temperature on CO ₂ recovery	73
5.4.5 Interaction of matric potential and temperature	74
5.4.6 Effect of matric potential and temperature on residual concentration.....	77
5.4.7 Implications of matric potential on CO ₂ recovery.....	79
5.5 Influence of start-up conditions on CO ₂ recovery	82
5.6 Non-mineralized fractions.....	84
5.6.1 Influence of environmental parameters on the non-mineralized yield coefficient (Y _{NC}).....	85
5.6.2 Physiological implications of non-mineralized fraction production	87
5.7.2 Non-mineralized fraction production rate.....	89
5.8 Conclusions.....	91

CHAPTER 6	93
6.1 Introduction.....	93
6.2 Significance of temperature in biofiltration	94
6.2.1 Effect of temperature on biodegradation kinetics	94
6.3 Role of water in biofiltration.....	95
6.3.1 Effect of water content on biofilter performance	96
6.4 Biofilter performance evaluation	97
6.5 Results and Discussion.....	98
6.5.1 Biofilter performance monitoring over the time course	98
6.5.2 Interaction between temperature and substrate concentration impacting EC.....	101
6.5.3 Effect of temperature and substrate concentration on biofilter performance	105
6.5.4 Correlation of EC with CO ₂ recovery.....	106
6.5.5 Impact of residual concentration on EC.....	108
6.6 Impact of start-up conditions on biofilter performance.....	110
6.6.1 Effect of lower start-up substrate concentration	110
6.7 Interaction of temperature and matric potential impacting EC	114
6.7.1 Impact of temperature and matric potential on biofilter performance	118
6.7.3 Correlation of EC with CO ₂ recovery at different matric potentials	120
6.8 Conclusions.....	121
CHAPTER 7	123
7.1 Introduction.....	123
7.1.2 Biofilm matrix	124
7.1.3 Relevance of biofilms in a biofilter	124
7.1.4 Co-existence of a heterogeneous community in a biofilter	125
7.1.5 Maintenance metabolism.....	126
7.2 Biofiltration with an unsaturated <i>Pseudomonas putida</i> biofilm	127
7.2.1 Gas phase carbon tracking	127
7.3 Microscopic observation of the biofilm samples	129

7.3.1 Confocal microscopy.....	129
7.3.2 Scanning electron microscopy (SEM).....	131
7.3.3 Carbon balance analysis of the biofilm run.....	133
7.4 Effect of shut down phase on the microbial physiology: endogenous CO ₂ production.....	134
7.5 Toluene degradation by the biofilm	136
7.5.1 Effect of substrate concentration on biofilm degradation	137
7.5.2 Effect of start-up substrate concentration on biofilm degradation.....	138
7.6 Conclusions.....	139
CHAPTER 8	140
8.1 Overall summary.....	140
8.2 Future work	148
8.2.1 Extension of the factorial design to other substrates.....	148
8.2.2 Metagenomics: To answer who is doing what?.....	148
8.2.3 Metabolomics and proteomics.....	149
8.2.4 Unsaturated biofilms under controlled environmental conditions	149
8.2.5 Exploring Start-up conditions and other substrates.....	150
8.2.6 What else could drive the carbon flux in the system.....	150
8.2.6 Characterisation of the polysaccharides	151
8.2.7 Impact of the polymers on pressure drop	151
REFERENCES.....	152
APPENDICES	176
A.1 CO ₂ Calibration data.....	176
A.2 GC Calibration data.....	177
A.3 Carbon content analysis for the liquid and solid phase.....	178
A.3.1 Shimadzu TOC-L unit Calibration data for total carbon (TC).....	178
A.3.2 Shimadzu TOC-L unit Calibration data for inorganic carbon (IC).....	179
A.3.2: Shimadzu SSM-5000A unit calibration data for total carbon (TC).....	180
A.4 Supplementary data for ANOVA analysis	181

A.4.1: 3X3 factorial analysis for temperature and substrate concentration influencing CO ₂ (Chapter 5.Table 5-2).....	181
A.4.2: 2X3 factorial analysis for temperature and matric potential influencing CO ₂ (Chapter 5.Table 5-2).....	184
A.4.3: 3X3 factorial analysis for temperature and substrate concentration influencing EC (Chapter 6.Table 6-2).....	187
A.4.4: 2X3 factorial analysis for temperature and matric potential influencing EC (Chapter 6.Table 6-5).....	190

LIST OF FIGURES

- Figure 1-1 :** A brief schematics of the structure of the thesis with the key investigation focus of the core experimental chapters 4
- Figure 2-1:** Various waste gas treatment technologies used for air pollution abatement. 8
- Figure 3-1:** A section view of the differential biofilter. 15
- Figure 3-2:** Process flow diagram of the lab scale biofilter setup. 16
- Figure 4-1:** Flow chart identifying plausible carbon end-points in the system after toluene degradation. 28
- Figure 4-2:** Section view of the differential biofilters used in this study. 39
- Figure 4-3:** Change in carbon flux through a control system without toluene feed over time (t_0 = initial time) and (t_F = final time), operated at a certain temperature and matric potential. 40
- Figure 4-4:** Fate of degraded carbon through the system during experimental run over the course of operation and various carbon end-points. 42
- Figure 4-5 :** Variations in the residual toluene concentration as a function of temperature at an inlet feed concentration of 120 ppm toluene and -10 cm_{H₂O} matric potential. 44
- Figure 4-6:** Evolution of CO₂ production in relation to the degradation of the toluene by the soil bed with time. This experiment was operated at 20 °C and -20 cm_{H₂O}. 45
- Figure 4-7:** Typical experimental runs for evaluating the endogenous CO₂ baseline at 40 °C and 20 °C at -10 cm_{H₂O} through pre-, operational and shut down phases. 46
- Figure 4-8:** Effect of temperature and matric potential on the endogenous CO₂ production rate of the soil bed. 47
- Figure 4-9:** Comparison of control soluble carbon contents in the liquid phase with the biofilter experimental runs. Unsaturated control was done at -10 cm_{H₂O}. 54
- Figure 4-10 :** Forrest plot for carbon balance closure for the experimental biofilters runs operated over various environmental parameters using meta-analysis (n=16). Where, TE is estimate of treatment effect. seTE is the standard error of treatment effect. 56
- Figure 5-1 :** Interaction plot of temperature and substrate concentration parameter impacting CO₂ recovery. Values represents mean with uncertainties at 95% confidence interval during steady state over a multi-day period from replicate runs. 67
- Figure 5-2 :** Tukey HSD plot illustrating the pair wise comparisons between combinations of various levels of temperature : toluene concentrations (x axis) with corresponding CO₂ recovery. Groups sharing the same letters as listed in the top of the graph are not significantly different ($p \text{ value} < 0.05$). 69

- Figure 5-3 :** CO₂ recovery as a function of residual outlet concentrations at various temperatures operated at -10 cm_{H₂O}. Values represents mean with uncertainties at 95% confidence interval during steady state over a multi-day period from replicate runs. 70
- Figure 5-4 :** Influence of matric potential and temperature on CO₂ recovery at an inlet concentration of 120 ppm toluene. Values represent the mean with uncertainties at 95% confidence interval during steady state over a multi-day period from replicate runs. 75
- Figure 5-5:** Tukey HSD plot illustrating the pair wise comparisons between combinations of various levels of temperature : matric potential (x axis) with corresponding CO₂ recovery. Groups sharing the same letters as listed at the top of the graph are not significantly different (*p value*<0.05). 76
- Figure 5-6:** Residual toluene concentration as a function of temperature and matric potential and its impact on CO₂ recovery. Values represent the mean with uncertainties at 95% confidence interval during steady state over a multi-day period from replicate runs. 79
- Figure 5-7:** Soil water release curve at the various matric potentials for the biofilter runs at 40 °C. Water content is reported on a dry weight basis (DWB). 80
- Figure 5-8 :** Comparison of inlet substrate concentration at constant feed (A) vs variable feed (B) to evaluate lower start-up conditions and its implications on mineralized CO₂ fractions. Experiments were operated at 40 °C and -10 cm_{H₂O}. Values represents mean with uncertainties at 95% confidence interval during steady state over a multi-day period from replicate runs (Constant inlet feeds). Error bars in the multiple feed experiment represents within run variations in steady state at 95 % confidence interval. 82
- Figure 5-9:** Start-up condition comparison for experiments operated at 20 °C and -10 cm_{H₂O}. Values represents mean with uncertainties at 95% confidence interval during steady state over a multi-day period from replicate runs. 84
- Figure 5-10:** Non-mineralized fraction (NmC) production rate as a function of temperature and matric potential at an inlet feed of 120 ppm toluene. 90
- Figure 5-11:** Non-mineralized production rate as a function of temperature operated at a matric potential of -10 cm_{H₂O} and inlet feed of 193 ppm toluene. 91
- Figure 6-1:** A typical time course for biofilters at an inlet feed concentration of 120 ppm. Biofilters operated at (a) 40 °C and -10 cm_{H₂O}. (b) 20 °C and -20 cm_{H₂O}. 99
- Figure 6-2 :** Interaction plot of substrate concentration and temperature impacting (*EC*) at -10 cm_{H₂O}. Values represents mean with uncertainties at 95% confidence interval during steady state over a multi-day period from replicate runs. 102
- Figure 6-3 :** Tukey HSD plot illustrating the pair wise comparisons between combinations of various levels of temperature: toluene concentration (X axis) in regards to the impact on *EC*. The groups sharing same letters are not significantly different from each other (*p-value*<0.05). 104

- Figure 6-4 :** Correlation of EC with CO_2 recovery for each set of operating conditions. I_{75} , I_{120} and I_{193} denote the inlet feed concentration. Values represent the means with uncertainties at 95% confidence interval during steady state over a multi-day period from replicate runs. 107
- Figure 6-5 :** Effect of residual outlet concentration on EC and CO_2 recovery as a function of operating temperature. Values represent the mean with uncertainties at 95% confidence interval during steady state over a multi-day period from replicate runs. 109
- Figure 6-6:** Experiments were studied at 40 °C at a matric potential of -10 cm_{H_2O} by varying the feed concentration in a step-wise manner from 75 → 120 → 193 → 75 → 193 → 75. (B) compared to constant feed at 120 and 193 ppm (A). 111
- Figure 6-7 :** Experiments were operated at 40 °C and an inlet feed of 120 ppm toluene and investigation was expanded across two matric potential of -10 cm_{H_2O} and -20 cm_{H_2O} . For the multi feed start-up conditions feeds were started at 75 ppm and increased to 120 ppm in a step wise manner. 112
- Figure 6-8 :** Interaction plot of matric potential and temperature impacting EC at an inlet feed concentration of 120 ppm toluene. Values represents mean with uncertainties at 95% confidence interval during steady state over a multi-day period from replicate runs. 116
- Figure 6-9:** Tukey's HSD plot illustrating the pair wise comparisons between combinations of various levels of temperature : matric potential (X axis) corresponding to EC . Groups sharing the same letters indicated at the top of the graph are not significantly different ($p\text{ value} < 0.05$). 117
- Figure 6-10:** Relationship between water content and EC operated over various matric potentials at 40 °C. Moisture content is reported on a dry weight basis. 119
- Figure 6-11 :** Correlation of EC with CO_2 recovery for each set of operating conditions. 121
- Figure 7-1 :** CO_2 recovery for the biofilm and soil runs at -10 cm_{H_2O} and 40 °C as a function of residual toluene concentration. 128
- Figure 7-2:** Biofilm sample visualization with CLSM. a) Photograph of the membrane at $t = 0$. b) Photograph of the biofilm established on the membrane taken at the end of the experiment. c) At $t = 0$, wheat germ agglutinin 647(WGA) stained image of the biofilm. d) 3D stacked confocal microscopy image of the biofilm. Sample was stained with wheat germ agglutinin 647(WGA) was used as it specifically binds to polysaccharides. 130
- Figure 7-3: Representative SEM micrograph of the biofilm samples taken at the end of the run illustrating the biofilm architecture (a-c).The micrograph (d) is the control membrane at $t=0$ without any culture. 132
- Figure 7-4:** The endpoints of the toluene degraded by *Pseudomonas putida* reported on a percent carbon basis after 120 days of operation. 134
- Figure 7-5:** Endogenous CO_2 profile of some experimental runs at different sets of environmental parameters after toluene feed was shut down. Biofilm and Soil-a

run was at 40 °C and -10cm_{H2O} while Soil-b was at 20 °C and -20 cm_{H2O} at an inlet feed of 120 ppm toluene. 135

Figure 7-6: Stain: Live Dead of the *Pseudomonas putida* biofilm deposited on the membrane. (a) Day 0 image without toluene feed. (b) Images after 120 days of toluene degradation (images were taken from different runs). 136

Figure 7-7 : Surface elimination capacities of the biofilm run over a range of residual toluene concentration. Experiments were operated at 40 °C and 10 cm_{H2O} over two inlet feed concentrations (75 and 120 ppm toluene) 137

Figure 7-8: Comparison of lower start-up conditions and its implication on biofilm performance operated at 40°C and -10 cm_{H2O} over constant inlet feed (A) and variable inlet feed (B). Values represent means over steady state at 95% CI. 139

Figure 8-1: Schematic representing specific and overlapping regulatory mechanisms eventually impacting CO₂ carbon end-point over the different environmental parameters. 141

List of Tables

Table 3-1: Antoine coefficients for toluene over various temperature ranges.	18
Table 3-2 : GC operating conditions for gas phase analysis.	21
Table 4-1: Compilation of the literature encompassing carbon mass balance studies in biofiltration of various pollutants.	35
Table 4-2: Carbon content analysis of the control soil samples for both wet soil samples and oven dried soil samples.	48
Table 4-3: Total carbon measurements for different experimental reactor systems and control runs for carbon loss test during analysis of fresh and oven dried samples.	50
Table 5-1: Biofilter operational parameters used for tracking the carbon fractions	65
Table 5-2: Summary of analysis of variance (ANOVA) results for the manipulated environmental parameters.	66
Table 5-3: The biomass yield on toluene reported by various biofilter studies.	85
Table 6-1: Experimental factors and different levels of investigations.	101
Table 6-2: Summary of analysis of variance (ANOVA) results for the temperature and substrate concentrations.	102
Table 6-3: EC for toluene reported at various operating conditions in the literature.	114
Table 6-4: Experimental factors and different levels of investigation.	114
Table 6-5: Summary of analysis of variance (ANOVA) results for the temperature and matric potential.	115

Nomenclature & Abbreviations

A_t	Diffusion tube cross sectional area	m^2
D	Diffusion coefficient at Pressure P and Temperature T	$m^2.s^{-1}$
D_{298}	Diffusion coefficient at 298 K and 1 atm	$m^2.s^{-1}$
T	Temperature	K
P	Pressure in the diffusion system	mm.Hg
p_v	Vapour pressure of toluene	mm.Hg
n	Temperature coefficient	-
C_{diff}	Concentration at the exit of diffusion tube	ppm
q_d	Diffusion rate	$m^3.s^{-1}$
F_g	Gas flow rate	$m^3.s^{-1}$
L	Length of diffusion flask	M
t_0	Initial time	Days
t_F	Final time	Days
G	Carbon content in gas phase	gC
S	Carbon content in solid phase	gC
S_E	Carbon leached from the soil	gC
S_D	Carbon accumulated in the soil.	gC
L	Carbon content in liquid phase	gC
L_D	Soluble degraded carbon in the liquid.	gC
R	Endogenous soil respiration	gC
ψ_m	Matric potential	$-cm_{H_2O}$

NmC	non-mineralized carbon fractions	gC
Y_{NC}	non-mineralized biomass yield coefficient	gNmC/gTC
EC	Elimination capacity	$\text{g m}^{-3} \text{ h}^{-1}$
SEC	Surface elimination capacity	$\text{g m}^{-2} \text{ h}^{-1}$
pCO_2	Net CO_2 production rate	$\text{g m}^{-3} \text{ h}^{-1}$
tCO_2	Total CO_2 produced	g.m^{-3}
rCO_2	Endogenous CO_2 of the soil bed	g.m^{-3}
C_i	Inlet concentration	g.m^{-3}
C_o	Outlet concentration	g.m^{-3}
V	Reactor bed volume	m^3
A_m	biofilm surface area	m^2
Q	flow rate	$\text{m}^3.\text{h}^{-1}$
NDIR	Non-dispersive infrared sensor	
CLSM	Confocal laser scanning microscope	
SEM	Scanning electron microscope	
TOC	Total organic carbon	
TC	Total carbon	
EPS	Extracellular polymeric substance	
SMP	Soluble microbial products	
PHB	Polyhydroxybutyrate	
WGA	Wheat germ agglutinin	
GC	Gas chromaography	
FID	Flame ionization detector	
HID	Helium ionization detector	
MW	Molecular weight	

-

Chapter 1

INTRODUCTION

1.1 Background: Motivation for the current research

The flow of carbon from the substrate through the unsaturated, metabolically restricted biofilm in biofilters is poorly understood. It is evident from the literature that a fraction of the carbon entering the system in many biofilm processes remains unaccounted for. The issue of missing carbon needs to be addressed quantitatively as it provides a context for better understanding and modelling of biofilter performance. In addition, knowledge of interaction between multiple environmental parameters can help address practical problems pertaining to process efficacy such as clogging and stability.

Biofilms are often growth restricted (e.g. - nutrient limited, etc.) especially in soil and various industrial processes such as biofiltration but possess the inherent ability to break down organic pollutants (Jorio et al., 2000a, Li et al., 2002, Xi et al., 2006). Biofilms proliferating in these dynamic environmental conditions are commonly unsaturated, operating at the air/solid interface. Many attempts have been made to close the carbon balance in these systems; however (10-50%) of the degraded carbon often remains untracked (Deshusses, 1997b, Morales, 1998, Song and Kinney, 2000, Cox et al., 2001, Avalos Ramirez et al., 2008, Girard et al., 2011). In spite of the importance of these growth restricted, unsaturated biofilm processes in engineered systems, certain aspects of their activity/metabolism remain unclear, particularly the ultimate fate of carbon entering these systems.

Commonly assumed carbon end-points for organic carbon substrates are CO₂, biomass and EPS. Other plausible carbon end-points include soluble microbial products (Meng et al., 2009, Jiang et al., 2010, Ni and Yu, 2011), soluble metabolites (Díaz et al., 2008), internal storage polymers (Reis et al., 2003) and volatile substances such as carbon monoxide (Haarstad et al., 2006). A common assumption is that the untracked carbon is utilised for microbial growth (biomass) but carbon extraction studies have not corroborated this hypothesis (Vance et al., 1987, Fürer and Deshusses, 2000, Song and Kinney, 2000). Accumulation of missing carbon within the system as biomass could clog up the reactor bed, contrary to reports in non-growth systems (Deshusses, 1997b, Singh et al., 2006b). Whilst microbes undoubtedly convert a portion of the organic substrates into soluble microbial products and other metabolites, their identities and relation to biodegradation of substrates remain to be fully investigated (Kim et al., 2005b, Díaz et al., 2008, Magbanua and Bowers, 2006). Even in the gaseous effluents, nothing other than CO₂ and untreated substrates has been widely reported. There have been limited reports of carbon monoxide reported in the off gas of some biodegradation processes (Haarstad et al., 2006, Hellebrand and Schade, 2008), and the possibilities of other unreported biogenic emissions cannot be ruled out. Thus the carbon balance in these systems is yet to be closed conclusively and the identity of the unaccounted carbon remains elusive.

1.2 Research Objectives:

Abatement of gaseous pollutants in biofiltration through a metabolically restricted biofilm system needs the fundamental question of missing carbon to be answered quantitatively. This project strived to address three key questions:

- 1) Where does the missing carbon go?
 - Solid, liquid or gas phase?

The key objective of this project was investigating the carbon flux through the system and tracking the missing carbon in various phases and how it is exiting or accumulating within the system. A robust analysis of the solid, liquid and gas phase was done to find the missing carbon. Two types of biofilms were used in this study

which would provide a basis for interpretation of experimental data: biofilms associated with soil and pure culture biofilms.

2) How do the environmental parameters influence the carbon end-points?

- Temperature, matric potential and substrate concentration (toluene)

Once the plausible end-points were conclusively tracked and identified, the primary focus was to investigate the impact of environmental parameters and their interactions on the carbon end-points.

3) How does a pure culture investigation corroborate the findings with soil biofilters?

- This offered a good perspective on the metabolic response of a pure culture compared to the heterogeneous community in the biofilter at similar conditions and to quantify the carbon end-points. In addition quantitative analysis of the biofilm itself through various microscopic techniques provided insight on the fate of missing carbon in the biofilm and specific staining for visualization.

This study provided a framework for interpretation of the magnitude and dispersal of end points and parameters influencing them. Thus a comprehensive investigation of these questions on carbon endpoint, product ratio and impact of environmental parameters entailed an empirical understanding of unsaturated biofilms in engineered and natural systems.

1.3 Thesis layout

A brief outline of the thesis structure is presented below with the key focus of investigation highlighted:

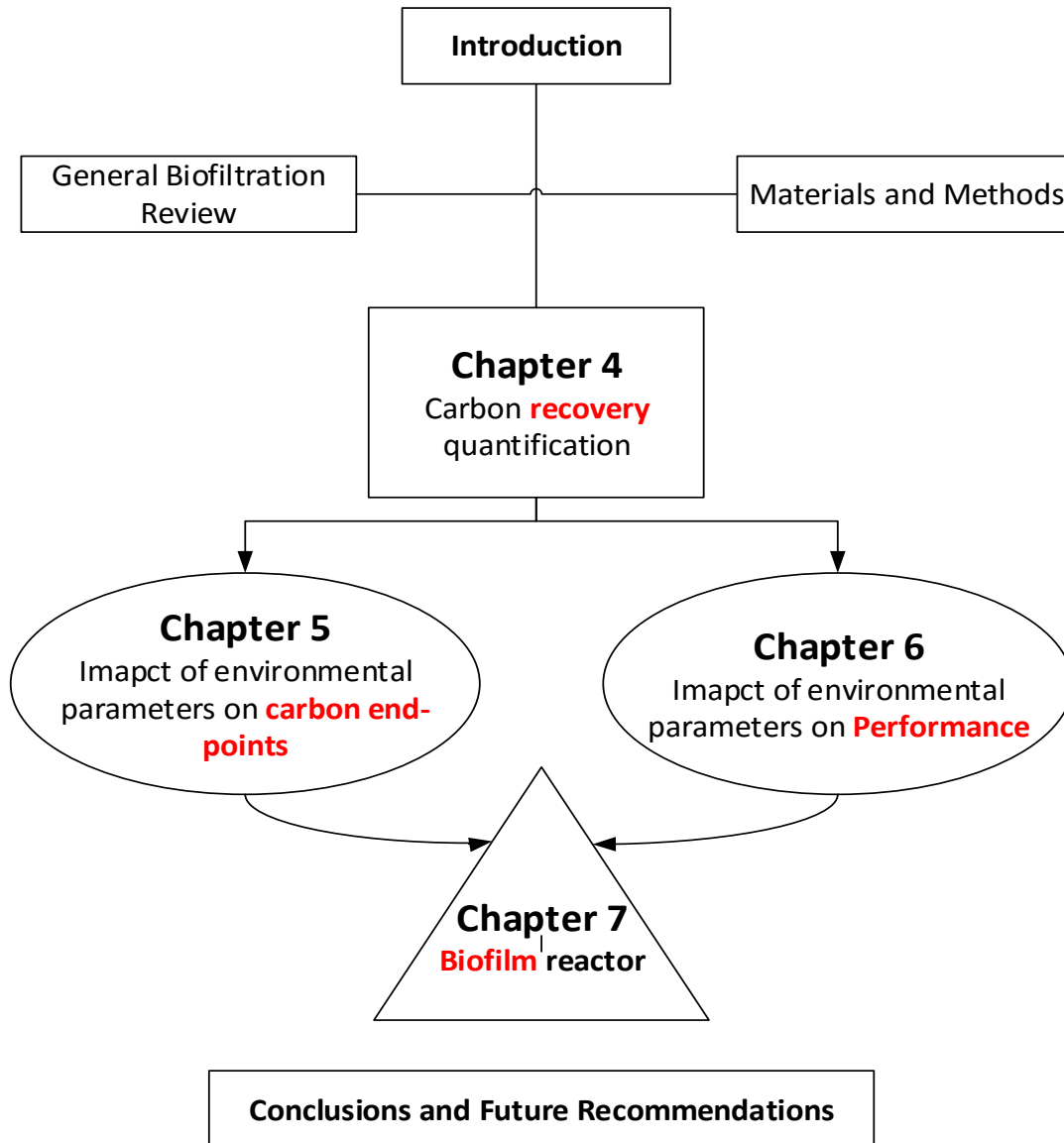


Figure 1-1 : A brief schematics of the structure of the thesis with the key investigation focus of the core experimental chapters

Chapter 2

GENERAL LITERATURE REVIEW: BIOTECHNIQUES FOR AIR POLLUTION

2.1 Biofiltration: Towards effective abatement of air pollution

In this era of looking for sustainable development, biofiltration for the abatement of industrial VOCs and other gas emissions from various anthropogenic sources offers a viable solution. In response to increasing public concerns, stringent environmental regulations have laid increasing emphasis on technology development for pollution abatement. Biofiltration is one of the earliest and still the most widespread full scale biotechnology for waste gas treatment with illustrated socio-economic and environmental benefits (Kennes, 2012). Biofiltration competes with various physical and chemical processes for air pollution control strategies (Devinny et al., 1999). It offers various advantages over conventional physio-chemical process such as lower capital and operational costs and delivering a cleaner and effective process for treating dilute gaseous emissions (Mudliar et al., 2010b). In spite of the importance of these biofilm processes in engineered systems, certain aspects of their activity/metabolism remain to be answered, particularly the ultimate fate of carbon entering these systems.

2.1.1 Types and sources of air pollutants

Air pollutants can be categorised into primary and secondary pollutants with the former released directly into the air whereas the latter form as a result of reactions happening in presence of a combination of pollutants in ambient air. Of late, emissions of volatile organic compounds (VOCs) were attributed to have crippled the air quality significantly throughout the world (Muñoz et al., 2015). VOCs are a major class of pollutants which are dispensed into the atmosphere through a myriad of channels including both natural and anthropogenic sources. Natural source includes volcanic eruptions, natural calamities, forest fires etc. But the major contribution

comes from various industrial sites (e.g. petrochemical refining, waste water treatment, food processing, paper and pulp, paint industry). The most common group of VOCs arising out of these sources are the BTEX compounds consisting of benzene, toluene, ethylbenzene and xylene (Vergara-Fernández et al., 2007b). Odorous compounds are also a concern and include ammonia (and other amines), nitrous oxide, styrene, hydrogen sulphide and other reduced sulphur compounds. Odorous compounds are released into the atmosphere from various sources like animal rearing premises, landfills and waste water treatment plants (Ralebitso-Senior et al., 2012).

2.1.2 Environmental and health hazards of VOCs

Volatile organic compounds (VOC) are a major source of air pollution with well documented environmental and health concerns (Mudliar et al., 2010b, Kennes, 2012). Environmental impacts of these pollutants includes stratospheric ozone depletion, ground level ozone formation and global warming (Mohammad et al., 2007). The BTEX group is specifically hazardous and can impose serious health implications ranging from central nervous system disorder, damage to organs like the liver and kidney and induce cancer upon chronic exposure (Gallastegui et al., 2013). Toluene is highly toxic and mutagenic, chronic exposure to even low doses can lead to a variety of health implications ranging from immunological, and neurological disorder (Nikiema et al., 2007b).

The adoption of emission trading schemes will compel industries to accurately assess their carbon footprints in the future. The ramifications of climate change is postulated to have far-ranging impacts on both humans and nature unless hazardous volatile organic carbon emissions are reduced and regulated earnestly (IPCC, 2014). The clamor for accurate accounting of hazardous VOCs and other greenhouse gases (e.g. methane) associated with biofilm processes critical to various industrial waste treatment, landfill sites and agricultural sources is also reaching a crescendo worldwide (Gentil et al., 2009). In the light of this present scenario, accountability for emissions and related carbon-based outputs is as much an obligation as is a necessity for improved process design of oxidative biofilm processes. Biofiltration has been widely

adopted and effective for waste gas treatment and hence a greater insights into the microbial response dynamics to the pollutants is warranted.

2.2 Process overview

Biofiltration provides a clean, cost effective, and environmentally friendly technology using mass transfer and microbial oxidation to degrade organic pollutants (Devinny et al., 1999, Groenestijn and Hesselink, 1993). The biofiltration process is used effectively for treating large streams of air contaminated with low concentrations (<1000 ppm) of pollutants (Iranpour et al., 2005). It has been successfully applied to treat a wide spectrum of organic and inorganic pollutants as well as a means to abate odours. The presence of numerous industrial establishments releasing significant amounts of hazardous pollutants has positioned biofiltration and related technologies as a promising option.

Biofilters are packed bed bioreactors degrading pollutants through a complex and diverse mixed culture of microorganisms forming a pollutant-degrading biofilm on the porous bed medium. Various natural packing materials such as bark, compost and soil are commonly used but synthetic packing materials are also used. A humidified, pollutant laden stream of air is passed through the porous packed bed where the pollutants are transferred from the gas phase to the biofilm and subsequently degraded. Air, volatile degradation products (typically CO₂ and water) and undegraded pollutants exit the reactor. A small flow of liquid condensate also typically exits the reactor (Delhom nie and Heitz, 2005).

Biofiltration involves a combination of complex elemental steps pertaining to mass transfer, biodegradation kinetics and the carbon flux influencing the ultimate fate of the degraded pollutants. The first step involves diffusion of the pollutants from the gas phase to the biofilm. Within the biofilm, the diffusion of pollutants are dependent on the particulate, water holding capacity and the thickness of the biofilm (Xavier et al., 2004, Bhaskaran et al., 2008) Then the microbiota in the biofilm uses the pollutant as a carbon/energy source to synthesize new cells and/or maintenance forming CO₂ and associated degradation products.

2.2.1 Types of waste gas treatment techniques

Enactment of laws and policies by governments across the world for controlling the hazards of air pollution from different VOCs had led to the development of various promising technologies along with the conventional ones. Implementation of strict emission limits on VOCs for the industrial facilities have been issued in view of the imminent hazards posed to human health and the environment. Figure 2-1 outlines the various air treatment options classified on the basis of their mode and nature of operation. Some of these physical and chemical processes lead to the generation of secondary pollutants which need further attention (e.g. spent adsorbent). Moreover there is a need for substantial investment for their operation and a few of them like incineration are energy consuming. In this regard, biological treatment methods are efficient, cost effective and a relatively green technology with a smaller environmental footprint (Delhoménie and Heitz, 2005, Mudliar et al., 2010a). Biological waste gas treatment includes biofilters, biotrickling filters and bioscrubbers all of which have been successfully used for a few decades (Kennes et al., 2009).

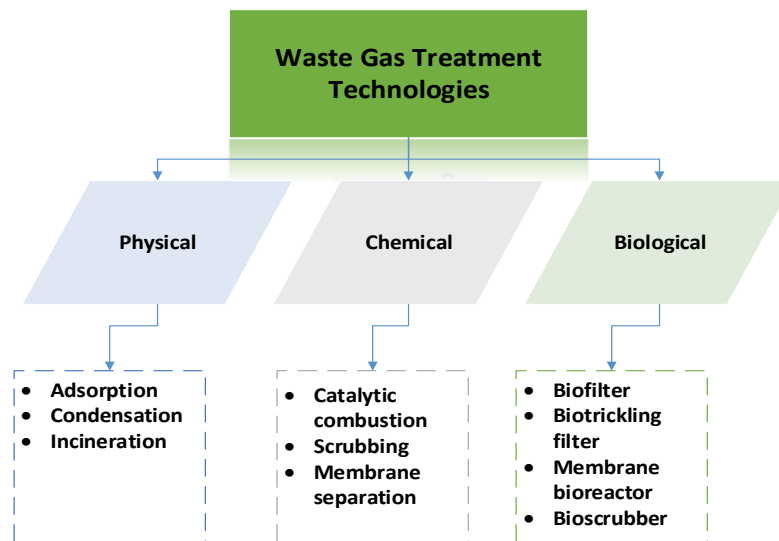


Figure 2-1: Various waste gas treatment technologies used for air pollution abatement.

2.3 Environmental parameters impacting biofiltration

2.3.1 Microbiological aspects for biofiltration

The heterogeneous microbial population that develops on exposure to pollutants is one vital aspect of biodegradation in engineered systems linking biological activity to the overall efficacy of the system performance. Biological degradation of organic pollutants is controlled by the microbiological activity and the influence of environmental parameters. Natural packing beds (e.g. soil, compost) play host to a plethora of indigenous species which harbor degradation capabilities. However synthetic packing beds require inoculation which is often targeted to specific pollutants to be abated. Selected strains offer the benefits of shorter acclimation period and good removal efficiency (Veiga and Kennes, 2001) but can be prone to transient operational parameters such as shut down periods and fluctuating contaminant concentrations (Kim et al., 2005a) . Hence a mixed microbial community ensures more stability and robustness to the engineered systems (Cabrol and Malhautier, 2011). So the evolution of the consortium within the biofilter encompassing various facets of microbial activity and co-existence could have implications on the eventual fate of the degraded pollutants (Watanabe and Hamamura, 2003).

The functional populations actually degrading the compounds of interest have been found to coexist and be outnumbered by diverse micro-consortia unrelated to the degradation of the target compound (Møller et al., 1996, Pedersen et al., 1997, Song and Kinney, 2000). Most of these secondary population do not contribute to the pollutant degradation and constitute an increase of additional carbon sources for cryptic growth (Villaverde and Fernández, 1997). Protozoa and mite graze upon the biomass in addition to the cell lysis products released in the system. Only a small fraction of the biomass has been found to be active and contributing to the actual degradation process (Sakuma et al., 2006). However microorganisms engage in various cooperative interactions within the ecosystem for their proliferation like syntrophic interactions (Schink, 2002) and quorum sensing (Chen et al., 2002). Pelz et al. (1999) illustrated the intricate metabolic networks across communities and role of interdependencies between primary and secondary degraders.

Recent studies have devoted efforts in deciphering the community structure and the change pertaining to a myriad of environmental conditions resulting in proliferation of different community than what proliferated initially. Microbial activity can suffer irreversible or temporary loss of activity owing to pollutant-induced stress by both short term chronic exposure or long term exposure to high concentration of pollutants (Tresse et al., 2003, Song and Kinney, 2005). Although, there have been reports of *P. putida* mt-2 showing progressive adaptation to toxic VOCs resulting in more stable and efficient process (Muñoz et al., 2009). Usually tolerance and adaptability towards toxic pollutants propels specific species as the dominant degrading community (Estrada et al., 2012). But the specific functional roles these populations play in species survival and proliferation has seldom been addressed in biofiltration research.

Biofilters are a complex and structured ecosystem exhibiting immense diversity (Malhautier et al., 2005, Friedrich et al., 2002). Of late much focus has been centered on identification and isolation of the micro-consortia in various waste gas treatment systems, thus expanding the horizons on microbial ecology. Good reactor performance was obtained with a biofilter containing fungi (Weber and Hartmans, 1996, Maestre et al., 2007). Also, fungi specifically feed on dead biomass and mobilize nutrients (Fermor and Wood, 1981) which could explain their ability to have higher degradation rates than bacteria in nutrient-limited conditions. Protozoa predation has also been linked to influence carbon mineralization in systems with high biomass production and as a means to control biomass accumulation (Cox and Deshusses, 1999) but their specific role is yet to be fully elucidated. Hence knowledge on the mechanism of carbon sharing within the system hosting a diverse micro-consortium is still limited.

Due to the complex nature of biological activity, the microbial ecology within a biofilter is still considered as a black box. Different bed medium (types of soil, compost) have characteristic composition of nutrients and micro-flora having different degradation pathways leading to various transformations product ratios in the system. It is important to link microbial diversity to various environmental parameters since pollutants intrinsic physico-chemical characteristics such as water solubility,

biodegradability and inhibitory effects influence the community structure as well as degradation activities (Khammar et al., 2005) This can be correlated to the different degradation fractions of pollutant consumption.

Micro-organisms need essential macronutrients like carbon and nitrogen for growth and survival. Other micronutrients like potassium, sulphur and trace elements are also critical for various metabolic cellular functions. The biofilter bed is usually derived from natural sources hosting a diverse micro-consortium and nutrients. In biofiltration, organic pollutants serve as the carbon source for the microbes utilizing it for both energy and growth requirements. The availability of nitrogen, constituting about (12%) of the bacterial cell mass is elemental to sustain biomass growth and degradation efficacy (Morgenroth et al., 1996, Song et al., 2003). Nitrogen limitation can adversely affect biofilter performance and is often the limiting nutrient (Morales, 1998, Moe and Irvine, 2001, Song et al., 2003). Other essential nutrients are sometimes supplied to the bed media. Also, cell lysis from the dead biomass releases the nutrients in soluble form, where they can be taken up by growing cells (Deviny et al., 1999).

Biomass growth is expected in systems supplied with a source of nutrients, but is less easily understood under nutrient-limited conditions (Cherry and Thompson, 1997). There could be N₂ fixation or supplemental nitrogen from the packing material in the system. But the presence of an assimilable form of nitrogen is necessary for uptake by the microbes. Some degraders are also known to be capable of N₂ fixation providing an additional source of nitrogen to the bed media (Hurek and Reinhold-Hurek, 1995, Bodelier and Laanbroek, 2004, Nikiema et al., 2007a). However the importance of N₂ fixation during biofiltration remains to be assessed. Overall, the nutrient cycle within the system holds immense value for effective degradation process kinetics.

2.3.3 Temperature

Biofiltration is influenced significantly by the operating temperature which regulates reaction rates during the oxidation of pollutants. Pollutant degradation generally increases with temperature until a certain point within the optimum range (Acuña et al., 1999). Temperatures beyond optimal for the microbial community hampers the

degradation rates because of inhibition and/or cell death at higher temperatures (Yoon and Park, 2002). However biofiltration has been successfully operated over a wide temperature range from 15 °C to 60 °C owing to the presence of both mesophilic and thermophilic microbial communities in natural materials (Mohammad et al., 2007, Ryu et al., 2009, Wang et al., 2012). Proper acclimatization helps in establishing an active community at a specific range of temperatures. Temperature changes bring along other constraints like drying of biofilter bed as the exothermic nature of the oxidation reactions induce evaporation of bed moisture. In addition, temperature influences the solubility of the gaseous pollutants into the liquid phase of the biofilm which is hampered at elevated temperature (Darlington et al., 2001). Recent studies have focused on optimization of performance in the thermophilic range to achieve better performance by the addition of yeast extract (Montes et al., 2014).

2.3.4 Water content

As a biological system, sufficient water content is essential for sustained performance of the biofilter (Devinny et al., 1999). Biofilters with a water content in the range of 50-60% usually have better performance. Reduction in water content of the bed is associated with a decline in biofilter performance whereas too much water causes mass transfer limitations (Delhoménie and Heitz, 2005). Water content is subjected to both operational and kinetic factors. Poor humidification of the inlet streams (Morales et al., 2003), metabolic heat from oxidation (Gostomski et al., 1997) and air flow mode can contribute to drying of the bed (Sakuma et al., 2009). Further, changing hydrodynamic conditions in the bed directly impacts the microbial community. Lower water content affects the osmoregulation and cell turgor pressure. It can further lead to major changes in the protein and DNA synthesis pathways (Dmitrieva and Burg, 2007). Often bacteria produce EPS for their enhanced water holding capacity to sustain biofilm activity (Van De Mortel and Halverson, 2004). Other changes range from a shift in community structure (Chowdhury et al., 2011) to inducing specific gene expression (Gülez et al., 2012) to successfully adapt to the changing water contents in the biofilter bed. Often fungal dominance is seen in drier conditions (Nikolova and Nenov, 2005).

2.3.4.1 Packing materials

The nature and type of packing materials are essential selection criteria to obtain effective abatement of pollutants where microbes can be immobilized. Some of the key characteristics of the packing materials are water holding capacity, porosity and adsorptive capacities (Dorado et al., 2010). Other important packing material characteristics include bed porosity and air permeability which defines the ability to easily move air through the biofilter (Sakuma et al., 2009). Organic packing materials like soil, compost and peat are naturally enriched with residual nutrients and a diverse microbial community but are prone to bed compaction and channelling. Whereas inorganic packing materials like polyurethane foam (PUF), lignite, lava rock offers better adsorptive capabilities, lower pressure drop and offer more stability but require inoculation (Ralebitso-Senior et al., 2012). Znad et al. (2007) found good performance on a biofilter operated with a mixture of ceramic and compost treating high loads of toluene at different flow modes. Packing material characteristics eventually influence the microbial metabolism based on the response to system inputs. Estrada et al. (2013b) reported 81% mineralization to CO₂ with a compost biofilter as opposed to 45% mineralization for a biofilter with perlite packing. This was attributed to unstable metabolism or possible metabolite accumulation during periods of high EC in the perlite biofilter. Kim and Deshusses (2008) experimentally determined the mass transfer coefficients of different packing materials, an important parameter which is useful for designing bioreactors. Current research is focused on evaluation of the performance of different packing materials as a function of various operating parameter to increase stability and performance of biofilters and biotrickling filters (Prenafeta-Boldú et al., 2008, Gallastegui et al., 2011b, Cabeza et al., 2013)

Chapter 3

MATERIALS AND METHODS

3.1 Differential biofilter

The reactor system used for this project was initially developed in our group by Beuger and Gostomski (2009) which was improved for online monitoring of the gas phase constituents to further enhance data logging (Detchanamurthy, 2013). In differential biofilters, the entire packing material is exposed to the same environmental conditions at any snapshot in time as compared to traditional column-based biofilters where environmental parameters vary along the length of the reactor. This unique reactor system though similar to other studies (Holden et al., 1997b, Dechesne et al., 2008, Gülez et al., 2010) is tailored for this project enabling accurate control of critical parameters impacting the biodegradation kinetics of the pollutants. This system entails continuous gas flow, uniform gas/liquid concentration exposure to the entire biofilm, controlled matric potential of unsaturated biofilm/soil, measurement and control of the liquid phase and access to the entire biofilm for a quantitative carbon analysis.

3.1.1 Components and configuration

The reactor is comprised of two cylindrical chambers, one for the gas phase and the second for the liquid phase separated by a semipermeable, hydrophilic membrane (Acetate plus, diameter 90 mm, 0.45 μm pore size, GE Water & Process Technology) placed on a metallic mesh (Fig. 3-1). The soil/biofilm is placed on this membrane at the gas/liquid interface. The cylindrical chambers are constructed from glass with an OD of 100 mm and a wall thickness of 5 mm. These are assembled between stainless steel plates with the top and bottom ones fitted with the requisite ports for the pollutant feeds, liquid lines and a welded temperature well for the temperature probe (RTD probe). The system is assembled with detachable threaded rods which pass

through the steel plates and are screwed firmly with nuts. The steel plates have machined slots for Viton o-rings (Dotmar Engineering Plastics Ltd, New Zealand) that provide an air-tight seal between the glass and steel surfaces. The inlet and outlet ports in the steel plates are connected via 2-layer flexible fluoropolymer tubing (SMC, Japan) with an OD of 4 mm. The liquid reservoir is connected to the external reservoir through tygon tubing (Cole-Parmer) which helps in adjusting the height to set the desired matric potential after filling the chamber through the suction cell principle (Section 3.2.3).

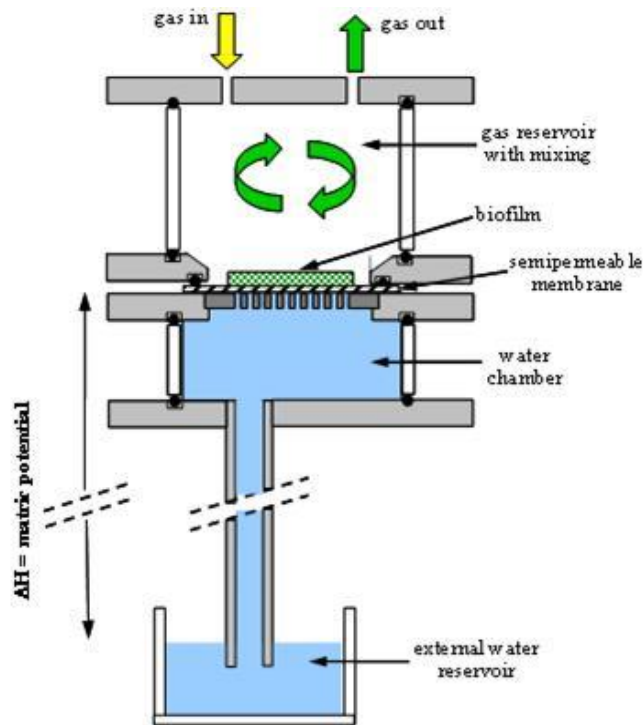


Figure 3-1: A section view of the differential biofilter.

3.2.1 Pollutant feed generation

Desired gas phase toluene concentrations are generated by a diffusion tube apparatus containing liquid toluene (pure HPLC grade) which adds at a constant mass rate of toluene to a flowing air stream depending on the water bath temperature and dimensions of the diffusion tube. It was placed in a water bath (GD100, Grant Instruments, Cambridge, England) with the ability to control temperature from 10-100 °C to achieve the desired toluene concentration. The diffusion system uses CO₂-free, dry compressed air (BOC, NZ Ltd) operated at a pressure of 200 kPa. A mass flow controller (M100B, MKS) control the flow rate of 25 ± 0.34 ml/min.

3.2.1.1 Diffusion system

The concept of a diffusion system was applied to the biofilter set-up for generating a continuous, steady stream of toluene-laden air feed in our group (Beuger and Gostomski, 2009, Detchanamurthy, 2013). A diffusion system is an effective approach to generate low concentration of desired solvents in a continuous stream of gas (Nelson, 1971). Under constant conditions of temperature, diffusion tube geometry and a concentration gradient, a uniform diffusion rate of the gas is achieved. The concentration gradient drives the diffusion across the tube (Altshuller and Cohen, 1960). The diffusion coefficient is affected by the temperature and pressure of the diffusion tube system and the diffusion coefficient (D) can be calculated as follows:

$$D = D_{298} \left[\frac{T}{298} \right]^n \frac{1}{P} \quad (\text{m}^2 \cdot \text{s}^{-1}) \quad 3-1$$

Where,

D = Diffusion tube cross sectional area (m²)

D_{298} = Diffusion coefficient at 298 K and 1 atm (m².s⁻¹)

T is temperature (K) and P is pressure in the diffusion system (mm.Hg)

The value of coefficient n varies between 1.6 and 2. According to Chen and Othmer (1964) a coefficient of 1.81 is used. Temperature governs the vapour pressure above the liquid (Altshuller and Cohen, 1960). The change in temperature will result in a change in vapour pressure (P_v) of the toluene, the Antoine relationship can be used to express it as follows:

$$\ln p_v = A - \frac{B}{T + C} \quad (\text{mm.Hg}) \quad 3-2$$

Where,

p_v = Vapour pressure of toluene (mm.Hg)

Factors A, B and C are found in the literature (Table 3-1) and p_v is the vapour pressure at temperature T. The coefficients used for the calculation are from (Pitzer and Scott, 1943).

Table 3-1: Antoine coefficients for toluene over various temperature ranges.

Temperature	A	B	C	Reference
273.1 – 297.9	4.23679	1426.448	-45.957	(Besley and Bottomley, 1974)
308.0-343.0	4.08	1346.94	-55.77	(McGarry, 1983)
420.0 - 580.0	4.54436	1738.123	0.394	(Ambrose et al., 1975)
273.0 – 323.0	4.14157	1377.578	-50.507	(Pitzer and Scott, 1943)

The toluene concentration in this diffusion system can be controlled through various ways. Changes in temperature and the dimensions of the diffusion tube can influence the diffusion rate. The volumetric flow rate of toluene (q_d) can be calculated by:

$$q_d = \frac{DA \ln\left[\frac{P}{P - P_v}\right]}{L} \quad (\text{m}^3 \cdot \text{s}^{-1}) \quad 3-3$$

Where,

q_d = Diffusion rate ($\text{m}^3 \cdot \text{s}^{-1}$)

D = Diffusion coefficient at Pressure P and Temperature T ($\text{m}^2 \cdot \text{s}^{-1}$)

A = Diffusion tube cross sectional area (m^2)

L = Length of diffusion flask (m)

Also the gas flow rate can be used to achieve the desired concentration by diluting the constant mass of toluene added to the stream and the concentration generated (C_{diff}) can be calculated by using the following equation (Nelson, 1971):

$$C_{diff} = \frac{q_d \times 10^6}{F_g} \quad (\text{ppm}) \quad 3-4$$

Where,

C_{diff} = Concentration at the exit of diffusion tube (ppm)

F_g = Gas flow rate ($\text{m}^3 \cdot \text{s}^{-1}$)

3.2.2 Temperature control

The reactor is housed inside a temperature controlled, wooden box insulated with polyethylene foam. Temperature is regulated by a temperature controller (LTR-5, LAE Electronics, Italy) which uses a light bulb (40-60 W) to generate heat inside the box by switching intermittently. There is an additional refrigeration unit with a thermostat (Tropicool-XC3000A, 12 V DC, Thermoelectric Refrigeration Ltd., New Zealand) which provides the necessary cooling load (temperature adjustable) for the

temperature controller to work against, particularly for maintaining temperatures slightly above or below ambient.

3.2.3 Matric potential control

The matric potential in the system is controlled by using the suction cell principle. The soil is placed on a wet, semipermeable membrane which is only permeable to water but not to air at differential pressures below its bubble point. The soil needs to be hydraulically connected by a liquid column to enable water content control. A syringe is used to create the vacuum in the internal chamber which then draws water from the external reservoir to fill up the chamber. The desired matric potential is implemented by changing the height between the membrane and the level of liquid in the external water reservoir which creates a vacuum on the membrane.

3.2.4 Soil characteristics

Biofilter performance is inherently dependent on the nature of the filter bed. Garden soil (Parkhouse Garden Supplies) is used as the filter bed material for this study. The soil is sieved through a US no 10 sieve (2 mm) and kept in a storage box at ambient temperature (18-26 °C) in the lab. The moisture content of the soil is analysed through standard gravimetric procedure of drying at 105 °C in an oven (LabServ) for 24 hours or until a constant weight was achieved. Soil samples are then put in a desiccator after drying for 15 minutes prior to gravimetric analysis. Triplicate samples ranging from 3-5 g are used for analysis. The moisture content of the soil did not change significantly over time.

3.3 Analytical procedures

Various analytical instruments were used to quantify the degradation products in the gas, solid and liquid phases throughout this study. Detailed methodologies are discussed in the subsequent sections.

3.3.1 Gas Analysis

Gas samples from the inlet and outlet streams are continuously withdrawn via sampling lines connected to a GC/FID (SRI-8610C, SRI instruments) fitted with a 10-

port valve (Valco, Houston, TX). Helium is used as a carrier gas (5 psi and 10 mL min⁻¹). Air (5 psi and 250 mL min⁻¹) and hydrogen (20 psi and 25 mL min⁻¹) is used for flame ignition. Air to the GC is supplied by the compressed air supply of the lab. A MXT-15m capillary column (Restek Corporation, US) is used for the analysis. Peak Simple Version 435 was used for data acquisition and processing. Online monitoring is regulated by the pre-set auto sampler programme for continuous operations and controlling the sampling cycles. At standard operating conditions, the biofilter inlets are measured in quadruplicate twice a day and outlets in quadruplicate thrice a day. Calibration curves generated for toluene are presented in Appendix I. Another SRI GC fitted with a HID detector was intermittently used by collecting gas samples in tedlar bags to look for other unreported biogenic components. A 1 ml SGE gastight syringe was used for manual injection. A portable CO sensor was also used to look for CO production in the reactor outlets.

Table 3-2 : **GC operating conditions for gas phase analysis.**

Parameter	Settings
Detector temperature	385 °C
Column temperature	180 °C
Injection temperature	120 °C
Purge time	90 minutes
Sample loop	1 ml

3.3.1.2 CO₂ analysis

CO₂ is measured using a NDIR CO₂ probe GMP 343 (Vaisala, Finland). Triplicate measurements of CO₂ are taken simultaneously along with the outlet measurements every day for three cycles. Over the purge time of 90 minutes, CO₂ data is logged every minute through the MI170 link software into the computer. A four-point CO₂ calibration curve (Appendix I) was generated from a standard calibration cylinder

(BOC, New Zealand Ltd) of 3000 ppm CO₂ in air. Calibration is periodically checked for linearity and drift.

3.4 Biofilter loading and start-up

Biofilters are autoclaved at 121°C for 30 minutes to eliminate any biological contamination before assembling. A 10mM phosphate buffer solution (PBS) at a pH of ~7.4 is used for the liquid phase. The glassware and the PBS solution was autoclaved for 20 minutes. Once the bottom half of the biofilter and the liquid reservoir chamber are mounted on the stand, the semipermeable membrane is wetted and placed on the metallic mesh. Approximately 8 g of soil is wetted with 2-3 ml PBS solution to make a uniform soil bed in a thin cylindrical shape using a circular metallic ring (ID 53 mm) to help outline the shape. The thickness of the bed is approximately 3 mm to avoid inter-particle mass transfer limitations. After this step, the cylindrical glass chamber for the gas phase mixing is placed on the upper half and the biofilter was sealed and thoroughly leak tested. A leak test is done after assembly by using a syringe fitted with a tubing connected to the outlet and blowing air while sealing the inlet. If the reactor is in operation leak test is carried out for troubleshooting by using soap solutions along the seal. Then the suction cell principle is applied to fill the liquid chamber and set the biofilter to the desired matric potential. All the biofilters are started from wet to dry conditions. This is done by briefly exposing the soil to 0 cm_{H₂O} matric potential akin to saturated condition before lowering it down to the desired height for operation at the corresponding matric potential. This period is followed by an equilibration period with air flow with no toluene is passed through the reactor. The endogenous CO₂ production of the soil at the specific operating temperature and matric potential are monitored followed by starting the toluene-laden air feed.

3.5 Biofilm reactor

3.5.1 Culture regeneration and cell plating

Toluene degraders were isolated from the same soil exposed to toluene in this biofilter set-up for a previous project (Detchanamurthy, 2013) and identified through 16s rDNA and 18s rDNA sequencing methods by Eco Gene Ltd (Auckland, NZ). Stock

cultures were kept in 40% glycerol/60% Luria Bertani (LB) media (Sigma Aldrich) (v/v) at -20 °C in 15 ml centrifuge tubes. Solid agar plates is made by adding 1.5% Agar-Agar (May Baker, England) to LB media solution. The autoclaved solution is cooled to room temperature and poured on sterile petri dishes inside a laminar biocabinet and allowed to solidify. The glycerol stock solution is used to inoculate a shake flask with LB media and is grown overnight at 37 °C in an incubator to regenerate the culture. The liquid cultures is then used to streak the agar plates and kept in the incubator at 37 °C for 4-5 days following which colonies appeared in the plates. The plates are subsequently kept at 4 °C for further use. For this study *Pseudomonas putida* strain was selected to do the pure culture biofilm reactors as this would allow generalizing the results with toluene degradation capability reported in the literature (Bordel et al., 2007b, Díaz et al., 2008). Most of the pure culture work pertaining to degradation of VOCs has been carried out in batch cultures and extrapolation of those results can vary in an engineered bioreactor environment. Hence there is a need to study them in bioreactors under controlled environmental conditions.

3.5.2 Biofilm Reactor loading and inoculation

Reactors and tubings were washed in 5% virkon solutions prior to autoclaving the glass and metallic components at 121 °C for 15 and 30 minutes respectively. The reactor assembly for the biofilm experiments were done inside a laminar biocabinet to maintain sterility and prevent contamination. *Pseudomonas putida* cultures were inoculated from the agar plates and grown overnight in Luria Bertani (LB) media in shake flasks at 37 °C in an incubator. The reactors were assembled in the same manner and the liquid cultures (120 ml) were aseptically poured on the semipermeable membrane slowly until the liquid LB media was drained and seeped into the liquid chamber beneath the membrane. PBS solution was used to wash out the LB media thoroughly to minimise residual LB media in the system. The membrane has a pore size of 0.45 µm which retains the bacteria on the membrane. After this, the reactor headspace and associated parts are assembled and the reactor was put inside the

insulated box for the starting the experiment after making the necessary feed connections to the ports. Following the biofilters assembly the toluene feeds is started.

3.5.3 Biofilm dry biomass measurements

From the same batch of *Pseudomonas putida* culture which was used to inoculate the biofilter, an equal volume (120 ml) was used to quantify the dry biomass present at time zero (t_0) for the reactor. The culture volume was centrifuged at 12000 x *g* for 20 minutes and the supernatant was decanted. The pellet was lyophilized to determine the dry biomass weight of the starting culture. At the end of the run a biofilm matrix was established on the membrane which was gel-like and sticky. Because of the different nature (solid) of the post run biofilm matrix, biomass dry weight was determined through the standard oven drying at 105 °C akin to soil analysis. This was done to maintain consistency of the analysis procedure.

3.5.4 Carbon quantification of the biofilm

The dry biomass was used to determine the carbon content using the Shimadzu SSA-5500 solid module of the TOC-L analyser (Shimadzu) The analyser measures total organic carbon based on the combustion catalytic oxidation/NDIR detection method. Dried biomass was homogenized using a mortar and pestle prior to analysis. The quantification of the liquid and soil carbon is discussed in detail in chapter 4.

3.6 Microscopic analysis

3.6.1 Confocal scanning laser microscopy (CLSM)

Representative biofilm samples were qualitatively analysed through confocal laser scanning microscopy (CLSM) to visualize the biofilm matrix and confirm plausible carbon fractions in the biofilm. Microscopy was done on a Leica TCS SP5 confocal microscope.

3.6.1.1 Polysaccharide staining

Samples were analysed by staining with wheat germ agglutinin-A647 (Invitrogen) which differentially stains polysaccharides (*Strathmann et al., 2002*). Stock solution of

the dye (1 mg/ml) in water was diluted to 10 µg/ml milli-Q water. The sample was washed with milli-Q water after staining to remove the excess stain that is not bound to material. Samples were then placed on a glass slide and covered with a glass cover slip. Excitation was at 561 nm, and an emission window was set from 643 - 751 nm. The dye fluoresced in red. Biofilm samples were analysed both before and after the experimental runs for comparison.

3.6.1.2 Live dead staining

A premixed sample of 1.67 mM propidium iodide and 1.67 mM syto-9 diluted in DMSO was used. Excitation was at 488 and 561 nm, with emission windows from 500 to 550 and 600 to 700nm. Working concentration of each dye was about 5 mM. Samples were incubated for about 5 minutes and put on a glass slide covered by a clear glass cover slip. Living cells stained in green, and dead cells stained in red as the propidium iodide quenches the green fluorescence. This does not always occur, and some cells may stain both green and red, indicating that they are in fact dead. This dye fluoresces only very weakly when not bound to DNA, so the sample could be viewed in this solution.

3.6.2 Scanning electron microscopy (SEM)

Biofilm matrix formed on the membrane was also used for visualization of the surface morphology using scanning electron microscopy (SEM). Small sections of the membrane were immersed in fixative consisting of 2.5% (v/v) glutaraldehyde (Electron Microscopy Sciences, Fort Washington, PA) in 0.1 M cacodylate buffer (Polysciences, Inc., Warrington, PA) with a final pH of 6.7. Samples were fixed for 5 – 6 h, rinsed 12 – 36 h in 0.1 M cacodylate buffer, dehydrated in ethanol for 12 – 36 h, and then critically point dried using a Denton DCP-1 (Denton Vacuum, Moorestown, NJ). Finally, the dried samples were subsequently mounted on a 12 mm aluminium stub using smoothest, 12 mm carbon tabs and gold-coated for 180 seconds using a JEOL fine coat ion sputter JFC-1100. The micrographs were taken using a JEOL FE-7000 scanning electron microscope working at a voltage of 5-8 kV and a working distance of 15 mm.

Chapter 4

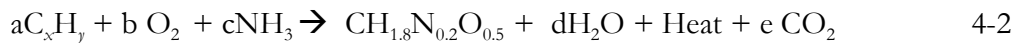
FATE OF THE DEGRADED CARBON IN BIOFILTRATION: CARBON RECOVERY

4.1 Carbon balance and fate of pollutants

The biofilms in oxidative microbial processes in the waste gas treatment industry degrade waste organic compounds (C_xH_y) to CO_2 , biomass and other metabolites (Deshusses, 1997a). It is essentially a biochemical reaction catalysed by the microorganisms proceeding via different pathways depending on nutrient availability. Under nutrient-limited conditions, a typical oxidation reaction for a hydrocarbon leads to the production of CO_2 , water and heat which can be represented as follows:



However, in the presence of sufficient nutrients, toluene (pollutant) oxidation results in the formation of biomass along with other degradation products (Delhomenie et al., 2005) :



Where, $CH_{1.8}N_{0.2}O_{0.5}$ represents a generic formula for biomass.

A major portion of the degraded organic carbon is released as CO_2 (Jorio et al., 2000a, Xi et al., 2006, Li et al., 2002). CO_2 production is often a good indicator of the biological activity of the microbes, which is a common mode for the evaluation of a biofilters performance efficacy (García-Peña et al., 2008b, Bester et al., 2011). So it is common practice to monitor CO_2 production whereas limited success has been achieved in exhaustively pinning down the carbon flux through the system to its final

end-points in different phases. Usually the focus of CO₂ measurement has been on optimization of the operating parameters to address stability and improve process efficacy. Attempts to close the carbon balance have been uneven, with 10-50 % of the degraded carbon missing (Deshusses, 1997b, Morales, 1998, Song and Kinney, 2000, Cox et al., 2001, Avalos Ramirez et al., 2008, Girard et al., 2011).

Determining the biofilm mass is often difficult in packed beds or soil, often requiring the carbon balance to be closed using the difference of other parameters (e.g. C-biomass, carbon content of cells, yield on nitrogen, COD/carbon conversion etc.) (Cox and Deshusses, 1999, Elmrini et al., 2004, Kroukamp and Wolfaardt, 2009, Bester et al., 2011). From the CO₂ measurements, the remaining carbon fractions are estimated as the difference from the net degraded carbon with the common assumption being the formation of biomass. The estimation of parameters based on differences come with their own experimental uncertainties and assumptions, therefore the simple carbon mass balance closure in these highly complex systems remains debatable. Hence, there is a pressing need to track the unaccounted carbon in these biofilm processes through a holistic approach. An illustration of how the carbon entering the system exits or accumulates within the system in the solid, gas and liquid phase is presented in Figure 4-1.

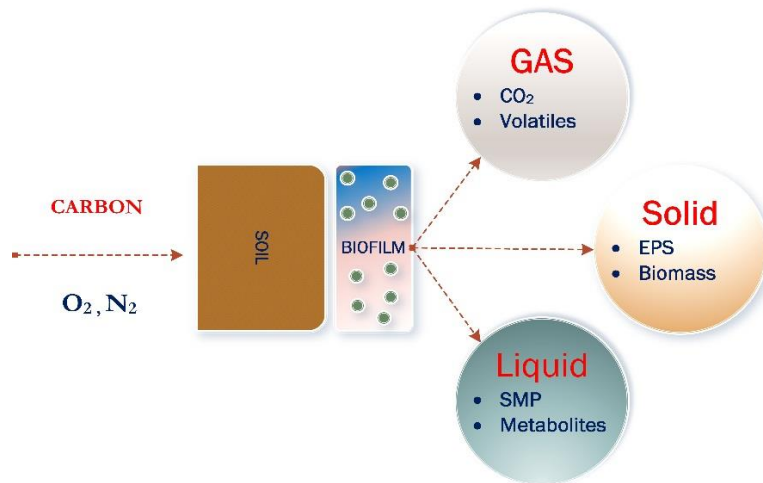


Figure 4-1: Flow chart identifying plausible carbon end-points in the system after toluene degradation.

Material balances follow the principle of conservation of mass, which states that mass can neither be created nor destroyed. So the carbon balance on a biofilter should account for all the carbon entering and leaving the system or accumulating within it. Hence, a systematic and rigorous framework of analysis is necessary to track down the missing carbon in solid, liquid and gaseous phase.

A robust material balance is pre-requisite in designing a new process and analysing an existing one. Considering the general mass balance equation:

$$\text{Input} + \text{Generation} = \text{Output} + \text{Consumption} + \text{Accumulation} \quad 4-3$$

Most biofilter research performs a molecular balance on the pollutant (e.g. toluene, methane) and explicitly focusses on the *Consumption* term (e.g. elimination capacity) as function of a variety of system inputs. As there is rarely any generation term for the pollutant, the mass balance for the pollutant simplifies to:

$$\text{Accumulation} = \text{Input} - \text{Output} - \text{Consumption} \quad 4-4$$

The material balances on reactive systems require a *generation* or *consumption* term on the other molecular compounds. A pollutant balance would not require a *generation* term and would not typically account for the other unknown quantities associated with the process. Hence, the common assumption of the unquantified carbon fractions accumulating as biomass in biofiltration studies needs to be tracked conclusively. For an initial tracking of this missing carbon fraction in the system, an elemental carbon balance is one approach, regardless of the molecular species to which the carbon atom belongs. Hence, a total mass balance on carbon will entail accounting for the various degraded by-products of the organic substrate. Balances on atomic species are in the form of $Input = Output$, since atoms can neither be created ($Generation = 0$) nor destroyed ($Consumption = 0$) in a chemical reaction. So this work is structured on the elemental balance for carbon:

$$Accumulation = Input - Output \quad 4-5$$

Where initially,

$$Input = C_{pollutant} \quad 4-6$$

**This is assuming CO₂ free air or it is accounted for.*

$$Output = C_{pollutant(gas)} + C_{CO_2(gas)} + C_{?(gas)} + C_{(Liquid)} \quad 4-7$$

$$Accumulation = C_{(Solid)} \quad 4-8$$

From preceding equations, the total carbon mass balance on the system becomes:

$$C_{Accumulation(Solid)} = C_{In(Gas)} - C_{Out(Gas)} - C_{Out(Liquid)} \quad 4-9$$

Tracking the carbon fraction in all three phases should account for the carbon end-points in the system encompassing the degradation products as a whole.

4.1.2 Gas phase end-points

In the biofiltration process, the off-gas stream is often analysed for CO₂ and unreacted pollutants as a measure of biofilter performance. CO₂ production is regarded as a good indicator of the microbial activity within the biofilters (Jorio et al., 2005,

Fang and Govind, 2006, Kroukamp and Wolfaardt, 2009, Bester et al., 2011). CO₂ recoveries from various studies have ranged from 40-90 % as a function of mode of operation and variable operational parameters (Deshusses, 1997b, Jorio et al., 2005, Grove et al., 2009, Wang et al., 2012). Cox et al. (2001) reported higher mineralization of 60% to CO₂ at thermophilic conditions as opposed to 46% for the mesophilic biofilter. Higher values of carbon recoveries as CO₂ of 58% for BTEX binary mixtures were obtained compared to single pollutants conversion which ranged from 31-53 % (García-Peña et al., 2008b). This was attributed to cross inhibition in the catabolic pathways for these closely related molecules. Hence, CO₂ production pattern is an important component in defining the product ratios of degraded carbon end-points.

The commonly used methods to analyse effluent gas streams includes gas chromatography with various detectors (TCD, FID) and CO₂ analysers. A few studies have attempted to analyse gas phase components by tracking effluent gas components through mass spectrometry but seldom reported anything other than CO₂ and un-degraded organic pollutants (Møller et al., 1996, Matteau and Ramsay, 1997, Kastner and Das, 2005, Domeño et al., 2010). However, the possibility of other unreported biogenic emissions in these systems cannot be ruled out definitively as yet. Further, the effluent gas stream could possibly be ingrained with aerosols, which can contain C-containing intermediates, un-degraded substrates and dissolved CO₂.

In this framework, the possibility of other unreported trace gases forming during the process is reinforced by limited reports of the formation of carbon monoxide during solid organic waste degradation (Haarstad et al., 2006, Hellebrand and Schade, 2008). Scarce reports in the literature of other gas phase components make a case for more robust experimental tracking. Presence of toxic intermediates in the gas phase needs to be tracked and quantified properly. Elucidating of various carbon end-points in the gas phase should contribute to the fundamental understanding of the degradation kinetics and metabolic pathways as a function of various environmental parameters.

4.1.3 Solid Phase end-points

In biofiltration, once the pollutants are transferred from the gas phase to the biofilms, the substrates are utilized as a carbon and/or energy source by the acclimatized micro consortium (Cabrol et al., 2012). Utilization of substrates which act as an electron donor to the catabolic and anabolic processes are dependent on the carbon flow in the system (Xiao and VanBriesen, 2006). The carbon substrate, apart from being mineralized to CO₂ and water for energy production, is partially diverted towards microbial growth and some non-growth associated products (Leson and Winer, 1991). These constituents form the solid phase accumulation in the system.

Studies delving into a carbon balance often assume the unaccounted carbon from the system is incorporated into the biomass or associated polymers and polysaccharides without robust quantification. But if the missing carbon reservoir were solely biomass or polysaccharides, this would cause clogging of the reactor beds which is not typically reported in growth-limited systems (Deshusses, 1997b, Singh et al., 2006b). In nutrient-limited conditions, maintenance metabolism assumes significance, which means no net increase in active biomass (Cherry and Thompson, 1997). Even in growth systems, limited clogging was reported indicating possible biological equilibrium between primary and secondary degraders (Diks et al., 1994). However clogging of bioreactors with nutrient addition are common and have been extensively covered in the literature (Weber and Hartmans, 1996, Delhoménie et al., 2003, Xi et al., 2006, Maestre et al., 2007, Yang et al., 2010, Dorado et al., 2012). Although, surprisingly little quantitative knowledge exists on the composition of the biofilm components proliferating in these bioreactor systems.

Biomass yield forms an important parameter in model development which can be quantified from carbon recovery estimates (Bordel et al., 2008, Grove et al., 2009). Various studies which assumed the fraction of degraded pollutant not appearing as CO₂ was going to biomass reported biomass yields in the range of 17-43 % per g carbon source (Grove et al., 2009, Singh et al., 2006b, Jorio et al., 2000b, Deshusses,

1997b). However, there is no exhaustive quantification and characterization of these carbon end-points.

When a reactor is running on maintenance requirements under nutrient-limited conditions, a complete conversion of substrate into CO₂ is expected (Weber and Hartmans, 1996). However, the CO₂ fraction is invariably less than the theoretical estimate and carbon may be assimilated by the biomass in some form. Bacteria produce extracellular polymeric substances (EPS) which make up a major fraction of biofilms and play a very important part in biofilm structure, activity and performance (Sutherland, 2001). The major EPS components are comprised of polysaccharides and proteins in varying fractions which also includes nucleic acids and lipids (Flemming and Wingender, 2010). They are sticky solid materials secreted by cells, and are involved in the formation of matrix structure and control microbial physiology.

Biofilms as dynamic systems respond to environmental conditions physiologically which leads to variations in EPS composition (Schmitt et al., 1995). The origins and composition of EPS are very complex. Therefore a number of factors may affect the EPS composition and quantity, such as the type of limiting substrate (electron donor and acceptor), nitrogen and phosphorous limitation, and desiccation (Nielsen et al., 1997). The C/N ratio of the influent also influences the composition of EPS in terms of carbohydrates and proteins (Durmaz and Sanin, 2003). Thus EPS has been related to the macro-scale characteristics of biofilms describing its microbial and structural properties (Ras et al., 2011) and its production is also linked to microbial growth and substrate utilization (Laspidou and Rittmann, 2002). Moreover EPS can be degraded by bacteria as a source of carbon and energy under substrate limited conditions (Kommedal et al., 2001). However, carbon extraction studies of microbial biomass in these systems are limited but seldom show significant carbon accumulation in the biofilms (Fürer and Deshusses, 2000, Song and Kinney, 2000, Vance et al., 1987). Nutrient limited systems rarely plug up which begs the question of other possible carbon sinks for biofilms in stationary phase degrading pollutants using maintenance kinetics.

4.1.4 Liquid phase end-points

In addition to making active biomass and EPS, bacteria also convert a fraction of the organic substrate into soluble microbial products (SMPs) (Namkung and Rittmann, 1986, de Silva and Rittmann, 2000). SMPs are defined as soluble organic matter resulting from intermediates or end-products of substrate degradation and endogenous cell decomposition (Boero et al., 1991, Barker and Stuckey, 1999, Magbanua and Bowers, 2006). They have a wide MW distribution, structure and function (Barker and Stuckey, 1999, Magbanua and Bowers, 2006, Rosenberger et al., 2006). A fractionation study by Jiang et al. (2010) studying SMPs in an activated sludge membrane system found proteins and carbohydrates as the major components of SMPs. SMPs are important because they are ubiquitously present and often comprise a major portion of soluble organic matter in the effluent of biological treatment systems (Rosenberger et al., 2006, de Silva and Rittmann, 2000).

The majority of the SMP research has been done with pure cultures or wastewater treatment systems. A few waste gas biofiltration studies conducting a carbon balance have also reported inorganic and organic carbon in the effluent liquid of the reactor, albeit at a variable percentage (3-39 %) depending on the mode of operation (growth and nutrient limited) (Kim et al., 2005b, Girard et al., 2011, Bester et al., 2011, Cox et al., 1998). However, the identities and the relation to biodegradation of the substrate to SMPs are yet to be determined conclusively in biofiltration. Some metabolic intermediates accumulation during various VOC treatment process has been shown to inflict a detrimental effects on the process culture and in some cases results in a more toxic form than the parent VOC being treated (Bordel et al., 2007a). Duetz et al. (1994) describe the TOL pathway for toluene in strains with the pWWO plasmids that results in toluene being first methyl-oxidized into benzyl alcohol which then leads to benzaldehyde, benzoic acid and catechol, these are then further cleaved at the meta-position. These metabolites have the potential to effect performance efficacy as they can be toxic to microbial communities (Ren and Frymier, 2002). Previously benzyl alcohol has been reported of having mutagenic effects on *Pseudomonas putida* 54G resulting in loss of toluene degradation capacity (Mirpuri et al., 1997).

Furthermore, system inputs like oxygen can become rate limiting within the biofilm resulting in a shift in metabolism forming other intermediates (Yang et al., 2002, Wilshusen et al., 2004, Kim et al., 2005b). Oxygen limitation in overloaded biofilms can lead to partially oxidized by-products such as carboxylic acids (Devinny and Hodge, 1995). Song and Kinney (2005) reported deterioration in biofilters performance under high toluene loadings suggesting rapid accumulation of reaction intermediates. Metabolic by-products during anaerobic degradation of toluene have also been demonstrated but further studies are warranted in aerobic biofilters in identifying transient intermediates (Beller et al., 1992). Even some CO₂ is retained in the liquid phase as carbonates by ionic equilibrium (Morales, 1998, Singh et al., 2006b, Gallastegui et al., 2011a). However, the identities of the carbon fractions in the liquid phase of the reactor are yet to be ascertained quantitatively in a controlled situation, and therefore could be a significant sink for the degraded carbon in engineered systems. Thus, it is evident from the literature thus far, for carbon balances conducted on biofilters, a variable percentage of carbon remains unaccounted for in the system. Usually the emphasis has been largely on process optimization and this fundamental question has met with limited success in the sporadic attempts made in the literature. Table 4 1 presents a compilation of the literature encompassing biofiltration of various VOC's so far, where in carbon mass balance has received attention. Whilst a conclusive understanding of the fate of the degraded carbon in these engineered system remains elusive.

Table 4-1: Compilation of the literature encompassing carbon mass balance studies in biofiltration of various pollutants.

No	Pollutant	Biofiltration Mode	Packing	Variables	Carbon Balance: Endpoints	Analytical Methods	Reference
1	Methyl ethyl ketone (MEK)	Biofilter : Non Growth	Compost: Horse manure + yard waste, redwood chips		C-CO ₂ : 82 ± 10 %	Gas Phase : GC FID, CO ₂ : Chemosorb column with TCD.	(Deshusses, 1997b)
2	Toluene	Biotrickling : Growth	Pall rings with <i>P. corrugata</i> + Protozoan	Toluene IL Nutrient supply	C- CO ₂ : 69%, Biomass: 13 % Liquid : 8 %	Gas Phase : GC FID &TCD, Biomass: Weighing of wet packing, Liquid: TOC	(Cox et al., 1998)
4	Toluene	Biotrickling : Growth	Pall rings with <i>P. corrugata</i> + Protozoa		C- CO ₂ : 68%, Biomass: 21 % Liquid : 6 %	Gas Phase : GC FID &TCD, Biomass: Weighing of wet packing + elemental balance, Liquid: TOC	(Cox and Deshusses, 1999)
6	Toluene	Biofilter : Growth	Peat enriched with nutrients	Toluene loads, ammonia addition	C-CO ₂ : 44.5 %, Carbonates:14.3%, Polymers: 32%, Biomass: 9.2 %	Gas Phase: GC TCD, Biodegradable fractions were analysed through a digestion protocol.	(Morales, 1998)
7	Toluene	Biofilter: Non Growth	Compost + bark and lava rocks		C- CO ₂ : 70 %	C-14 toluene: scintillation, Gas Phase : GC FID &TCD, infrared CO ₂ analyser	(Fürer and Deshusses, 2000)
8	Toluene	Vapour phase Bioreactor (VPB): Growth	Porous silicate pellets	Air flow : Unidirectional (UD), Directionally switching (DS)	Assumption : EPS	Gas Phase: GC-FID and CO ₂ analyser. Biofilm analysis: COD , dehydrogenase activity	(Song and Kinney, 2000)
9	Toluene, Benzene	Biofilter: Non Growth	Cylindrical activated carbon (CAC)	Inlet load (IL) and gas flow rate	Toluene - CO ₂ : 64% Benzene- CO ₂ : 51% Assumption: Biomass and solute	Gas Phase : GC FID & HP CC, CO ₂ analyser and bacterial counts	(Li et al., 2002)

No	Pollutant	Biofiltration Mode	Packing	Variables	Carbon Endpoints	Balance:	Analytical Methods	Reference
10	Ethanol	Biofilter Growth	: Polypropylene rings	Temperature	C-biomass : 10.6 % Unaccounted: 35%		Gas Phase : GC FID &TCD, Biomass dry weight , Biofilm:TOC	(Cox et al., 2001)
11	Toluene and acetone	TBAB	Coal particles	Inlet load (IL) and Gas flow rate	Stoichiometric cal: C-CO ₂ : 90 %		Gas Phase : GC/FID, THC, and CO ₂ analyzer .S-COD	(Chang and Lu, 2003)
12	Ethanol	Biofilter Growth	: Sugarcane bagasse with <i>Candida utilis</i>	Inlet load (IL)and Gas flow	C- CO ₂ :(16-76.3) % C-biomass:(2,8-5.7)%, Acetaldehyde:(1-7.8%), Ethyl acetate:(14-20%)		CO ₂ : GC with TCD Cell no for biomass calculation.	(Christen et al., 2002)
13	Xylene	Biofilter	Spherical peat	Inlet load (IL)and Gas flow	C- CO ₂ - 82% Assumption: Biomass and solute		Gas Phase : THA and CO ₂ analyser	(Elmrini et al., 2004)
14	Styrene	Biofilter Growth	: Peat and Ceramic	Inlet load (IL)and Gas flow	CO ₂ - 78.5% (peat) Biomass : 9.2 % Degradation product		Gas Phase: GC/MS and FID, Viable cell no NA plates	(Jang et al., 2004)
15	Toluene	TBAB	Inorganic	Non-use /backwashing	C_CO ₂ : 63.2% C-Liquid :15.5 % Unaccounted: 20.9		Gas Phase : GC FID and TOC	(Kim et al., 2005a)
16	Toluene, styrene, methyl ethyl ketone and methyl isobutyl ketone	Trickle bed air biofilter (TBAB)	Pelletized diatomaceous earth	Interchanging VOC's	C_CO ₂ : 63% C-Liquid: 20 % Unaccounted: 15%		Gas Phase : GC FID and TCD. Liquid: TOC analyzer	(Kim et al., 2005c)

No	Pollutant	Biofiltration Mode	Packing	Variables	Carbon Endpoints	Balance:	Analytical Methods	Reference
17	Toluene	Biofilter Growth	: Wood chips + propylene spheres inoculated with activated sludge	Inlet load (IL)and Gas flow	CO ₂ : 83% approx. Explicit balance attempted	not	Gas Phase : GC FID and TCD, Leachate: TOC	(Xi et al., 2006)
18	Citrate and glucose	Bioreactor	Biofilm	Inlet load (IL)	C- CO ₂ : 25% ,C-Liquid :72% ,C-cells 4%		CEMS, TOC	(Kroukamp and Wolfaardt, 2009)
19	Octane	Biofilter Growth	: Compost and perlite 50/50(v/v)	Inlet concentration plus a shutdown period	CO ₂ recovery : 0.25 mol/molC Remaining carbon assumed as biomass.		Gas Phase : GC FID and CO ₂ analyser	(Grove et al., 2009)
20	Methane	Biotrickling: Growth	Inorganic packing	CH ₄ and nitrate	CO ₂ recovery : 82% Accumulation in biofilter: 15%		Gas Phase : THC and CO ₂ analyser, Lixiviate: Ion chromatograph, UV detector, TOC	(Girard et al., 2011)
21	Toluene and p-xylene	Biofilter	Inert material	Inlet load (IL)	p-xylene: 74% gCO ₂ gC ⁻¹ Toluene: 72% gCO ₂ gC ⁻¹ Accumulation based on conversion of an empirical biomass formula to carbon accumulation rate: 5-8%		Gas Phase : GC FID and total hydrocarbon analyser, CO ₂ : NDIR CO ₂ analyser, Leachate: TOC	(Gallastegui et al., 2011a)
22	Toluene	Biotrickling Growth	: Granular activated carbon (GAC)	Concentration, gas flow rate and temperature (55 °C and ambient)	C in CO ₂ : 69 % C in biomass: 30.5 %		Gas Phase : GC FID and CO ₂ analyser. Leachate: TOC analyser Fluorescence spectroscopy	(Wang et al., 2012)

4.2 Results and Discussion

4.2.1 Differential Biofilter

The differential biofilter used in this research enabled accurate control of environmental parameters such as water content, pollutant concentration and temperature (Beuger and Gostomski, 2009). The advantage of a differential reactor is that the microbes in the soil are exposed to the same controlled environmental parameters at any snapshot in time. In contrast, a column biofilter is exposed to transient conditions along its length. The pollutant concentration changes along the length of the column and without much control over the water content in the bed. Heat generated from the oxidation reactions also leads to temperature variations within the bed. Thus, through this investigation on the carbon recovery as a function of controlled environmental parameters could provide valuable insights on the microbial response to system inputs, substrate utilization and its ultimate fate after transformation.

The fate of degraded carbon in the system was robustly tracked in the solid, liquid and the gas phases independently. This helped to track the carbon flux through the system. The primary focus of this chapter is illustrating the analytical approach and discussion of the experimental results pertaining to the explicit carbon balance closure independent of the influence of the environmental parameters on the flow of carbon in to the various outputs (solid, liquid, gas). Experimental runs over multiple parameters were investigated and the degraded carbon was quantified. The impact of various environmental parameters on the carbon recovery and product ratios has been analysed in the subsequent chapters.

4.2.2 Carbon balance model for the differential biofilter

The differential biofilter experimental system entailed carbon flux tracking through the system independently in the gas, liquid and solid phases. Figure 4-2 illustrates a section view of the differential biofilter used for this study. All the three phases are interconnected with a dynamic gas phase and stationary solid and liquid phases. In the gas reservoir, the gas contacts the biologically active solid phase. The solid phase is hydraulically connected to the water chamber through a semipermeable hydrophilic membrane. This necessitates consideration of the carbon quantified in each phase and their contribution to the carbon mass balance in totality. Hence, the carbon flux through this system is explained through a series of mass balance equations by explaining the rationale behind their incorporation in the final carbon balance calculations.

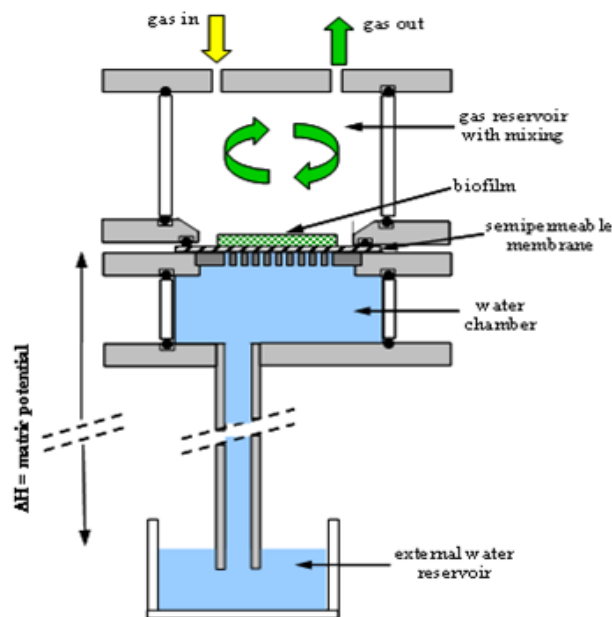


Figure 4-2: Section view of the differential biofilters used in this study.

For a control system without any pollutant feed, there is endogenous CO_2 production from the soil bed that can be tracked in the gas phase. Simultaneously there is a natural flux of the soluble fraction of the carbon from the soil to the liquid phase. At time zero (t_0) the carbon content of the soil can be termed as S_1 (gC). The liquid phase for a control comprising of PBS (phosphate buffer saline) solution at t_0 has negligible carbon content, $L_1 = \sim 0$ (gC). With time, a portion of the initial carbon in the soil is extracted into the liquid reservoir (S_E). The carbon flux rate for both the endogenous CO_2 production and soil extract in the liquid reservoir for this system is influenced by temperature and matric potential. For the illustration of the carbon flux concept in this system a typical operation at a temperature of X °C and a matric potential of $-Y$ $\text{cm}_{\text{H}_2\text{O}}$ is considered. Figure 4-3 presents a pictorial depiction of the carbon flux in a control system

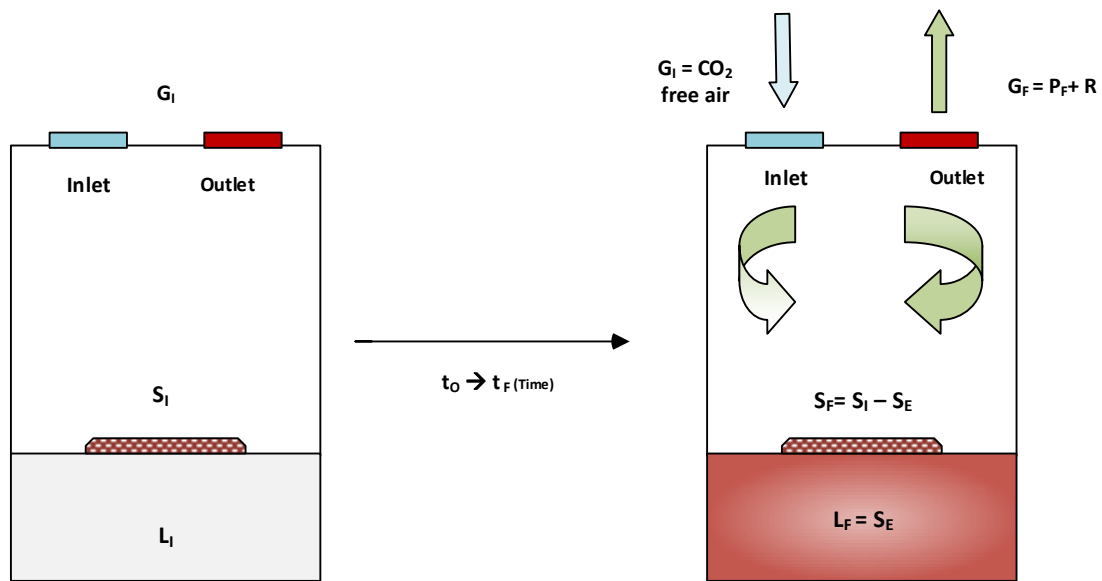


Figure 4-3: Change in carbon flux through a control system without toluene feed over time (t_0 = initial time) and (t_F = final time), operated at a certain temperature and matric potential.

From Figure 4-3 two equations can be derived for carbon content from t_0 (initial) to t_F (final). At time t_F , carbon content in the gas and soil phase can be represented as:

$$\text{Gas}_{\text{final}} = G_{\text{F}} = G_{\text{I}} + R \text{ (gC)}$$

$$\text{Soil}_{\text{final}} = S_{\text{I}} - S_{\text{E}} \text{ (gC)}$$

$$\text{Liquid}_{\text{final}} = S_{\text{E}} \text{ (gC)}$$

Where, all carbon fraction quantification are in (gC). Variables are defined as follows:

G= Carbon content in gas phase

R= Endogenous soil respiration

S= Carbon content of soil

L= Carbon content of liquid

Subscripts _{O,I&F} = Denotes time zero (o), initial (i) and final concentrations (f).

S_E= Carbon leached from the soil

t= Time (days)

Now this system prior to pollutant addition can be compared to a typical experimental run with pollutant feed and distribution of biodegradation products over various phases. Once the biofilter equilibrates to the operating temperature and matric potential with a steady endogenous CO₂ production rate, the pollutant feed is started. Over the time course of biofilter operation, plausible carbon fractions and its eventual end-points are depicted in Figure 4-4. Further, an equation was derived for calculating the carbon balance for the experimental runs accounting for the natural carbon flux (without toluene feed) and differentiating the total accumulated carbon from the degraded fractions.

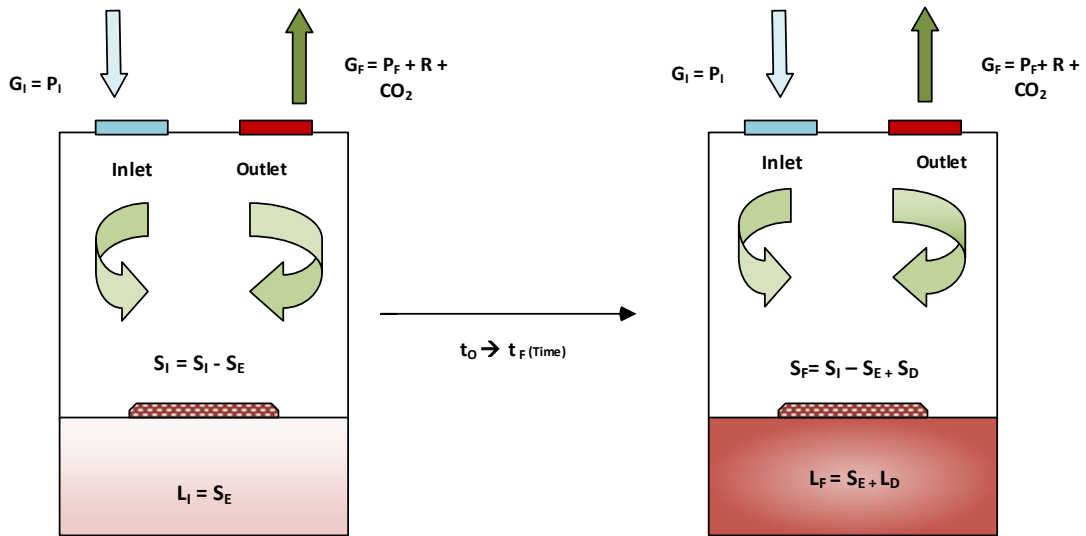


Figure 4-4: Fate of degraded carbon through the system during experimental run over the course of operation and various carbon end-points.

Where, all carbon fraction quantification are in (gC). Variables are defined as follows:

G = Carbon content in gas phase

R = Endogenous soil respiration

S = Carbon content of soil

L = Carbon content of liquid

P = Pollutant concentration on a carbon basis

Subscript $_{0,I \& F}$ = Denotes time zero ($_0$), initial ($_I$) and final concentrations ($_F$).

S_E = Carbon leached from the soil

S_D = Carbon accumulated in the soil.

L_D = Soluble degraded carbon in the liquid.

T = Time length of the experimental run.

Now after the experimental run, the net carbon deposited in the soil will be:

$$S_F = S_I - S_E + S_D \quad 4-10$$

Rearranging Eq (4-10) we get.

$$S_E = S_I - S_F + S_D \quad 4-11$$

In the liquid phase net carbon deposited is given by:

$$L_F = S_E + L_D \quad 4-12$$

Rearranging Eq (4-12) we get.

$$S_E = L_F - L_D$$

Now combining Eq 2 and 4 we get,

$$S_I - S_F + S_D = L_F - L_D \quad 4-13$$

Again rearranging Eq (4-13)

$$S_D + L_D = S_F - S_I + L_F$$

Now, combining the quantified carbon fraction from the three phases the following carbon mass balance becomes:

$$\text{Carbon balance} = (G_I - G_F = R - CO_2 + S_D + L_D) \quad 4-14$$

Equation (4-14) was used for calculating the carbon mass balance for the experimental runs in this study. Quantified carbon represents the total degraded carbon from the pollutant which was tracked in the various phases by quantification of the components as depicted in the previous equation. Analytical procedures are discussed in the subsequent sections.

4.2.4 Carbon flux tracking in various phases

4.2.4.1 Gas phase carbon end-points quantification

Toluene and carbon dioxide concentration at both the inlet and outlet were tracked on-line for each set of experiments. Figure 4-5 presents a typical experiment showing the evolution of the residual outlet concentrations implying degradation rates for three biofilters as a function of temperature. Inlet feed concentration was kept constant for each experimental run throughout the time course of operation.

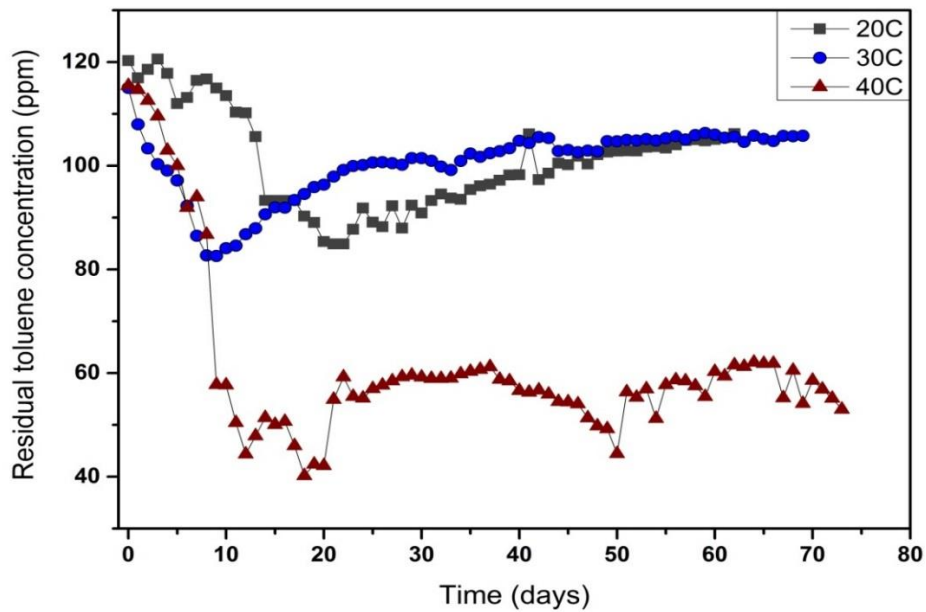


Figure 4-5 : Variations in the residual toluene concentration as a function of temperature at an inlet feed concentration of 120 ppm toluene and $-10 \text{ cm}_{\text{H}_2\text{O}}$ matric potential.

A key component in the gas phase is the CO_2 production which is a major carbon end-point and an effective indicator of the biofilter efficacy. Throughout this study the degradation was well correlated with the CO_2 production in the system. Figure 4-6 shows typical experimental results for inlet and outlet toluene with the corresponding CO_2 concentrations. Importance of the pre and post run experimental phase evaluated without toluene feed to determine the endogenous CO_2 production is discussed in the subsequent section. Online monitoring of the gas phase carbon fractions enabled to understand the dynamic response of the system and have a continuous tracking of the carbon flux in one phase.

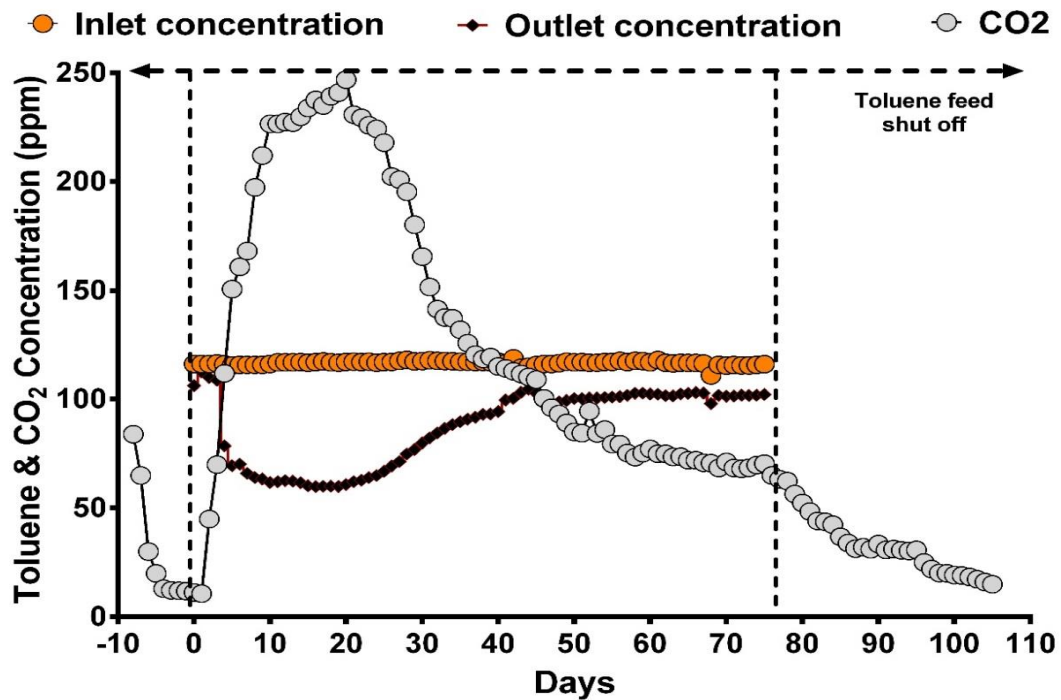


Figure 4-6: Evolution of CO₂ production in relation to the degradation of the toluene by the soil bed with time. This experiment was operated at 20 °C and -20 cm_{H₂O}.

The endogenous CO₂ production rate of the soil was required as part of the mass balance outlined in section 4.2.2. This rate was a function of both temperature and matric potential. Changes in these parameters can affect the endogenous CO₂ respiration rate of the soil microbes. This made it imperative to establish the baseline for each set of operating condition. This was done by passing CO₂-free compressed air (no toluene) through the reactor until it reached a steady CO₂ production rate at the operating conditions before starting the toluene feed. Upon achieving steady state at the applied matric potential and operating temperature, the toluene feed was started. At the end of the run, the toluene feed was stopped to monitor the endogenous CO₂ production pattern post-run. CO₂ production in typically dropped by ~30-50 % in the absence of toluene (Figure 4-7).

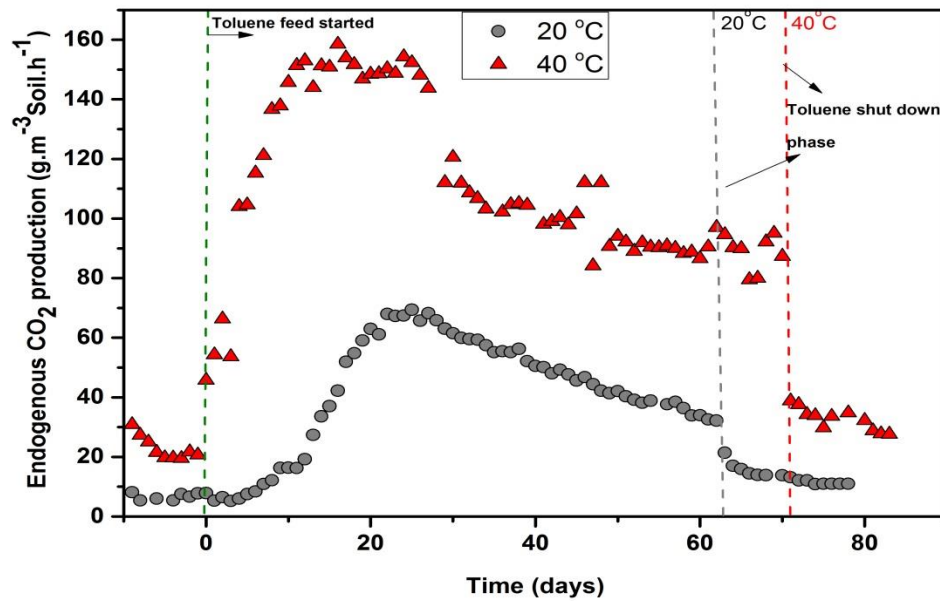


Figure 4-7: Typical experimental runs for evaluating the endogenous CO₂ baseline at 40 °C and 20 °C at -10 cm_{H₂O} through pre-, operational and shut down phases.

So there was a sudden change in the process culture kinetics switching from active metabolism to survival mode utilizing available resources. This implied that the resulting CO₂ production after stopping the toluene feed was a likely combination of soil respiration and utilization of internal storage polymers from toluene-degrading organisms or utilization of accumulated EPS by the multispecies microenvironment. However, with time, the CO₂ production rate approached the pre-start up value. This indicates a fixed endogenous activity at a particular set of environmental parameters (Figure 4-8). Hence, the net endogenous CO₂ production rate was identified for each set of conditions. This was accounted for quantification of carbon recovery as CO₂.

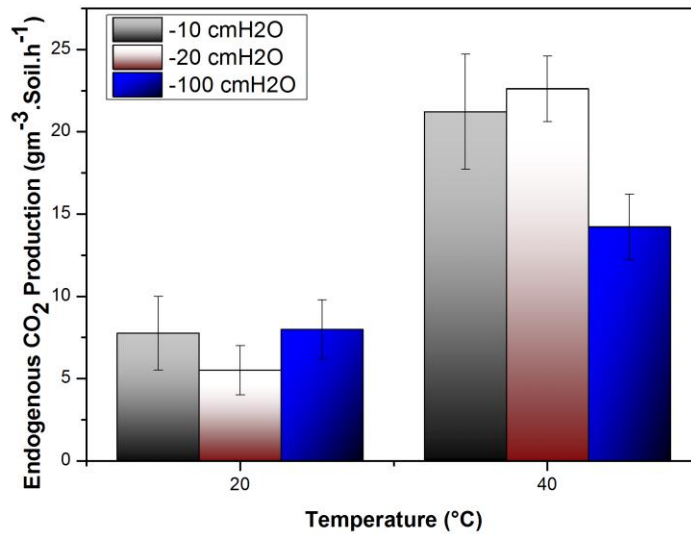


Figure 4-8: Effect of temperature and matric potential on the endogenous CO₂ production rate of the soil bed.

4.4 Solid phase carbon end-points quantification

4.4.1 Control soil sampling

The quantification of the carbon fractions in soil was the most critical of the three phases partly because of the presence of natural organic carbon fractions. Soil samples are a mix of fragmented structures of clay, silt and sand and natural substances like barks and other organic remains. This made quantitating total carbon in the samples more prone to variations by just taking representative samples through mixing and subsampling without further sample pretreatment. Mechanically homogenizing the soil sample using a mortar and pestle after segregating it through a US no 10 sieve (2mm) decreased the measurement uncertainty to approximately < 3% from around 8-10 % observed by just sub sampling. Hence this procedure was adopted throughout the study as a sample preparation step for soil carbon content analysis.

Secondly, the Shimadzu TOC analyser solid module reports the carbon fractions on a percent and/or weight basis with respect to the wet sample weight. This required an estimation of the soil moisture content separately to estimate the carbon content on an oven-dry weight basis. So an additional method of directly using the oven dried soil for carbon content analysis was tested and compared to wet soil sample analysis. This enabled simultaneous determination of the moisture content and direct estimation of the carbon content on an oven-dry weight basis. Table 4-2 presents the total carbon (TC) content data for both wet soil samples and oven-dried soil samples to elucidate the presence of any significant deviations between the two sampling methodology and reliability in particular.

Table 4-2: Carbon content analysis of the control soil samples for both wet soil samples and oven dried soil samples.

Sample type	gC/g _{DW} Soil ^a (%)	gC/g _{DW} Soil ^b (%)	gC/g _{DW} Soil ^c (%)	Cumulative gC/g _{DW} (%)
Oven dried soil (OD)	10.52±0.33	10.99±0.49	10.71±0.26	10.88±0.24
Wet soil (WW)	13.27±0.26	10.64±0.25	8.50±0.63	10.87±0.55

*Reported values with superscripts (a,b,c) are means from three independent measurements at 95 % CI.

From the analytical results presented in Table 4-2, independent observations over a long time frame (~2.5 years) yielded fairly consistent results for the oven dried samples (OD) with a coefficient of variation (CV = 7%). But there was more variability for the fresh soil samples analysed on a wet weight basis (WW) with a coefficient of variation (CV = 16%). Although cumulatively pooling the samples (OD, n=26; WW, n=28) for both the sampling methods by unpaired two sample t-test did not show significant difference ($p\text{-value} < 0.05$) among the means for both the test methods repeated every 6 months. The carbon content was 10.88 ± 0.24 % for the OD method whilst it was 10.87 ± 0.55 % for the WW method. However the OD method was more precise for soil analysis and further tested for biofilter soil samples.

4.4.2 Biofilter soil sampling

The soil from the biofilters invariably differs in physical and chemical properties than the control soil, particularly after the deposition of extracellular polymeric substances (EPS) and other soluble microbial products (SMP) during the course of biodegradation. Unlike the control soil from storage, soil beds in the biofilters are exposed to different environmental parameters while simultaneously undergoing carbon influx and outflux over a period of time (~70 - 120 days). During this period, it is exposed to transient residual pollutant concentrations resulting in carbon accumulation in the soil (EPS) from degradation of the pollutants. This happens simultaneously with the outflux of SMP's (soluble microbial products) from the degradation along with the natural soluble fraction from the soil to the liquid phase which causes the biofilter soil carbon content to change with time. Hence the static phase of the biofilter including the soil bed and the interconnected liquid reservoir cumulatively account for the net carbon deposited from toluene degradation.

Secondly, the biofilter soil samples are comparatively wetter than the control soil from the storage. In addition, the variable carbon accumulation in the form of SMP's and EPS as a function of different environmental parameters are bound to impact the physico-chemical characteristics and texture of the soil. Thus both the methodology of oven dried (OD) and wet soil sample (WW) used for control soil analysis were again tested for biofilter soil samples to check for any volatile carbon loss or analytical variance Table 4-3. These two methodologies were tested for both control biofilter systems (without toluene feed) and for post-run experimental biofilter samples.

Table 4-3: Total carbon measurements for different experimental reactor systems and control runs for carbon loss test during analysis of fresh and oven dried samples.

Sampling methods	C/g _{DW} Soil ^a (%)	% C/g _{DW} Soil ^b (%)	% C/g _{DW} Soil ^c (%)	% C/g _{DW} Control Soil ^d (%)
Soil-OD	12.13±0.50	11.63±0.81	8.90±0.20	9.64±0.41
Soil-WW	11.92±0.40	10.47±0.33	17.43±0.43	9.53±0.13

* Reported values with superscripts (a,b,c,d) are means from independent measurements at 95 % CI

Post run biofilter soil samples were homogenized and randomly sub sampled for independent analysis with the two methodologies (OD vs WW) over different experimental runs. The analyses were consistent across a multitude of biofilter samples and a control biofilter set up at a matric potential of $-10 \text{ cm}_{\text{H}_2\text{O}}$ without any toluene feed. As discussed previously regarding control soil analysis, both the methods yielded consistent results for the samples from the biofilters without any significant statistical difference for the means ($p \text{ value} < 0.05$). Although, the analyses for the biofilter samples has less variance which could be partly due to equilibration at specific matric potentials maintained in the biofilters leading to an even distribution of carbon through the hydraulically connected pores. The results were analysed with two samples unpaired t-test.

However, for the results presented for sample (Soil^c) there were significant differences between the carbon content results between the two methods. These were tracked down to a post run biofilter disassembly issue. Over the course of the experiments, condensation often results in the inner surface of the upper chamber and in the base of reactor plates holding the cylindrical glass chamber sealed with a Viton o-ring. Although the reactor design pulls the excess condensate into the reservoir if it flows down the wall, during the disassembly process of the reactor post run if care is not

taken, it rolls on to the soil bed, which happened in this particular instance. It led to overestimation of the moisture content (Mc) at around 75 ± 3 % on a dry weight basis (dwb). This estimation was much higher than other Mc analysis at runs operated at a matric potential of $-10 \text{ cm}_{\text{H}_2\text{O}}$ which were around 61 ± 4 % (dwb). Hence, this significant difference in analysis result occurred as an effect of the correction factor for the moisture in the sample. Also the presence of extracellular polymeric substances (EPS) in variable amount as a function of environmental parameters could absorb more water in case of flooding because of their water holding capacity (Or et al., 2007a). So for sampling wet reactor samples, even though it is possible to avoid flooding by following a careful disassembly procedure at the end of the run, the oven dried sampling of soil was considered for consistent analytical precision and accuracy. In addition, homogenization of the samples yielded much better results and particularly with biofilter soil samples containing EPS that got very sticky when wet.

4.5 Liquid phase carbon end-points quantification

PBS (phosphate buffer saline) solution at a pH of ~ 7.4 was filled in the liquid reservoir as discussed previously in Chapter 3. Initially at time zero (T_0), the autoclaved PBS solution contained 0.2 ± 0.003 mg/l total carbon and hence was treated as insignificant ($L_I = \sim 0$ gC). Before starting the biofilter operation, the liquid reservoir was hydraulically connected to the soil through the semipermeable membrane at the applied matric potential. The natural carbon flux from the soil and the soluble fraction of the degradation products to the liquid phase were influenced by matric potential and length of operation. The effect of temperature was not independently explored in this study. At the end of the biofilter runs, $S_E + L_D$ (Section 4.2.2) were analysed cumulatively through quantification of the total carbon (TC) in the liquid phase for L_F .

4.5.1 Soluble carbon fractions in soil

An essential prerequisite was to determine the water-extractable fraction of the soil carbon used for the biofilter bed. The carbon content of the soil extracts were independently quantified through a combination of different experimental methods. Soil:PBS were mixed randomly at (8:100 w/v soil-to-solution ratio) and (8:500 w/v

soil-to-solution ratio) keeping the same volume of soil as used in the biofilters and held for variable lengths of time. Several methods suggested fairly quick equilibration in terms of mixing and centrifuging the supernatant for extractable carbon fraction analysis (Ghani et al., 2003, Jones and Willett, 2006). However because of the long biofilter experiments, samples were set up in submerged conditions and kept for a variable time spanning from 5 days to 2 years in static conditions with intermittent mixing. Subsequent total carbon analysis suggested fairly consistent values indicating complete extraction was achieved within < 5 days. These values gave the total water-extractable carbon from the soil sample used for this study assuming all of the soluble carbon was dissolved in the water phase.

This was followed by another control set up of soil:PBS in the ratio akin to the reactor set-up with (8:500 w/v soil-to-solution ratio) albeit in saturated conditions. The mixture was kept in a conical flask and put in a magnetic stirrer hot plate operated at 200 rpm and 35 °C for 5 days. These results were similar to the quantified values of the set up discussed in the previous paragraph. Equating these values to the total initial soil carbon the water extractable carbon fraction in soil was approximately 16 ± 4 % of the carbon content in soil.

4.5.2 Implications of soluble carbon flux in the liquid phase

The soluble carbon fraction of the soil estimated in submerged conditions serves as a good context for experimental set-up which was primarily operated at unsaturated conditions. Carbon flux in the liquid phase would be much slower at unsaturated conditions and was tested at a matric potential of $-10 \text{ cm}_{\text{H}_2\text{O}}$ for varying periods of time. Control biofilters were set up without any toluene feed through the system. CO_2 free dry air was passed through the reactor to monitor the endogenous CO_2 production and the liquid reservoirs were analysed for the extractable carbon fractions from the soil. The liquid carbon content with different controls was compared with the experimental runs as a function of environmental parameters (Figure 4-9). From Figure 4-9 it implies that unlike the submerged controls, in the unsaturated system the extractable carbon flux progression into the liquid reservoir was considerably slower. Probably more controls would be required to conclusively determine if it reached

equilibrium by 60 days although the values were similar at the end of 20 days. But it does indicate that even more time would be required for the extractable fraction to flux into the liquid phase for lower matric potentials ($-20 \text{ cm}_{\text{H}_2\text{O}}$ and $-100 \text{ cm}_{\text{H}_2\text{O}}$) studied in this project. Operations as a function of decreasing matric potential decreases the the water content of soil impairing the hydrated pathways which hampers the carbon flux. Secondly all the extractable carbon did not diffuse into the liquid phase as the total carbon content values from the unsaturated controls and almost all the experimental runs were significantly lower than the extractable carbon values. In addition, the experimental runs were undergoing carbon accumulation (L_D) in varying amounts depending on the environmental parameters over time in conjunction with the S_E flux.

Hence the carbon content for the unsaturated controls should increase with time to reach equilibrium if monitored for longer time, in particular at lower matric potentials. However unless the flux rate is constant which do not change under the transient biofilter operating conditions, extrapolating this value to the calculations may not give accurate quantification. During the course of the experimental runs, degradation of toluene releases water as a by-product that partly wets the soils and eventually equilibrates to the operated matric potential. This phenomenon could profoundly impact the flux of both $S_E + L_D$ to the liquid phase pertaining to the extent of biodegradation taking place. Thus S_E , the flux for any experimental run was not an independent process but was simultaneously being influenced by the biodegradation kinetics. Hence, additional controls at each set of conditions would not have contributed to the analytical accuracy and was not pursued. So the primary objective of quantifying the fate of the degraded carbon was accounted by the model carbon balance equations derived for this system (section 4.4.2). So the carbon accumulation in the interconnected static phases of solid and liquid phase has been considered cumulatively and independently for each biofilter runs. This helped to conclusively track the carbon end-points which was one of the key focuses of this work.

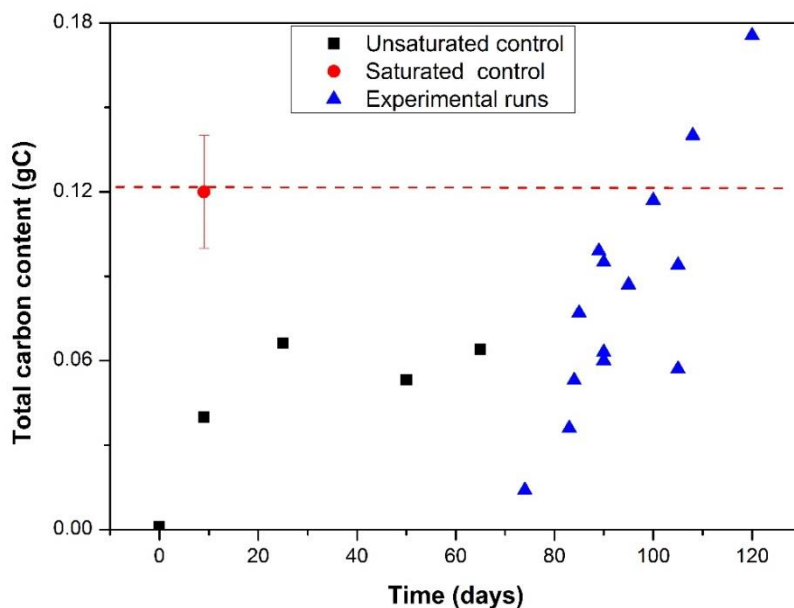


Figure 4-9: Comparison of control soluble carbon contents in the liquid phase with the biofilter experimental runs. Unsaturated control was done at $-10 \text{ cm}_{\text{H}_2\text{O}}$.

4.6 Carbon end-points quantification: Carbon balance

A primary objective of this study was to track and quantify all the degraded toluene on a carbon basis. Plausible carbon end-points in the gas, liquid and the solid phase were quantified to track the carbon flux through the system. On-line monitoring of the toluene and CO_2 was done in the gas phase. Toluene was the sole organic fraction detected by the GC fitted with a FID detector and no other hydrocarbons were detected in the outlet stream. Gas samples were also tested with a HID detector but nothing else was detected. The possibility carbon monoxide using a handheld device (Vaisala) in the degradation products was also explored but it was not detected. The solid and the liquid phase were independently quantified for the carbon accumulation over the experimental period. These fractions were included into the carbon balance equations derived for this experimental system (Sec. 4.4.2). Carbon recovery was

tracked over independent biofilter runs operated as a function of various environmental parameters as discussed in the next section.

4.6.1 Carbon balance: Data analysis and error propagation

The carbon fractions (gC) in the inlets and outlets were determined independently for each experimental run (μ). Each measurement had its own associated uncertainties. To estimate the carbon balance closure (CB) the ratio was calculated as: $CB = \mu_{\text{outlet}}/\mu_{\text{inlet}}$. Standard error approximation was done by the Delta Method which is based on Taylor series expansion to find variance in functions for independent random variables (Weisberg, 2005). Simply converting the CB into percentage to report the relative uncertainty is not a robust way to report error. Hence a new data set with the corresponding approximated standard errors were calculated for each independent experiment. Analysis was done using R statistical software (Team, 2015) using the car package (Fox and Weisberg, 2010, Fox et al., 2015). Once the estimates were calculated, a combined mean of the whole study was estimated along with a 95% confidence interval through meta-analysis (inverse variance) using the package meta (Schwarzer, 2015) using R statistical software.

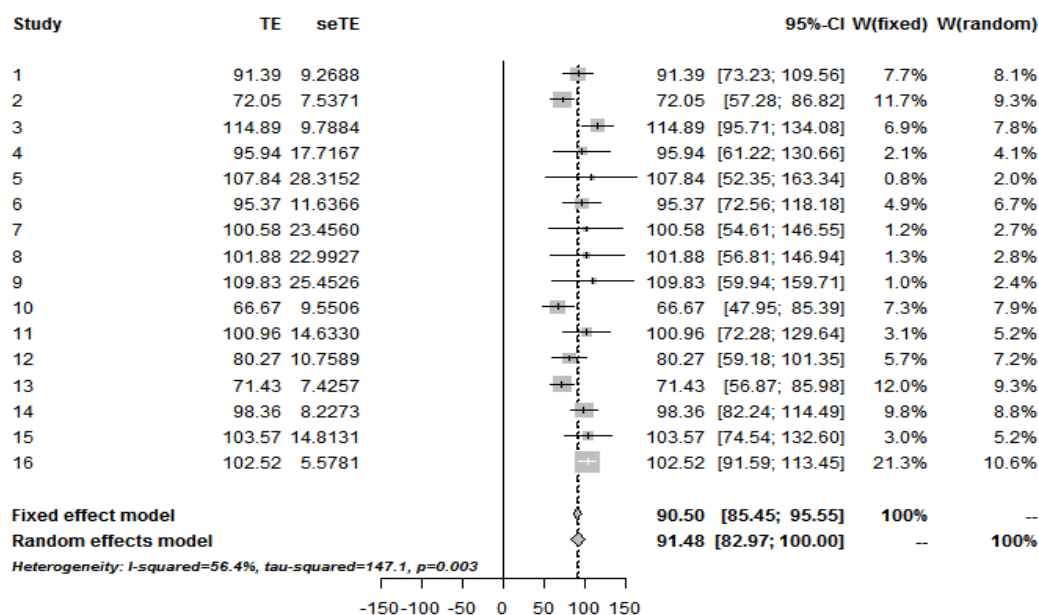


Figure 4-10 : Forrest plot for carbon balance closure for the experimental biofilters runs operated over various environmental parameters using meta-analysis (n=16). Where, TE is estimate of treatment effect. seTE is the standard error of treatment effect.

4.7 Conclusions

The cumulative carbon balance closure achieved over the entire set of biofilter runs independent of the varying environmental parameters (n=16) was 90.50 % [85.45;95.55] at 95 % confidence interval using the assumption of a fixed effect model. Considering the measurement uncertainty and the associated statistical rigour for data analysis, the quantitative carbon recovery estimation can be postulated to have accounted for all the degraded carbon without any missing carbon. A significant contributor to the experimental uncertainty in this work comes from soil partly owing to less degradation with non-growth mode of operation. However the results gave evidence of a significant carbon sink in the system which can vary as a function of environmental parameters. Subsequent chapters in the thesis focused on the variation in this product ratio of CO₂ fractions to the non-mineralized fraction over

temperature, matric potential and toluene concentration at various levels and combinations.

Chapter 5

INFLUENCE OF ENVIRONMENTAL PARAMETERS ON THE CARBON END-POINTS

5.1. Introduction

Biofilters are packed bed bioreactors using microbial consortiums to form a pollutant degrading biofilm (Mudliar et al., 2010b). It is a parameter driven process where each critical parameter influences the process in a specified way. However there are combinations of environmental parameters at play exerting its own unique influence and by interactions between other parameters. Most biofiltration studies have focussed on the impact of these critical parameters like temperature, matric potential and substrate concentration on process optimization and efficacy for specific influence rather than potential interaction across levels (Francesc et al., 2012, Estrada et al., 2012, Zamir et al., 2014, Vergara-Fernández et al., 2012). Understanding the interactions of various environmental parameters on substrate metabolism pertaining to various end products could help solve operational problems like clogging and start-up times. In addition, knowledge of the carbon end-points could bridge the connection between functionalities, community structure and metabolic response if coupled with high throughput molecular biology techniques.

The fate of degraded carbon in the system is defined by the physiological response of the micro-ecosystem encompassing both primary and secondary degraders as impacted by the operating conditions. These processes cumulatively influence the degradation process that reflects on the carbon end-points. Tracking the recovered CO₂ fraction as a function of various environmental parameters could provide interesting insights on their interactions pertaining to their impact on carbon-endpoints and removal rates of

biofilters. The focus of this study was to track the variations in product ratios as CO₂ and non-mineralized fractions as a function of temperature, matric potential and substrate concentration.

5.2 Impact of temperature on the fate of transformed carbon

Like any biological system, temperature is a critical operational parameter for the biofiltration process (Delhom nie and Heitz, 2005, Mudliar et al., 2010b). Temperature is a defining factor for microbial activity both in terms of proliferation and biodegradation rates in engineered systems (Devinny et al., 1999, Jin et al., 2007, Vergara-Fern andez et al., 2012). As biofilters are often exposed to fluctuating temperatures, tracking the temperature mediated impact on degradation end-products provides a vital link to the mechanistic understanding of the microorganism's physiological response. Microbial adaptation to the variations in temperature and its associated implication on the microenvironment is the key to growth and survival. The influence of temperature should reflect on the fate of the degradation products in response to the metabolic pathways of the active degrading community. So unravelling the various facets of substrate utilization, carbon end-points in particular could lead to a better understanding of the fate of pollutant in the biofilter.

5.2.1 Temperature mediated response on substrate utilization

Temperature variations in biofilters have a profound effect on the physical, biological and chemical aspects of biofiltration process parameters (Darlington et al., 2001, Veiga and Kennes, 2001). Temperatures below the optimal range inhibit microbial growth. It can structurally affect the lipids in the cell membrane hampering membrane transport machinery (D'Amico et al., 2003, Nedwell, 1999). Darlington et al. (2001) found a greater effect on substrate affinity than microbial activity at 20 °C. Higher temperatures can lead to drier conditions due to excess evaporation of bed moisture (Mohammad et al., 2007). Dry conditions can favor fungal proliferation over bacteria (Nikolova and Nenov, 2005). Another potential problem is temperature increases can decrease the solubility of pollutants and oxygen (Zhu et al., 2004). Zamir et al. (2014) reported a significant decrease in removal efficiency from 70-100% at 35 °C to 25% at

40 °C attributed to a decreased solubility of *n*-hexane at high temperature. High temperature can also induce protein denaturation and cell death as observed by Kong et al. (2013). However, limited knowledge exists on the effect of temperature on microbial community and metabolic pathways for biodegradation of volatile organic compounds.

Usually microorganisms have a higher and lower limit of temperature for survival separated by an “optimum temperature range” associated with maximum growth and degradation. The majority of the biofiltration reports are in the 15-40 °C temperature range (Delhomenie et al., 2005, Jin et al., 2007, Shareefdeen et al., 2009, Vergara-Fernández et al., 2012). Thermophilic biofiltration, while less well studied, has reported higher activity over the 45-70 °C range (Mohammad et al., 2007, Luvsanjamba et al., 2007, Montes et al., 2014). However, most biofiltration research focuses on the impact of temperature on activity and performance without correlating it to the product ratios. Only a few studies have reported mineralization and biomass accumulation patterns over a temperature range. Wang et al. (2012) reported lower biomass accumulation (30% of the removed toluene) at 55 °C as opposed to 47% in biofilters operated at ambient conditions (20-30 °C). In one of the earlier studies, Cox et al. (2001) found higher mineralization of ethanol (60 %) at higher temperature of 53 °C to 46 % at ambient temperature (22 °C). So a general consensus of higher temperature increasing VOC mineralization is accepted. This indicates a temperature-driven phenomenon of regulating the diversion of substrate degradation end-points. But detailed knowledge on the intrinsic relationship of temperature with other environmental parameters on the fate of the degraded carbon is still limited.

5.2.2 Link between temperature and community to degradation products.

Variation in temperature also affects the community structure in a biofilter, ultimately influencing degradation end-products. Lu et al. (1999) found rod shaped bacteria as the dominant community at 15 °C which changed to a predominance of bacilli and cocci at 50 °C in a biofilters treating BTEX vapors. Cox et al. (2001) found rod-shaped bacteria, yeasts and fungi in moderate concentration at the high temperature biofilter

operating at 53 °C implying the presence of thermophilic ethanol degrading community. They also observed greater microbial diversity in the biofilters at ambient temperature than at higher temperatures. The biofilter mineralized 60 % of the ethanol at 53 °C as opposed to 46 % at ambient temperature. Gallastegui et al. (2013) attributed a two-fold higher mineralization to CO₂ for toluene than ethylbenzene to the dominant degrading community in the biofilter speculated to be fungi. However the individual contribution of bacteria and fungi was not ascertained. They postulated a synergistic interaction between the bacteria and fungi which was previously reported to influence the mineralization of aromatic hydrocarbons by Li et al. (2008). These adaptations to temperature can influence a change in community structure with substrate degrading capability. Evolution of different community would imply different metabolic pathways which could affect the fate of carbon.

Microorganisms can thrive within a certain temperature range through regulating physiological and metabolic activities. Kong et al. (2013) found lower metabolic activities in thermophilic biofilters compared to mesophilic biofilters during the early phases but showed comparable values over long term operation (181 days). This study gave interesting insights on the temperature-microorganism dynamics in biofilters. These temperature-mediated attributes have illustrated a direct impact on the eventual degradation of the pollutants by the microbial adaptation to the changing environment. This implies a significant influence of temperature on the fate of degraded pollutants and various transformation product ratios in the system.

5.3 Water potential in unsaturated media

Usually water is present in two forms in soil and other porous media, bound and mobile. Bound water is not available to the microorganisms, only the mobile water held between the pores can be used for microbial activity. In biofiltration, water availability in the bed can be measured using the concept of water potential (ψ). This is the free energy of the water in a system and is cumulatively comprised of, osmotic potential (ψ_{π}), matric potential (ψ_m), gravitational potential (ψ_g), pressure potential (ψ_p) and overburden potential (ψ_{Ω}) (Papendick and Campbell, 1981). Mobile water is held

between pores by capillary forces and gravitational forces. At saturation, the pores are completely filled with water resulting in zero water potential (ψ) (Papendick and Campbell, 1981). As the water potential (ψ) decreases, water is drained out of the pores generating drier conditions and making it more difficult for the microorganism to utilize the water for their metabolic activity.

5.3.1 Transient water content dynamics in biofiltration

Limited water availability has a detrimental effect on the process culture involved in bioremediation (Coronado et al., 2014). Both organic and inorganic packing materials have been used in biofiltration with varying hydrodynamic properties. Organic material offers the advantage of residual inorganic nutrients and better water holding capacities whereas inorganic packing are more robust and possess higher surface areas (Dorado et al., 2010). The water content of the packing material is critical to the microbial community and pollutant abatement. Change in water content in the packing materials is driven by both operational and kinetic parameters. Drying of packing bed can occur due to incomplete humidification of inlet air stream (Morales et al., 2003). Sakuma et al. (2009) reported drying at the inlet port of a biofilter reduced its performance. Microbial oxidation is an exothermic process; the metabolic heat generated from pollutant oxidation can increase the bed temperature thereby lowering the bed water content (Gostomski et al., 1997, Mysliwiec et al., 2001). Thus accurate mechanism for maintaining optimal water content is vital to the microbial process as water related stress can induce physiological response that can be detrimental to process efficacy.

5.3.2 Microbial response to water stress

Microbes exhibit an intricate set of physiological adaptations to transient hydration dynamics in unsaturated media like soil. Lower water potential could result in a drastic change to osmotic potential which directly affects the osmoregulation and cell turgor pressure. Cellular dehydration can also cause protein denaturation and structural damage to DNA. Drier conditions can impair nutrient flux as water serves as a transport medium for nutrients to cells (Or et al., 2007b). Most bacteria produce extracellular polysaccharides (EPS) for their increased water holding capacity in low

water content habitats (Van De Mortel and Halverson, 2004, Holden et al., 1997a). Schimel et al. (2007) illustrated the microbial response via allocation of resources upon decreasing water potential. They proposed that during stressed conditions microbes are compelled to produce protective molecules such as osmolytes and chaperones to maintain cellular integrity.

Various studies have linked water stress response to specific gene expressions. *Pseudomonas putida* induces alginate synthesis in response to an imposed water stress of -0.04 MPa along with genes responsible for trehalose biosynthesis (Gülez et al., 2012). Johnson et al. (2011) found increased expression of genes involved with trehalose and exopolysaccharide biosynthesis and reduced expression of genes responsible for flagella biosynthesis under lower water potential of -0.25 MPa in *Sphingomonas wittichi* strain RW1. They also found significant changes in membrane fatty acid components. Dmitrieva and Burg (2007) illustrated damage to the protein and DNA synthesis pathways as direct response to water stress.

Changing the water potential influences the microbial community depending on the inherent acclimatization machinery at its disposal (Harris, 1981). Often the significant effects of water stress can shift the community structure over time. Sun et al. (2002) found an increase in bacterial population with increasing moisture content while the actinomycetes and moulds decreased. Lower surface colonization by *P. putida* KT2440 at negative water potentials was reported by Descene et al. (2008). They attributed this to limited bacterial motility due to shallow liquid films at the surface of the pores in the experimental system. Prenafeta-Boldú et al. (2012) reported sustained biofilter degradation by a mixed bacterial and fungal community in xerophilic conditions (water content was ~20%) dominated by fungi, especially *Exophiala oligosperma*. Fungi are known to thrive in low moisture conditions which can influence the degradation end-products as the metabolic responses vary among different groups of microbial communities.

5.3.3 Effect of matric potential on carbon recovery

Mineralization of the pollutants to CO₂ serves as a good estimate of the microbial activity in the system (Jorio et al., 2005, Kroukamp and Wolfaardt, 2009). Variation in CO₂ recovery fractions with changing matric potential could mean adaptation of the microbes to the imposed water stress. Lower matric potential brings in physical constraints like impaired solute diffusivity and microbial motility owing to reduction in hydrated pathways (Or et al., 2007a). This could render the process biologically limited due to reduced water availability for cellular function. Microorganisms produce extracellular polysaccharides (EPS) for their increased water holding capacity in low water content habitats (Van De Mortel and Halverson, 2004, Holden et al., 1997a). Also at the optimal matric potential requisite cellular functions for maintenance can be easily met through catabolic energy generation process leading to higher CO₂ recovery. This shift in substrate degradation products towards non-mineralized fractions as a function of matric potential could have immense significance in elucidating carbon-endpoints.

Lower matric potential results in reduced water availability in the pores causing the microorganisms to expend more energy for maintaining cellular activity and prevent dehydration. In response to the drier environment, genes for producing important solutes like ectoine (LeBlanc et al., 2008), and protective proteins like chaperonin are induced (Kato et al., 2004). Water stress related constraints could potentially trigger a stress response maintaining intracellular osmolyte concentration to maintain cell turgor pressure (Van De Mortel and Halverson, 2004). Carbon from the substrate is required for production of osmolytes. The generation of osmolytes has been well documented as a mechanism induced in response to environmental stress. But at lower matric potential, the drier environment can hinder optimal carbon flow affecting osmolyte accumulation (Kakumanu and Williams, 2014). So a community with better adaptive capabilities over a range of water content would ensure efficient pollutant abatement and survival.

Drier conditions at lower matric potentials are known to facilitate fungal proliferation in biofilters because of their ability to thrive under such conditions (Prenafeta-Boldú et

al., 2008, Gallastegui et al., 2013). It underlines the effect on microbial activity in response to transient gradients in water contents in unsaturated surfaces commonly encountered in soils (Long and Or, 2009). However the fate of degraded carbon is dependent on the dominant degrading community which gains predominance with time. Estrada et al. (2013a) did a comparative study with a VOC mixture on bacterial and fungal biofiltration. They found higher VOC mineralization by bacteria (~63 %) compared to fungi (~43 %). Thus the eventual fate of the degraded carbon can be significantly influenced by variations in matric potential and its associated effects on the microenvironment.

5.4 Results and Discussion

5.4.1 Influence of environmental parameters on the CO₂ recovery

Quantifying carbon-end points for biofilters operated over multiple levels of environmental parameters revealed variations in product ratios comprising of mineralized and non-mineralized fractions as previously discussed in Chapter 4. Since the CO₂ production was concurrently monitored with the degraded toluene it was an effective tool to understand the carbon flux through the system. The term CO₂ recovery is calculated on a percent carbon basis from the net CO₂ produced per gram of toluene degraded and corrected for the endogenous CO₂ production (gC-CO₂/gC - Toluene). Temperature, matric potential and substrate concentration were the three critical environmental parameters which were postulated to impact the substrate utilization and carbon endpoints. These parameters were studied at three levels in various combinations to track their influence on CO₂ recovery (Table 5-1).

Table 5-1: Biofilter operational parameters used for tracking the carbon fractions

Parameters	Variable	Units
Inlet feed concentration	75,120,193	ppm
Temperature	20,30,40	°C
Matric potential	10,20,100	-cmH ₂ O
Reactor bed material	Soil/Biofilm	m ³ or m ²
Operation period	80-120	Days

Each biofilter was operated at various levels of these factors. For each parameter categorical levels were chosen to cover a wide spectrum of effect from low to high groups. Each factor was controlled for the time course of operation. Only the residual toluene exiting the reactor varied depending on the metabolic activity for each specific operating condition.

The environmental parameters were analysed through a mixed factorial approach from (three temperatures, three inlet feed concentrations and three matric potentials). A two-way ANOVA on a 3x3 factorial run between temperature and substrate concentration suggested significant interactions between both the parameters, $F(4,111) = 13$, $p\text{-value} < 0.05$. Another two-way ANOVA between temperature and matric potential 2x3 also showed significant main effects for each parameter than the interaction term. ANOVA results are presented in Table 5 2. The simple main effect of each factor on subsequent levels of the other factor was further explored to interpret the variations in CO₂ recovery observed across various levels of the parameters.

Table 5-2: Summary of analysis of variance (ANOVA) results for the manipulated environmental parameters.

a)	DF	Sum of Squares	Mean Square	F Value	P Value
Temperature	2	1578	789	33.76	3.5e-14 ***
Inlet toluene concentration	2	9068	4534	194.09	<2e-16 ***
Interaction	4	1182	296	12.65	1.6e-08***
Residual	111	2593	23		
b)	DF	Sum of Squares	Mean Square	F Value	P Value
Temperature	1	5923	5923	236	<2e-16 ***
Matric potential	2	26370	13185	526	<2e-16 ***
Interaction	2	39	20	0.785	0.46
Residual	104	2606	25		

5.4.2 Interaction of temperature and substrate concentration

Biofilter runs were studied at temperatures of 20 °C, 30 °C and 40 °C at a corresponding inlet feed concentration of 75 ppm, 120 ppm and 193 ppm toluene. Each biofilter was operated at these various levels of temperature and inlet feed by keeping the matric potential constant at $-10 \text{ cm}_{\text{H}_2\text{O}}$. The residual toluene varied depending on the metabolic activity at the operating conditions. Therefore, the simple main effects of each level of temperature against the subsequent levels of inlet toluene concentration were further analysed (Figure 5-1). The impact of these interactions on toluene degradation is discussed in Chapter 6.

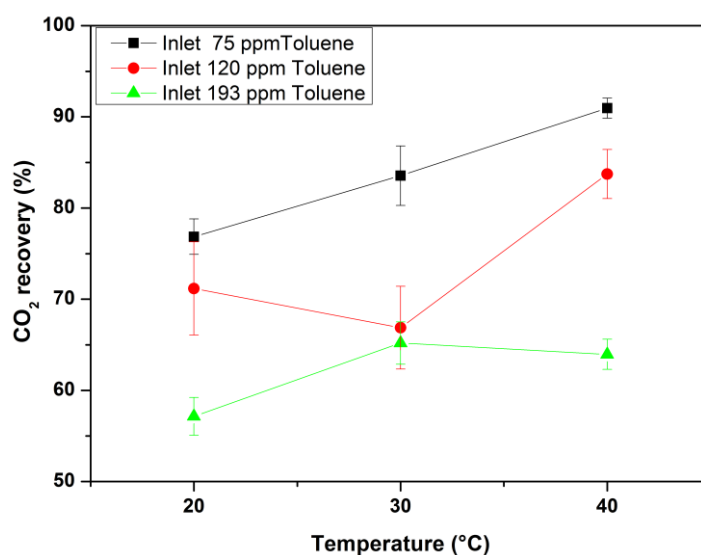


Figure 5-1 : Interaction plot of temperature and substrate concentration parameter impacting CO₂ recovery. Values represents mean with uncertainties at 95% confidence interval during steady state over a multi-day period from replicate runs.

Toluene mineralization to CO₂ evolved through the time course of the experimental run and varied as a function of specific combination of environmental parameters. At a feed concentration of 120 ppm toluene, CO₂ recovery increased with temperature (Figure 5-1). Around 71 % CO₂ was recovered at 20 °C followed by 66% at 30 °C. The highest recovery of 81% was observed at 40 °C. The variation in carbon recovery

as a function of temperature does imply its underpinning role in influencing metabolic pathways for substrate utilization as a function of residual substrate concentration exposure.

To further this study, the same temperature and matric potential conditions were operated at a lower inlet feed concentration of 75 ppm toluene to generate lower residual toluene concentrations than what was achieved at feeds of 120 ppm toluene. The toluene mineralization trend was similar with more of it being mineralized at higher temperatures (Figure 5-2). At the lower inlet toluene concentrations, the fraction of carbon mineralized to CO₂ increased. For operations at 40 °C, around 90% was mineralized to CO₂ followed by 82 % at 30 °C and 76 % at 20 °C. As the inlet feed concentration was increased to 193 ppm toluene, mineralized CO₂ fractions further decreased. However, at this higher feed concentration, the mineralized fraction does not differ significantly (*p-value* <0.05) as a function of temperature. Thus CO₂ recovery was influenced by the interaction of both the parameters at various levels of operations. At lower inlet feed concentrations, temperature was the dominant parameter influencing mineralization to CO₂ while at the highest inlet feed concentration, substrate concentration became dominant irrespective of the operating temperatures.

Each temperature interacted differently with variation in feed concentrations eventually resulting in a distinct mineralization pattern. At 40 °C, mineralization to CO₂ decreased linearly (R=0.98) with increase in feed concentration followed by 20 °C (R=0.98). At 30 °C toluene mineralization was highest at 75 ppm feed but then mineralization dropped and plateaued over the higher feed concentrations. Temperature played a dominant role over the lower feed concentrations but at higher feed, substrate concentration seems to have negated the impact of higher temperature.

As both the parameters were found to have significant interaction from the ANOVA analysis (Table 5-2), a further post hoc analysis was carried out. CO₂ recovery data was accessed through pairwise comparison of the means at each set of conditions through Tukey's HSD procedure at 95 % confidence interval (Figure 5-2). There were many

combinations which were found to be significantly different. In summary, 40 °C was significantly different from 20 °C and 30 °C at lower feed concentrations. However 20 °C and 30 °C were not significantly different across the substrate concentration range studied.

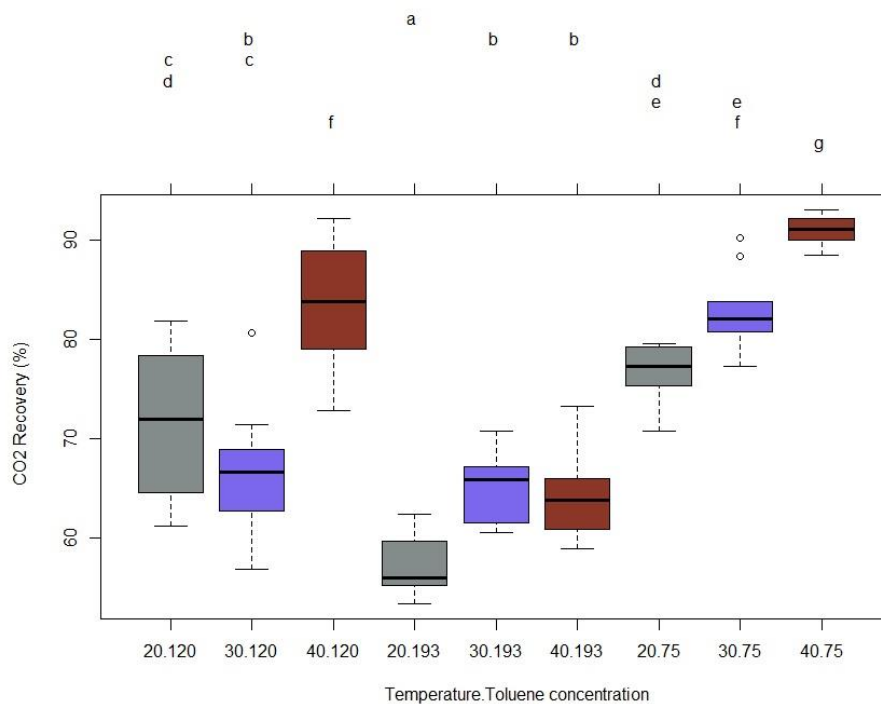


Figure 5-2 : Tukey HSD plot illustrating the pair wise comparisons between combinations of various levels of temperature : toluene concentrations (x axis) with corresponding CO₂ recovery. Groups sharing the same letters as listed in the top of the graph are not significantly different (p value < 0.05).

5.4.3 Effect of inlet feed and temperature on residual toluene concentration

In this differential biofiltration set-up, due to degradation the biofilm associated with the soil were only exposed to the residual outlet concentration while the inlet feed was constantly maintained at the desired concentration level. These inlet concentrations

determined the maximum start-up residual concentrations to which the microbes could be exposed to for each biofilter run. The subsequent residual concentration evolved over time, influenced by the environmental parameters at each set of conditions. The impact of this residual toluene concentration on the CO₂ recovery is presented in Figure 5-3.

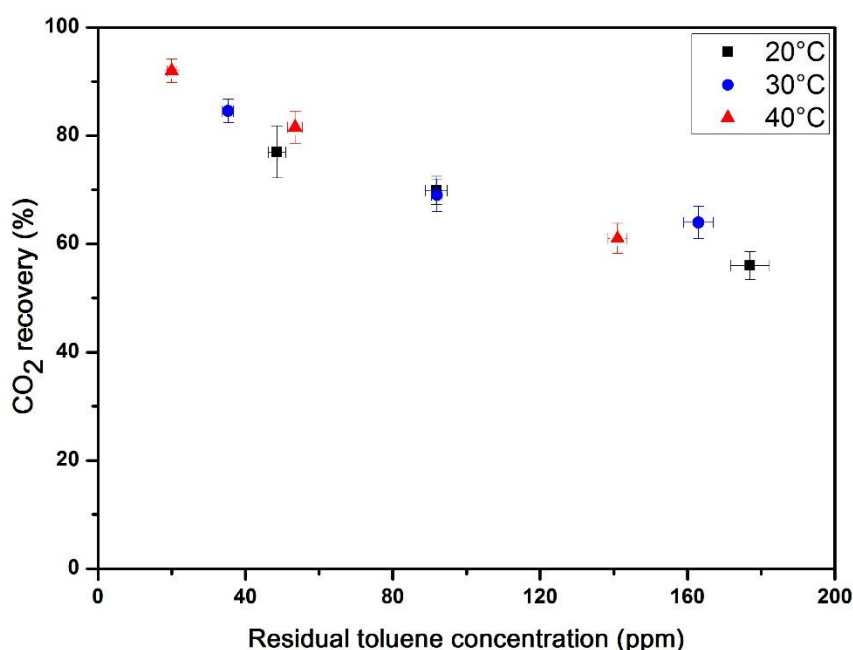


Figure 5-3 : CO₂ recovery as a function of residual outlet concentrations at various temperatures operated at -10 cm_{H₂O}. Values represents mean with uncertainties at 95% confidence interval during steady state over a multi-day period from replicate runs.

The residual toluene concentration and CO₂ recovery in the differential biofilter were both impacted by temperature. Residual substrate concentration for each inlet feed concentration varied as a function of the operating temperature. Operations at 40 °C resulted in the lowest residual concentration followed by 30 °C and 20 °C for all range of inlet feed concentrations investigated. This can be attributed to higher temperature (40 °C) increasing the metabolic activity resulting in lower residual toluene concentrations owing to increased degradation of toluene. Usually higher temperature

increases the enzymatic reactions and cell growth rates double with every 10 °C increase within a certain optimum range which results in higher cellular activities for degraders (Cho et al., 2007). Biofilters operated in the thermophilic range display increased microbial activity for a wide range of VOC's (Ryu et al., 2009, Wang et al., 2012). The increased activity at 40 °C exposes the microbes to lower residual concentrations as opposed to operations at 20-30 °C.

Interaction between substrate concentration and temperature can simultaneously have a significant effect in regulating the overall process metabolism which can be tangibly observed as quantified fractions of recovered CO₂. As can be seen from Figure 5-3, lower residual concentration corresponded to higher CO₂ recovery for all the operating temperatures. The highest mineralization was found at 40 °C and decreased with higher residual concentration which was associated with lower temperatures. In the residual toluene concentration range of less than 100 ppm toluene, CO₂ recovery was linearly correlated with temperature and residual toluene concentrations.

However at a residual concentration greater than 100 ppm toluene, CO₂ recovery became independent of the operating temperature. Even though 40 °C was still at a lower residual concentration, the CO₂ recovery was not statistically different for all the three temperatures (*p-value* <0.05). So although activity was increased at higher temperatures, the mineralization pattern was not affected. This implies a similar metabolic response from the active community across all the temperatures. This may happen because a particular community dominates beyond a level of substrate concentration. Another possibility could be higher residual concentrations might have affected the non-degrading community in some way. Under favourable environmental conditions, they can contribute to increased mineralization by predation (Cox and Deshusses, 1999, Woertz et al., 2002, Bhaskaran et al., 2008). But this would make a strong case if the non-mineralized fractions were produced at a fixed rate. From the analysis in chapter 6 it was found otherwise and non-mineralized fractions showed significant variations with parameters. It is possible grazing by a non-degrader like protozoa could be happening in varying magnitude in parallel as a function of environmental parameters (Tso and Taghon, 2006). But further work would be

required to confirm this through stable isotope probing in conjunction with community fingerprinting tools.

Alternately, higher concentrations can influence the fraction of the active degrading community due to substrate toxicity. Kim et al. (2005c) found impaired degradation capability at higher inlet concentrations which can simultaneously alter microbial metabolism especially in a nutrient-limited system. Higher residual toluene can increase the stress on the process culture which can lead to variation in degradation products from CO₂ recovery to other non-mineralized fractions. Factors such as substrate toxicity at higher residual concentration could contribute to microbial inactivity (Song and Kinney, 2005). Various stress responses for microbes have been elucidated which includes production of internal storage polymers like PHA's under nutrient limited conditions (Poblete-Castro et al., 2012).

Tracking the influence of interaction between environmental parameters on the fate of various degraded fractions can help to understand the process culture's metabolic response. Under nutrient-limited conditions, the assumption is there is no net biomass growth in biofilters (Cherry and Thompson, 1997). Since CO₂ recovery was never 100 %, it suggests a diversion of degraded carbon towards other products as influenced by the environmental parameters. For a nutrient-limited system, a plausible sink would be accumulation of EPS, storage polymers and soluble microbial products (SMP).

There are reports of microbes producing more EPS at lower temperatures (Le Bihan and Lessard, 2000). For this work reduced CO₂ recoveries at higher residual toluene concentrations at lower temperature may have induced accumulation of non-mineralized fractions (Figure 5-3). Less CO₂ recovery is an indication of the culture possibly producing EPS and other internal storage polymers for survival and associated benefits of nutrient pooling (Xavier and Foster, 2007). This further illustrates the interdependence and effect of multiple environmental parameters on the fate of degraded carbon in these engineered systems.

5.4.4 Implications of temperature on CO₂ recovery

Usually higher mineralization to CO₂ at increased temperatures may be coupled with maintenance requirements which are expected to take precedence in a nitrogen-limited system with the assumption of no active growth. The flow of electrons from the substrate leads to energy generation with a part of it dissipated as heat (Xiao and VanBriesen, 2006). In a nutrient-limited system with a continuous source of carbon/energy, the active population can be driven by the requisite energy for maintenance without any active growth. The performance of two reactors degrading ethanol at mesophilic and thermophilic temperature was monitored by Cox et al. (2001). Although the removal efficiencies were similar for both the reactors, there was marked difference in the amounts of CO₂ production and biomass accumulation. Higher temperature showed greater mineralization to CO₂ (60 %) as opposed to 46 % at ambient conditions. In another study treating toluene, 70% of the toluene was mineralized to CO₂ at an operating temperature of 55 °C, which was higher than 53 % observed at operations at ambient temperature (20-30 °C) (Wang et al., 2012). Although an increase in temperature increases the metabolic activity of microbes, it can also simultaneously increase the maintenance requirements of the process culture (Cox et al., 2001). The microbes, as postulated to be in maintenance mode must have had energy to expend on maintenance requirements for the cells to stably survive through catabolic conversions. Without the supplement of nitrogen, the metabolic pathways are likely to be directed towards more energy generation unless there is an apparent advantage for the microbes to produce EPS. This was reflected in the higher CO₂ recovery at the highest temperatures.

Thus varying mineralization suggests microbial adaptation to different temperatures indicating a change in metabolic pathways which could affect the fate of carbon in the system. Tracking the temperature mediated response to degradation end-products could provide a vital link to the mechanistic understanding of the microorganism's physiological response. Temperatures not favourable to the degraders may result in decreased substrate affinity and/or impaired microbial activity putting stress on the microbes. Various stress response for microbes have been elucidated which includes

production of internal storage polymers like PHA's under nutrient limited conditions. This could essentially alter the carbon endpoints in various phases. This difference in carbon recoveries as a function of temperature implies a critical role in metabolic pathways for substrate utilization. Secondly, variations in temperature can also affect the community structure evolution in a biofilter (Nadarajah et al., 2007, Wang et al., 2012) which can ultimately influence the various degradation end-products. Change in community structure after long term operations at different operating temperature has been reported (Mohammad et al., 2007). This suggests a significant effect of operating parameters such as temperature on microbial activity possibly owing to lack of adaptation of the dominant degrading community leading to temporal change in community structure. Kong et al. (2013) found differences in the microbial metabolic characteristics and microbial community in thermophilic and mesophilic biofilters degrading toluene. However the dissimilarity decreased with time over longer term operation of up to 296 days. It was suggested that long term exposure can help in the proliferation of an aptly adapted community. Estrada et al. (2013a) reported variations in mineralization for bacterial and fungal biofilters degrading a VOC mixture at similar conditions. Bacteria had a higher fraction of mineralization (63 %) compared to fungi (43 %). This could translate into different specific degradation rates across communities which are also likely to influence the fate of degradation products.

5.4.5 Interaction of matric potential and temperature

Water content is another critical operational parameter influencing biodegradation kinetics (Delhoménie and Heitz, 2005). Clearly, as both residual substrate concentration and temperature were interacting to influence the CO₂ recovery at a constant matric potential of -10 cm_{H₂O}, it became imperative to extend the investigation to lower levels of matric potentials. So the parameters were investigated through a 2x3 factorial design. CO₂ recovery at temperatures of 20 °C and 40 °C were investigated at three levels of matric potential of -10 cm_{H₂O}, -20 cm_{H₂O} and -100 cm_{H₂O} at an inlet feed concentration of 120 ppm toluene. From the 2-way ANOVA analysis there were significant main effects for both the parameters Table 5-2 without much

interaction. There was a variation in CO₂ recovery pattern at 20 °C and 40 °C throughout the entire range of operating matric potentials (Figure 5-4)

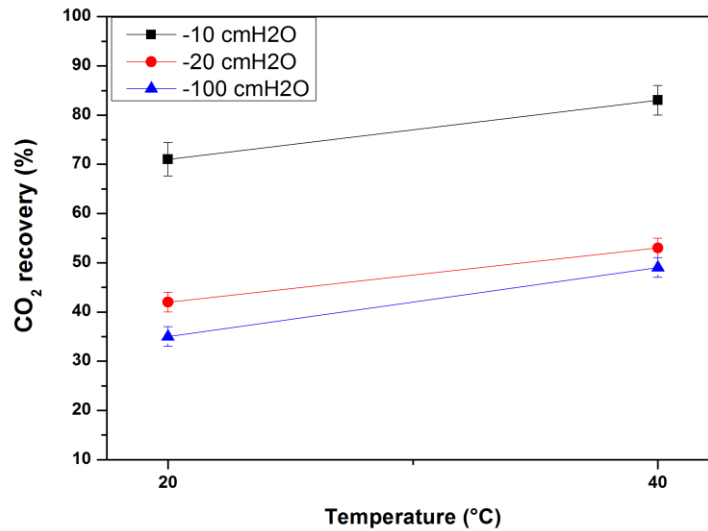


Figure 5-4 : Influence of matric potential and temperature on CO₂ recovery at an inlet concentration of 120 ppm toluene. Values represent the mean with uncertainties at 95% confidence interval during steady state over a multi-day period from replicate runs.

Lower matric potential resulted in lower CO₂ recovery independent of the operating temperature. From Figure 5-4 it is apparent that there was a significant decrease in mineralisation at 40 °C with decrease in matric potential to -20 cm_{H₂O}. CO₂ recovery dropped from 81 % to 54 %. At -100 cm_{H₂O}, CO₂ recovery decreased to 48 %. However at 20 °C, CO₂ recovery significantly dropped from 71% at -10 cm_{H₂O} to 48% at -20 cm_{H₂O}. But further dropped to 35 % at -100 cm_{H₂O}. On the other hand 40 °C had more mineralization at -10 cm_{H₂O} and decreased by ~ 50 % at -20 cm_{H₂O} and then did not vary significantly at the lower matric potential of -100 cm_{H₂O}. These results compares well with the general trend previously reported in the literature of decrease in mineralization at lower matric potential (drier conditions). Gallastegui et al. (2011b) found only 32 % of xylene being recovered as CO₂ along with reduced removal efficiency during intermittent water supply leading to low moisture content in the biofilter operated at ambient temperature. Vergara-Fernández et al. (2012) found 80 %

mineralization of n-pentane at packing material moisture content of 80 % for a biofilter operated at 25 °C. But it was not clear if the moisture content was on a wet or dry basis. Also comparing results on percent moisture may not be an accurate representation of the true water content as its variable for different packing even at same matric potential. However no study was found to directly compare the results which investigated water content and temperature interactions impacting CO₂ recovery in biofilters.

Since there was significant main effects for both temperature and matric potential (Table 5-2), further post hoc analysis was done. CO₂ recovery data was accessed through pairwise comparison of the means at each set of conditions through Tukey's HSD procedure at 95 % confidence interval (Figure 5-5).

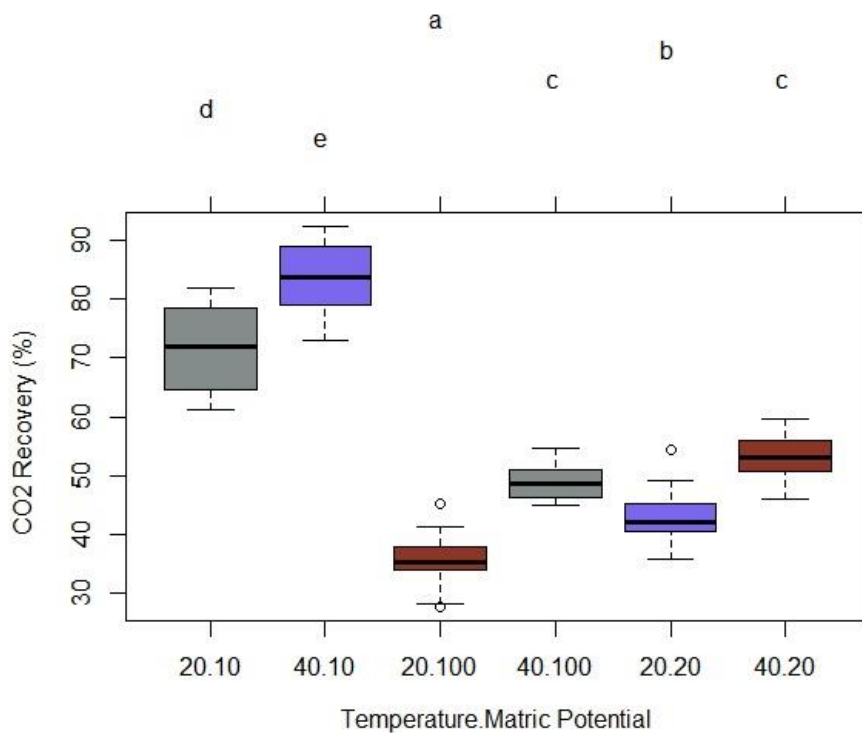


Figure 5-5: Tukey HSD plot illustrating the pair wise comparisons between combinations of various levels of temperature : matric potential (x axis) with corresponding CO₂ recovery. Groups sharing the same letters as listed at the top of the graph are not significantly different ($p\ value < 0.05$).

Tukey's HSD analysis (Figure 5-5) evaluated the presence of significant differences among all the pair wise comparisons. Means at combinations of 40 °C at -20 cm_{H2O} and -100 cm_{H2O} were not significantly different. Also the least difference was between operations at 20 °C at -10 cm_{H2O} and -20 cm_{H2O}. Otherwise, most of the means were significantly different from each other. The highest difference was found between 40 °C at -10 cm_{H2O} and 20 °C at -100 cm_{H2O} resulting in highest and lowest fractions of CO₂ recovery respectively.

5.4.6 Effect of matric potential and temperature on residual concentration

In addition to the interactions between temperature and matric potentials investigated at an inlet feed concentration of 120 ppm toluene, the residual toluene concentrations varied as a function of operating conditions (Figure 5-6). At -20 cm_{H2O}, CO₂ recovery values were within 10 % with a higher fraction at 40 °C. Both set of conditions had a residual toluene concentration of 88-101 ppm with 20 °C at the higher concentrations. However at -10 cm_{H2O} there was significant variation in CO₂ recovery between the two temperatures; 81 % was mineralized at 40 °C and only 71 % at 20 °C. Concurrently there was a significant difference in the residual toluene concentrations as well, with 53 ppm at 40 °C and 88 ppm at 20 °C. This can be attributed to higher microbial activity at 40 °C resulting in improved degradation. But since the CO₂ recovery was also driven by increased activity at higher temperature it can be attributed to a greater push for catabolic conversion of the pollutants at higher temperature. As discussed previously higher maintenance requirements could be the driving force for energy generation.

Further investigations at lower matric potentials from -20 cm_{H2O} to -100 cm_{H2O} showed a decrease in mineralization pattern in varying amounts. At 40 °C, CO₂ recovery did not differ significantly from -20 cm_{H2O} to -100 cm_{H2O} (53-49%). The residual toluene concentration for 40 °C at -100 cm_{H2O} was 94 ppm which was also close to the 88 ppm observed at -20 cm_{H2O}. However for -100 cm_{H2O} at 20 °C, CO₂ recovery decreased significantly to 35%. Although the residual concentrations for -20 cm_{H2O} and -100 cm_{H2O} did not vary significantly from 98-104 ppm toluene, decrease in mineralization

can be attributed to the effect of lower matric potential becoming the dominant parameter. Temperature may have contributed to a certain extent simultaneously in imposing maintenance requirements.

So it can be deduced that CO₂ recovery was impacted by the influence of environmental parameters with one parameter becoming dominant at a specific set of condition. As can be seen from Figure 5-6 temperature factor became dominant at higher matric potential of -10 cm_{H₂O}. Higher temperature resulted in a more active process culture with possibly higher maintenance requirements which also significantly improved the carbon mineralization. At -20 cm_{H₂O} both the temperature and matric potential did not show a huge impact on carbon mineralization which were fairly close. However as the matric potential was further decreased to -100 cm_{H₂O}, matric potential seemed to have become dominant having significantly impacted the biofilter at 20 °C as opposed to 40 °C. Alternately 40 °C may have negated the effects of lower matric potential as mineralization did not changed significantly from operations at -20 cm_{H₂O}. So the combined effect of temperature and matric potential resulted in a huge shift in toluene degradation towards the non-mineralized fraction (~81% → ~35%).

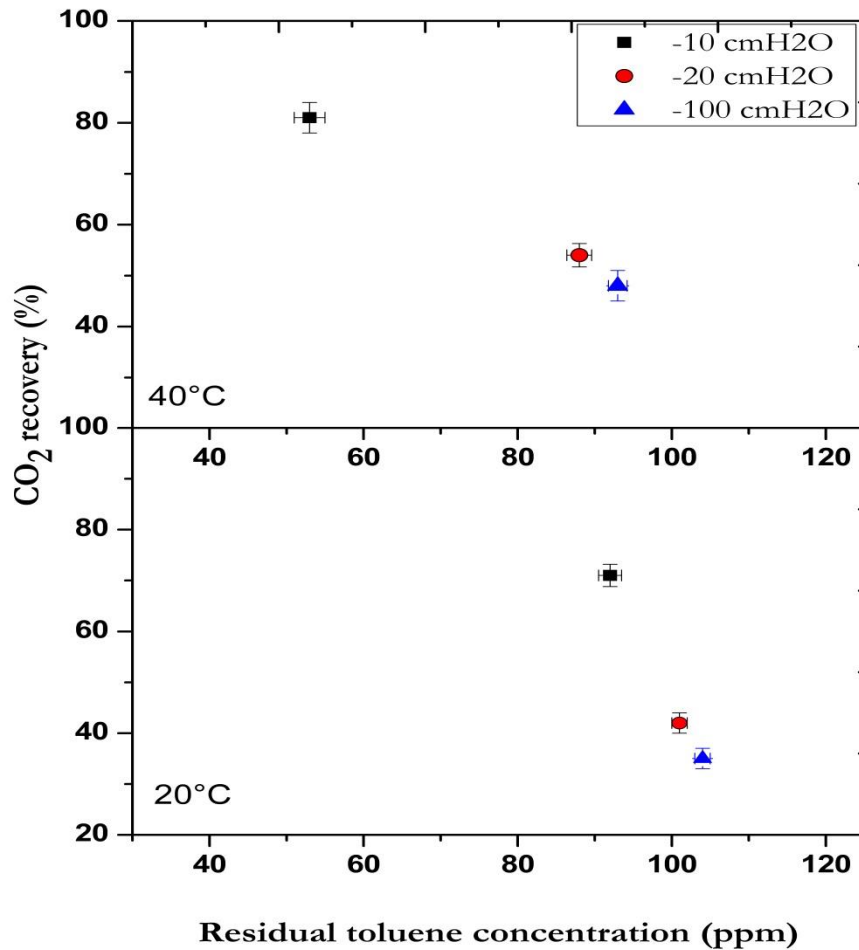


Figure 5-6: Residual toluene concentration as a function of temperature and matric potential and its impact on CO₂ recovery. Values represent the mean with uncertainties at 95% confidence interval during steady state over a multi-day period from replicate runs.

5.4.7 Implications of matric potential on CO₂ recovery

For this study matric potential was controlled to regulate the water content of the soil. Water content plays a crucial part in microbial proliferation and pollutant degradation. Water content of the soil was measured after the experimental runs. Figure 5-7 presents the water retention curve at the investigated range of matric potential for this study.

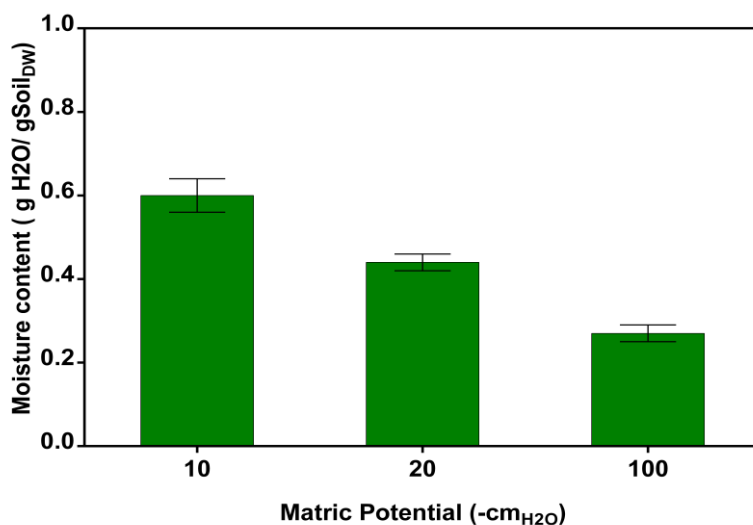


Figure 5-7: Soil water release curve at the various matric potentials for the biofilter runs at 40 °C. Water content is reported on a dry weight basis (DWB).

Gravimetric analysis of the post run biofilter soil revealed soil water content of 0.6 g/g at -10 cm_{H₂O} to 0.45 g/g at -20 cm_{H₂O} on a dry weight basis. Soil water content was further reduced to 0.27 g/g at -100 cm_{H₂O}. Mineralization of the pollutants to CO₂ serves as a good estimate of the resource allocation impacting carbon end-points in response to environmental stress, matric potential in this case. It could be a greater demand for energy to meet cellular functionalities. As previously discussed, without nutrient addition, growth is not expected in the long term run as residual nutrients from the soil bed is likely to be exhausted soon. Thus the requirements for energy could specifically be for maintenance purposes which influenced the fate of degraded carbon due to resource allocation. Moreover lower matric potential brings in physical constraints like impaired solute diffusivity and microbial motility owing to reduction in hydrated pathways (Or et al., 2007a). This can trigger a shift in community structure capable of better adaptation to the specific conditions. Thus variations in the CO₂ recovery fraction with changing matric potentials indicates possible adaptation of microbes to the imposed water stress at each level of operating temperature. These adaptations could also be a change in metabolic pathways at a specific set of conditions.

Lower CO₂ recovery with decreasing matric potential could be due to the process being metabolically impaired due to reduced water availability for cellular function. This can trigger varied survival strategies at the diverse community level by gene expression for specific tasks to maintain cellular functionalities ultimately impacting carbon end-points. Lower matric potential can change the degrading community in different proportions due to the imposed water stress. Fungi have a different metabolic response to bacteria to drier conditions and these changing dynamics can influence the net fraction of pollutant mineralization. Low water content puts pressure to prevent dehydration on the cell membrane. This could potentially trigger a stress response for maintaining intracellular osmolyte concentration to maintain cell turgor pressure (Van De Mortel and Halverson, 2004). Carbon accumulation from the substrate could be channelized towards production of osmolytes. Generation of osmolytes has been well documented as a mechanism induced in response to environmental stress. Decrease in CO₂ recovery with lower matric potential could be survival mechanism in response to decreasing matric potential (Schimel et al., 2007).

However the interaction between parameters at different levels of operation is likely to go through a transition phase both in terms of metabolic and community structure response. Nasrin et al. (2011) suggested a two pronged microbial response to water potential (matric potential + osmotic potential). Lower water potential up to $(-2 \times 10^3 \text{ cm}_{\text{H}_2\text{O}})$ kills a certain fractions and a further decrease results in proliferation of an adapted community with reduced activity. Fungal prevalence was found over bacteria in a biofilters treating ethylbenzene and toluene at low moisture content range of 15-30% (Gallastegui et al., 2013). However they reported the presence of synergism between the microbes mineralizing the aromatic hydrocarbons. Coexistence of different communities would impact the mineralization pattern due to difference in metabolic response among them. Further microbiological work is warranted to elucidate the functionalities and metabolic responses regulating the fate of the degraded pollutants to better understand the interactions.

5.5 Influence of start-up conditions on CO₂ recovery

Toluene mineralization to CO₂ varied as a function of inlet feed concentration which corresponds to the residual substrate concentration exposure at start up. Toluene concentrations at start-up could have a significant influence on the microbial consortium's community structure, activity and acclimatization as concentrations were generally quite higher for a number of days than the eventual steady state values. This hypothesis was investigated by monitoring the impact on toluene mineralization to CO₂ on changing the feed concentrations in a step wise manner from low to high at start-up and vice-versa at 40 °C and -10 cm_{H₂O} (Figure 5-8). Influence on the removal rates is discussed in Chapter 6.

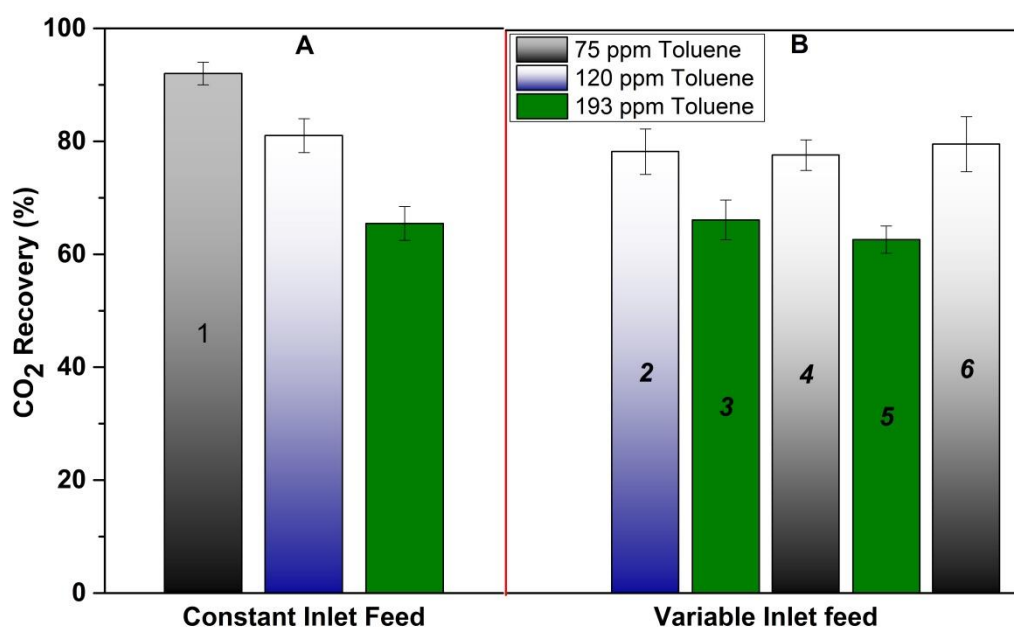


Figure 5-8 : Comparison of inlet substrate concentration at constant feed (A) vs variable feed (B) to evaluate lower start-up conditions and its implications on mineralized CO₂ fractions. Experiments were operated at 40 °C and -10 cm_{H₂O}. Values represents mean with uncertainties at 95% confidence interval during steady state over a multi-day period from replicate runs (Constant inlet feeds). Error bars in the multiple feed experiment represents within run variations in steady state at 95 % confidence interval.

The implications of start-up substrate concentration and transient feed conditions on CO₂ recovery was investigated over 200 days. In part (B), the influence of lower start-up feed concentration was investigated to compare with the three range of constant inlet feed concentration studied throughout this project (Figure 5-8,A). In part B, after the experiment at the inlet feed of 75 (1), the feed concentration was increased in a step wise manner to 120 ppm (2) and 193 ppm (3) respectively. On increasing the feed concentration from low to high no significant change in the CO₂ recovery pattern was found compared to the separate experiments where the feed concentration was constant for the entire length of the experiment (Figure 5-8,A). So for phase (4) the impact of changing the feed concentration from higher feed to lower feed was investigated. From the inlet feed of 193 ppm (3) the feed concentration was changed back to 75 ppm (4) and this cycle was repeated through phase (5) and (6). There was no impact on the CO₂ recovery at inlet feed of 193 ppm similar to phase (3). However the CO₂ recovery at an inlet feed of 75 ppm over the two cycles was 78 ± 1.5 % compared to 90 % observed at start-up (1). So exposure to higher feed concentration had an impact on the carbon-endpoints. The influence of exposure to a higher feed concentration was further investigated at 20 °C and -10 cm_{H₂O} (Figure 5-9). For monitoring this an experiment running at a feed concentration of 193 ppm toluene (20 °C) was switched to a lower feed concentration of 75 ppm and compared to operations at similar conditions with constant feed concentration (75 ppm) throughout (Figure 5-9,A). A similar pattern of decrease in CO₂ recovery of 63 % was observed upon exposure to higher feeds at start-up as opposed to 76 % at lower feed concentrations throughout. So exposure to higher concentration can be attributed to incur irreversible changes to metabolic response of the process culture which was different at the initial acclimated response at the same concentration.

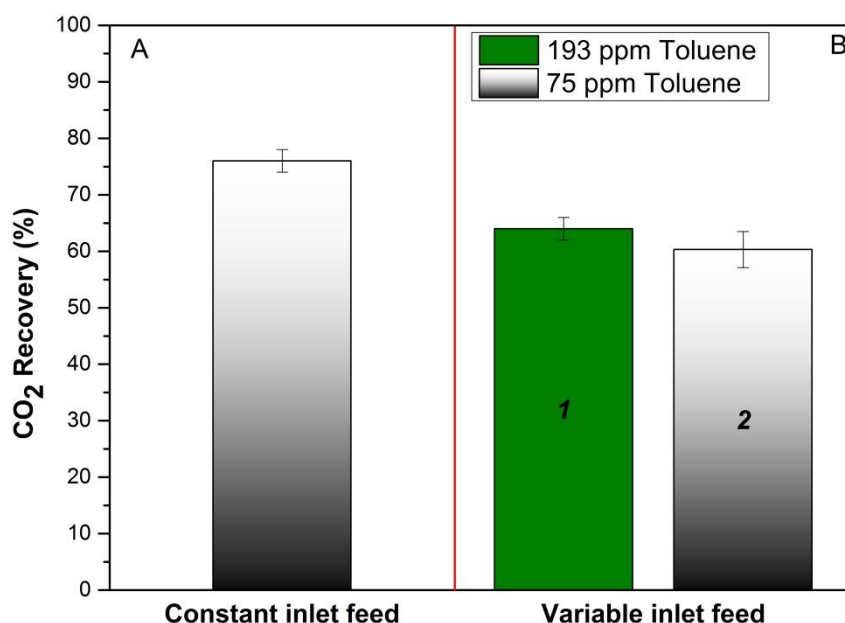


Figure 5-9: Start-up condition comparison for experiments operated at 20 °C and 10 cm_{H₂O}. Values represents mean with uncertainties at 95% confidence interval during steady state over a multi-day period from replicate runs.

5.6 Non-mineralized fractions

Non-mineralized fractions were monitored for the entire biofilter run by tracking the difference between the degraded toluene and the net CO₂ recovered. They were quantified at the end of each biofilter runs in the solid and liquid phases as non-mineralized carbon fractions (NmC) accumulated over the course of the experiment. The non-mineralized biomass yield coefficient (Y_{NC}), is defined as the carbon amount produced per unit toluene degraded on a carbon basis (g NmC/ g toluene C). The significant interaction between the environmental parameters which impacted the mineralized fractions discussed previously also holds true for the non-mineralized fractions as well. Therefore the focus of this section is on understanding the underlying push for the microbes to direct degradation products towards non-mineralized carbon fractions as a function of environmental parameters. The yield

coefficient quantified from the degraded toluene fractions in the solid and liquid phases ranged from $Y_{NC} = 0.08-0.65$. The non-mineralized fraction is postulated to include extra polymeric substances (EPS), soluble microbial products (SMP) in the absence of any active growth without nutrient addition, (nitrogen source in particular). These impacts of environmental parameters raise an important question of whether these resulted because of a shift in metabolic pathways or community structure.

5.6.1 Influence of environmental parameters on the non-mineralized yield coefficient (Y_{NC})

Microbes regulate the allocation of resources towards various processes involving growth and maintenance in response to the environmental conditions pertaining to nutrient availability, stress and other changing parameters (Schimel et al., 2007). Few biofiltration studies delving into performance optimization have evaluated the biomass yield coefficients for various VOCs. The available studies were done over a wide range of environmental conditions and involved addition of supplemental nutrients to the system (Table 5-3). This invariably made the growth of active biomass inevitable.

Table 5-3: The biomass yield on toluene reported by various biofilter studies.

Pollutant	Biomass yield (g Biomass/g Pollutant)	References
Toluene	0.708	(Shareefdeen and Baltzis, 1994)
Toluene	0.60	(Song and Kinney, 2000)
Toluene	0.34	(Gallastegui et al., 2011a)
Toluene	0.08-0.65*	Current study
Toluene	0.83	(García-Peña et al., 2005)
Toluene	0.81	(Dorado et al., 2012)

* Assumed no active biomass, only non-mineralized fraction

In the biofilm matrix, biomass can be roughly fragmented into various fractions encompassing active biomass, inert biomass, extra polymeric substances (EPS) and soluble microbial products (SMP) (Lapidou and Rittmann, 2002). The active biomass fraction is regulated by the growth rates and cell yield whilst inert biomass is

accumulated through endogenous decay and cell death in addition to maintenance requirements. Comparing the cumulative biomass yields in the present study to the literature values will help in putting the estimated biomass yield coefficients in context (Table 5-3). Active biomass growth was not expected for the current nutrient limited system and the non-mineralized carbon fraction can be attributed to EPS, SMP and internal storage polymers. Hence the range of non-mineralized yield was in general lower compared to values reported earlier. Thus the quantified carbon fractions in this study can be assumed to be comprised of non-mineralized yield (Y_{NC}).

For studies with nutrient supplements, there is a push for the process culture to form new active biomass along with polymeric substances to form a biofilm matrix. For biofiltration of toluene, Dorado et al. (2012) reported a biomass yield coefficient of 0.809 g biomass /g toluene. The biofilter was operated at a temperature of 23 ± 2 °C at different pollutant concentrations ranging from 400 ± 30 ppm_v at start-up, to 1000 ± 150 ppm_v over the steady state period. Earlier, Song and Kinney (2000) assumed a generic biomass formula and observed an average yield coefficient of 0.36 g biomass C/g toluene C from the total biomass yield. A much lower biomass yield coefficient of 0.34 g biomass/ g toluene was reported for a biofilters operated at 23 ± 0.2 °C at varying inlet loads from 21-89 gC.m⁻³.h⁻¹ (Gallastegui et al., 2011a). These results imply that the diversion of the carbon and energy sources towards specific anabolic and catabolic processes was most likely influenced by the environmental conditions.

Flow of carbon from the substrate are either diverted towards energy generation or biomass synthesis (Yu et al., 2001). Grove et al. (2009) suggested a favourable range of yield coefficients of 0.17 – 0.43 g biomass / g carbon for most substrates. High biomass yields causes clogging of the bed which leads to practical problems such as increased pressure drop and decline in biofilter performance. Hence the current results compare well with the literature values with the assumption of no active biomass growth without any supplemental nutrient addition. So the range of non-mineralized yield coefficients obtained at each set of combinations ranging from 0.08-0.65 g NmC/g toluene C can be attributed to various non-growth associated carbon end-points of toluene degradation.

In addition, biomass yield is also an important parameter for model development (Xiao and VanBriesen, 2006, Bordel et al., 2008). Often for modelling purposes the yield parameter is determined cumulatively without an accurate quantification of the active biomass and non-growth fractions. The process of energy allocation for both cellular biosynthesis and maintenance happens simultaneously and both the process can happen at different rates (Russell and Cook, 1995). An assumption of a generic biomass formula for quantifying the non-growth carbon fractions could lead to gross overestimation or underestimation of the carbon in the biomass yields. Biomass composition varies for different species and is dependent on environmental conditions (Xiao and VanBriesen, 2006). Moreover, the non-growth associated products are not differentiated where carbon content could significantly change in EPS, SMP etc. as a function of biofilm age and the nature of substrate. Thus calculating a yield on a generic formula could lead to significant difference in the biomass yields estimation on a carbon basis. Therefore the non-mineralized yield results in this study can be interpreted and adequately linked to the metabolic response as a function of environmental parameters. This opens up possibilities of gaining better insights into the plausible mechanism regulating these diversions towards the specific carbon-endpoints.

5.6.2 Physiological implications of non-mineralized fraction production

Maintenance metabolism assumes significance over active growth in a biofilters which is nutrient limited (Grove et al., 2009). However maintenance requirements are necessary at all times in addition to active biomass production which occurs during growth from energy derived from substrate utilization (Cherry and Thompson, 1997). Changing environmental conditions can significantly impact maintenance requirements which can increase under stress conditions. Maintenance requirements are relatively lower under high specific growth rate favouring biomass growth and metabolite production (Pirt, 1982). Several studies have reported lower biomass yields at higher temperatures attributing it to increased cellular maintenance requirements with temperature (Cox et al., 2001, Cho et al., 2007, Luvsanjamba et al., 2007). Nasrin et al.

(2011) reported that lower matric potential also impairs biomass yield and can initiate a change in microbial community structure. So these stress conditions may affect the metabolic pathways by either a reduction in the fraction of the active community or impaired activity itself at specific set of conditions. Simultaneously, there can be a shift in community structure with changes in environmental parameters (Cabrol et al., 2012, Bhaskaran et al., 2008, Wallenstein and Hall, 2012, Kong et al., 2013). Observed yields (Y_{NC}) for the non-mineralized fraction can be linked to these stress related diversion of resources regulating microbial metabolism.

For both growth and maintenance, the bioenergetics in the cells is mediated through the catabolic and anabolic reactions which happen separately. But they are intricately coupled with the total energy expenditure which is partitioned into biomass and maintenance functions (Russell and Cook, 1995). However cells are not capable of utilizing all the energy for cellular functions. Xiao and VanBriesen (2006) estimated a 60% average energy capture efficiency. The rest of the energy is dissipated into the system as heat. But this energy capture efficiency is not constant and is subject to change with different substrates, strains and environmental conditions. (Von Stockar et al., 2006) suggested that for low growth systems, only a small amount of biomass is formed per substrate consumed as opposed to a high growth system where biomass formed per substrate consumed would be high. Zafar et al. (2014) correlated the variance in maintenance energy expenditure to changing specific growth rates and yields cumulatively comprising of biomass and PHB production.

Thus the empirical results observed for the variance in non-mineralized biomass yields can also be interpreted through the energy dependent kinetics. At a certain set of combinations, more precisely at lower matric potential, higher substrate concentrations or higher temperature, the additional stress can increase the maintenance requirements. Without any driving force for biomass growth in the absence of nitrogen, resource allocation is most likely diverted towards metabolic pathways for production of storage polymers. So the variance in non-mineralized yield observed can be possibly attributed to the influence and interactions of environmental parameters which made it imperative for the microbial community to adapt. These can involve a

shift in community structure with the pre dominance of a single community or co-existence of a diverse active community degrading toluene. Further metagenomics work is required to conclusively determine if there is a change in the active community fractions with changing conditions.

5.7.2 Non-mineralized fraction production rate

As discussed previously, degraded toluene and the concomitant CO₂ production was continuously monitored which helped in evaluating the non-mineralized fractions accumulation in the solid and the liquid phases. It was further used to quantify the production rate of the non-mineralized fractions as a function of environmental parameters (Figure 5-10). Analysing the production rate for each set of conditions will help to deduce if it was being produced at a fixed rate, independent of the environment parameters. It can be hypothesized that if the non-mineralized production was happening at a fixed rate CO₂ recovery will have to increase with improved degradation. However if the non-mineralized production rate varies it will imply the influence of environmental parameters on the diversion of substrate utilization products to its eventual fate in the system.

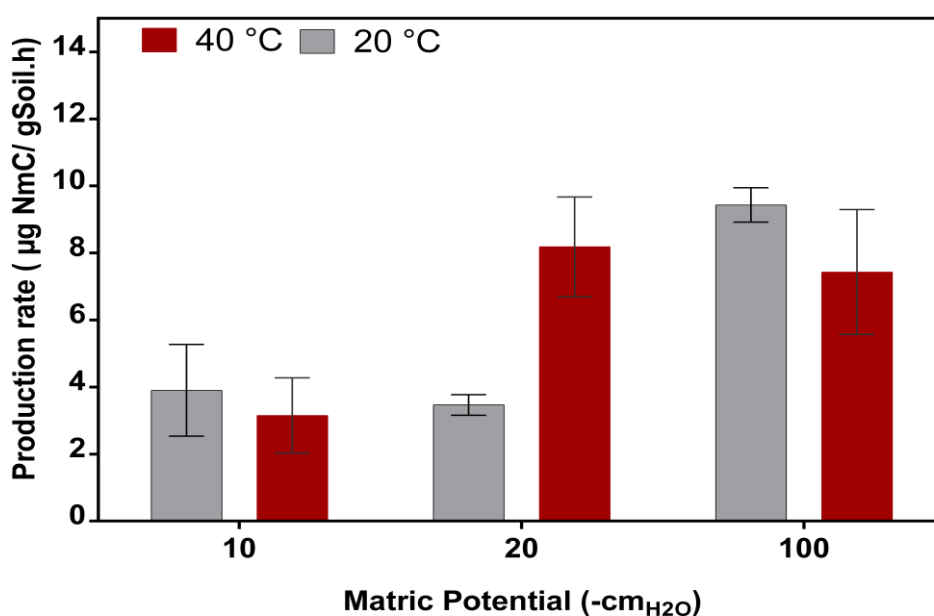


Figure 5-10: Non-mineralized fraction (NmC) production rate as a function of temperature and matric potential at an inlet feed of 120 ppm toluene.

The non-mineralized production rate varied with changing environmental parameters. Although the absolute values obtained cannot be compared directly as it is dependent on the elimination capacities which also varied. The EC was in general 2-fold higher at 40 °C than observed at 20 °C, impact on EC is discussed in detail in Chapter 7.

One hypothesis is if the active culture remained same metabolic response to transient conditions can influence the product ratios. It is also possible that cells have a constant physiological maintenance requirement at a particular set of environmental condition. However the overall bioenergetic requirements are cumulatively defined by the dynamics of the whole community along with other non-degraders. Secondly, at certain conditions like lower matric potential, if there were reduction in the fraction of active community as a function of environmental parameters maintenance requirements would also change along with the non-mineralized production rate.

Furthermore, of all the combinations of environmental parameters, only operations at matric potential of $-10 \text{ cm}_{\text{H}_2\text{O}}$ and an inlet feed of 193 ppm toluene resulted in a yield fraction which was not significantly different ($p\text{-value} < 0.05$) across the three temperatures investigated (Figure 5-1). For the set of conditions presented in Figure 5-11, the non-mineralized production rate again varied with a higher rate observed at 40 °C. However the similar yield coefficients observed for all the temperature was different from the carbon recovery results obtained at any other set of conditions. This similarity in the non-mineralized fractions indicates towards a similar metabolic pathway under the conditions. Although it could also happen from the survival of one dominant group of community capable of degrading toluene at this set of conditions, in particular higher substrate feed. This may have resulted during the start-up phase with the exposure of the community to a high residual toluene concentration at 193 ppm toluene. Exposure to certain concentration of toluene can be toxic to some community while an adapted community may survive (Delhomenie et al., 2005). So only the activity of the community was influenced by the temperature whilst the

metabolic response remained the same. Thus the observed variance in the non-mineralized production rate and the yield coefficients can be attributed to have been simultaneously impacted by the operating parameters. This implies that the non-mineralized production rate may not be fixed but is parameter driven. However conclusive evidence can be drawn only if the functionalities of the active group within the communities are traced to their metabolic response.

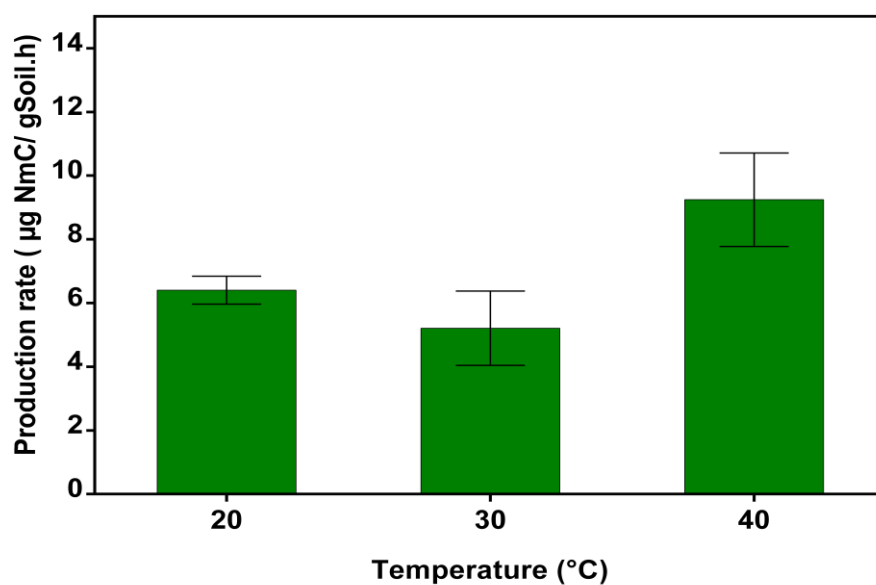


Figure 5-11: Non-mineralized production rate as a function of temperature operated at a matric potential of $-10 \text{ cm}_{\text{H}_2\text{O}}$ and inlet feed of 193 ppm toluene.

5.8 Conclusions

CO_2 recovery at various levels of the three critical environmental parameters of temperature, matric potential and substrate concentrations was investigated. Tracking the mineralization pattern over multiple parameters provided valuable insights of the interactions between them pertaining to the eventual fate of the degraded toluene in the system. Quantifying the mineralized fraction was a helpful tool in garnering qualitative knowledge on the changes in metabolic pathways happening at the macroscopic level within the community as a function of environmental parameters.

Studies on the start-up conditions showed the implications of exposure to high substrate concentrations that caused irreversible changes to the metabolic response of the community. Mineralization was lower upon exposure to high concentration intermittently and switching back to a lower concentration as opposed to a continuous exposure at the lower concentration from start-up. This response was not seen on exposure from low to high concentrations.

Chapter 6

EFFECT OF ENVIRONMENTAL PARAMETERS ON BIOFILTER PERFORMANCE

6.1 Introduction

Stringent environmental regulations for carbon emissions have compelled various industries and other anthropogenic sources to reduce and/or abate their carbonaceous pollutants for its detrimental impact on health and environment. In the past decade biofiltration has emerged as a viable solution to ameliorate low concentrations of VOCs as opposed to other conventional methods (Kennes, 2012). Biofiltration has been applied successfully to degrade a variety of VOC's like toluene (Sun et al., 2013), benzene (Aly Hassan and Sorial, 2010), α -pinene (Jin et al., 2007), formaldehyde (Maldonado-Diaz and Arriaga, 2015), xylene (Gallastegui et al., 2011b), octane (Grove et al., 2009) and BTEX compounds simultaneously (García-Peña et al., 2008a, Prenafeta-Boldú et al., 2012) . Elimination capacity (*EC*) is routinely used to quantify the degrading capacity of a biofilter. Various studies have investigated the influence of critical environmental parameters like temperature, matric potential and substrate concentration on *EC* (Gallastegui et al., 2011a, Lebrero et al., 2012, Rene et al., 2015, Picone et al., 2013, Wang et al., 2012). However limited knowledge exists on the interaction of these parameters at different levels and its impact on biofilter performance. So the focus of this chapter is to investigate the interactions between temperature, matric potential and substrate concentration and their impact on the biofilters performance.

6.2 Significance of temperature in biofiltration

For a biological system temperature is a vital environmental parameter influencing the reaction kinetics and plays a pivotal role in establishing the micro-flora. Optimal temperature facilitates the growth and survival of microorganisms which consequently regulates reaction rates during oxidation of pollutants. Pollutant degradation generally increases with temperature until a certain point within the optimum range (Acuña et al., 1999). Temperatures on either side of the optimal range have varied consequences impacting the biofiltration process.

6.2.1 Effect of temperature on biodegradation kinetics

Temperature has a dynamic effect on the biodegradation process affecting the microconsortia, metabolism and mass transfer. Usually a higher temperature increases the enzymatic reactions and cell growth doubles every 10 °C within a certain optimum range. This results in higher cellular activities for thermophiles than mesophiles (Cho et al., 2007). The degradation of pollutants in a biofilter is mostly accomplished by mesophilic organisms at ambient temperatures (15-40 °C) (Delhoménie and Heitz, 2005). This is the common range of operation for most biofilter studies. However this has constrained extending its applicability for high temperature industrial waste gases from pulp, paper, food and chemical manufacturing (Cho et al., 2007). One way, albeit an expensive one, is to cool these gases to 40 °C (Cox et al., 2001). However thermophilic biofilters offers a more viable solution for implementing industrial scale biofilters at large. Although it also brings in other constraints like changing moisture content of the bed owing to evaporation and the effect on Henry's constant of hydrophobic compounds in particular which inhibits biodegradation of the pollutants.

However thermophilic biotreatment of waste gases have been the applied successfully. High removal efficiency (up to 95%) was achieved for H₂S containing malodourous gas at 60 °C from thermophilic microorganisms sourced from compost (Ryu et al., 2009). High loads of BTEX compounds were treated achieving higher removal rates under thermophilic conditions (50 °C) than mesophilic reactors (Mohammad et al., 2007). On the contrary a few studies have reported a decline in biofilter performance

when switching from mesophilic to thermophilic conditions owing to cell death at high temperatures (Lu et al., 1999, Yoon and Park, 2002). But this decline could be due to lack of aptly adapted species to high temperature after long term proliferation in the mesophilic range.

Although biofiltration has been applied over a wide range of temperature it can significantly influence the microbial diversity (Cabrol and Malhautier, 2011). Temperature effect on community structure can be substantiated from the findings of Kong et al. (2013) where metabolic characteristics evolved over the time course in both the mesophilic (20-25 °C) and thermophilic(55 °C) operations. In another study evaluating the community structure over different operational temperature range, there was fungal dominance in the mesophilic reactor and bacterial proliferation in the thermophilic reactor (Mohammad et al., 2007). Temperature impacted both the *EC* and spore formation by *Fusarium solani* degrading n-pentane (Vergara-Fernández et al., 2012). Wang et al. (2012) found enrichment of thermophilic bacteria *Brevibacillus sp.* and *Anoxybacillus sp.* in the thermophilic biofilter at 55 °C whilst mesophilic bacteria such as *Delftia sp.* and *Strenotopomonous sp.* in the biofilter at ambient temperature (20-30 °C) over long term operations. This suggests a significant influence of the nature and length of exposure of temperature on the community structure. Evolution of an adapted and tolerant community could be a pivotal step in regulating biofilter performance.

6.3 Role of water in biofiltration

Water is an important precursor for microbial growth and effective biodegradation of organic compounds in engineered systems (Devinny et al., 1999). Optimal water content for operating biofilters ranges from 40-60 % on a wet basis (Bohn and Bohn, 1999). Low water content can reduce microbial activity and cause bed desiccation where as too much water leads to mass transfer limitations and bed compaction (Delhoménie and Heitz, 2005).

Typically physico-chemical characteristics regulate the water holding capacities of various bed materials. So the optimal water content varies for different bed media. However for microorganism, it is the water availability which influences microbial activity. Water availability can be quantified by water potential (ψ). It describes the energy status of water associated with the bed material comprising of several components of which osmotic potential and matric potential affects microbial activity (Papendick and Campbell, 1981). Osmotic potential is defined by the solutes in water while matric potential is due to the adsorption and capillary action of the solid phase. Matric potential is the dominant component in unsaturated porous media like non-saline soil.

6.3.1 Effect of water content on biofilter performance

In spite of the importance of water for microbial degradation, less attention has been paid to establish a coherent link between performance and water content. Many studies have reported loss in biofilter performance efficacy due to drying of support media over the operational period. Beuger and Gostomski (2009) illustrated the importance of water content with a compost biofilters treating toluene resulting in a 50% decrease in elimination capacity over a matric potential of $-20 \text{ cm}_{\text{H}_2\text{O}}$ to $-100 \text{ cm}_{\text{H}_2\text{O}}$. Similar results were reported by Cabeza et al. (2013) using compost degrading α -pinene. Manzoni et al. (2011) attributed decreased microbial activity in dry soil to diffusional constraints of solutes as opposed to biological limitations on the soil microbial communities. Toluene degradation rates were found to decrease with experiments done on unsaturated soils microcosms at water-filled porosity (WFP) ranging from 6-30% (Picone et al., 2013). Sakuma et al. (2009) demonstrated improved toluene degradation of 1.2-1.7 times on a biofilter fitted with lower irrigation system. This showed the effect of bed drying on microbial activity. Recently Danaee et al. (2014) explored the feasibility of using water super adsorbents in biofilters resulting in better performance which could decrease the need for frequent irrigation and sustain biofilter performance longer without being affected by bed drying. Higher water content can also be detrimental to degradation of hydrophobic VOC's. Bagherpour et al. (2005) investigated the effect of irrigation and packing water content on the

performance of a biofilter treating alpha-pinene. They attributed impaired performance to irrigation as pore blocking caused higher pressure drop and mass transfer resistance as a result of an increased water thickness layer.

Although recent advances have enabled elucidation of water stress responses of microorganisms in regards to gene expression and community structure, there exists a shortage of insight on the mechanism of metabolic pathways in engineered systems (Dechesne et al., 2008, Gülez et al., 2012, Coronado et al., 2014). Johnson et al. (2011) stressed the need to elucidate different stress responses observed in more comparable scenarios in low water conditions in soil. Hence, little is known about how microbial physiological response and adaptation to water stress in biofilters would influence degradation of volatile organic compounds.

6.4 Biofilter performance evaluation

Pollutant concentrations at the inlet and outlet were tracked for the time course of the reactor. Concomitant CO₂ production was also monitored simultaneously as described in chapter 4. Terminologies used to express the performance evaluation of the reactors are illustrated below. Elimination capacity, EC (g.m⁻³.h⁻¹) is the measure of the degradation of the pollutant per unit bed volume of the biofilter over a period of time.

$$EC = (C_i - C_o) \frac{Q}{V} \quad 6-1$$

Where,

C_i = Inlet concentration (g.m⁻³)

C_o = Outlet concentration (g.m⁻³)

Q = flow rate (m³.h⁻¹)

V = reactor bed volume (m³).

The CO₂ production rate is the net CO₂ production resulting from the pollutant degradation. It was corrected for the endogenous CO₂ production of the soil bed for each set of environmental conditions of temperature and matric potential.

$$pCO_2 = (tCO_2 - rCO_2) \frac{Q}{V} \quad 6-2$$

Where,

pCO_2 = Net CO₂ Production rate (g m⁻³ h⁻¹)

tCO_2 = Total CO₂ produced (g.m⁻³)

rCO_2 = Concentration of endogenous CO₂ of the soil bed (g.m⁻³)

6.5 Results and Discussion

6.5.1 Biofilter performance monitoring over the time course

The interaction between the environmental parameters and biofilter performance was studied simultaneously for the same set of conditions discussed previously in Chapter 5. The biofilters performance was determined by online monitoring of the net change in the pollutant concentration between the inlet and outlet. CO₂ production was concurrently tracked during biofilter operation. The residual concentration evolved over the time course of the biofilter runs as a function of environmental parameters. So the subsequent residual concentration for the time course of the experiment was a measure of performance and /or substrate concentration exposure for the microbes degrading the pollutant source. Corresponding volumetric removal rates termed as the elimination capacity (*EC*) (g.m⁻³.h⁻¹) were evaluated from the net differences in the inlet and outlet concentrations tracked throughout the experimental run.

Subsequent sections in this chapter will discuss the *EC* as influenced by different levels of the three critical environmental parameters of temperature, tension and substrate concentration. Any correlations between biofilter performance and the fate of degraded carbon into mineralized and non-mineralized fractions will also be explored. A typical time course graph for a biofilter run at two different set of conditions (Figure 6-1) illustrates the evolution and tracking of the system components for the length of the biofilter experiments.

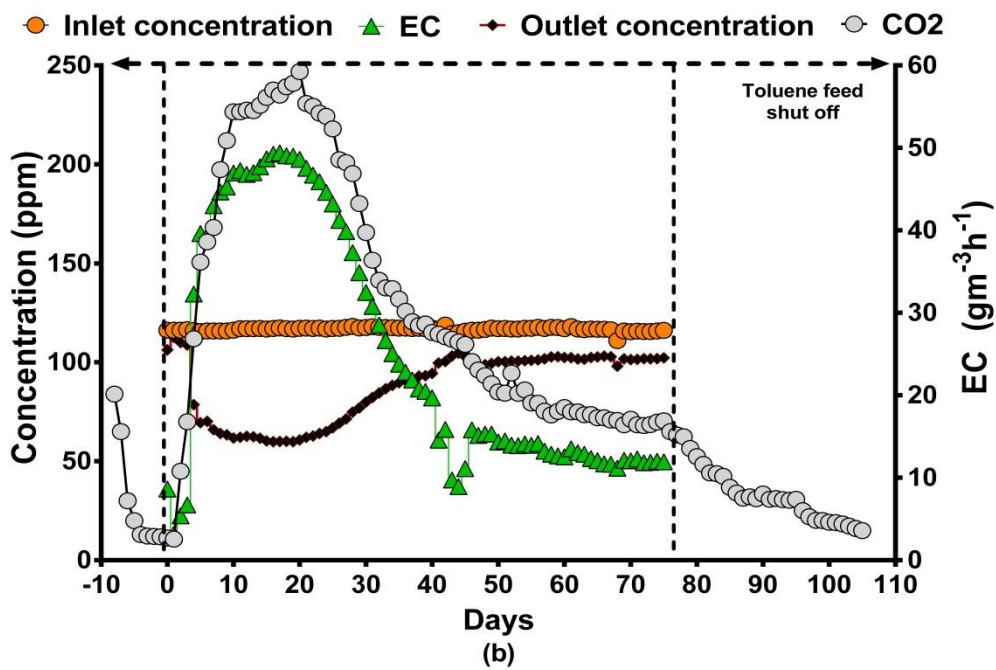
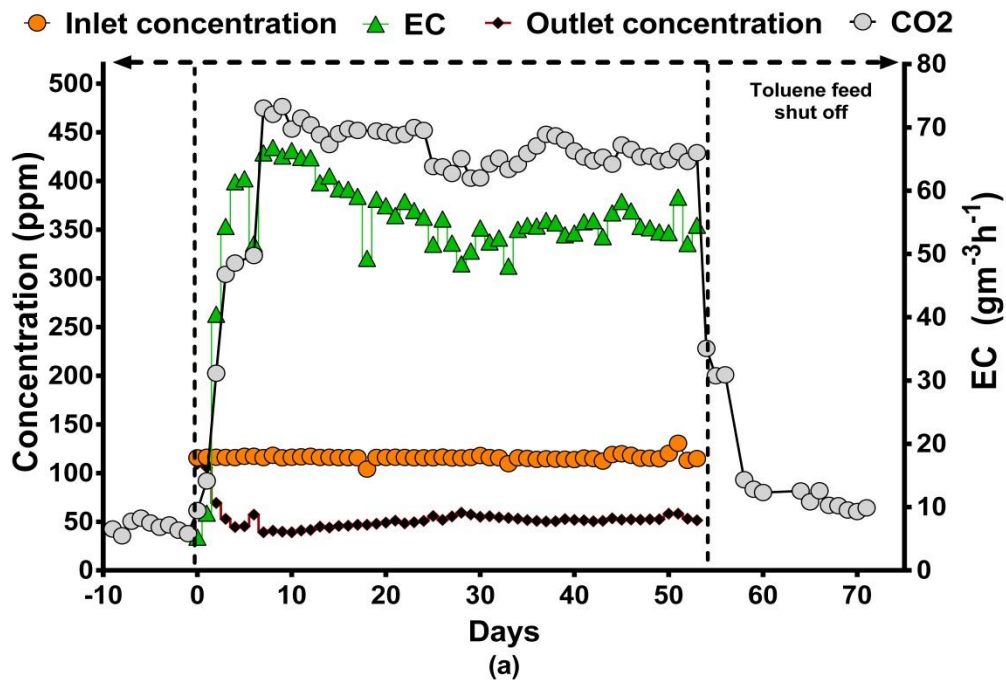


Figure 6-1: A typical time course for biofilters at an inlet feed concentration of 120 ppm. Biofilters operated at (a) 40 °C and -10 cm_{H2O}. (b) 20 °C and -20 cm_{H2O}.

Over the operational period, the outlet concentration of the biofilters varied under different temperatures resulting in different removal rates. Lower outlet concentration was an indication of higher degradation rates which was found at 40 °C in particular. Biofilters operating at 40 °C (Figure 6-1a) had a rapid start-up phase synonymous with initial acclimatization of the process culture. It reached EC_{max} values of around $62 \pm 4 \text{ g.m}^{-3}.\text{h}^{-1}$ and subsequently settled to a stable degradation rate for the length of the operation. The steady state EC was around $55 \pm 2.5 \text{ g.m}^{-3}.\text{h}^{-1}$. It reached steady state around day 12 and remained stable throughout the length of operation. This higher removal rates were correlated with higher CO_2 production which stayed above 400 ppm throughout the operation.

From Figure 6-1 (b) it can be seen that the biofilter rapidly acclimatized in the start-up phase and reached an EC_{max} of $48 \text{ g.m}^{-3}.\text{h}^{-1}$ by day 20. After the peak performance, EC declined until day 44. Thereafter the performance was stable for around 30 days with a steady state EC of $13 \pm 2.5 \text{ g.m}^{-3}.\text{h}^{-1}$. CO_2 production also tracked the EC for the whole period. However in contrast to the biofilter at 10 $\text{cm}_{\text{H}_2\text{O}}$ (Figure 6-1 a) CO_2 production was much lower, ranging around 70 ppm for the steady state period.

These parameters were tracked for the entire period of operation at various combinations of the investigated environmental parameters. Elimination capacity in general, correlated with the CO_2 production for the entire experiment. This is an indication of the impact of these environmental parameters on biodegradation kinetics as CO_2 production tracked EC implying degradation. The impact of these environmental parameters and their interactions at various levels eventually influencing the biofilters performance are discussed in detail in the subsequent sections in this chapter.

6.5.2 Interaction between temperature and substrate concentration impacting *EC*

Temperature and substrate concentration parameter were investigated at different levels to understand its influence on the elimination capacity (*EC*) of the biofilters. Experiments were investigated by a mixed level 3x3 factorial design to track their influence on the elimination capacities (Table 6-1). Each biofilter was operated at every combination of temperature and inlet feed concentration while keeping the matric potential constant at $-10 \text{ cm}_{\text{H}_2\text{O}}$.

Table 6-1: Experimental factors and different levels of investigations.

Factors	Levels			Units
Temperature	20	30	40	°C
Inlet toluene concentration	75	20	193	ppm

In the differential biofilter, only the residual toluene exiting the reactor varied depending on the variance in metabolic activity for each set of operating conditions. This was used to quantify the performance of the biofilters at each set of conditions. Performance for all the parameters were statistically analysed to interpret the impact on biofilters efficacy. A two-way ANOVA (Table 6-2) suggested significant interactions between temperature and substrate concentration affecting the biofilters performance, $F(4,122) = 40$, $p < 0.05$.

Table 6-2: Summary of analysis of variance (ANOVA) results for the temperature and substrate concentrations.

	DF	Sum of Squares	Mean Square	F Value	P Value
Temperature	2	25238	12619	1431	<2e-16 ***
Inlet toluene concentration	2	447	223	25	8.55e-10 ***
Interaction	4	1412	353	40.04	<2e-16 ***
Residual	111	978	9		

Signif. codes: 0 '***' 0.001 '**' 0.01 '*' 0.05 '.' 0.1 ' ' 1

Variation in residual toluene concentrations tracked from the outlet measurements determined the *EC* as a function of temperature and inlet substrate concentration for biofilters operated at a matric potential of $-10 \text{ cm}_{\text{H}_2\text{O}}$ (Figure 6-2).

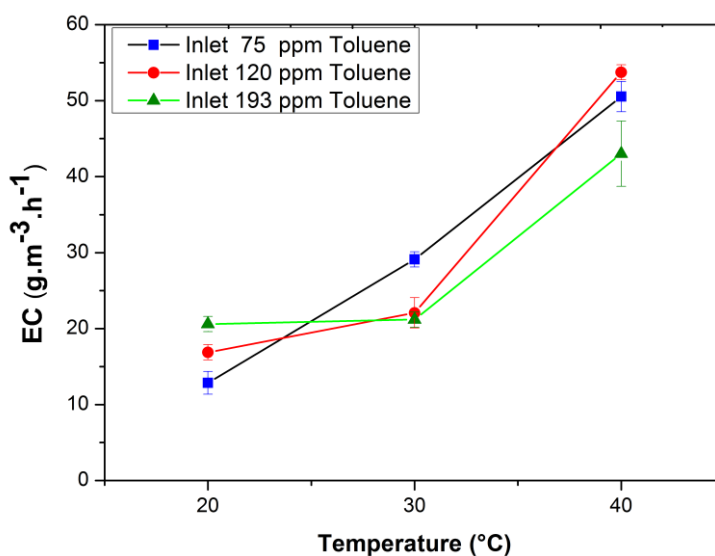


Figure 6-2 : Interaction plot of substrate concentration and temperature impacting (*EC*) at $-10 \text{ cm}_{\text{H}_2\text{O}}$. Values represents mean with uncertainties at 95% confidence interval during steady state over a multi-day period from replicate runs.

The *EC* varied for the biofilters operated at different levels of the environmental parameters. From Figure 6-2, a general trend of improved performance (*EC*) at the highest temperature (40 °C) was found irrespective of the feed concentrations. The *EC* was also simultaneously impacted at different feed levels for each set of conditions. However there was no clear trend for any of the feed concentrations at each temperature. These kinds of performance patterns over various sets of conditions suggest an intrinsic relationship of substrate concentrations and temperatures. There was significant interaction found between temperature and substrate concentrations using a 2-way analysis of variance (ANOVA) test (Table 6-2). Therefore the simple main effects for each level of temperature against subsequent levels of substrate concentrations were further analysed.

At the lowest feed concentration of 75 ppm toluene, *EC* increased with temperature. As the feed concentrations were increased, a general decline in performance was noticed, more pronounced at the highest feed of 193 ppm toluene. *EC* values over the three feed concentrations at 20 °C and 30 °C varied by 10-20 % respectively. However *EC* decreased by ~30% at 40°C from 120 ppm to 193 ppm without significantly affecting performance at 20-30°C.

In general each temperature had a distinct pattern of *EC* over the range of feed concentrations studied. At 20 °C, the *EC* did not change significantly over the inlet feed range (120-193 ppm). Operation at 30 °C followed a similar course at different feed concentrations. However, 30 °C had a higher *EC* at the lowest feed concentration than what was obtained at 20 °C. Biofilters at 40°C degraded more than the other temperatures with an average *EC* of $53 \pm 3 \text{ g.m}^{-3}.\text{h}^{-1}$ at 75 - 120 ppm inlet feed concentrations. Thereafter, *EC* decreased to $42 \pm 2 \text{ g.m}^{-3}.\text{h}^{-1}$ at the higher feed concentration of 193 ppm toluene. Further post hoc analysis was done to test the significance of these differences among parameters Figure 6-3. Each pairwise combination was accessed by Tukey's HSD test at a significance level of (0.05). From Tukey's HSD test, most of the differences in *EC* over various combinations of environmental parameters were found to be significant ($p\text{-value}<0.05$). The only *EC*'s

that were not significantly different ($p\text{-value}<0.05$) were between 20 °C and 30 °C at feed concentrations of 120-193 ppm toluene. It suggests a clear dependence on multiple environmental parameters which had a combined influence on the biofilters performance. These results illustrated the importance of temperature and substrate concentration in being pivotal to achieving optimum performance.

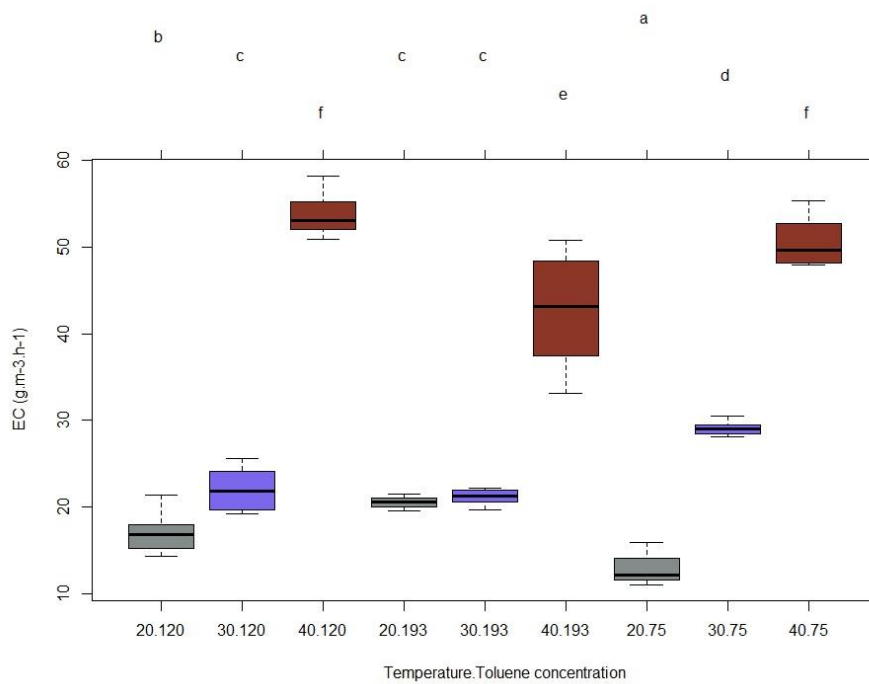


Figure 6-3 : Tukey HSD plot illustrating the pair wise comparisons between combinations of various levels of temperature: toluene concentration (X axis) in regards to the impact on EC. The groups sharing same letters are not significantly different from each other ($p\text{-value}<0.05$).

6.5.3 Effect of temperature and substrate concentration on biofilter performance

Figure 6-2 shows the intricate relationship between the key operational parameters like temperature and substrate concentration influencing biofilter performance. Both these critical parameters impacts biofilter performance independently by impacting varied aspects of the process. Most biological systems shows improved activity up to a certain optimal temperature beyond which activity starts to decrease (Cho et al., 2007). Simultaneously inlet pollutant concentrations and load also significantly affect the biofiltration treatment process (Xi et al., 2006, Muñoz et al., 2009). Removal rates declined upon increasing the feed concentrations above a critical level (Moussavi et al., 2009). Temperature and substrate concentration also influence the microbial community structure depending on the set of operating conditions (Borin et al., 2006, Cabrol and Malhautier, 2011, Kong et al., 2013). Thus it is important to understand the interactions between different levels of these parameters which play a role in influencing the efficacy of biofilter systems.

Biofilters operated at different temperatures showed variance in metabolic activity as a function of temperature. Higher *EC* was observed at 40 °C for the range of substrate feed concentrations investigated. These results compares well to the general trends reported in the literature (Vergara-Fernández et al., 2007a, Zamir et al., 2014, Montes et al., 2014). However, higher temperatures can decrease the solubility for a range of pollutants which hampers mass transfer to the biofilm. Henry's coefficient for toluene significantly increases from 0.21 at 20 °C to 0.79 at 50 °C (Mohammad et al., 2007). But since the highest *EC* was observed at 40 °C, it can be attributed to a temperature induced enhancement in metabolic activity compared to 20 °C.

So the implications of temperature and substrate concentration are vital for the performance of the system. Since there were significant interactions between both temperature and substrate concentration, a transition effect of microbial response was expected at some level of parameters. At the lowest feed concentration, performance

increased with temperature. But since performance did not vary significantly over the 20-30 °C temperature range at feed concentration of 120-193 ppm, it suggests an increasing influence of substrate concentration. However the *EC* increased at 40 °C and 120 ppm feed concentration, providing the metabolic push but there was a significant drop in *EC* by ~30% at 193 ppm. It is possible that the increasing substrate concentration nullified the improved metabolic activity at higher temperature. This can be attributed to the combined effect of both the parameters interacting in pushing the performance in opposite directions. Both microbial diversity and biochemical reactions could have caused it, as they can be influenced by the interaction between the environmental parameters. However microbial community structure needs to be further explored to relate performance to species functionalities in the micro-ecosystem within the biofilter. Hence prior knowledge on the interactions between the critical parameters at play in biofiltration simultaneously at any given point in time could help in stable and efficient operations in the long term.

6.5.4 Correlation of *EC* with CO₂ recovery

From these results, it was apparent that *EC* was significantly influenced by the variation in temperature and substrate feed concentrations. *EC* is a measure of the metabolic activity of the microbes degrading the pollutants. Thus these *EC* results were compared to the concurrent CO₂ recovery to investigate linkages between the two dependent variables as a function of environmental parameters.

From Figure 6-4 at the lowest feed concentrations (75 ppm), both *EC* and CO₂ recovery increased linearly with temperature. Operations at 40 °C resulted in highest mineralization to CO₂ of 90 ± 2 % along with an *EC* of 50.4 ± 2 g·m⁻³·h⁻¹ followed by 30 °C and 20 °C. Linear regression fit showed a good correlation with a $R^2 = 0.96$. As the feed concentration was increased to 120 ppm toluene, the fraction mineralized to CO₂ was lower at all temperatures along with the *EC*.

For the higher feed concentrations at 193 ppm toluene, CO₂ recovery was not significantly different for all the three temperatures (p -value < 0.05) with a decrease in

EC observed for 40 °C and 30 °C from the lower feed values. Consequently linear regression fit did not show any correlation ($r^2 = 0.005$). But *EC* at 40 °C was approximately 2-fold higher than 20-30 °C which were not significantly different ($p\text{-value} < 0.05$). These results may further support the hypothesis previously discussed in regards to mineralization. At the highest feed concentration there could be one dominant degrading community which resulted in a constant mineralization fraction owing to the metabolic pathways. The increase in *EC* with increase in temperature could be attributed to elevated activity of the same active community while the pathways remained the same. Alternately it is possible that the metabolic response became independent of the substrate concentration beyond a critical level.

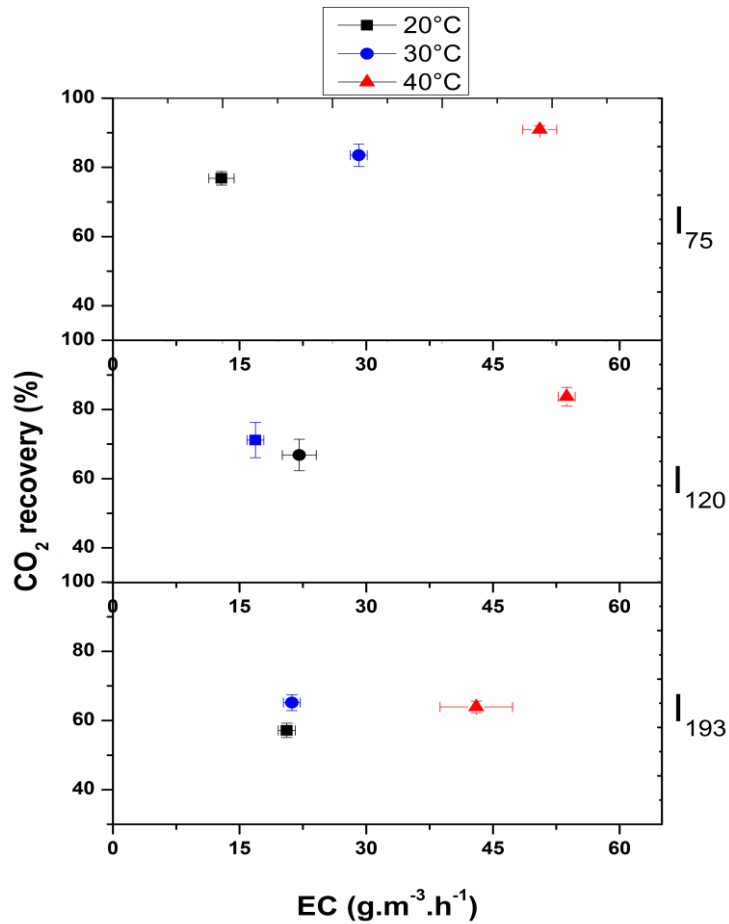


Figure 6-4 : Correlation of *EC* with CO₂ recovery for each set of operating conditions. I₇₅, I₁₂₀ and I₁₉₃ denote the inlet feed concentration. Values represent the means with uncertainties at 95% confidence interval during steady state over a multi-day period from replicate runs.

6.5.5 Impact of residual concentration on *EC*

For the differential biofilters, residual toluene concentration varied which is a measure of performance at specific inlet feed conditions to evaluate the volumetric removal rates (*EC*) for each set of conditions. This is a key variable in a differential biofilter as this concentration is consistent through the pore space of the soil bed. The results demonstrated that CO₂ recovery was influenced by the substrate concentration of the microbes which was found to be temperature driven. Thus *EC*s of the biofilters were further compared to the resulting residual concentrations at the operated temperatures and inlet feed concentrations. From the plots in Figure 6-5, residual concentration above 100 ppm seems detrimental to microbial activity. The *EC* at 30 °C gradually declined while at 20 °C it plateaued over higher concentrations. At 40 °C the performance was greater for each feed concentration resulting in the lowest range of residual toluene concentration. However higher performance at 40 °C was hampered by an approximately ~30% drop in *EC* at a residual concentration of 140 ± 4 ppm toluene. As previously illustrated in Chapter 5, there was an influence of higher residual substrate concentration to lower CO₂ recovery along with the operating temperature. Thus residual concentration can be attributed to play a role in influencing both metabolic and community dynamics impacting *EC* and CO₂ recovery albeit in varied proportions simultaneously.

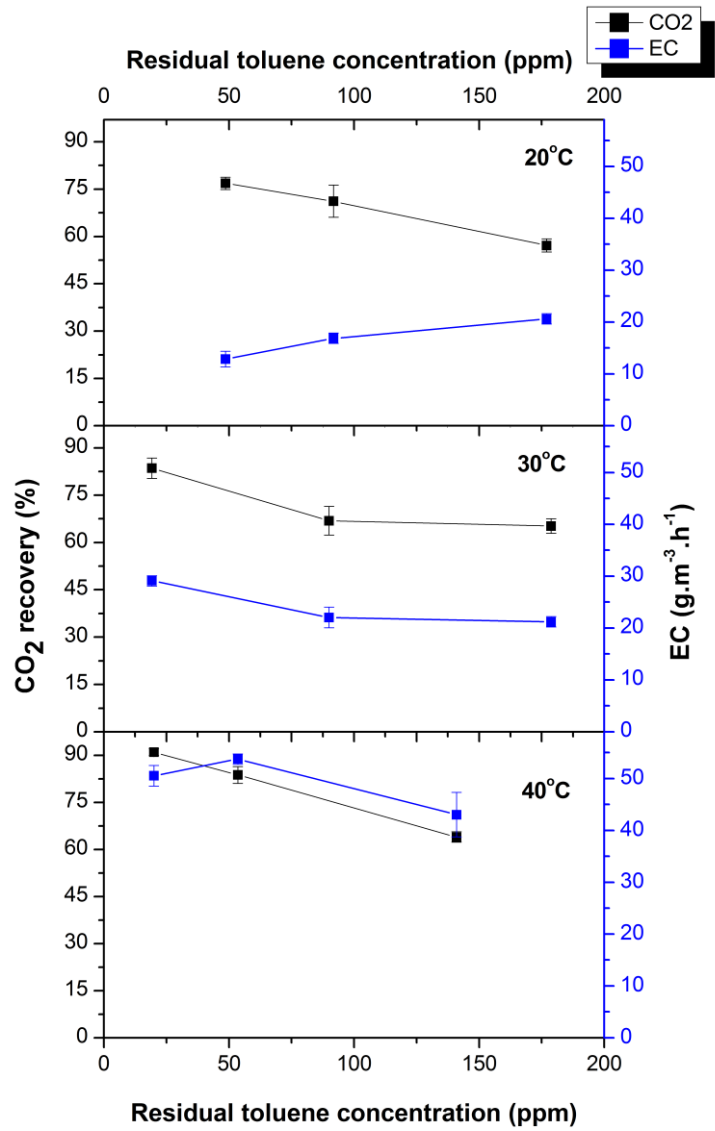


Figure 6-5 : Effect of residual outlet concentration on *EC* and *CO₂* recovery as a function of operating temperature. Values represent the mean with uncertainties at 95% confidence interval during steady state over a multi-day period from replicate runs.

6.6 Impact of start-up conditions on biofilter performance

6.6.1 Effect of lower start-up substrate concentration

Lower EC_s were observed at biofilter runs with higher start-up feed exposures ranging from 120-193 ppm feed concentrations (Figure 6-4). In this differential biofilters, at time zero, the microbes were exposed to the inlet feed concentration. This concentration decreased during the start-up period as the microbes in the soil adapted to degrade toluene. The magnitude of the residual concentrations was a function of various operating parameters resulting in varied residual concentrations (Figure 6-1). However start-up conditions did not influence the subsequent CO_2 recovery on going from lower to higher feed concentrations. It was reproducible irrespective of the start-up feed concentration exposure across different temperatures (Chapter 5). Its corresponding effect on EC is discussed in the next section. It raises an interesting question of the possible effect of the start-up conditions on performance. Thus it was hypothesized that start-up conditions may have an impact on performance.

For the investigations over the course of this study operations at 40 °C and 75 ppm toluene feed at -10 cm_{H_2O} resulted in the lowest residual concentrations of around 20 ± 2 ppm of all the runs (Figure 6-4). This set of condition had the lowest start-up residual feed concentrations as well which eventually resulted in the highest fraction of CO_2 recovery ($90 \pm 2\%$) along with a higher EC ($50.4 \pm 2 \text{ g.m}^{-3}.\text{h}^{-1}$). This was postulated to the activity of a well-acclimatized culture generating energy for cellular functionalities in maintenance mode without any supplemental nutrient addition. From a practical point of view, a higher mineralization and EC would be an optimal operational requirement. So the investigation was further extended to test the hypothesis on performance by increasing the inlet feed concentrations at this set of conditions in a step wise manner (Figure 6-6).

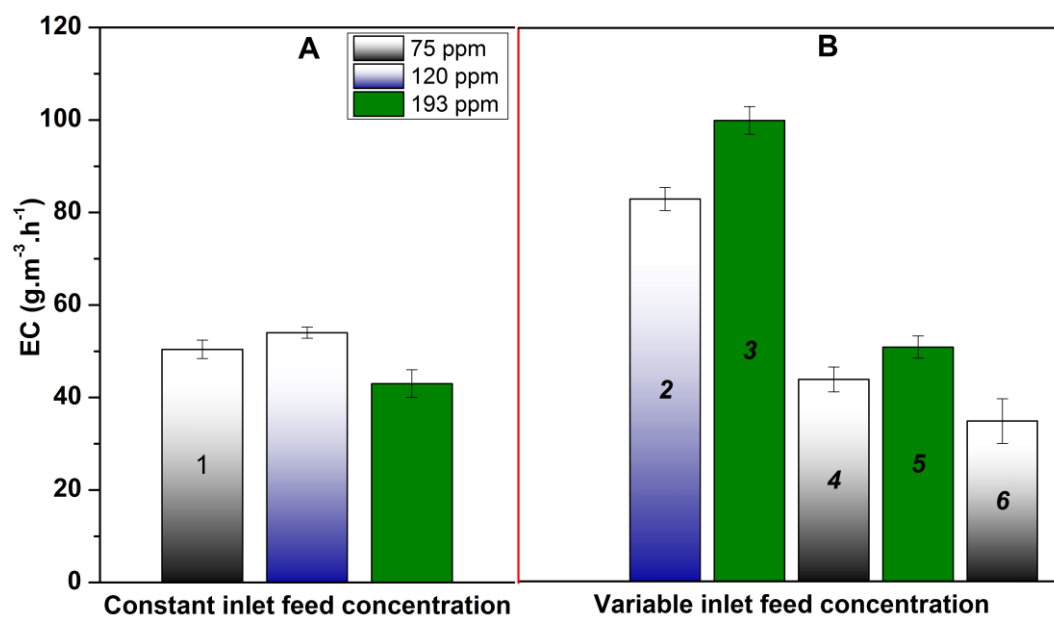


Figure 6-6: Experiments were studied at 40 °C at a matric potential of -10 cm_{H₂O} by varying the feed concentration in a step-wise manner from 75 → 120 → 193 → 75 → 193 → 75. (B) compared to constant feed at 120 and 193 ppm (A).

Variable inlet feed experiment starting from a low start-up concentration of 75 ppm resulted in significantly higher performance increasing linearly with higher feed concentration (Figure 6-6.B). Upon increasing the feed to 120 ppm (2) inlet feed, an EC of $80 \pm 2 \text{ g.m}^{-3}.\text{h}^{-1}$ was observed as opposed to $55 \pm 2.5 \text{ g.m}^{-3}.\text{h}^{-1}$ when started at 120 ppm. Increasing to 193 (3) ppm inlet feed improved the performance significantly, reaching an EC_{max} of $127 \pm 2 \text{ g.m}^{-3}.\text{h}^{-1}$ and then had a slow downward progression to $100 \pm 3 \text{ g.m}^{-3}.\text{h}^{-1}$.

This run was further subjected to a step-wise sequential change in the feed condition from 75 ppm (4) to the higher feed concentrations of 193 ppm (5) with time and back to 75 ppm (6). During the operation at inlet feed of 193 ppm (5) toluene EC remained at $> 80 \text{ g.m}^{-3}.\text{h}^{-1}$ for close to 30 days of operation before further declining to reach a steady state EC of $50 \pm 3 \text{ g.m}^{-3}.\text{h}^{-1}$. After lowering the feed concentration again to 75 ppm (6) EC stabilized at $34 \pm 3 \text{ g.m}^{-3}.\text{h}^{-1}$. The biofilter with the constant feed

starting at 193 ppm only briefly reached an EC_{max} of $62 \pm 2 \text{ g}\cdot\text{m}^{-3}\cdot\text{h}^{-1}$ before reaching a steady state EC of $38 \pm 3 \text{ g}\cdot\text{m}^{-3}\cdot\text{h}^{-1}$. This significantly improved performance can be attributed to a possible favourable start-up conditions entailing in acclimatization of a very active degrading community. During this period, the necessary enzyme machinery is also induced due to the presence of a carbon source (García-Peña et al., 2005). This follows a period of adaption for primary degraders eventually contributing to the microbial diversity in the biofilter ecosystem (Cabrol and Malhautier, 2011). Higher diversity can contribute to performance through the evolution of a community which is fit to survive and stably function (Cabrol et al., 2012). This effect on performance of lower start-up substrate concentrations was further investigated at a lower matric potential of $-20 \text{ cm}_{\text{H}_2\text{O}}$ at $40 \text{ }^\circ\text{C}$ and increasing the inlet feed from 75 to 120 ppm toluene (Figure 6-7).

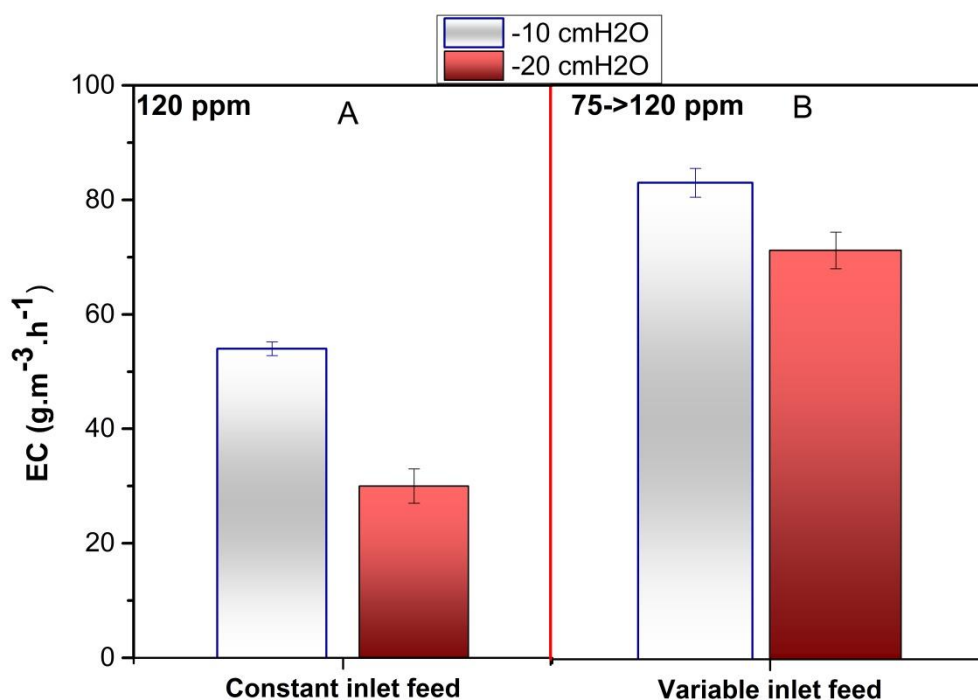


Figure 6-7 : Experiments were operated at $40 \text{ }^\circ\text{C}$ and an inlet feed of 120 ppm toluene and investigation was expanded across two matric potential of $-10 \text{ cm}_{\text{H}_2\text{O}}$ and $-20 \text{ cm}_{\text{H}_2\text{O}}$. For the multi feed start-up conditions feeds were started at 75 ppm and increased to 120 ppm in a step wise manner.

Exposure to a lower start-up substrate concentration had a similar effect of improved performance at lower matric potential as well. Performance increased two-fold for the biofilters upon exposure to lower inlet feed at start-up. Consequently it resulted in lower residual concentration for the process culture. Since in this differential biofilter microbial community is exposed to only the residual concentration irrespective of the inlet feeds. Further discussion on the influence of residual concentration from the perspective of time dependent exposure influence of toluene on the process culture regulating the performance is discussed in the next section.

Various removal rates for toluene have been reported in the literature under a plethora of operating conditions (Table 6-3). Better performances usually ranged from 50-90 $\text{g.m}^{-3}.\text{h}^{-1}$ with good removal efficiencies. In this study, change in just the start-up conditions significantly improved the *EC* by almost 2-fold which was comparable to *ECs* reported in the literature. This was achieved without any supplemental nutrient addition or inoculation of an adapted culture across different operating conditions. It further presses the importance of culture acclimatization/exposure to lower VOC concentrations to help establish a diverse and active microbial community. Contrary to the traditional norms of high concentration exposure to enrich a specialized culture, establishment of a diverse and greater fraction of a better adapted community to the substrate can probably withstand higher concentrations longer. This may be a more feasible option to achieve better performance without nutrient addition. But further metagenomics work is necessary to quantify the functionalities of the community and changes happening at the microscale. Nonetheless operations at conditions resulting in higher performance along with a good mineralization rate could help address critical practical problems like clogging and long term stability.

Table 6-3: *EC* for toluene reported at various operating conditions in the literature.

EC (g.m⁻³.h⁻¹)	Packing and Inoculum	Temperature (°C)	Reference
50	Perlite with <i>Paecilomyces lilacinus</i>	28	(Vigueras et al., 2008)
138	ABONLIR (commercial soil)	RT* (18-30)	(Gallastegui et al., 2013)
95	Compost	RT*	(Maestre et al., 2007)
80	Compost	RT*	(Estrada et al., 2013b)
97	Coir Pith without nutrient addition	Ambient (31±1)	(Krishnakumar et al., 2007)
90	Cattle bone Porcelite	RT*(21-24)	(Sakuma et al., 2009)
100	Garden soil	40 (controlled)	Present study

*RT: room temperature

6.7 Interaction of temperature and matric potential impacting *EC*

Water and temperature profoundly impact biofilter performance (Vergara-Fernández et al., 2012). Most of the studies on these parameters were done by keeping one parameter constant and by varying the second parameter to study the main effects (Mohammad et al., 2007, Sakuma et al., 2009, Gülez et al., 2010, Gallastegui et al., 2011b, Wang et al., 2012). The focus of this investigation was to investigate the presence of any interactions between these two parameters in impacting the *EC*. For this study the feed concentration (120 ppm) was kept constant and the temperatures and matric potentials were varied. Experiments were investigated by a mixed level 3 x 2 factorial design to track their influence on the *EC* (Figure 6-4).

Table 6-4: Experimental factors and different levels of investigation

Factors	Levels			Units
Temperature	20	-	40	°C
Matric potential	10	20	100	-cm _{H2O}

The biofilters were operated at various combinations of temperature and matric potentials and the *EC* was tracked for the time course of the experimental runs. A two-way ANOVA (Table 6-5) suggests significant interaction between temperature and matric potential, $F(2,104) = 127$, $p < 0.05$.

Table 6-5: Summary of analysis of variance (ANOVA) results for the temperature and matric potential.

	DF	Sum of Squares	Mean Square	F Value	P Value
Temperature	1	9557	9557	414	<2e-16 ***
Matric potential	2	3264	1632	71	<2e-16 ***
Interaction	2	5855	2928	127	<2e-16 ***
Residual	104	2399	23		

Signif. codes: 0 '***' 0.001 '**' 0.01 '*' 0.05 '.' 0.1 ' ' 1

Lower matric potentials resulted in lower elimination capacities independent of the operating temperatures. *EC* also increased at higher temperatures with 40 °C resulted in a much higher *EC*s for each level of matric potentials than the subsequent run at 20 °C. This variation in *EC* pattern at 20 °C and 40 °C at specific matric potentials can be attributed to the interaction effect between the two parameters. These were substantiated from the 2 -way ANOVA analysis (Table 6-5). As there was significant interaction between both the parameters, the simple main effects of the various operating conditions were investigated to elucidate the specific differences among the parameters (Figure 6-8). Matric potential and temperature effect on the *EC* of the biofilters was interpreted for each set of conditions to identify its combined impact on the performance. At the highest matric potential of $-10 \text{ cm}_{\text{H}_2\text{O}}$ the difference in performance between 40 °C and 20 °C was the highest; 40 °C resulted in more than two fold increase in *EC* than at 20 °C. An overall decrease in *EC* at lower matric potential was observed for both the temperatures. For operations at 20 °C, the *EC* was not impacted over the matric potential range studied. However the biofilter runs at 40 °C followed a different pattern with an *EC* of $54 \pm 1.2 \text{ g.m}^{-3}.\text{h}^{-1}$ at the matric potential of $-10 \text{ cm}_{\text{H}_2\text{O}}$ and then decreased by $\sim 50\text{-}70\%$ at $-20 \text{ cm}_{\text{H}_2\text{O}}$ and $-100 \text{ cm}_{\text{H}_2\text{O}}$.

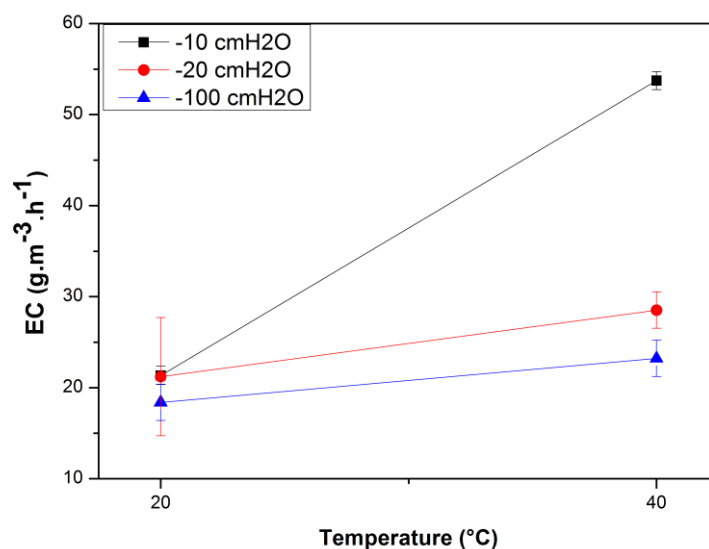


Figure 6-8 : Interaction plot of matric potential and temperature impacting EC at an inlet feed concentration of 120 ppm toluene. Values represents mean with uncertainties at 95% confidence interval during steady state over a multi-day period from replicate runs.

Since there was significant interaction between temperature and matric potential which was found through the 2-way analysis of variance (ANOVA) further post hoc analysis was done to analyse the differences between each level of the investigated environmental parameters. EC data was accessed through pairwise comparison of the means at each set of conditions through Tukey's HSD procedure at 95 % confidence interval (Figure 6-9).

From Tukey's HSD test most of the differences in EC over various combinations of temperature and matric potentials were found to be significant ($p\text{-value} < 0.05$). However EC s were not significantly different at ($p\text{-value} < 0.05$) between matric potentials of -10 cm_{H_2O} , -20 cm_{H_2O} and -100 cm_{H_2O} operated at $20\text{ }^\circ\text{C}$. Other sets of EC s which were not significantly different at ($p\text{-value} < 0.05$) were found between operations at $40\text{ }^\circ\text{C}$ and -100 cm_{H_2O} and $20\text{ }^\circ\text{C}$. So the lowest EC at $40\text{ }^\circ\text{C}$ found at the lowest potential (-100 cm_{H_2O}) was not significantly different from the EC s at $20\text{ }^\circ\text{C}$. Similar performance at these two temperatures is usually not expected unless there is

second parameter at play. It can be attributed to the dominant effect of matric potential lowering the performance at 40 °C where otherwise higher *EC*s were observed. Lower performance at 20 °C and -10 cm_{H2O} can be postulated to lower microbial activity associated with lower temperature, indicating an intricate relationship between temperature and matric potential in influencing biofilters performance.

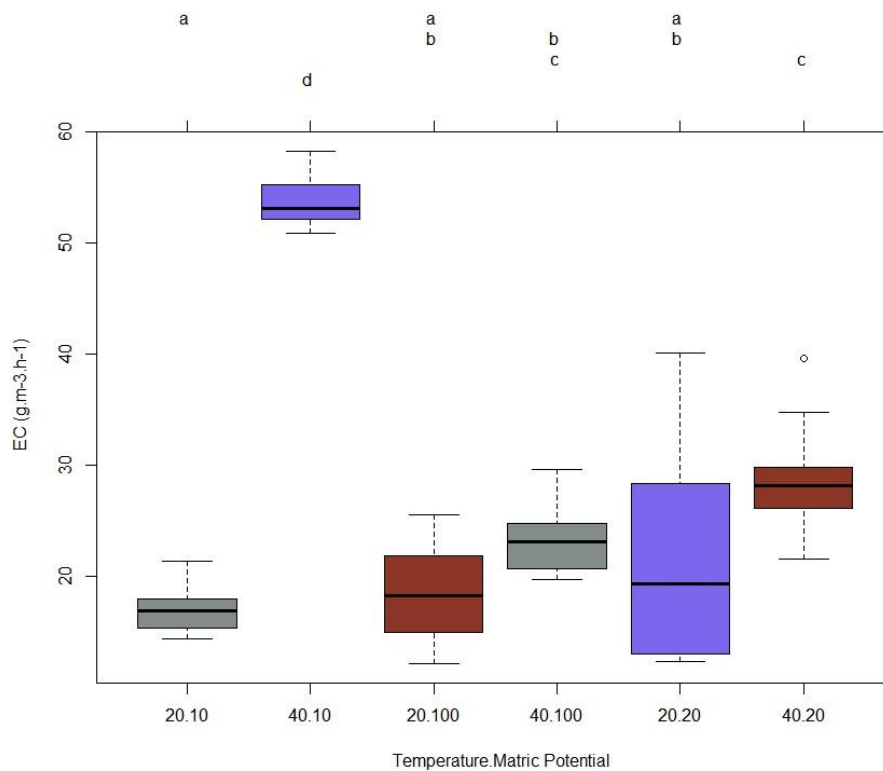


Figure 6-9: Tukey's HSD plot illustrating the pair wise comparisons between combinations of various levels of temperature : matric potential (X axis) corresponding to *EC*. Groups sharing the same letters indicated at the top of the graph are not significantly different (p value < 0.05).

6.7.1 Impact of temperature and matric potential on biofilter performance

Water is a critical component in microbial degradation in unsaturated media such as soil. It influences mass transfer in soil pores, through the biofilm and has potential implications for microbial physiology (Holden et al., 1997b, Or et al., 2007a, Manzoni et al., 2011). This implies that a decrease in matric potential can severely inhibit the degradation capacity of the biofilters. The substrate degradation rates were critically influenced by the matric potential as illustrated in the preceding section. However operations at each temperature played a significant role simultaneously for the range of investigated matric potentials in influencing the overall microbial response to pollutant degradation.

Overall the process culture can be argued to have thrived and acclimatized within the constraints of both temperature and matric potentials. As discussed previously, higher temperature improves metabolic activity while lower matric potential impairs the degradation capability of the microbes. Under a constant carbon source without any supplemental nutrient addition, cells can accomplish normal maintenance requirements unless there is a major stress from a dominant parameter to increase maintenance requirements. Operations at the highest matric potential of $-10 \text{ cm}_{\text{H}_2\text{O}}$ were not found to be major limiting factor for degradation whilst temperature pushed the performance higher. However, further investigations over different matric potentials would be needed. But stable and better degradation rates were achieved at $-10 \text{ cm}_{\text{H}_2\text{O}}$ correlated with higher CO_2 production to what was observed at lower matric potentials of $-20 \text{ cm}_{\text{H}_2\text{O}}$ and $-100 \text{ cm}_{\text{H}_2\text{O}}$. This is most likely due to relatively favourable conditions at $-10 \text{ cm}_{\text{H}_2\text{O}}$ for the microbes in degrading the carbon source while attaining maintenance requirements.

These results were in general agreement with previously reported trends in the literature. Beauger and Gostomski (2009) reported a 50% decrease in *EC* in changing the matric potential from $-20 \text{ cm}_{\text{H}_2\text{O}}$ to $-300 \text{ cm}_{\text{H}_2\text{O}}$. Poor abatement of p-xylene was found ($33 \pm 7 \%$) in the absence of water irrigation in spite of fungal proliferation

(Gallastegui et al., 2011b). Removal efficiencies improved to 100% on continued periodic irrigation. Sakuma et al. (2009) illustrated the importance of irrigation in biofilters with a 1.2-1.7 times higher toluene elimination in biofilters fitted with lower irrigation system as opposed to the control ones. Similar reduction in removal efficiency was reported by Cabeza et al. (2013) with a decrease in moisture content of the compost sourced from municipal wastes from 66 % to 51 % on a dry weight basis. So the water content has been illustrated to play a pivotal role in pollutant attenuation. The water content of the biofilters maintained at the controlled matric potentials for these investigations are presented in Figure 6-10.

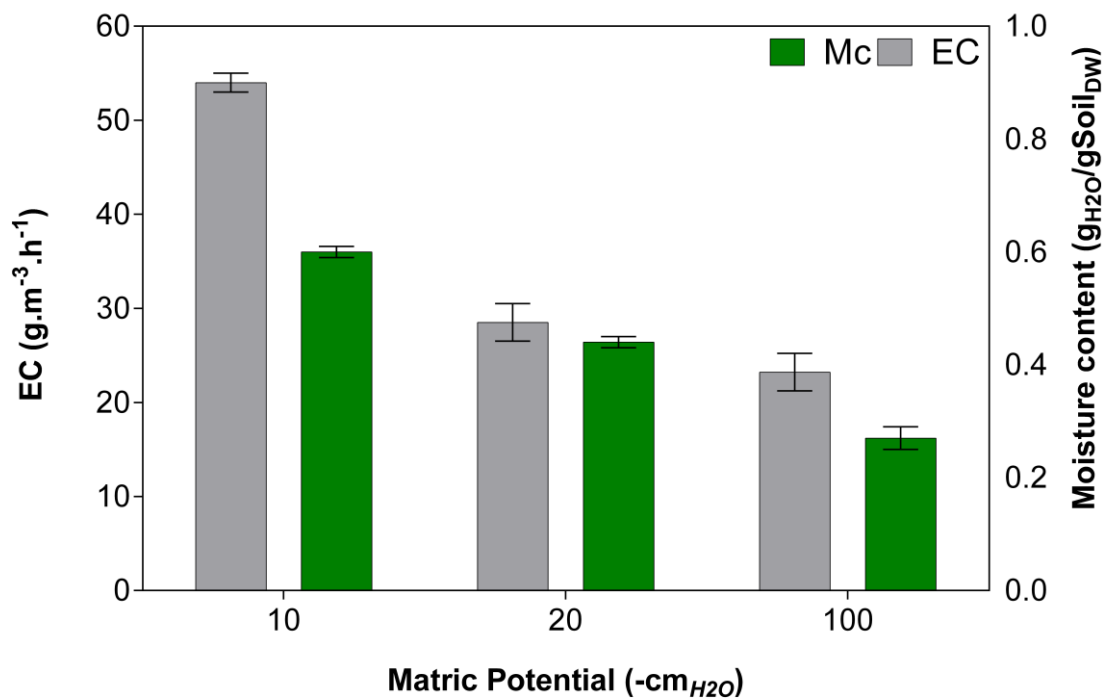


Figure 6-10: Relationship between water content and *EC* operated over various matric potentials at 40 °C. Moisture content is reported on a dry weight basis.

There was a clear dependency of biofilters performance on the water content depicted in Figure 6-10. Biofilters operated at -10 cm_{H2O} had a moisture content of 0.60 g_{H2O}/gSoil_{DW} on a dry weight basis. The soil is usually expected to be drier at lower matric potentials. The water content of the soil followed this trend. The biofilter at -20

$\text{cm}_{\text{H}_2\text{O}}$ had 0.44 $\text{g}_{\text{H}_2\text{O}}/\text{gSoil}_{\text{DW}}$ moisture content. The moisture content further decreased to 0.27 $\text{g}_{\text{H}_2\text{O}}/\text{gSoil}_{\text{DW}}$ for the biofilters operated at the higher matric potential of -100 $\text{cm}_{\text{H}_2\text{O}}$. However gravimetric water content does not always quantify the water available to the microbes in most cases but the conditions in general were drier with lower matric potential.

So the detrimental effects of lower matric potential on microbial degradation translates due to both physico-chemical and physiological effects imposed on the microbes. Drier conditions associated with higher matric potential limits the hydrated pathways in soil which hampers solute diffusivity (Or et al., 2007b). Lower water availability can impose stress on the cell membranes to prevent dehydration and maintain membrane integrity, thus increasing maintenance requirements. Microbes need to adapt to decrease in water potential through regulation of cellular turgor pressure to prevent dehydration by mobilizing osmolyte concentration (Van De Mortel and Halverson, 2004). Failure to do so will make the microbes susceptible to irreversible damage and possible cell lysis. Dechesne et al. (2008) attributed decreased surface colonization at lower matric potential to impaired microbial motility of *P. putida* KT2440. On the other side too much water is also detrimental to the degradation process as it affects the packing material. It can cause bed compaction and impact the sorption capacity of the packing (Dorado et al., 2010). These factors could cumulatively contribute to lower degradation rates with lower matric potentials. Thus matric potential and its associated kinetic and systemic impacts on the microbial community is one of the critical factors for biofilters performance.

6.7.3 Correlation of *EC* with CO_2 recovery at different matric potentials

The performance of the biofilters influenced by the interaction of temperature and matric potential illustrated the impact on microbial activity. Variation in *EC* suggests a possible change in metabolic response at the operated set of environmental parameters. This was further compared to the CO_2 recovery pattern evolved for the combination of environmental parameters (Figure 6-11).

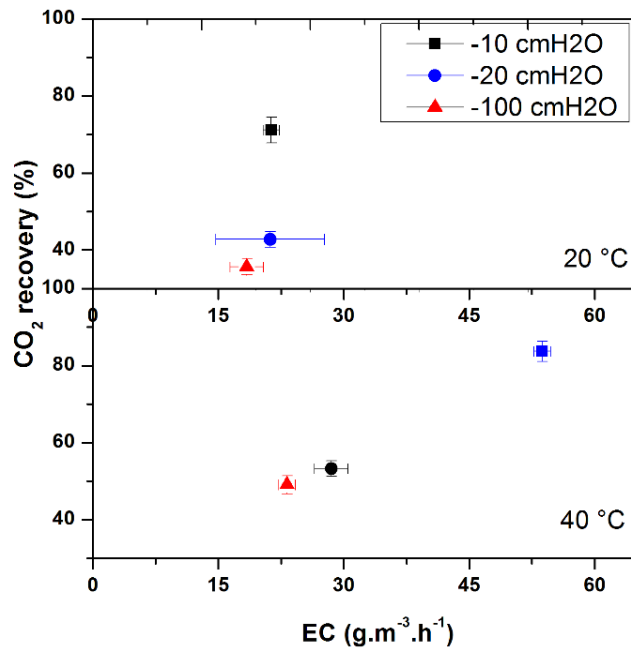


Figure 6-11 : Correlation of EC with CO_2 recovery for each set of operating conditions.

From the results presented in Figure 6-11, a non-linear relationship was found across the different matric potential operated at temperatures of 20 °C while CO_2 recovery correlated with EC at 40 °C. While the EC over -20 cm_{H_2O} to -100 cm_{H_2O} were not significantly different ($p\text{-value} < 0.05$) mineralization varied over this range. Similarly at 40 °C the EC dropped with decreasing matric potential, particularly from -20 cm_{H_2O} to -100 cm_{H_2O} where CO_2 recovery was not significantly different ($p\text{-value} < 0.05$). So the overall performance did not show a direct link with mineralization pattern although both the dependent variables were impacted by the interactions of the environmental parameters.

6.8 Conclusions

Biofilter performance was significantly influenced by the interactions between the environmental parameters. Investigations on temperature and substrate concentrations suggested dominance of temperature in regulating EC at lower feed concentrations. At 40 °C, the EC decreased at higher feed concentrations, while for operations at 20-30 °C the EC were not significantly different at higher concentrations. Similarly

temperature and matric potential also had a significant interaction between them. Although 40 °C in general resulted in 2-fold higher *EC* than at 20 °C, *EC* decreased with a decrease in matric potential from -10 cm_{H₂O} to -100 cm_{H₂O} for both the temperatures. The lowest *EC* at 40 °C at -100 cm_{H₂O} was not significantly different from the *ECs* observed at 20 °C. This suggests a transition in the influence of the temperature and matric potential at different levels of operations. However there was no correlation between *EC* and mineralization at the lowest temperature and highest inlet feeds even though both the dependent variable has been found to be independently impacting the variables. Further, results for the influence of start-up conditions showed markedly improved performance by 2-3 fold using lower feed start-up conditions as opposed to initial exposure to higher feeds. This knowledge could help in operations with improved efficacy and help avert problems related to clogging and stability.

Chapter 7

CARBON RECOVERY FROM A BIOFILTER WITH AN UNSATURATED *Pseudomonas putida* BIOFILM UNDER CONTROLLED ENVIRONMENTAL PARAMETERS

7.1 Introduction

Significant advances have been made to gain new insights into the biofilms in environmental remediation pertaining to community structure, stress response and gene expression (Kroukamp and Wolfaardt, 2009, Yang et al., 2010). Even so, to date, advanced biofilm research cannot be extrapolated to explain the dynamics of biofilm processes in engineered systems, particularly waste gas treatment. There is a need for investigation of biofilm in reactors systems with controlled parameters to compare results from studies done with suspended cultures and other microcosms. Biofilms found in waste gas treatment are exposed to a myriad of transient environmental conditions which regulates its structure and stability (Cabrol et al., 2012). Establishment of a biofilm offers distinctive advantages to the communities against environmental stressors (Singh et al., 2006a). Even though excessive biomass accumulation is detrimental to an effective biofilter operation, knowledge of its composition pertaining to microbial ecology and degradation products is limited. In particular, the current understanding of the mechanisms of synthesis and regulation of extracellular polysaccharides is yet to fully explain their structural intricacy and functional variability. Hence conclusive quantification of this components and its correlation to environmental parameters is warranted. The focus of this chapter was to test a pure culture (*Pseudomonas putida*) under the similar set of conditions investigated with soil and quantify the carbon end-points.

7.1.2 Biofilm matrix

Extracellular polymeric substances make up a major fraction of biofilms and play a very important part in biofilm structure, activity and performance (Sutherland, 2001). The EPS is composed of a mix of polysaccharides, proteins, nucleic acids and lipids in varying proportions (Flemming and Wingender, 2010). Biofilms as a dynamic system responds to environmental conditions physiologically which leads to variations in EPS composition (Schmitt et al., 1995). Biofilm composition is dependent on a variety of factors ranging from substrate type to environment parameters (Nielsen et al., 1997). Thus EPS has been related to the macro-scale characteristics of biofilms describing its microbial and structural properties (Ras et al., 2011)

Enumeration of the biofilm activity in terms of active and dead biomass could provide substantial insight in quantitating the EPS production, as a very low fraction of biofilm dry weight consists of active biomass (Arcangeli and Arvin, 1992, Tresse et al., 2003). Cell uses electrons from the electron donor substrate to provide the energy to build active biomass and also produce other associated substrate utilization products such as EPS and SMP (Laspidou and Rittmann, 2002). The carbon source has been documented to play a role in the physicochemical properties of EPS (Ye et al., 2011). However the nature and components of substrate utilization products reflects a fragmented view of the process, the general consensus emerging does not establish a universal theory allowing *a priori* estimation of the fate of degrading pollutants.

7.1.3 Relevance of biofilms in a biofilter

Biofilms are ubiquitous in nature, from engineered porous media in our everyday surroundings, to the microorganisms in landfills, to a biofilter treating industrial air emissions (Costerton et al., 1995). Biofilm formation is dependent upon a combination of factors encompassing hydrodynamic and biochemical variables (Characklis and Marshall, 1990). Microbes participating in biodegradation processes usually proliferate as a biofilm with bacterial colonies encased within an extensive extracellular polymeric matrix both in saturated and unsaturated environments (Costerton et al., 1995). Biofilm development and its characteristics are defined by the prevailing

environmental conditions which regulates the thriving micro-consortia (Characklis and Marshall, 1990). Despite significant advances in biofiltration process kinetics, some fundamental aspects concerning the biofilm process in these systems need to be studied. Particularly, the issue of an accurate carbon balance remains largely ignored.

Biofilms are often growth restricted (e.g. nutrient limitations) in soil and industrial process but possess the inherent ability to break down organic pollutants. Biofilm growth and metabolism are influenced by factors ranging from nutrient limitations, substrate surface loading, hydrodynamic conditions and the physiology of the proliferating microorganisms (Or et al., 2007b). The viability and resilience of biofilm communities in engineered reactors is also postulated to some bacterial species cell-to-cell signalling known as quorum sensing influencing functionality relating to pollutant attenuation (Shrout and Nerenberg, 2012). Linking the metabolic response to the degradation process as influenced by the environmental conditions could enhance the understanding related to functionalities in the biofilm matrix.

EPS helps to regulate the hydrodynamics in the biofilms and soil and demonstrates a profound effect on the soil structure, affecting microbial habitat and activity in the vadose zone (Or et al., 2007b). Often these physical constraints leads to diversion of substrates away from energy generation and biomass production to other metabolic pathways (e.g. storage polymers, EPS) (Roberson and Firestone, 1992). Soil bacterial aggregation and pooling of resources enables successful adaptation to hydrological variation and nutrient flux in unsaturated soils (Or et al., 2007a). However the nature and fate of carbon end-points in the system as influenced by microbial adaptation to transient conditions would allow a better understanding of the degradation process.

7.1.4 Co-existence of a heterogeneous community in a biofilter

The heterogeneous microbial population development on exposure to pollutants is one of the vital yet least investigated aspects of biodegradation in engineered systems. The microbial diversity in a biofilter throws up an interesting question of secondary populations growing on syntrophic interactions and playing a role in nutrient cycle through consumption of products from cell lysis, EPS matrix and the bed itself

(Cabrol and Malhautier, 2011). The functional population actually degrading the substrate of interest co-exists and can be outnumbered by a diverse micro-consortia (Møller et al., 1996, Song and Kinney, 2000, Pedersen et al., 1997). Various studies have used the 16S rDNA/RNA approach to study microbial diversity in waste gas treatment. However still there is a lot to know about the activity and functionality in a biofilter at the community level.

Overall heterogeneity in the system comprising of primary and secondary degraders does influence the degradation process and performance. Fungi feed on dead biomass and mobilize nutrients and are considered more resilient than bacteria to transient environmental conditions like low moisture and pH (Fermor and Wood, 1981, Kennes and Veiga, 2001). Protozoa predation is linked to carbon mineralization in systems with high biomass production and as a means to control biomass accumulation (Cox and Deshusses, 1999). In addition, these non-toluene degraders can increase alternative carbon sources for cryptic growth (Villaverde et al., 1997). Bhaskaran et al. (2008) illustrated the grazing of nematodes and rotifers in efficient control of pressure drop and nutrient recycling in a biofilter degrading toluene. These effects of community structure play a part in the metabolic response of the process culture which can influence the fate of carbon in the system.

7.1.5 Maintenance metabolism

In nutrient limited conditions, maintenance energy is a pivotal driving force which encompasses various non-growth associated requirements such as cell motility, osmoregulation and proof reading (van Bodegom, 2007). Apart from these physiological requirements other important functions which come under the domain of maintenance expenditure includes shifts in metabolic pathways, accumulation of biopolymers and energy spilling reactions (van Bodegom, 2007). The term maintenance coefficient is attributed as a pivotal parameter for microbial homeostasis in the absence of growth. Maintenance metabolism assumes significance over active growth in biofilters which are nutrient limited (Grove et al., 2009). Maintenance requirement is a parallel process in addition to the biomass yield which occurs during growth upon substrate utilization (Cherry and Thompson, 1997). Maintenance

requirements are subjected to the impact of changing environmental conditions and can increase under unfavourable conditions. Maintenance requirements are lower under high specific growth rate favouring biomass growth and metabolite production (Pirt, 1982). So investigations on a non-growth system over multitude of environmental parameters would help in tracking the implications of maintenance requirements in regulating the carbon-endpoints in the system.

7.2 Biofiltration with an unsaturated *Pseudomonas putida* biofilm

Experiments were set up with a biofilm of *Pseudomonas putida* isolated from the soil used in the biofilters as discussed previously in Chapter 3. The biofilters were operated at a matric potential of $-10 \text{ cm}_{\text{H}_2\text{O}}$ and $40 \text{ }^\circ\text{C}$ by varying the inlet toluene feed concentrations with no supplemental nutrient addition. Subsequently the fate of degraded carbon was tracked over the three phases and the biofilm was used for confirming carbon end-points accumulation as EPS and other associated products with specific lectin binding stains.

7.2.1 Gas phase carbon tracking

Carbon fractions in the gas phase were analysed as described previously in chapter 4. Correlation with the concomitant CO_2 production can be related to substrate utilization by an active biofilm (Bester et al., 2011). Figure 7-1 compares the CO_2 recovery fraction for the biofilm runs with the soil biofilters at the same matric potential and temperature as a function of residual toluene concentration.

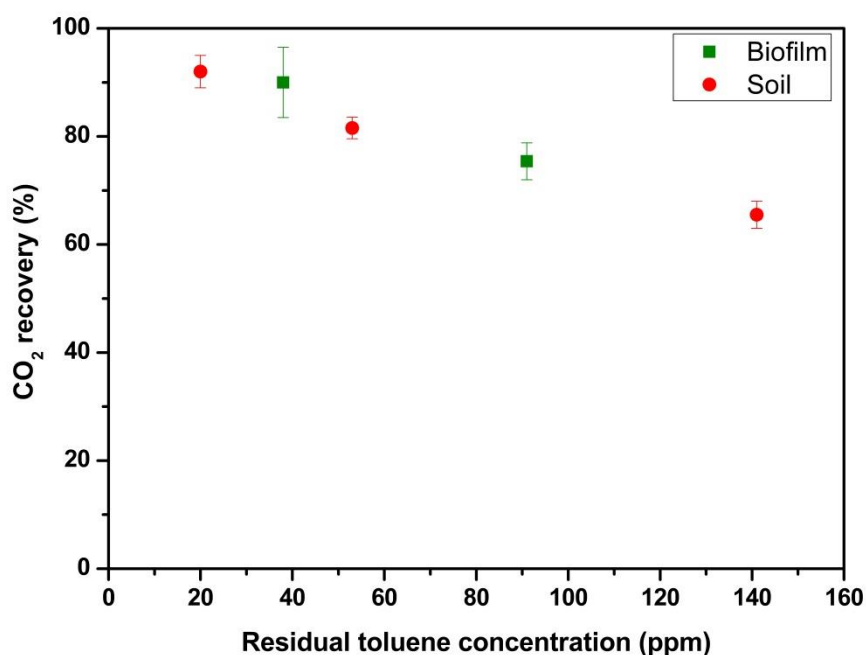


Figure 7-1 : CO₂ recovery for the biofilm and soil runs at -10 cm_{H₂O} and 40 °C as a function of residual toluene concentration.

The *Pseudomonas putida* biofilm resulted in a net CO₂ recovery of 90% and 75% respectively at inlet feeds of 75 ppm and 120 ppm toluene. These values compares well with the soil runs at similar set of conditions. This serves as a good validation for the soil studies in terms of the metabolic pathways influencing the carbon end-points. Some differences in mineralization pattern between the biofilm and soil may exist which can be attributed to the existence of a mixed community in the soil as opposed to the pure culture. However from these results *Pseudomonas putida* may be one of the dominant degrading communities at this set of conditions as evident from the comparable mineralized fractions.

Further, CO₂ recovery varied for both soil and biofilm operations at 40 °C and -10 cm_{H₂O} as a function of inlet feed concentrations with different residual toluene concentration (Figure 7-1). A general declining trend in CO₂ recovery with increasing residual toluene concentration was observed. The biofilm runs at the same inlet feed concentration of 120 ppm had a higher residual toluene concentration of 90 ppm

compared to the soil run which was at 53 ppm, which can be attributed to the heterogeneous nature of soil microbes. However the corresponding CO₂ recovery for the biofilm is within <5% of the soil runs. Although it raises vital questions regarding changes happening in the soil bed in terms of microbial structure and diversity which can regulate performance and degradation products. Hence further pure culture work is required to gain insights pertaining to the effect of substrate concentration on the microbial community along with metagenomic analysis of the pre and post run cultures thriving in the soil bed.

7.3 Microscopic observation of the biofilm samples

7.3.1 Confocal microscopy

Biofilm samples were qualitatively analysed through confocal laser scanning microscopy (CLSM) to identify carbon fractions in the biofilm. Samples were analysed by staining with wheat germ agglutinin (WGA-647) which differentially stains polysaccharides (Strathmann et al., 2002). Photograph of the biofilm established on the membrane and the subsequent confocal microscopy image of the sample is presented in Figure 7-2. It confirms the presence of polymeric substances in the biofilm as can be visualized from the micrographs with red fluorescence resulting from lectin binding to the polysaccharides, where the biofilm at $t = 0$ (Figure 7-2) shows no EPS. These images further corroborate the presumption of non-mineralized fractions accumulation in the solid phase as quantified from carbon balance results. In biofiltration, long-term accumulation of polymeric substances creating operational problems like clogging leading to increased pressure drops has been a long standing issue (Dorado et al., 2012). So carefully choosing the range of critical environmental parameters which would direct more degraded pollutant fractions towards mineralization could have a beneficial practical application.

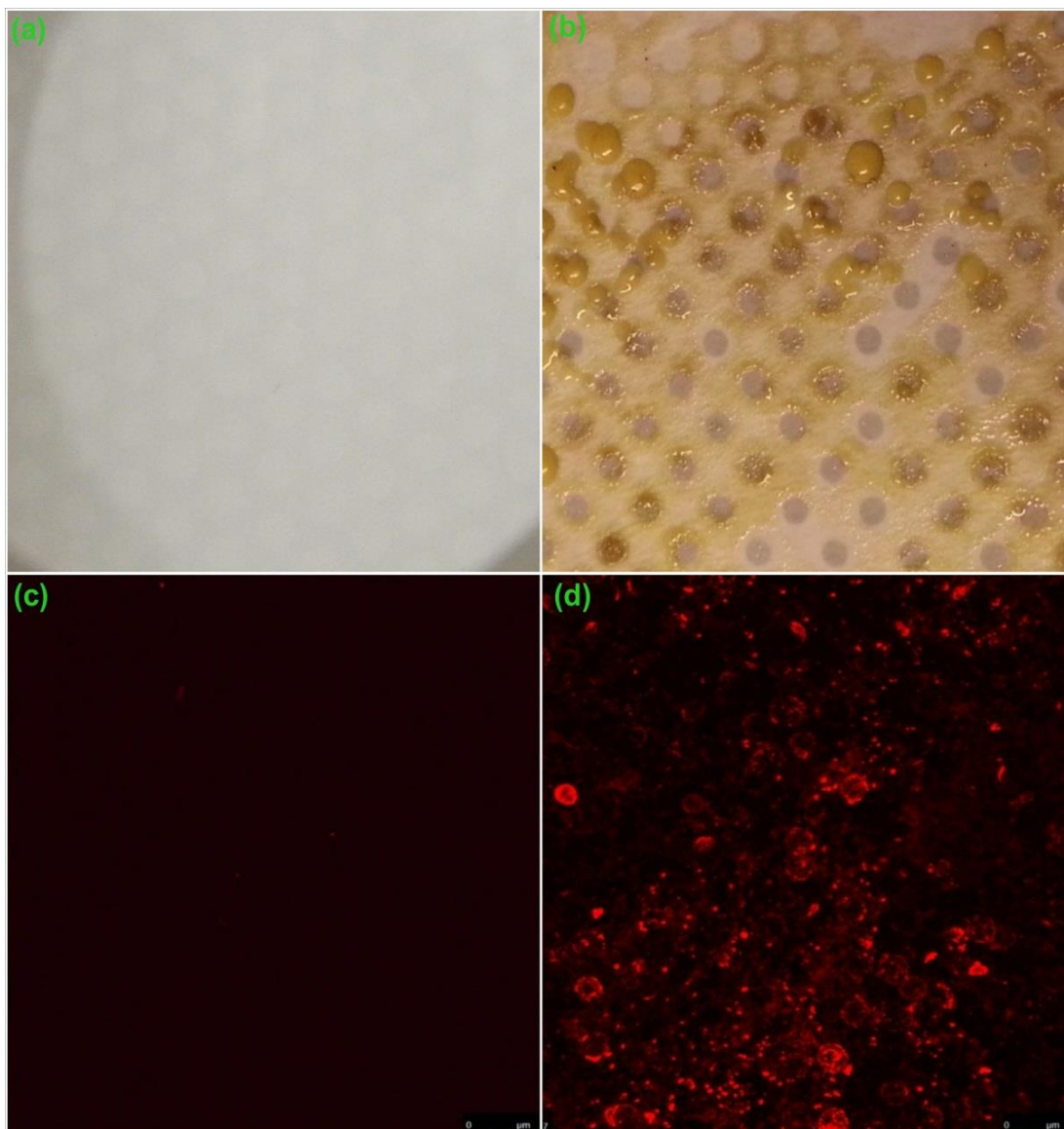


Figure 7-2: Biofilm sample visualization with CLSM. a) Photograph of the membrane at $t=0$. b) Photograph of the biofilm established on the membrane taken at the end of the experiment. c) At $t=0$, wheat germ agglutinin 647(WGA) stained image of the biofilm. d) 3D stacked confocal microscopy image of the biofilm. Sample was stained with wheat germ agglutinin 647(WGA) as it specifically binds to polysaccharides.

7.3.2 Scanning electron microscopy (SEM)

The biofilm samples were further analysed by scanning electron microscopy (SEM) upon confirmation of the presence of extracellular polymeric substances (EPS). SEM images showed the surface morphology and architecture of the biofilm matrix (Figure 7-3). The biofilm established on the membrane can be assumed to be mostly composed of EPS in the absence of any active biomass growth without any supplemental nutrient addition. Although there is a possibility of nitrogen fixation occurring but it would have resulted in improved degradation which was not observed as discussed later. Small circular shapes were presumed to be collapsed bacterial cells enmeshed within the matrix (Figure 7-3 a & c). Possible reason for this artefact could be due to drying of the sample before fixing in the stub or the fixing process itself. However the focus of the SEM micrographs was to visualize the biofilm morphology which was evident in Figure 7-3. The extensive polymeric matrix established in a non-growth system indicates apparent advantages towards survival and maintenance. This could include nutrient pooling and better water holding capacities (Holden et al., 1997a, Van De Mortel and Halverson, 2004). The fraction of degraded carbon channelized towards the non-mineralized fraction was found to be parameter driven from this study.

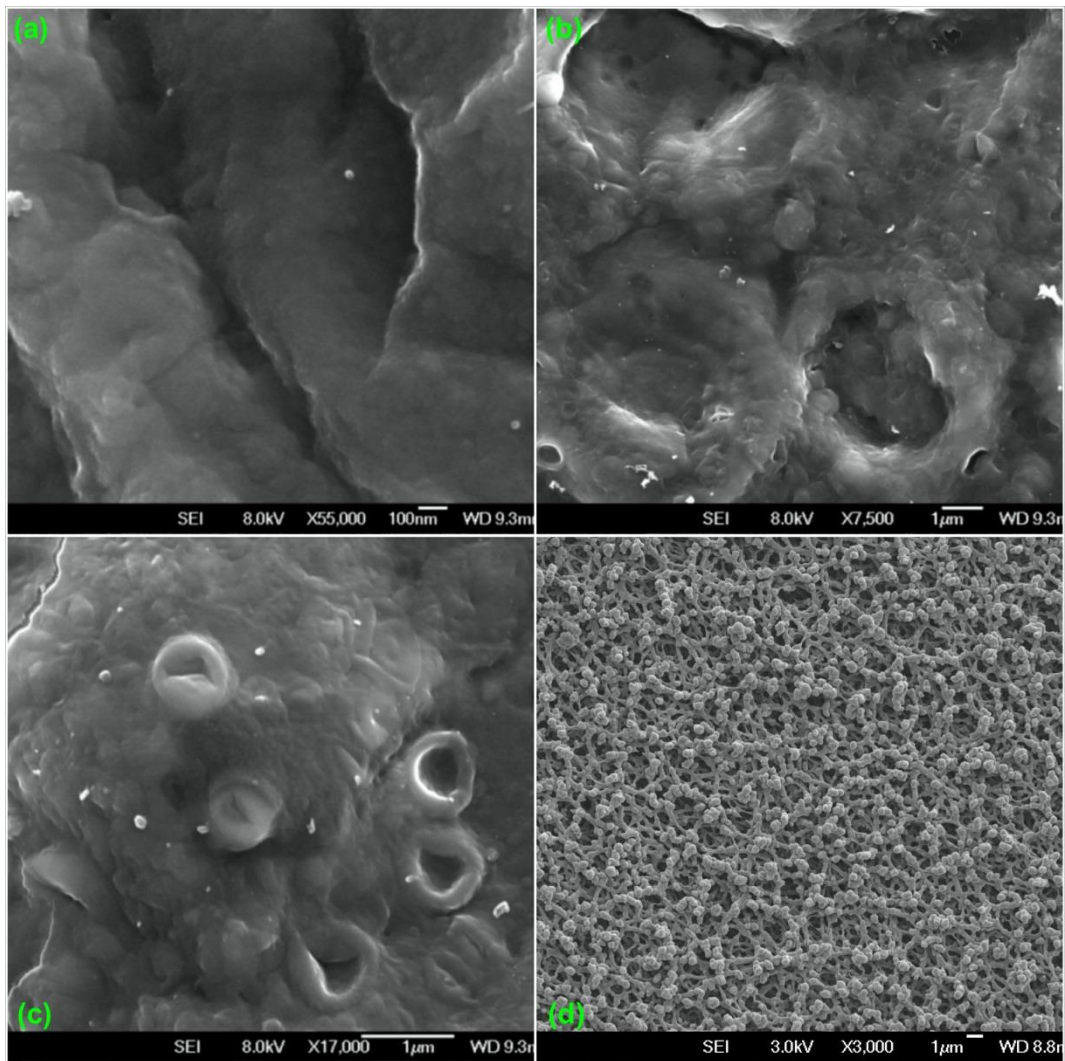


Figure 7-3: Representative SEM micrograph of the biofilm samples taken at the end of the run illustrating the biofilm architecture (a-c).The micrograph (d) is the control membrane at $t=0$ without any culture.

7.3.3 Carbon balance analysis of the biofilm run

The biofilter was operated at a matric potential of $-10 \text{ cm}_{\text{H}_2\text{O}}$ and $40 \text{ }^\circ\text{C}$ with an inlet feed concentrations of 120 ppm toluene. The degraded toluene was tracked in the gas, liquid and solid phase similarly to the soil runs on a carbon basis (Figure 7-4). For the biofilm reactor, 79% of the degraded carbon was mineralized to CO_2 . Solid and liquid phase accounted for $\sim 18 \%$ of the degraded carbon. The liquid phase in the biofilm was PBS without any nutrient supplements with negligible carbon content at start-up. The 10 % carbon tracked in the liquid phase is likely a combination of soluble microbial products (SMP) from the toluene degradation which accumulated over the time course of the experiment. Overall the mass balance closure of $97 \pm 5 \%$ was achieved by tracking the carbon end-points in the different phases.

Since the CO_2 recovery was never 100 % for this non-growth system, it indicated the accumulation of the remaining fraction in the solid and liquid phase. Likewise a clear biofilm deposition was visible on the semipermeable membrane at the end of the run (Figure 7-2b). This was postulated to be extracellular polysaccharides (EPS) which can be an important carbon sink during nutrient-limited growth (Weber and Hartmans, 1996). Also EPS has been demonstrated to have a higher C/N ratio than viable biomass (Leddy et al., 1995), thus suggesting negligible nitrogen requirement for providing a carbon sink from toluene oxidation (Wilshusen et al., 2004). There is also a possibility of polyhydroxybutyrate (PHB) production at excess residual toluene concentrations through overflow metabolism. *Pseudomonas putida* are known to produce PHB's (Velázquez et al., 2007, Escapa et al., 2012). However clearly there would be a limit to the amount of carbon that could be deposited as PHB without additional cell growth. In addition alginate production by *Pseudomonas putida* has been specifically linked to environmental stress from lower matric potential (Gülez et al., 2012). Although biofilters might also have additional secondary degraders in a mixed ecosystem capable of utilizing the EPS survival apart from the primary producers (Zhang and Bishop, 2003). Confirmation of these carbon end-points for the non-

mineralized fractions in pure culture serves as a good validation for the soil runs. A replicate biofilm run at the same set of condition was used for a qualitative study of the biofilm matrix discussed in the subsequent section.

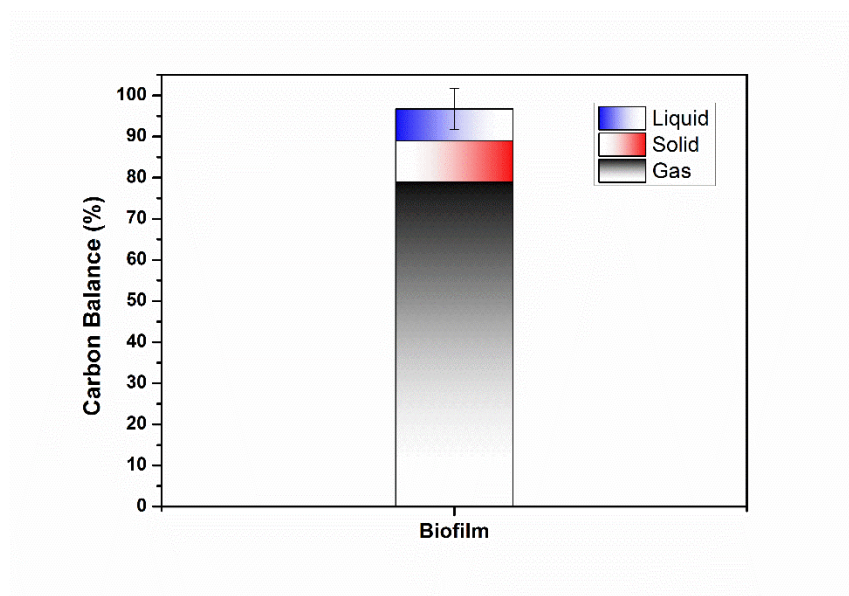


Figure 7-4: The endpoints of the toluene degraded by *Pseudomonas putida* reported on a percent carbon basis after 120 days of operation.

7.4 Effect of shut down phase on the microbial physiology: endogenous CO₂ production

Biofilter runs were monitored for the endogenous CO₂ production after the toluene feed was shut off (Figure 7-5). It was done to test two possible hypothesis pertaining to endogenous respiration and survival of the process culture in the absence of any carbon and or/energy source. On the assumption of the production of some sort of cellular reserve (e.g. PHB) and subsequent utilization of cellular reserves, the CO₂ production should eventually tail off upon exhaustion of the accumulated carbon reserves. This was observed for the soil runs where the post-run CO₂ production approached the pre-run range. Both quantitative and qualitative analysis of carbon end-points gave conclusive evidence of variable fraction of non-mineralized carbon fraction in the system. Hence after 120 days of operation of the pure culture biofilm

run, the toluene feed was shut off and CO₂-free air was fed into the system to monitor the dynamic response of the CO₂ production in the absence of carbon source.

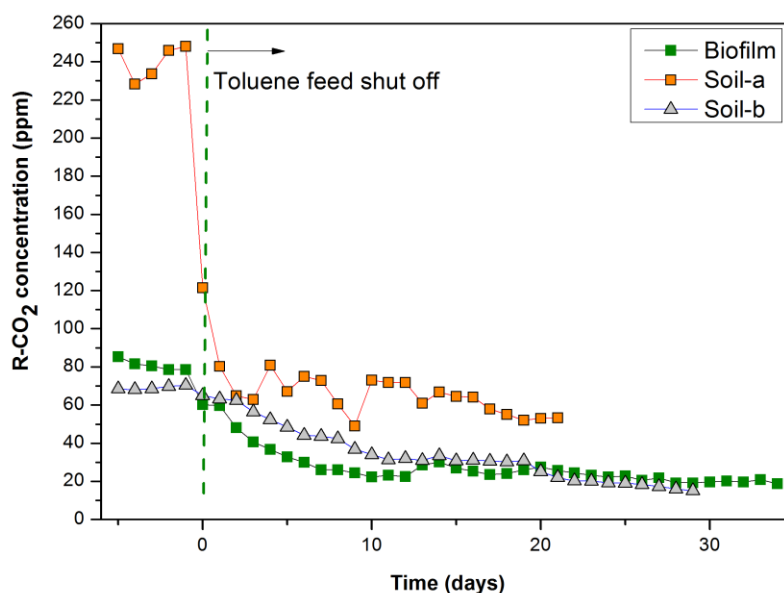


Figure 7-5: Endogenous CO₂ profile of some experimental runs at different sets of environmental parameters after toluene feed was shut down. Biofilm and Soil-a run was at 40 °C and -10cm_{H₂O} while Soil-b was at 20 °C and -20 cm_{H₂O} at an inlet feed of 120 ppm toluene.

CO₂ production gradually decreased by ~20-66 % upon shut down of toluene feed and subsequently stabilized. After monitoring it for 34 days, as stable CO₂ production persisted the experiment was stopped for further analysis. To confirm the presence of respiring bacteria, live dead stain was used with CLSM at the end of the run (Figure 7-6. b). Red fluorescence indicates dead cells whereas green fluorescence represents the live cells. A greater fraction of dead cells can be seen on the membrane at the end of the run. Presence of live cells confirms the hypothesis of endogenous respiration without pollutant feed. The can be validated from the CO₂ production profile (Figure 7-5). However the confocal micrograph does represent a substantial fraction of red fluorescence indicating dead cells. So it can be speculated to toxicity induced death owing to toluene or death happening over the experimental run due to nutrient

limitation. This is further substantiated from a separate micrograph at Day 0 showing significantly greater fraction of live cells (Figure 7-6.a). However for the time zero micrograph done independently only a quarter of the culture medium was poured on the membrane to what was used for starting the experimental runs. The idea was to look for dead versus live fractions at start-up. So the cell density was substantially lower for this micrograph.

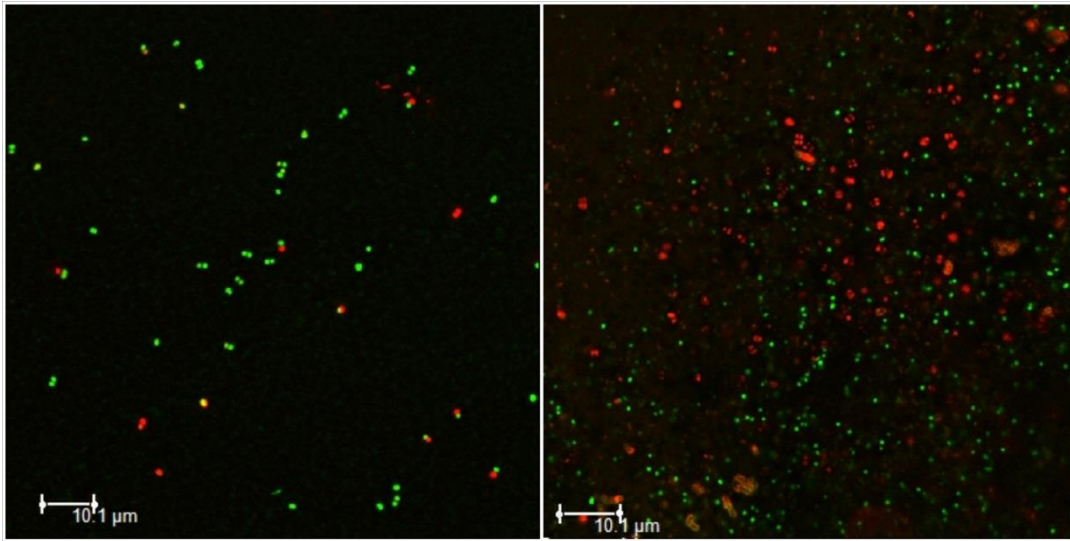


Figure 7-6: Stain: Live Dead of the *Pseudomonas putida* biofilm deposited on the membrane. (a) Day 0 image without toluene feed. (b) Images after 120 days of toluene degradation (images were taken from different runs).

7.5 Toluene degradation by the biofilm

Removal of toluene by the biofilm was quantified as surface elimination capacity (SEC) normalized to the whole biofilm surface area in the membrane. The surface elimination capacity is calculated as:

$$SEC = (C_i - C_o) \frac{Q}{A_m} \quad (g.m^{-2}.h^{-1}) \quad 7-1$$

Where,

C_i = Inlet toluene concentration (ppm)

C_o = Outlet toluene concentration (ppm)

Q = flow rate ($\text{m}^3 \cdot \text{h}^{-1}$)

A_m = biofilm surface area (m^2)

7.5.1 Effect of substrate concentration on biofilm degradation

Biofilm runs were investigated at two inlet feed concentration of 75 ppm and 120 ppm toluene to monitor the degradation rates under nutrient limited conditions (Figure 7-7). Under this operating mode toluene supports the microbial maintenance requirements without cellular growth as the carbon and energy source.

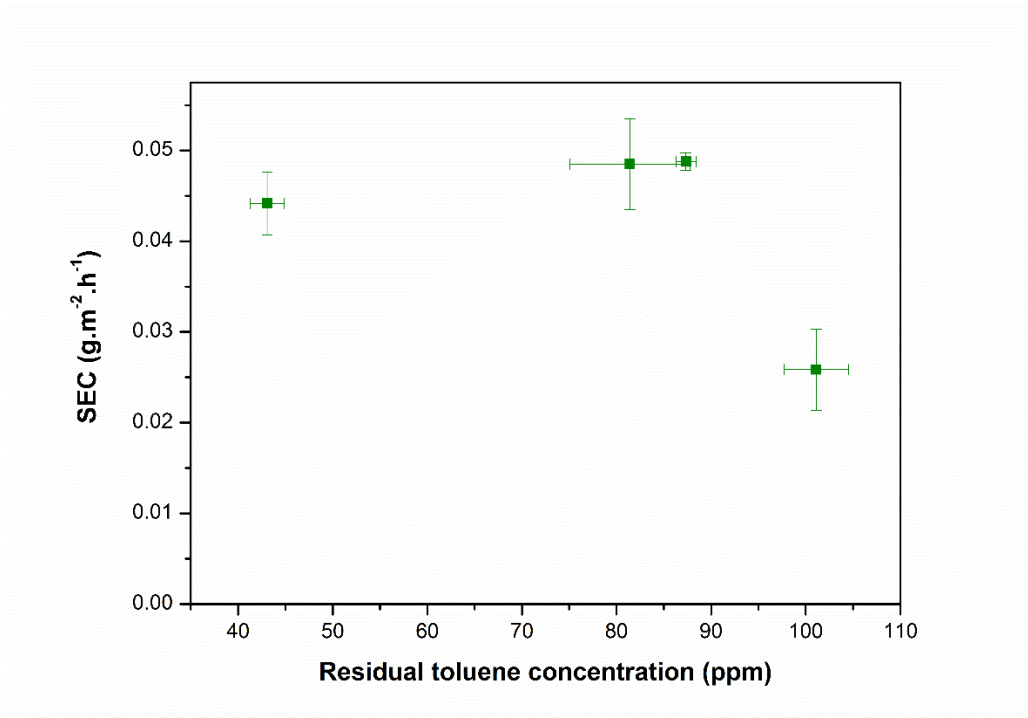


Figure 7-7 : Surface elimination capacities of the biofilm run over a range of residual toluene concentration. Experiments were operated at 40 °C and 10 $\text{cm}_{\text{H}_2\text{O}}$ over two inlet feed concentrations (75 and 120 ppm toluene)

Toluene degradation rates were not significantly different over the residual concentration range below 100 ppm. However there was a significant drop in performance at residual concentration above 100 ppm toluene. This compares well to

the soil runs where performance declined over this range discussed in chapter 6. Also, the mineralization of toluene to CO₂ became independent in soil biofilters runs above this range which suggest a change in metabolic response of the community in response to exposure to different substrate concentrations. Similar response in the *Pseudomonas putida* biofilm further substantiates this phenomenon at a pure culture level that may translate to other communities in a heterogeneous microbial community inside a biofilters. Although, these needs to be investigated over higher concentration range with different degraders to gain more insights on physiological responses influencing metabolic end products.

7.5.2 Effect of start-up substrate concentration on biofilm degradation

Soil biofilm activity was influenced by toluene exposure and as residual concentration evolved with time exposure to subsequently higher concentration at start-up impacted the process culture as discussed in chapter 6. This was found in the soil start-up experiments and hence the hypothesis was tested on the pure culture run. The biofilm run was started at 75 ppm inlet feed and upon reaching steady state a step change in feed concentration was made to 120 ppm toluene (Figure 7-8). The SEC values increased upon increasing the feed concentration to 120 ppm. This SEC was almost double compared to the independent runs at constant feed of 120 ppm that only had a higher start-up residual concentration as the remaining conditions were kept similar. Hence a clear impact of start-up concentrations can be deduced from these results which lead to the question of the nature of the resulting impact.

There can be a different set of induced response at the enzymatic level as a function of substrate concentration exposure apart from substrate toxicity. Under a constant carbon source the culture can be expected to be in maintenance mode with a steady degradation rate. However the response of *Pseudomonas putida* to lower start up concentration akin to soil runs indicates a probable activation/acclimatization of a greater fraction of the cells in the system as opposed to exposure at higher feeds. This can be linked to the instant increase in SEC after step up in feed as opposed to operation at constant feed which could have impaired some fraction at the start itself.

As a greater fraction of dead cells were observed at the end of the biofilm run at the constant feed of 120 ppm, death owing to toluene toxicity cannot be discounted. On the other hand it does illustrate the possibility of achieving greater performance if process culture is acclimatized at lower substrate concentrations initially.

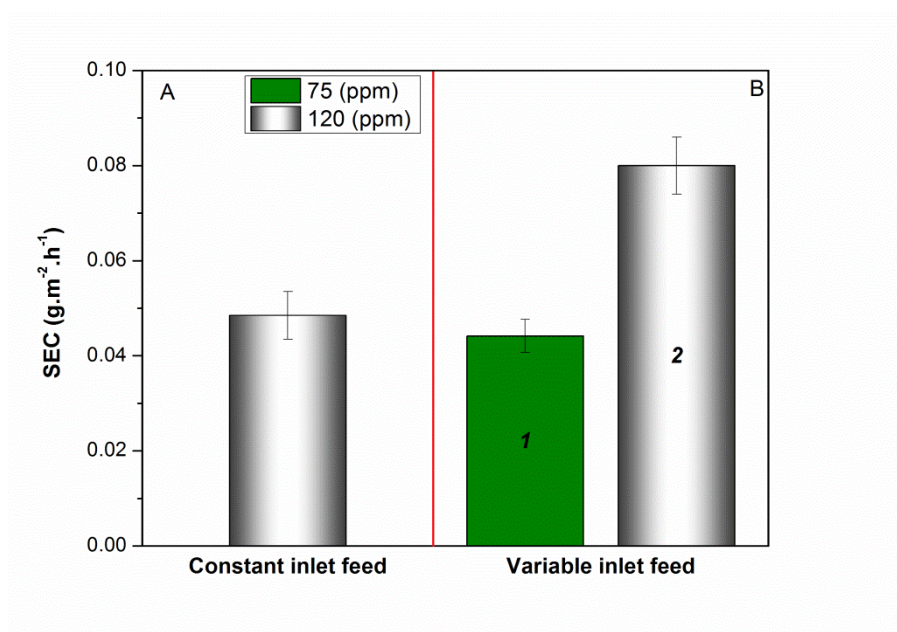


Figure 7-8: Comparison of lower start-up conditions and its implication on biofilm performance operated at 40°C and -10 cm_{H₂O} over constant inlet feed (A) and variable inlet feed (B). Values represent means over steady state at 95% CI.

7.6 Conclusions

Pure culture runs with *Pseudomonas putida* served as good validation for the soil biofilter run in terms of tracking the carbon end-points and monitoring recovery at specific set of conditions. Further microscopic observations with WGA-647 helped in conclusively linking the non-mineralized fractions to extracellular polysaccharide accumulation in the system. In addition, subsequent investigations on the start-up conditions showed good reproducibility with the biofilm comparable to the trends in the soil runs. Significantly improved degradation of 2-3 times was achieved at variable substrate feed conditions that at constant feeds. It showed the positive effect on microbial activity and the impact of start-up conditions at lower substrate conditions.

Chapter 8

CONCLUSIONS AND FUTURE WORK

8.1 Overall summary

In this work a key fundamental question of accurate quantification of the fate of degraded carbon in an engineered system for waste gas treatment was investigated. The carbon balance has not been addressed in a holistic way in biofiltration prior to this. Challenges exist in generalizing results postulated from assumptions of unaccounted carbon ending up as biomass without explicitly measuring all the potential outputs. The most common limitations pertaining to previous carbon balance closure attempts are discontinuous sampling in time, lack of control over parameters and direct sampling of the biofilm.

The unique differential reactor system used for this study exposes the process culture (soil or biofilm) to the same set of conditions at any snapshot in time. This facilitates the exploration for linking degradation products to metabolic response in a way traditional systems do not allow, as conditions change along the length in other biofiltration systems, which are normally integral plug-flow reactors.

This reactor set-up was used to quantify and track the carbon fractions in the gas, solid and liquid phases by the carbon balance equation devised for this system. Toluene and soil was used as a model component to generalize and critique with previous results. Experiments were operated in a non-growth mode without any supplemental nutrient addition. Quantitative closure of carbon balance was $90 \pm 5\%$ at a significance level of $\alpha = 0.05$. Within the experimental uncertainties associated with combining measurements from different sources and the applied statistical analysis to the data set, the carbon balance closure was achieved conclusively. Subsequently the toluene end-points were tracked as CO_2 production and the accumulated non-mineralized fraction within the solid and liquid phases.

The carbon balance results offered a new perspective while robustly tracking the ultimate fate of the carbon in the system degrading toluene, and the rationale can be extended to various other VOCs (Chapter 4). The distribution of carbon endpoints observed as CO₂ and accumulated non-mineralized fractions in the soil and the liquid phase varied as a function of the environmental parameters temperature, residual toluene concentration and matric potential (Figure 8-1). This made it imperative to comprehensively explore and establish a quantitative framework that determined their coupled impact on the CO₂ recovery across a wide range of independent variables. This offers space to critique the influence of each independent parameter in combination across different levels which can otherwise be masked. On-line monitoring of CO₂ throughout the experiment (coupled with the fraction of toluene degraded) makes it a robust tool in interpreting the metabolic response of the system.

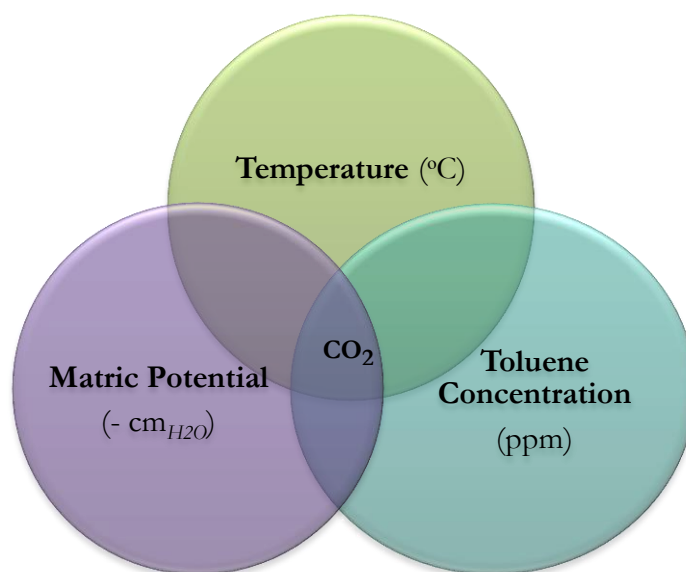


Figure 8-1: Schematic representing specific and overlapping regulatory mechanisms eventually impacting CO₂ carbon end-point over the different environmental parameters.

Tracking the carbon end-points as a function of various environmental parameters could provide interesting insights on their interactions pertaining to their impact on carbon-endpoints in biofilters. Biodegradation is driven by a myriad of environmental parameters co-existing and impacting the process in parallel. However, often these

parameters are investigated in isolation by keeping the other independent variables constant rather than investigating potential interaction across different levels of the independent parameters. Few studies have reported increasing VOC mineralization trends with increasing temperature without accurate control over the conditions. More so the matric potential as just the bed moisture content is reported without any control for the operational period. Thus concrete knowledge of the fate of carbon with variations in different environmental parameters remains elusive. Without a structured study it remains debatable whether the increasing VOC mineralization trend with increase in temperature will hold true with increasing substrate concentration or decreasing matric potential. The fate of the degraded carbon in the system is regulated by the physiological response of both the active degraders and non-degraders to the changing environmental parameters.

This study aimed to answer an open question of how interactions between environmental parameters impact carbon end-points. It tracked the variations in product ratios as the fraction of degraded toluene mineralized to CO₂ and non-mineralized fractions under controlled environmental conditions using a differential biofilter. A wide range of parameters defines the efficacy and microbial response ranging from temperature, type and concentration of substrate, water content, packing bed materials and community structure. Of these, three critical and omnipresent parameters central to any biofiltration process were investigated for which the reactor set-up is tailored to control robustly: temperature, matric potential and toluene concentration. In this study a factorial design approach was used to explore potential interactions and the main effects between three critical parameters over a wide range for each parameter chosen as categorical factors. The levels of each factor were chosen categorically to cover a widest possible range within the constraints allowing decent pollutant removal without critically impairing microbial functionalities.

A 3x3 factorial design of temperature (20 °C, 30 °C, 40 °C) and substrate concentration (75 ppm, 120 ppm, 193 ppm) was completed keeping the matric potential constant at -10 cm_{H₂O}. A 2-way ANOVA showed significant interaction

between the parameters. CO₂ recovery varied (~ 65 - 90%) as a function of operations at different combination of parameters. The combination of higher temperature (40 °C) and lower substrate concentration (75 ppm) resulted in the highest CO₂ recovery at 90%. However at the higher substrate concentration (193 ppm) this parameter had a significant (main) effect, as CO₂ recovery became independent of temperature across the three levels and were not significantly different at (*p-value* < 0.05). The investigation was extended by a (2x3) factorial design of temperature (20 °C and 40 °C) over three levels of matric potentials (-10 cm_{H₂O}, -20 cm_{H₂O} and -100 cm_{H₂O}) at a constant inlet feed of 120 ppm toluene. A 2-way ANOVA suggested significant effects for each parameter without an interaction component. CO₂ recoveries varied from (~35-81%) over the parameter combinations. Matric potential, controlled at each level to control the water content, resulted in a range from 0.60 - 0.27 g_{H₂O}/g_{SoilDW}, drier conditions were observed at lower matric potentials. While higher temperature (40 °C) lead to more CO₂ recovery (81%), with decreasing matric potential CO₂ recoveries decreased. Operations at 20 °C and -100 cm_{H₂O} resulted in the lowest CO₂ recovery observed in this study (35 %).

The simple assumption of a microbial population in maintenance mode degrading a carbon source is 100 % CO₂ recovery which was not true. Operations at those conditions with a major portion of degraded carbon accumulating in system could lead to clogging of bed and increase pressure drop affecting biofilter performance. Variations in CO₂ recovery (35-90%) as a function of environmental parameters sheds light on the processes underpinning biodegradation such as changing metabolic pathways, community structure and maintenance requirements.

Results showing CO₂ recovery becoming independent of the operating temperatures at higher toluene concentrations is contrary to the previously reported trends in the literature which were mostly evaluated by keeping concentration constant. This illustrated the importance of garnering knowledge on how the system behaves across other levels of independent variables where there is interaction between them that directly alters the dependent variable. This is indicative of microbial adaptation in the face of transient environmental parameters and the specific influences they bring to

the ecosystem. Temperature increases maintenance metabolism while in parallel can be outside the optimal range for a fraction of the community. Higher maintenance requirements can push the CO₂ recovery up for catabolic reactions to generate energy while the system can simultaneously witness a change in community structure. On the other hand toluene is toxic to many microorganisms and only specialized communities having the requisite mechanism in place can survive and use the organic pollutants. Its effect can range from inducing mutations to killing other communities due to toxicity. Thereby changing the dynamics of the system coexisting and possibly embracing niche phenomena such as cryptic growth and synergistic interaction. Also lower matrix potential reduces water availability which impairs microbial motility, induce gene expression to maintain cellular functionalities and initiate a change in community structure. This directly impacts metabolic pathways and maintenance requirements.

The cumulative quantification of the non-mineralized carbon fractions (NmC) of the degraded toluene over time was also critical on two fronts; it enabled tracking the ultimate fate of the degraded carbon and provided a vital link to interpret the variation in CO₂ product with the environmental parameters. Especially in a non-growth system with the assumption of no active biomass, these fractions can help explain metabolic responses which active biomass growth can hide and gets difficult to isolate and quantify from the inert fractions. Assumptions of unaccounted carbon going to biomass can be misconstrued as few studies addressing community culture have reported that the active fraction involved in degradation only constitutes ~5% of the ecosystem. The results from this study found the non-mineralized fraction to range from 0.08-0.65 (g NmC/ g toluene C) and postulated to be comprised of non-growth (inert) components like EPS and SMPs. Biomass yields range for various VOCs in the literature ranged from 0.34 – 0.83 g biomass / g carbon however normally were supplemented with nutrients including nitrogen without differentiating the inert fractions. While clogging is widely reported in biofiltration, a variable portion is most likely inert non-growth fractions like EPS and non-specialized biomass which may not have anything to do with biodegradation. Recent advances in sequencing techniques applied to biofilter packing bed revealed significant variation in community profile

from pre run to post run stages without identifying active fractions. Thus the common use of assuming a generic biomass formula approximately estimating 50% carbon can lead to erroneous results for biomass yield prediction without using an accurate carbon balance. The carbon content is also dependent on biofilm age, composition and specific communities. Current results further strengthen this proposition where even without active growth, significant variations in non-mineralized fractions occurred. At operations with lower matric potentials in particular at $-100 \text{ cm}_{\text{H}_2\text{O}}$, drier conditions induced resource allocations towards better adaptability by producing EPS and in parallel support a transition in community structure towards fungi. While EPS have the advantages of efficient nutrient pooling and its water holding capacity giving producers distinct headway. Thus, knowing the physiological response of the system as a function of carbon end-points offers the possibility of addressing operational problems like clogging plaguing biofilter operations. Carefully choosing parameters can ensure degradation products deviation towards mineralized CO_2 and keeping biomass yields at minimum.

Simultaneous impact of these parameters on biofilter performance was evaluated through ANOVA similarly to the carbon end point for degraded toluene. Elimination capacity (EC) is routinely used to quantify the degrading capacity of a biofilter. Various studies have investigated the influence of critical environmental parameters like temperature, matric potential and substrate concentration on EC. Few studies have addressed the interaction of mixed substrate on biofilter performance which showed both inhibition and stimulation in presence of mixed substrates. While the impact on EC across critical parameters like temperature, matric potential and substrate concentration and the impact of their interaction remains limited till date.

Biofilter performance was influenced by the interaction between the parameters. At the lowest inlet concentration (75 ppm), *EC* increased as function of temperature, while over higher substrate concentrations, *EC* did not vary much. Also for the 2x2 factorial design with temperature and matric potential, the interaction was significant between them. *EC* at the highest matric potential ($-10 \text{ cm}_{\text{H}_2\text{O}}$) was 2-fold higher for $40 \text{ }^\circ\text{C}$ ($50.4 \pm 2 \text{ g.m}^{-3}.\text{h}^{-1}$) than $20 \text{ }^\circ\text{C}$. However at lower matric potentials, interaction

between the parameters was at play which influenced the *EC*. The lowest *EC* at 40 °C was $23 \pm 2 \text{ g.m}^{-3}.\text{h}^{-1}$ at $-100 \text{ cm}_{\text{H}_2\text{O}}$, which was not significantly different from the *EC*s observed at 20 °C over the entire investigated matric potential range (*p-value* < 0.05).

Comparing *EC* to concurrent CO_2 recovery suggested that the two dependent variables are not always coupled and varied independently as a function of environmental parameters. From the trends observed for CO_2 recovery and *EC* at the higher substrate feed concentrations; it follows that CO_2 recoveries became independent of temperature and a general lower *EC* was observed compared to other set of conditions. At the highest feed concentration, there could be one dominant degrading community which resulted in a constant mineralization fraction owing to the metabolic pathways. The increase in *EC* with increase in temperature could be attributed to elevated activity of the same active community while the pathways remained the same. Alternately it is possible that the metabolic response became independent of the substrate concentration beyond a critical level. However there was no correlation between *EC* and CO_2 recovery at the lowest temperature (20 °C) compared to 40 °C. While the parameters independently impacted both the dependent variables, the comparison enabled an understanding of the intricate linkage between microbial activity and metabolic pathway regulation by the community.

In this differential biofilter, at time zero, the microbes were exposed to the inlet feed concentration which gradually decreased with time as a function of degradation at specific set of conditions. Lower *EC* values were observed at biofilter runs with higher start-up feed exposures ranging from 120-193 ppm. The hypothesis of possible implications of start-up conditions at lower feed and subsequent operations at variable feed concentrations was also tested. CO_2 recovery was not influenced by operations at low to higher feed concentration while upon decreasing the feed concentration from 193 ppm to 75 ppm, CO_2 recovery was 75% compared to 90% at constant feeds at same set of conditions. However there was a substantial increase in *EC* by 2-3 fold when varying the inlet feed concentration starting from 75 ppm compared to a constant feed concentration at 193 ppm. Although over the longer term, *EC* declined and was comparable to a constant feed concentration, a greater amount of degradation

was achieved over similar timeframe (90 days). It could be related to microbial diversity or better acclimatization of large fraction of active degraders that could have been impaired upon exposure to high concentration at start-up. An impact on the culture acclimatization process can be deduced from these results which can have good practical implications for improved process efficacy.

Pure culture runs with *Pseudomonas putida* (Chapter 7) served as a good validation for comparing the empirical results from the soil biofilter run in terms of tracking the carbon end-points and monitoring recovery at specific set of conditions. It yielded comparable CO₂ recovery (85%) at lower substrate concentration (75 ppm) and 40 °C compared to soil (90%). CO₂ recovery was also comparable for operations at 120 ppm. Further microscopic observations with WGA-647, a specific lectin binding stain helped in conclusively linking the non-mineralized fractions to extracellular polysaccharide accumulation in the system. Thus this work provides a good framework for understanding the fate of degraded carbon and the implication of multiple parameters having a combined interaction which is critical in influencing the metabolic response and community structure in the biofilter.

In addition, subsequent investigations on the start-up conditions showed good reproducibility with the biofilm which is comparable to the trends in the soil runs. Significantly improved degradation (2-3 times) was achieved at variable substrate feed conditions (75 → 120 ppm) than at constant feed concentration of 120 ppm. It substantiated the positive effect on microbial activity and the impact of start-up conditions at lower substrate conditions observed with soil runs pertaining to the active degraders.

Overall, using the CO₂ recovery fraction in this differential bioreactor was effective for studying the interaction of the three critical environmental parameters of temperature, matric potential and substrate concentrations through a factorial design. Tracking the carbon end-points pattern over multiple parameters provided valuable insights on the interactions between them pertaining to the eventual fate of the degraded toluene in the system. These results helped to establish an empirical framework providing a

coherent link between carbon end-points, metabolic pathways and community structure as influenced by the environmental parameters.

8.2 Future work

8.2.1 Extension of the factorial design to other substrates

The presence of interactions and main effects over multiple parameters investigated showed the importance of understanding the contribution of parameters cumulatively. The factorial design matrix can be extended over a broad range of factors and levels to can further help to gain better insights of the process kinetics pertaining to metabolic response and community structure with other VOCs. Generation of this empirical information could be invaluable to the field and contribute immensely towards making informed decision in commissioning industrial projects in deciding operational parameters. It would also serve as a good baseline for doing more fundamental research in terms of having a sense of systemic behaviours across different environmental parameters.

8.2.2 Metagenomics: To answer who is doing what?

This work provided a good framework to delve into the possibility of deciphering the functionalities of the complex heterogeneous community coexisting in the ecosystem. It could benefit from incorporating next generation RNA/DNA molecular sequencing techniques to identify the functionally active community especially with stable isotope probing (e.g. C¹³). The labelled genetic material can be isolated which allows for better identification of the active degrading community. DNA and RNA work can be used complementarily as both offers new dimension and will provide a picture of the active community. This will help relate environmental parameters influencing the wider community structure and differentiate active degraders which actually drive the biodegradation rates. This work will be strengthened by the unique differential biofilter which enables accurate control of parameters while enabling direct use of labelling thereby negating prior serum bottle work. The results from the current project pertaining to variations in carbon end-points across multiple levels of environmental parameters would help to choose the desired operational parameters

specifically aimed at labelling the active degraders. Like operation at a lower matric potential, higher temperature and lower substrate concentrations can test the hypothesis if drier conditions just makes the fungi happy or they are actually the active degraders. Contrasting it with higher matric potential and lower temperatures can correlate if bacteria were more active and quantification will enable to relate community structure change to both physiological response and biodegradation rates.

8.2.3 Metabolomics and proteomics

Further metabolomic approaches would form a critical basis of future work in detailing metabolic pathways. In this reactor system the possibility of using labelled isotopes (C^{13}) coupled with GC-MS, LC-MS, NMR and other chemometric tools can be very useful in metabolic profiling under different environmental stressors. These carbon end-points results can aid to critique a maintenance model under low/non-growth conditions. It will also generate important system data including specific metabolic rates for the different compounds under growth and non-growth conditions. Further transcriptome and proteomic study directed at gene expression under different environmental conditions can have profound implications towards understanding microbial response under transient conditions. Often microbes regulate gene expression to adapt to environmental stimuli. The investigation of mRNA gene expression data could be used for heterologous expression for upscaling secondary metabolite production that have good therapeutic implications.

8.2.4 Unsaturated biofilms under controlled environmental conditions

Often data collected from batch studies cannot be extrapolated to engineered systems owing to plethora of stressors associated with it as opposed to relatively favourable conditions under batch conditions. The pure culture work with biofilm reactors is a good approach to extrapolate information which is a much better representation of conditions in practical biofiltration operation as opposed to microcosm/batch studies. This work can extend into investigations with other pure cultures, in particular with prior knowledge about its functionality in the system from gene sequencing work.

While *Pseudomonas putida* was tested in this study there are four other degraders isolated from the same soil source also used for another project previously. Either these strains can be tested individually or the system can be operated as mixed cultures. This would help in comparing both performance and carbon end-points across the three systems: soil, pure culture biofilm, mixed culture biofilms. Correlating performance and carbon end-points between pure culture bacteria, fungi and mixed cultures to soil runs can offer new insights in microorganism's physiological response under similar conditions as well as variations across parameters.

8.2.5 Exploring Start-up conditions and other substrates

The implications of the start-up condition results offer the possibility of extending the experimental parameters further. Much lower start-up concentration conditions can be tested, and then the variable feed can be used over significantly higher substrate concentrations. This start-up condition can be tested over other pollutant sources. If this start-up concept pans out equivocally to other substrates it could have application in operating stable and more efficient engineered process. Also knowledge in regards to the effect of activity and quantity of the active community structure in response to start-up conditions will be immensely valuable.

8.2.6 What else could drive the carbon flux in the system

While the system was operated without supplemental nitrogen, there is the possibility of N_2 fixation. Although from the results achieved it can be speculated otherwise as an incremental increase in EC would have been observed and no significant biomass growth was observed either. Previously, upon addition of a nitrogen source to the liquid reservoir, biomass growth was observed which indicates that the system was indeed nitrogen limited. However to definitively confirm this hypothesis, N_2 could be replaced by argon. The role of N_2 -fixing bacteria can be investigated through monitoring metabolism kinetics and carbon end-points upon the change.

Another phenomenon which could influence the mineralization pattern is the role of predators (e.g. protozoa, mites) in the system and their response to changing environmental parameters. Experiments with pre-treated soil aimed at neutralizing the

predators could offer interesting insights on the co-existence and specific influence of the predators on substrate metabolism.

8.2.6 Characterisation of the polysaccharides

A good extension of the current work can be followed up by characterization of the polysaccharides in both solid and liquid phases in terms of molecular weight distribution, types and solubility. Further exploration can be done in studying the differentiation between external (EPS) and internal storage polymers (e.g. PHB). This will be helpful in understanding phenomenon like overflow metabolism. The identities of the carbon fractions in the liquid and solid phase of the bioreactors are yet to be ascertained quantitatively in a controlled situation in biofiltration. This can serve as a key indicator to physiological response under different environmental conditions.

8.2.7 Impact of the polymers on pressure drop

A column biofilter can be used to test some of the implications of the results from this study in terms of the influence of polymers on pressure drop. Solubility of polymers can lead to a significant sink in the leachate while consumer-producer dynamics would throw light on the plausible reasons for the biofilters not plugging up. This is a bottleneck in attaining good operational stability and efficacy.

References

- ACUÑA, M. E., PÉREZ, F., AURIA, R. & REVAH, S. 1999. Microbiological and kinetic aspects of a biofilter for the removal of toluene from waste gases. *Biotechnology and Bioengineering*, 63, 175-184.
- ALTSHULLER, A. & COHEN, I. 1960. Application of diffusion cells to production of known concentration of gaseous hydrocarbons. *Analytical Chemistry*, 32, 802-810.
- ALY HASSAN, A. & SORIAL, G. A. 2010. Removal of benzene under acidic conditions in a controlled Trickle Bed Air Biofilter. *Journal of Hazardous Materials*, 184, 345-349.
- AMBROSE, D., LAWRENSON, I. & SPRAKE, C. 1975. The vapour pressure of naphthalene. *The Journal of Chemical Thermodynamics*, 7, 1173-1176.
- ARCANGELI, J. P. & ARVIN, E. 1992. Toluene biodegradation and biofilm growth in an aerobic fixed-film reactor. *Applied Microbiology and Biotechnology*, 37, 510-517.
- AVALOS RAMIREZ, A., BÉNARD, S., GIROIR-FENDLER, A., JONES, J. P. & HEITZ, M. 2008. Treatment of methanol vapours in biofilters packed with inert materials. *Journal of Chemical Technology & Biotechnology*, 83, 1288-1297.
- BAGHERPOUR, M. B., NIKAZAR, M., WELANDER, U., BONAKDARPOUR, B. & SANATI, M. 2005. Effects of irrigation and water content of packings on alpha-pinene vapours biofiltration performance. *Biochemical Engineering Journal*, 24, 185-193.
- BARKER, D. J. & STUCKEY, D. C. 1999. A review of soluble microbial products (SMP) in wastewater treatment systems. *Water Research*, 33, 3063-3082.
- BELLER, H. R., REINHARD, M. & GRBIĆ-GALIĆ, D. 1992. Metabolic by-products of anaerobic toluene degradation by sulfate-reducing enrichment cultures. *Applied and Environmental Microbiology*, 58, 3192-3195.

- BESLEY, L. & BOTTOMLEY, G. 1974. Vapour pressure of toluence from 273.15 to 298.15 K. *The Journal of Chemical Thermodynamics*, 6, 577-580.
- BESTER, E., KROUKAMP, O., HAUSNER, M., EDWARDS, E. A. & WOLFAARDT, G. M. 2011. Biofilm form and function: carbon availability affects biofilm architecture, metabolic activity and planktonic cell yield. *Journal of Applied Microbiology*, 110, 387-398.
- BEUGER, A. L. & GOSTOMSKI, P. A. 2009. Development of a biofilter with water content control for research purposes. *Chemical Engineering Journal*, 151, 89-96.
- BHASKARAN, K., NADARAJA, A. V., BALAKRISHNAN, M. V. & HARIDAS, A. 2008. Dynamics of sustainable grazing fauna and effect on performance of gas biofilter. *Journal of Bioscience and Bioengineering*, 105, 192-197.
- BODELIER, P. L. E. & LAANBROEK, H. J. 2004. Nitrogen as a regulatory factor of methane oxidation in soils and sediments. *FEMS Microbiology Ecology*, 47, 265-277.
- BOERO, V., ECKENFELDER JR, W. & BOWERS, A. 1991. Soluble microbial product formation in biological systems. *Water Science & Technology*, 23, 1067-1076.
- BOHN, H. L. & BOHN, K. H. 1999. Moisture in biofilters. *Environmental Progress*, 18, 156-161.
- BORDEL, S., MUÑOZ, R., DÍAZ, L. F. & VILLAYERDE, S. 2007a. Predicting the Accumulation of Harmful Metabolic Byproducts During the Treatment of VOC Emissions in Suspended Growth Bioreactors. *Environmental Science & Technology*, 41, 5875-5881.
- BORDEL, S., MUÑOZ, R., DÍAZ, L. F. & VILLAYERDE, S. 2007b. New insights on toluene biodegradation by *Pseudomonas putida* F1: influence of pollutant concentration and excreted metabolites. *Applied Microbiology and Biotechnology*, 74, 857-866.
- BORDEL, S., MUÑOZ, R., DÍAZ, L. F. & VILLAYERDE, S. 2008. Mechanistic model for evaluating the performance of suspended growth bioreactors for the off-gas treatment of VOCs. *Biochemical Engineering Journal*, 38, 395-405.

- BORIN, S., MARZORATI, M., BRUSETTI, L., ZILLI, M., CHERIF, H., HASSEN, A., CONVERTI, A., SORLINI, C. & DAFFONCHIO, D. 2006. Microbial succession in a compost-packed biofilter treating benzene-contaminated air. *Biodegradation*, 17, 79-89.
- CABEZA, I., LÓPEZ, R., GIRALDEZ, I., STUETZ, R. & DÍAZ, M. 2013. Biofiltration of α -pinene vapours using municipal solid waste (MSW)–Pruning residues (P) composts as packing materials. *Chemical Engineering Journal*, 233, 149-158.
- CABROL, L. & MALHAUTIER, L. 2011. Integrating microbial ecology in bioprocess understanding: the case of gas biofiltration. *Applied Microbiology and Biotechnology*, 1-13.
- CABROL, L., MALHAUTIER, L., POLY, F., LEPEUPLE, A. S. & FANLO, J. L. 2012. Bacterial dynamics in steady-state biofilters: beyond functional stability. *FEMS Microbiology Ecology*.
- CHANG, K. & LU, C. 2003. Biofiltration of toluene and acetone mixtures by a trickle-bed air biofilter. *World Journal of Microbiology and Biotechnology*, 19, 791-798.
- CHARACKLIS, W. G. & MARSHALL, K. C. 1990. "Physical and Chemical Properties of Biofilms", In W.G. Characklis and K.C. Marshall (eds.), *Biofilm*, John Wiley, New York.p. 93- 130.
- CHEN, N. & OTHMER, D. 1964. Correspondence. Correlations for the Coefficients of Gaseous Diffusion. *Industrial & Engineering Chemistry Fundamentals*, 3, 279-280.
- CHEN, X., SCHAUDER, S., POTIER, N., VAN DORSSELAER, A., PELCZER, I., BASSLER, B. L. & HUGHSON, F. M. 2002. Structural identification of a bacterial quorum-sensing signal containing boron. *Nature*, 415, 545-549.
- CHERRY, R. S. & THOMPSON, D. N. 1997. Shift from growth to nutrient-limited maintenance kinetics during biofilter acclimation. *Biotechnology and Bioengineering*, 56, 330-339.
- CHO, K.-S., YOO, S.-K. & RYU, H. W. 2007. Thermophilic biofiltration of benzene and toluene. *Journal of microbiology and biotechnology*, 17, 1976-1982.

- CHOWDHURY, N., MARSCHNER, P. & BURNS, R. G. 2011. Soil microbial activity and community composition: impact of changes in matric and osmotic potential. *Soil Biology and Biochemistry*, 43, 1229-1236.
- CHRISTEN, P., DOMENECH, F., MICHELENA, G., AURIA, R. & REVAH, S. 2002. Biofiltration of volatile ethanol using sugar cane bagasse inoculated with *Candida utilis*. *Journal of Hazardous Materials*, 89, 253-265.
- CORONADO, E., ROGGO, C. & VAN DER MEER, J. R. 2014. Identification of genes potentially involved in solute stress response in *Sphingomonas wittichii* RW1 by transposon mutant recovery. *Frontiers in Microbiology*, 5, 585.
- COSTERTON, J. W., LEWANDOWSKI, Z., CALDWELL, D. E., KORBER, D. R. & LAPPIN-SCOTT, H. M. 1995. Microbial biofilms. *Annual Reviews in Microbiology*, 49, 711-745.
- COX, H. H. J. & DESHUSSES, M. A. 1999. Biomass control in waste air biotrickling filters by protozoan predation. *Biotechnology and Bioengineering*, 62, 216-224.
- COX, H. H. J., NGUYEN, T. T. & DESHUSSES, M. A. Year. Elimination of toluene vapors in biotrickling filters: performance and carbon balances, Paper 98-WAA.04P. In: *Proc. Annual Meeting and Exhibition of the Air and Waste Management Association*, San Diego, CA, June 14-18, 1998. AWMA, Pittsburgh, PA. 15 pp. In, 1998. 14-18.
- COX, H. H. J., SEXTON, T., SHAREEFDEEN, Z. M. & DESHUSSES, M. A. 2001. Thermophilic biotrickling filtration of ethanol vapors. *Environmental Science & Technology*, 35, 2612-2619.
- D'AMICO, S., MARX, J.-C., GERDAY, C. & FELLER, G. 2003. Activity-stability relationships in extremophilic enzymes. *Journal of Biological Chemistry*, 278, 7891-7896.
- DANAEE, S., FAZAEIPOOR, M. H., GHOLAMI, A., ATAIEI, S. A. & AFZALI, D. 2014. Modelling and experimental investigation on the application of water super adsorbents in waste air biofilters. *Environmental Technology*, 1-9.

- DARLINGTON, A. B., DAT, J. F. & DIXON, M. A. 2001. The biofiltration of indoor air: air flux and temperature influences the removal of toluene, ethylbenzene, and xylene. *Environmental Science & Technology*, 35, 240-246.
- DE SILVA, D. & RITTMANN, B. E. 2000. Nonsteady-state modeling of multispecies activated-sludge processes. *Water Environment Research*, 72, 554-565.
- DECHESSNE, A., OR, D., GÜLEZ, G. & SMETS, B. F. 2008. The porous surface model, a novel experimental system for online quantitative observation of microbial processes under unsaturated conditions. *Applied and Environmental Microbiology*, 74, 5195-5200.
- DELHOMÉНИЕ, M.-C., BIBEAU, L., GENDRON, J., BRZEZINSKI, R. & HEITZ, M. 2003. A study of clogging in a biofilter treating toluene vapors. *Chemical Engineering Journal*, 94, 211-222.
- DELHOMÉНИЕ, M.-C. & HEITZ, M. 2005. Biofiltration of air: a review. *Critical Reviews in Biotechnology*, 25, 53-72.
- DELHOMÉНИЕ, M. C., BIBEAU, L. & HEITZ, M. 2005. A study of the biofiltration of high-loads of toluene in air: Carbon and water balances, temperature changes and nitrogen effect. *Canadian Journal of Chemical Engineering*, 83, 153-160.
- DESHUSSES, M. A. 1997a. Biological waste air treatment in biofilters. *Current Opinion in Biotechnology*, 8, 335-339.
- DESHUSSES, M. A. 1997b. Transient Behavior of Biofilters: Start-Up, Carbon Balances, and Interactions between Pollutants. *Journal of Environmental Engineering*, 123, 563-568.
- DETCANAMURTHY, S. 2013. *Impact of different metabolic uncouplers on the specific degradation rate of toluene in a differential biofiltration reactor*. University of Canterbury.
- DEVINNY, J. & HODGE, D. 1995. Formation of acidic and toxic intermediates in overloaded ethanol biofilters. *Journal of the Air and Waste Management Association*, 45, 125-131.
- DEVINNY, J. S., DESHUSSES, M. A. & WEBSTER, T. S. 1999. *Biofiltration for air pollution control*, CRC.

- DÍAZ, L. F., MUÑOZ, R., BORDEL, S. & VILLAVERDE, S. 2008. Toluene biodegradation by *Pseudomonas putida* F1: targeting culture stability in long-term operation. *Biodegradation*, 19, 197-208.
- DIKS, R. M. M., OTTENGRAF, S. P. P. & VRIJLNAD, S. 1994. The existence of a biological equilibrium in a trickling filter for waste gas purification. *Biotechnology and Bioengineering*, 44, 1279-1287.
- DMITRIEVA, N. I. & BURG, M. B. 2007. Osmotic stress and DNA damage. *Methods in Enzymology*, 428, 241-252.
- DOMEÑO, C., RODRÍGUEZ-LAFUENTE, Á., MARTOS, J., BILBAO, R. & NERÍN, C. 2010. VOC removal and deodorization of effluent gases from an industrial plant by photo-oxidation, chemical oxidation, and ozonization. *Environmental science & technology*, 44, 2585-2591.
- DORADO, A. D., BAEZA, J. A., LAFUENTE, J., GABRIEL, D. & GAMISANS, X. 2012. Biomass accumulation in a biofilter treating toluene at high loads—Part 1: Experimental performance from inoculation to clogging. *Chemical Engineering Journal*, 209, 661-669.
- DORADO, A. D., LAFUENTE, J., GABRIEL, D. & GAMISANS, X. 2010. The role of water in the performance of biofilters: Parameterization of pressure drop and sorption capacities for common packing materials. *Journal of Hazardous Materials*, 180, 693-702.
- DUETZ, W. A., DE JONG, C., WILLIAMS, P. A. & VAN ANDEL, J. 1994. Competition in chemostat culture between *Pseudomonas* strains that use different pathways for the degradation of toluene. *Applied and Environmental Microbiology*, 60, 2858-2863.
- DURMAZ, B. & SANIN, F. D. 2003. Effect of carbon to nitrogen ratio on the physical and chemical properties of activated sludge. *Environmental Technology*, 24, 1331-1340.
- ELMRINI, H., BREDIN, N., SHAREEFDEEN, Z. & HEITZ, M. 2004. Biofiltration of xylene emissions: bioreactor response to variations in the pollutant inlet concentration and gas flow rate. *Chemical Engineering Journal*, 100, 149-158.

- ESCAPA, I. F., GARCÍA, J. L., BÜHLER, B., BLANK, L. M. & PRIETO, M. A. 2012. The polyhydroxyalkanoate metabolism controls carbon and energy spillage in *Pseudomonas putida*. *Environmental Microbiology*, 14, 1049-1063.
- ESTRADA, J. M., HERNÁNDEZ, S., MUÑOZ, R. & REVAH, S. 2013a. A comparative study of fungal and bacterial biofiltration treating a VOC mixture. *Journal of Hazardous Materials*, 250, 190-197.
- ESTRADA, J. M., QUIJANO, G., LEBRERO, R. & MUÑOZ, R. 2013b. Step-feed biofiltration: a low cost alternative configuration for off-gas treatment. *Water research*, 47, 4312-4321.
- ESTRADA, J. M., RODRÍGUEZ, E., QUIJANO, G. & MUÑOZ, R. 2012. Influence of gaseous VOC concentration on the diversity and biodegradation performance of microbial communities. *Bioprocess and Biosystems Engineering*, 35, 1477-1488.
- FANG, Y. & GOVIND, R. 2006. CO₂ Response to Doses of Organic Solvents Biodegraded in a Batch Biofilter. *Water, Air, & Soil Pollution*, 175, 33-48.
- FERMOR, T. & WOOD, D. 1981. Degradation of bacteria by *Agaricus bisporus* and other fungi. *Journal of General Microbiology*, 126, 377.
- FLEMMING, H.-C. & WINGENDER, J. 2010. The biofilm matrix. *Nat Rev Micro*, 8, 623-633.
- FOX, J. & WEISBERG, S. 2010. *An R companion to applied regression*, Sage.
- FOX, J., WEISBERG, S., ADLER, D., BATES, D., BAUD-BOVY, G., ELLISON, S., FIRTH, D., FRIENDLY, M., GORJANC, G. & GRAVES, S. 2015. Package 'car'.
- FRANCESC, X. P.-B., OMAR, O., MARC, A. & FRANCESC, C. 2012. Assessment of Process Limiting Factors During the Biofiltration of Odorous VOCs in a Full-Scale Composting Plant. *Compost Science & Utilization*, 20, 73-78.
- FRIEDRICH, U., PRIOR, K., ALTENDORF, K. & LIPSKI, A. 2002. High bacterial diversity of a waste gas-degrading community in an industrial biofilter as shown by a 16S rDNA clone library. *Environmental Microbiology*, 4, 721-734.

- FÜRER, C. & DESHUSSES, M. A. Year. Biodegradation in Biofilters: Did the Microbe Inhale the VOC?, in Proceeding of the A&WMA 93rd Annual Meeting. 2000: Salt Lake City, Utah. p. 13. *In*, 2000.
- GALLASTEGUI, G., ÁVALOS RAMIREZ, A., ELÍAS, A., JONES, J. P. & HEITZ, M. 2011a. Performance and macrokinetic analysis of biofiltration of toluene and p-xylene mixtures in a conventional biofilter packed with inert material. *Bioresource Technology*, 102, 7657-7665.
- GALLASTEGUI, G., BARONA, A., ROJO, N., GURTUBAY, L. & ELÍAS, A. 2013. Comparative response of two organic biofilters treating ethylbenzene and toluene after prolonged exposure. *Process Safety and Environmental Protection*, 91, 112-122.
- GALLASTEGUI, G., MUÑOZ, R., BARONA, A., IBARRA-BERASTEGI, G., ROJO, N. & ELÍAS, A. 2011b. Evaluating the impact of water supply strategies on p-xylene biodegradation performance in an organic media-based biofilter. *Journal of Hazardous Materials*, 185, 1019-1026.
- GARCÍA-PEÑA, I., HERNÁNDEZ, S., AURIA, R. & REVAH, S. 2005. Correlation of biological activity and reactor performance in biofiltration of toluene with the fungus *Paecilomyces variotii* CBS115145. *Applied and Environmental Microbiology*, 71, 4280-4285.
- GARCÍA-PEÑA, I., ORTIZ, I., HERNANDEZ, S. & REVAH, S. 2008a. Biofiltration of BTEX by the fungus *Paecilomyces variotii*. *International Biodeterioration & Biodegradation*, 62, 442-447.
- GARCÍA-PEÑA, I., ORTIZ, I., HERNANDEZ, S. & REVAH, S. 2008b. Biofiltration of BTEX by the fungus *Paecilomyces variotii*. *International Biodeterioration & Biodegradation*, 62, 442-447.
- GENTIL, E. C., Aoustin, E. & CHRISTENSEN, T. H. 2009. Greenhouse gas accounting and waste management. *Waste Management & Research*.
- GHANI, A., DEXTER, M. & PERROTT, K. 2003. Hot-water extractable carbon in soils: a sensitive measurement for determining impacts of fertilisation, grazing and cultivation. *Soil Biology and Biochemistry*, 35, 1231-1243.

- GIRARD, M., RAMIREZ, A. A., BUELNA, G. & HEITZ, M. 2011. Biofiltration of methane at low concentrations representative of the piggery industry— Influence of the methane and nitrogen concentrations. *Chemical Engineering Journal*, 168, 151-158.
- GOSTOMSKI, P. A., SISSON, J. B. & CHERRY, R. S. 1997. Water content dynamics in biofiltration: The role of humidity and microbial heat generation. *Journal of the Air and Waste Management Association*, 47, 936-944.
- GROENESTIJN, J. W. & HESSELINK, P. G. M. 1993. Biotechniques for air pollution control. *Biodegradation*, 4, 283-301.
- GROVE, J. A., ZHANG, H., ANDERSON, W. A. & MOO-YOUNG, M. 2009. Estimation of carbon recovery and biomass yield in the biofiltration of octane. *Environmental Engineering Science*, 26, 1497-1502.
- GÜLEZ, G., DECHESNE, A. & SMETS, B. F. 2010. The Pressurized Porous Surface Model: An improved tool to study bacterial behavior under a wide range of environmentally relevant matric potentials. *Journal of Microbiological Methods*, 82, 324-326.
- GÜLEZ, G., DECHESNE, A., WORKMAN, C. T. & SMETS, B. F. 2012. Transcriptome dynamics of *Pseudomonas putida* KT2440 under water stress. *Applied and Environmental Microbiology*, 78, 676-683.
- HAARSTAD, K., BERGERSEN, O. & SØRHEIM, R. 2006. Occurrence of carbon monoxide during organic waste degradation. *Journal of the Air & Waste Management Association*, 56.
- HARRIS, R. 1981. Effect of water potential on microbial growth and activity. *Water potential relations in Soil Microbiology*, 9, 23-95.
- HELLEBRAND, H. J. & SCHADE, G. W. 2008. Carbon Monoxide from Composting due to Thermal Oxidation of Biomass. *Journal of Environmental Quality*, 37, 592-598.
- HOLDEN, P. A., HALVERSON, L. J. & FIRESTONE, M. K. 1997a. Water stress effects on toluene biodegradation by *Pseudomonas putida*. *Biodegradation*, 8, 143-151.

- HOLDEN, P. A., HUNT, J. R. & FIRESTONE, M. K. 1997b. Toluene diffusion and reaction in unsaturated *Pseudomonas putida* biofilms. *Biotechnology and Bioengineering*, 56, 656-670.
- HUREK, T. & REINHOLD-HUREK, B. 1995. Identification of grass-associated and toluene-degrading diazotrophs, *Azoarcus* spp., by analyses of partial 16S ribosomal DNA sequences. *Applied and Environmental Microbiology*, 61, 2257-2261.
- IPCC 2014. *Climate Change 2014: Impacts, Adaptation, and Vulnerability. Part A: Global and Sectoral Aspects. Contribution of Working Group II to the Fifth Assessment Report of the Intergovernmental Panel on Climate Change* [Field, C.B., V.R. Barros, D.J. Dokken, K.J. Mach, M.D. Mastrandrea, T.E. Bilir, M. Chatterjee, K.L. Ebi, Y.O. Estrada, R.C. Genova, B. Girma, E.S. Kissel, A.N. Levy, S. MacCracken, P.R. Mastrandrea, and L.L. White (eds.)], Cambridge, United Kingdom and New York, NY, USA, Cambridge University Press.
- IRANPOUR, R., COX, H. H., DESHUSSES, M. A. & SCHROEDER, E. D. 2005. Literature review of air pollution control biofilters and biotrickling filters for odor and volatile organic compound removal. *Environmental Progress*, 24, 254-267.
- JANG, J. H., HIRAI, M. & SHODA, M. 2004. Styrene degradation by *Pseudomonas* sp. SR-5 in biofilters with organic and inorganic packing materials. *Applied Microbiology and Biotechnology*, 65, 349-355.
- JIANG, T., KENNEDY, M. D., SCHEPPER, V. D., NAM, S.-N., NOPENS, I., VANROLLEGHEM, P. A. & AMY, G. 2010. Characterization of Soluble Microbial Products and Their Fouling Impacts in Membrane Bioreactors. *Environmental Science & Technology*, 44, 6642-6648.
- JIN, Y., GUO, L., VEIGA, M. C. & KENNES, C. 2007. Fungal biofiltration of α -pinene: Effects of temperature, relative humidity, and transient loads. *Biotechnology and Bioengineering*, 96, 433-443.
- JOHNSON, D. R., CORONADO, E., MORENO-FORERO, S. K., HEIPIEPER, H. J. & VAN DER MEER, J. R. 2011. Transcriptome and membrane fatty acid analyses reveal different strategies for responding to permeating and non-

- permeating solutes in the bacterium *Sphingomonas wittichii*. *BMC microbiology*, 11, 250.
- JONES, D. L. & WILLETT, V. B. 2006. Experimental evaluation of methods to quantify dissolved organic nitrogen (DON) and dissolved organic carbon (DOC) in soil. *Soil Biology and Biochemistry*, 38, 991-999.
- JORIO, H., BIBEAU, L. & HEITZ, M. 2000a. Biofiltration of Air Contaminated by Styrene: Effect of Nitrogen Supply, Gas Flow Rate, and Inlet Concentration. *Environmental Science & Technology*, 34, 1764-1771.
- JORIO, H., BIBEAU, L., VIEL, G. & HEITZ, M. 2000b. Effects of gas flow rate and inlet concentration on xylene vapors biofiltration performance. *Chemical Engineering Journal*, 76, 209-221.
- JORIO, H., BRZEZINSKI, R. & HEITZ, M. 2005. A novel procedure for the measurement of the kinetics of styrene biodegradation in a biofilter. *Journal of Chemical Technology and Biotechnology*, 80, 796-804.
- KAKUMANU, M. L. & WILLIAMS, M. A. 2014. Osmolyte dynamics and microbial communities vary in response to osmotic more than matric water deficit gradients in two soils. *Soil Biology and Biochemistry*, 79, 14-24.
- KASTNER, J. R. & DAS, K. C. 2005. Comparison of chemical wet scrubbers and biofiltration for control of volatile organic compounds using GC/MS techniques and kinetic analysis. *Journal of chemical technology and biotechnology*, 80, 1170-1179.
- KATOH, H., ASTHANA, R. & OHMORI, M. 2004. Gene expression in the cyanobacterium *Anabaena* sp. PCC7120 under desiccation. *Microbial ecology*, 47, 164-174.
- KENNES, C. 2012. Biotechniques for air pollution control and bioenergy. *Journal of Chemical Technology & Biotechnology*, 87, 723-724.
- KENNES, C., RENE, E. R. & VEIGA, M. C. 2009. Bioprocesses for air pollution control. *Journal of Chemical Technology and Biotechnology*, 84, 1419-1436.
- KENNES, C. & VEIGA, M. C. 2001. **Bioreactors for Waste Gas Treatment.**
- KHAMMAR, N., MALHAUTIER, L., DEGRANGE, V., LENSİ, R., GODON, J. J. & FANLO, J. L. 2005. Link between spatial structure of microbial

- communities and degradation of a complex mixture of volatile organic compounds in peat biofilters. *Journal of Applied Microbiology*, 98, 476-490.
- KIM, D., CAI, Z. & SORIAL, G. A. 2005a. Behavior of trickle-bed air biofilter for toluene removal: Effect of non-use periods. *Environmental Progress*, 24, 155-161.
- KIM, D., CAI, Z. & SORIAL, G. A. 2005b. Impact of interchanging VOCs on the performance of trickle bed air biofilter. *Chemical Engineering Journal*, 113, 153-160.
- KIM, D., CAI, Z. & SORIAL, G. A. 2005c. Impact of interchanging VOCs on the performance of trickle bed air biofilter. *Chemical Engineering Journal*, 113, 153-160.
- KIM, S. & DESHUSSES, M. A. 2008. Determination of mass transfer coefficients for packing materials used in biofilters and biotrickling filters for air pollution control. 1. Experimental results. *Chemical Engineering Science*, 63, 841-855.
- KOMMEDAL, R., BAKKE, R., DOCKERY, J. & STOODLEY, P. 2001. Modelling production of extracellular polymeric substances in a *Pseudomonas aeruginosa* chemostat culture. *Water Science and Technology*, 43, 129.
- KONG, X., WANG, C. & JI, M. 2013. Analysis of microbial metabolic characteristics in mesophilic and thermophilic biofilters using Biolog plate technique. *Chemical Engineering Journal*, 230, 415-421.
- KRISHNAKUMAR, B., HIMA, A. M. & HARIDAS, A. 2007. Biofiltration of toluene-contaminated air using an agro by-product-based filter bed. *Applied Microbiology and Biotechnology*, 74, 215-220.
- KROUKAMP, O. & WOLFAARDT, G. M. 2009. CO₂ production as an indicator of biofilm metabolism. *Applied and Environmental Microbiology*, 75, 4391-4397.
- LASPIDOU, C. S. & RITTMANN, B. E. 2002. A unified theory for extracellular polymeric substances, soluble microbial products, and active and inert biomass. *Water Research*, 36, 2711-2720.
- LE BIHAN, Y. & LESSARD, P. 2000. Monitoring biofilter clogging: biochemical characteristics of the biomass. *Water Research*, 34, 4284-4294.

- LEBLANC, J. C., GONÇALVES, E. R. & MOHN, W. W. 2008. Global response to desiccation stress in the soil actinomycete *Rhodococcus jostii* RHA1. *Applied and environmental microbiology*, 74, 2627-2636.
- LEBRERO, R., ESTRADA, J. M., MUÑOZ, R. & QUIJANO, G. 2012. Toluene mass transfer characterization in a biotrickling filter. *Biochemical Engineering Journal*, 60, 44-49.
- LEDDY, M. B., PHIPPS, D. W. & RIDGWAY, H. F. 1995. Catabolite-mediated mutations in alternate toluene degradative pathways in *Pseudomonas putida*. *Journal of Bacteriology*, 177, 4713-4720.
- LESON, G. & WINER, A. M. 1991. Biofiltration: an innovative air pollution control technology for VOC emissions. *Journal of the Air & Waste Management Association*, 41, 1045-1054.
- LI, G. W., HU, H. Y., HAO, J. M. & FUJIE, K. 2002. Use of Biological Activated Carbon to Treat Mixed Gas of Toluene and Benzene in Biofilter. *Environmental Technology*, 23, 467-477.
- LONG, T. & OR, D. 2009. Dynamics of Microbial Growth and Coexistence on Variably Saturated Rough Surfaces. *Microbial Ecology*, 58, 262-275.
- LU, C., LIN, M.-R. & CHU, C. 1999. Temperature effects of trickle-bed biofilter for treating BTEX vapors. *Journal of Environmental Engineering*, 125, 775-779.
- LUVSANJAMBA, M., SERCU, B., KERTÉSZ, S. & VAN LANGENHOVE, H. 2007. Thermophilic biotrickling filtration of a mixture of isobutyraldehyde and 2-pentanone. *Journal of Chemical Technology & Biotechnology*, 82, 74-80.
- MAESTRE, J. P., GAMISANS, X., GABRIEL, D. & LAFUENTE, J. 2007. Fungal biofilters for toluene biofiltration: Evaluation of the performance with four packing materials under different operating conditions. *Chemosphere*, 67, 684-692.
- MAGBANUA, B. S. & BOWERS, A. R. 2006. Characterization of soluble microbial products (SMP) derived from glucose and phenol in dual substrate activated sludge bioreactors. *Biotechnology and Bioengineering*, 93, 862-870.

- MALDONADO-DIAZ, G. & ARRIAGA, S. 2015. Biofiltration of high formaldehyde loads with ozone additions in long-term operation. *Applied Microbiology and Biotechnology*, 99, 43-53.
- MALHAUTIER, L., KHAMMAR, N., BAYLE, S. & FANLO, J.-L. 2005. Biofiltration of volatile organic compounds. *Applied Microbiology and Biotechnology*, 68, 16-22.
- MANZONI, S., SCHIMEL, J. P. & PORPORATO, A. 2011. Responses of soil microbial communities to water stress: results from a meta-analysis. *Ecology*, 93, 930-938.
- MATTEAU, Y. & RAMSAY, B. 1997. Active compost biofiltration of toluene. *Biodegradation*, 8, 135-141.
- MCGARRY, J. 1983. Correlation and prediction of the vapor pressures of pure liquids over large pressure ranges. *Industrial & Engineering Chemistry Process Design and Development*, 22, 313-322.
- MENG, F., CHAE, S. R., DREWS, A., KRAUME, M., SHIN, H. S. & YANG, F. 2009. Recent advances in membrane bioreactors (MBRs): Membrane fouling and membrane material. *Water Research*, 43, 1489-1512.
- MIRPURI, R., JONES, W. & BRYERS, J. D. 1997. Toluene degradation kinetics for planktonic and biofilm-grown cells of *Pseudomonas putida* 54G. *Biotechnology and Bioengineering*, 53, 535-546.
- MOE, W. M. & IRVINE, R. L. 2001. Effect of Nitrogen Limitation on Performance of Toluene Degrading Biofilters. *Water Research*, 35, 1407-1414.
- MOHAMMAD, B. T., VEIGA, M. C. & KENNES, C. 2007. Mesophilic and thermophilic biotreatment of BTEX-polluted air in reactors. *Biotechnology and Bioengineering*, 97, 1423-1438.
- MØLLER, S., PEDERSEN, A. R., POULSEN, L. K., ARVIN, E. & MOLIN, S. 1996. Activity and three-dimensional distribution of toluene-degrading *Pseudomonas putida* in a multispecies biofilm assessed by quantitative in situ hybridization and scanning confocal laser microscopy. *Applied and Environmental Microbiology*, 62, 4632-4640.

- MONTES, M., VEIGA, M. C. & KENNES, C. 2014. Optimization of the performance of a thermophilic biotrickling filter for α -pinene removal from polluted air. *Environmental Technology*, 35, 2466-2475.
- MORALES 1998. Start-up and the effect of gaseous ammonia additions on a biofilter for the elimination of toluene vapors. *Biotechnology and Bioengineering*, 60, 483-491.
- MORALES, M., HERNÁNDEZ, S., CORNABÉ, T., REVAH, S. & AURIA, R. 2003. Effect of drying on biofilter performance: modeling and experimental approach. *Environmental Science & Technology*, 37, 985-992.
- MORGENROTH, E., SCHROEDER, E. D., CHANG, D. P. Y. & SCOW, K. M. 1996. Nutrient limitation in a compost biofilter degrading hexane. *Journal of the Air & Waste Management Association*, 46, 300-308.
- MOUSSAVI, G., BAHADORI, M. B., FARZADKIA, M., YAZDANBAKHSH, A. & MOHSENI, M. 2009. Performance evaluation of a thermophilic biofilter for the removal of MTBE from waste air stream: Effects of inlet concentration and EBRT. *Biochemical Engineering Journal*, 45, 152-156.
- MUDLIAR, S., GIRI, B., PADOLEY, K., SATPUTE, D., DIXIT, R., BHATT, P., PANDEY, R., JUWARKAR, A. & VAIDYA, A. 2010a. Bioreactors for treatment of VOCs and odours—a review. *Journal of Environmental Management*, 91, 1039-1054.
- MUDLIAR, S., GIRI, B., PADOLEY, K., SATPUTE, D., DIXIT, R., BHATT, P., PANDEY, R., JUWARKAR, A. & VAIDYA, A. 2010b. Bioreactors for treatment of VOCs and odours – A review. *Journal of Environmental Management*, 91, 1039-1054.
- MUÑOZ, R., HERNÁNDEZ, M., SEGURA, A., GOUVEIA, J., ROJAS, A., RAMOS, J. & VILLAVARDE, S. 2009. Continuous cultures of *Pseudomonas putida* mt-2 overcome catabolic function loss under real case operating conditions. *Applied Microbiology and Biotechnology*, 83, 189-198.
- MUÑOZ, R., MALHAUTIER, L., FANLO, J.-L. & QUIJANO, G. 2015. Biological technologies for the treatment of atmospheric pollutants. *International Journal of Environmental Analytical Chemistry*, 95, 950-967.

- MYSLIWIEC, M. J., VANDERGHEYNST, J. S., RASHID, M. M. & SCHROEDER, E. D. 2001. Dynamic volume-averaged model of heat and mass transport within a compost biofilter: I. Model development. *Biotechnology and bioengineering*, 73, 282-294.
- NADARAJAH, N., ALLEN, D. G. & FULTHORPE, R. R. 2007. Effects of transient temperature conditions on the divergence of activated sludge bacterial community structure and function. *Water Research*, 41, 2563-2571.
- NAMKUNG, E. & RITTMANN, B. E. 1986. Soluble microbial products (SMP) formation kinetics by biofilms. *Water Research*, 20, 795-806.
- NEDWELL, D. 1999. Effect of low temperature on microbial growth: lowered affinity for substrates limits growth at low temperature. *FEMS Microbiology Ecology*, 30, 101-111.
- NELSON, G. O. 1971. Controlled test atmospheres; principles and techniques. *Controlled test atmospheres; principles and techniques*. Ann Arbor Science.
- NI, B.-J. & YU, H.-Q. 2011. Microbial Products of Activated Sludge in Biological Wastewater Treatment Systems: A Critical Review. *Critical Reviews in Environmental Science and Technology*, 42, 187-223.
- NIELSEN, P. H., JAHN, A. & PALMGREN, R. 1997. Conceptual model for production and composition of exopolymers in biofilms. *Water Science and Technology*, 36, 11-19.
- NIKIEMA, J., BRZEZINSKI, R. & HEITZ, M. 2007a. Elimination of methane generated from landfills by biofiltration: a review. *Reviews in Environmental Science and Biotechnology*, 6, 261-284.
- NIKIEMA, J., DASTOUS, P.-A. & HEITZ, M. 2007b. Elimination of Volatile Organic Compounds by Biofiltration: A Review. *Reviews on environmental health*, 22, 273-294.
- NIKOLOVA, N. & NENOV, V. 2005. BTEX degradation by fungi. *Water Science & Technology*, 51, 87-93.
- O'DONNELL, A. G., YOUNG, I. M., RUSHTON, S. P., SHIRLEY, M. D. & CRAWFORD, J. W. 2007. Visualization, modelling and prediction in soil microbiology. *Nat Rev Micro*, 5, 689-699.

- OR, D., PHUTANE, S. & DECHESNE, A. 2007a. Extracellular Polymeric Substances Affecting Pore-Scale Hydrologic Conditions for Bacterial Activity in Unsaturated Soils. *Vadose Zone Journal*, 6, 298-305.
- OR, D., SMETS, B. F., WRAITH, J. M., DECHESNE, A. & FRIEDMAN, S. P. 2007b. Physical constraints affecting bacterial habitats and activity in unsaturated porous media – a review. *Advances in Water Resources*, 30, 1505-1527.
- PAPENDICK, R. I. & CAMPBELL, G. S. 1981. Theory and Measurement of Water Potential¹. In: PARR, J. F., GARDNER, W. R. & ELLIOTT, L. F. (eds.) *Water Potential Relations in Soil Microbiology*. Soil Science Society of America.
- PEDERSEN, A. R., MØLLER, S., MOLIN, S. & ARVIN, E. 1997. Activity of toluene-degrading *Pseudomonas putida* in the early growth phase of a biofilm for waste gas treatment. *Biotechnology and Bioengineering*, 54, 131-141.
- PELZ, O., TESAR, M., WITTICH, R. M., MOORE, E. R., TIMMIS, K. N. & ABRAHAM, W. R. 1999. Towards elucidation of microbial community metabolic pathways: unravelling the network of carbon sharing in a pollutant-degrading bacterial consortium by immunocapture and isotopic ratio mass spectrometry. *Environmental Microbiology*, 1, 167-174.
- PICONE, S., GROTENHUIS, T., VAN GAANS, P., VALSTAR, J., LANGENHOFF, A. & RIJNAARTS, H. 2013. Toluene biodegradation rates in unsaturated soil systems versus liquid batches and their relevance to field conditions. *Applied Microbiology and Biotechnology*, 97, 7887-7898.
- PIRT, S. 1982. Maintenance energy: a general model for energy-limited and energy-sufficient growth. *Archives of Microbiology*, 133, 300-302.
- PITZER, K. S. & SCOTT, D. W. 1943. The Thermodynamics and Molecular Structure of Benzene and Its Methyl Derivatives¹. *Journal of the American Chemical Society*, 65, 803-829.
- POBLETE-CASTRO, I., ESCAPA, I. F., JÄGER, C., PUCHALKA, J., LAM, C. M. C., SCHOMBURG, D., PRIETO, M. A. & DOS SANTOS, V. A. M. 2012. The metabolic response of *P. putida* KT2442 producing high levels of

- polyhydroxyalkanoate under single-and multiple-nutrient-limited growth: Highlights from a multi-level omics approach. *Microb Cell Fact*, 11, 34.
- PRENAFETA-BOLDÚ, F. X., ILLA, J., VAN GROENESTIJN, J. W. & FLOTATS, X. 2008. Influence of synthetic packing materials on the gas dispersion and biodegradation kinetics in fungal air biofilters. *Applied Microbiology and Biotechnology*, 79, 319-327.
- PRENAFETA-BOLDÚ, F. X., GUIVERNAU, M., GALLASTEGUI, G., VIÑAS, M., HOOG, G. S. & ELÍAS, A. 2012. Fungal/bacterial interactions during the biodegradation of TEX hydrocarbons (toluene, ethylbenzene and p-xylene) in gas biofilters operated under xerophilic conditions. *FEMS Microbiology Ecology*, 80, 722-734.
- RALEBITSO-SENIOR, T. K., SENIOR, E., DI FELICE, R. & JARVIS, K. 2012. Waste gas biofiltration: advances and limitations of current approaches in microbiology. *Environmental science & technology*, 46, 8542-8573.
- RAS, M., LEFEBVRE, D., DERLON, N., PAUL, E. & GIRBAL-NEUHAUSER, E. 2011. Extracellular polymeric substances diversity of biofilms grown under contrasted environmental conditions. *Water Research*, 45, 1529-1538.
- REIS, M. A. M., SERAFIM, L. S., LEMOS, P. C., RAMOS, A. M., AGUIAR, F. R. & VAN LOOSDRECHT, M. C. M. 2003. Production of polyhydroxyalkanoates by mixed microbial cultures. *Bioprocess and Biosystems Engineering*, 25, 377-385.
- REN, S. & FRYMIER, P. D. 2002. Estimating the toxicities of organic chemicals to bioluminescent bacteria and activated sludge. *Water Research*, 36, 4406-4414.
- RENE, E. R., KAR, S., KRISHNAN, J., PAKSHIRAJAN, K., LÓPEZ, M. E., MURTHY, D. & SWAMINATHAN, T. 2015. Start-up, performance and optimization of a compost biofilter treating gas-phase mixture of benzene and toluene. *Bioresource Technology*, 190, 529-535.
- ROBERSON, E. B. & FIRESTONE, M. K. 1992. Relationship between desiccation and exopolysaccharide production in a soil *Pseudomonas* sp. *Applied and Environmental Microbiology*, 58, 1284.
- ROSENBERGER, S., LAABS, C., LESJEAN, B., GNIRSS, R., AMY, G., JEKEL, M. & SCHROTTER, J. C. 2006. Impact of colloidal and soluble organic material

- on membrane performance in membrane bioreactors for municipal wastewater treatment. *Water Research*, 40, 710-720.
- RUSSELL, J. B. & COOK, G. M. 1995. Energetics of bacterial growth: balance of anabolic and catabolic reactions. *Microbiological Reviews*, 59, 48-62.
- RYU, H.-W., YOO, S.-K., CHOI, J. M., CHO, K.-S. & CHA, D. K. 2009. Thermophilic biofiltration of H₂S and isolation of a thermophilic and heterotrophic H₂S-degrading bacterium, *Bacillus* sp. TSO3. *Journal of Hazardous Materials*, 168, 501-506.
- SAKUMA, T., HATTORI, T. & DESHUSSES, M. A. 2006. Comparison of Different Packing Materials for the Biofiltration of Air Toxics. *Journal of the Air & Waste Management Association*, 56, 1567-1575.
- SAKUMA, T., HATTORI, T. & DESHUSSES, M. A. 2009. The effects of a lower irrigation system on pollutant removal and on the microflora of a biofilter. *Environmental Technology*, 30, 621-627.
- SCHIMEL, J., BALSER, T. C. & WALLENSTEIN, M. 2007. Microbial stress-response physiology and its implications for ecosystem function. *Ecology*, 88, 1386-1394.
- SCHINK, B. 2002. Synergistic interactions in the microbial world. *Antonie Van Leeuwenhoek*, 81, 257-261.
- SCHMITT, J., NIVENS, D., WHITE, D. C. & FLEMMING, H. C. 1995. Changes of biofilm properties in response to sorbed substances-an FTIR-ATR study. *Water Science and Technology*, 32, 149-156.
- SCHWARZER, G. 2015. Meta: general package for meta-analysis. *R package version*, 4.1-0.
- SHAREEFDEEN, Z. & BALTZIS, B. C. 1994. Biofiltration of toluene vapor under steady-state and transient conditions: Theory and experimental results. *Chemical Engineering Science*, 49, 4347-4360.
- SHAREEFDEEN, Z., SHAIKH, A. A. & AHMED, A. 2009. Steady-state biofilter performance under non-isothermal conditions. *Chemical Engineering and Processing: Process Intensification*, 48, 1040-1046.

- SHROUT, J. D. & NERENBERG, R. 2012. Monitoring Bacterial Twitter: Does Quorum Sensing Determine the Behavior of Water and Wastewater Treatment Biofilms? *Environmental Science & Technology*, 46, 1995-2005.
- SINGH, R., PAUL, D. & JAIN, R. K. 2006a. Biofilms: implications in bioremediation. *TRENDS in Microbiology*, 14, 389-397.
- SINGH, R., RAI, B. & UPADHYAY, S. 2006b. Performance evaluation of an agro waste based biofilter treating toluene vapours. *Environmental Technology*, 27, 349-357.
- SONG, J. & KINNEY, K. A. 2000. Effect of vapor-phase bioreactor operation on biomass accumulation, distribution, and activity: Linking biofilm properties to bioreactor performance. *Biotechnology and Bioengineering*, 68, 508-516.
- SONG, J. & KINNEY, K. A. 2005. Microbial response and elimination capacity in biofilters subjected to high toluene loadings. *Applied Microbiology and Biotechnology*, 68, 554-559.
- SONG, J. H., RAMIREZ, J. & KINNEY, K. A. 2003. Nitrogen utilization in a vapor-phase biofilter. *Water Research*, 37, 4497-4505.
- STRATHMANN, M., WINGENDER, J. & FLEMMING, H.-C. 2002. Application of fluorescently labelled lectins for the visualization and biochemical characterization of polysaccharides in biofilms of *Pseudomonas aeruginosa*. *Journal of Microbiological Methods*, 50, 237-248.
- SUN, D., LI, J., XU, M., AN, T., SUN, G. & GUO, J. 2013. Toluene removal efficiency, process robustness, and bacterial diversity of a biotrickling filter inoculated with *Burkholderia sp.* Strain T3. *Biotechnology and Bioprocess Engineering*, 18, 125-134.
- SUN, Y., QUAN, X., CHEN, J., YANG, F., XUE, D., LIU, Y. & YANG, Z. 2002. Toluene vapour degradation and microbial community in biofilter at various moisture content. *Process Biochemistry*, 38, 109-113.
- SUTHERLAND, I. W. 2001. The biofilm matrix—an immobilized but dynamic microbial environment. *TRENDS in Microbiology*, 9, 222-227.
- TEAM, R. C. 2015. R: A language and environment for statistical computing. Vienna, Austria; 2014. URL <http://www.R-project.org>.

- TRESSE, O., LESCOB, S. & RHO, D. 2003. Dynamics of living and dead bacterial cells within a mixed-species biofilm during toluene degradation in a biotrickling filter. *Journal of Applied Microbiology*, 94, 849-854.
- TSO, S.-F. & TAGHON, G. L. 2006. Protozoan grazing increases mineralization of naphthalene in marine sediment. *Microbial Ecology*, 51, 460-469.
- VAN BODEGOM, P. 2007. Microbial maintenance: a critical review on its quantification. *Microbial Ecology*, 53, 513-523.
- VAN DE MORTEL, M. & HALVERSON, L. J. 2004. Cell envelope components contributing to biofilm growth and survival of *Pseudomonas putida* in low-water content habitats. *Molecular Microbiology*, 52, 735-750.
- VANCE, E., BROOKES, P. & JENKINSON, D. 1987. An extraction method for measuring soil microbial biomass C. *Soil Biology and Biochemistry*, 19, 703-707.
- VEIGA, M. & KENNES, C. 2001. Parameters affecting performance and modeling of biofilters treating alkylbenzene-polluted air. *Applied Microbiology and Biotechnology*, 55, 254-258.
- VELÁZQUEZ, F., PFLÜGER, K., CASES, I., DE EUGENIO, L. I. & DE LORENZO, V. 2007. The phosphotransferase system formed by PtsP, PtsO, and PtsN proteins controls production of polyhydroxyalkanoates in *Pseudomonas putida*. *Journal of Bacteriology*, 189, 4529-4533.
- VERGARA-FERNÁNDEZ, A., LARA MOLINA, L., PULIDO, N. A. & AROCA, G. 2007a. Effects of gas flow rate, inlet concentration and temperature on the biofiltration of toluene vapors. *Journal of Environmental Management*, 84, 115-122.
- VERGARA-FERNÁNDEZ, A., MOLINA, L. L., PULIDO, N. A. & AROCA, G. 2007b. Effects of gas flow rate, inlet concentration and temperature on the biofiltration of toluene vapors. *Journal of Environmental Management*, 84, 115-122.
- VERGARA-FERNÁNDEZ, A., SALGADO-ÍSMODES, V., PINO, M., HERNÁNDEZ, S. & REVAH, S. 2012. Temperature and moisture effect on spore emission in the fungal biofiltration of hydrophobic VOCs. *Journal of Environmental Science and Health, Part A*, 47, 605-613.
- VIGUERAS, G., SHIRAI, K., MARTINS, D., FRANCO, T. T., FLEURI, L. F. & REVAH, S. 2008. Toluene gas phase biofiltration by *Paecilomyces lilacinus* and

- isolation and identification of a hydrophobin protein produced thereof. *Applied microbiology and biotechnology*, 80, 147-154.
- VILLAVERDE, S. & FERNÁNDEZ, M. T. 1997. Non-toluene-associated respiration in a *Pseudomonas putida* 54G biofilm grown on toluene in a flat-plate vapor-phase bioreactor *Applied Microbiology and Biotechnology*, 48, 357-362.
- VILLAVERDE, S., MIRPURI, R. G., LEWANDOWSKI, Z. & JONES, W. L. 1997. Physiological and chemical gradients in a *Pseudomonas putida* 54G biofilm degrading toluene in a flat plate vapor phase bioreactor. *Biotechnology and Bioengineering*, 56, 361-371.
- VON STOCKAR, U., MASKOW, T., LIU, J., MARISON, I. W. & PATINO, R. 2006. Thermodynamics of microbial growth and metabolism: an analysis of the current situation. *Journal of Biotechnology*, 121, 517-533.
- WALLENSTEIN, M. D. & HALL, E. K. 2012. A trait-based framework for predicting when and where microbial adaptation to climate change will affect ecosystem functioning. *Biogeochemistry*, 109, 35-47.
- WANG, C., KONG, X. & ZHANG, X.-Y. 2012. Mesophilic and thermophilic biofiltration of gaseous toluene in a long-term operation: Performance evaluation, biomass accumulation, mass balance analysis and isolation identification. *Journal of Hazardous Materials*, 229–230, 94-99.
- WATANABE, K. & HAMAMURA, N. 2003. Molecular and physiological approaches to understanding the ecology of pollutant degradation. *Current Opinion in Biotechnology*, 14, 289-295.
- WEBER, F. J. & HARTMANS, S. 1996. Prevention of clogging in a biological trickle-bed reactor removing toluene from contaminated air. *Biotechnology and Bioengineering*, 50, 91-7.
- WEISBERG, S. 2005. *Applied linear regression*, John Wiley & Sons.
- WILSHUSEN, J. H., HETTIARATCHI, J. P. A., DE VISSCHER, A. & SAINT-FORT, R. 2004. Methane oxidation and formation of EPS in compost: effect of oxygen concentration. *Environmental Pollution*, 129, 305-314.
- WOERTZ, J., VAN HEININGEN, W., VAN EEKERT, M., KRAAKMAN, N., KINNEY, K. & VAN GROENESTIJN, J. 2002. Dynamic bioreactor

- operation: effects of packing material and mite predation on toluene removal from off-gas. *Applied microbiology and biotechnology*, 58, 690-694.
- XAVIER, J., PICIOREANU, C. & VAN LOOSDRECHT, M. 2004. A modelling study of the activity and structure of biofilms in biological reactors. *Biofilms*, 1, 377-391.
- XAVIER, J. B. & FOSTER, K. R. 2007. Cooperation and conflict in microbial biofilms. *Proceedings of the National Academy of Sciences*, 104, 876-881.
- XI, J., HU, H.-Y. & QIAN, Y. 2006. Effect of operating conditions on long-term performance of a biofilter treating gaseous toluene: Biomass accumulation and stable-run time estimation. *Biochemical Engineering Journal*, 31, 165-172.
- XIAO, J. & VANBRIESEN, J. M. 2006. Expanded thermodynamic model for microbial true yield prediction. *Biotechnology and Bioengineering*, 93, 110-121.
- YANG, C., CHEN, H., ZENG, G., YU, G. & LUO, S. 2010. Biomass accumulation and control strategies in gas biofiltration. *Biotechnology Advances*, 28, 531-540.
- YANG, H., MINUTH, B. & ALLEN, D. G. 2002. Effects of Nitrogen and Oxygen on Biofilter Performance. *Journal of the Air & Waste Management Association*, 52, 279-286.
- YE, F., PENG, G. & LI, Y. 2011. Influences of influent carbon source on extracellular polymeric substances (EPS) and physicochemical properties of activated sludge. *Chemosphere*, 84, 1250-1255.
- YOON, I.-K. & PARK, C.-H. 2002. Effects of gas flow rate, inlet concentration and temperature on biofiltration of volatile organic compounds in a peat-packed biofilter. *Journal of Bioscience and Bioengineering*, 93, 165-169.
- YOU-QING, L., HONG-FANG, L., ZHEN-LE, T., LI-HUA, Z., YING-HUI, W. & HE-QING, T. 2008. Diesel pollution biodegradation: synergetic effect of Mycobacterium and filamentous fungi. *Biomedical and Environmental Sciences*, 21, 181-187.
- YU, H., KIM, B. J. & RITTMANN, B. E. 2001. The roles of intermediates in biodegradation of benzene, toluene, and p-xylene by *Pseudomonas putida* F1. *Biodegradation*, 12, 455-463.

- ZAFAR, M., KUMAR, S., DHIMAN, A. & PARK, H.-S. 2014. Maintenance-energy-dependent dynamics of growth and poly (3-hydroxybutyrate)[P (3HB)] production by *Azohydromonas lata* MTCC 2311 using simple and renewable carbon substrates. *Brazilian Journal of Chemical Engineering*, 31, 313-323.
- ZAMIR, S. M., FERDOWSI, M. & HALLADJ, R. 2014. Effects of Loading Type and Temperature on Performance, Transient Operation, and Kinetics of n-Hexane Vapor Removal in a Biofilter. *Water, Air, & Soil Pollution*, 225, 1-10.
- ZHANG, X. & BISHOP, P. L. 2003. Biodegradability of biofilm extracellular polymeric substances. *Chemosphere*, 50, 63-69.
- ZHU, X., SUIDAN, M. T., PRUDEN, A., YANG, C., ALONSO, C., KIM, B. J. & KIM, B. R. 2004. Effect of substrate Henry's constant on biofilter performance. *Journal of the Air & Waste Management Association*, 54, 409-418.

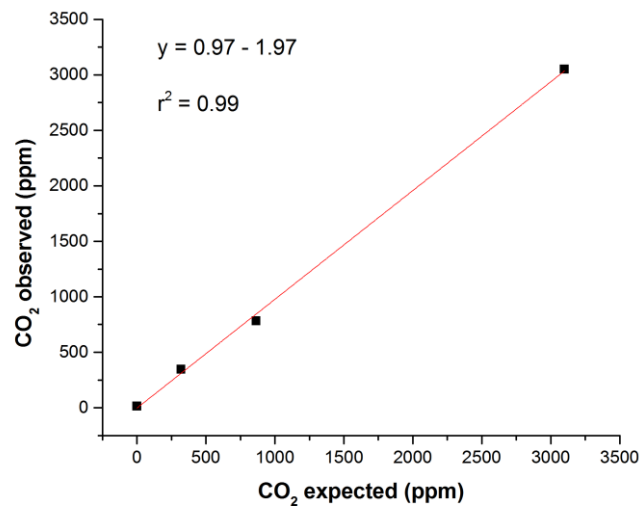
Appendices

A.1 CO₂ Calibration data

CO₂ was analysed using the GMP343 Carbon dioxide probe (Vaisala, Finland). The carbon dioxide probe was calibrated against a bottled nitrogen and a standard CO₂ calibration cylinder (3000 ppm). High purity nitrogen gas was used for calibrating the zero value. For calibrating the CO₂ sensor, an accurate mixture of nitrogen and standard CO₂ calibration gas was produced using a gas mixing unit. The operating temperature was ambient and the mass flow was set at a pressure of 200 kPa. The calibration results for measurement range 0-3000 ppm are presented in

Appendix. Table 1: CO₂ calibration data for the analyser.

Reference Gas (ppm)	Observed Gas (ppm)
0	13.07
320	346
865	782
3100	3050



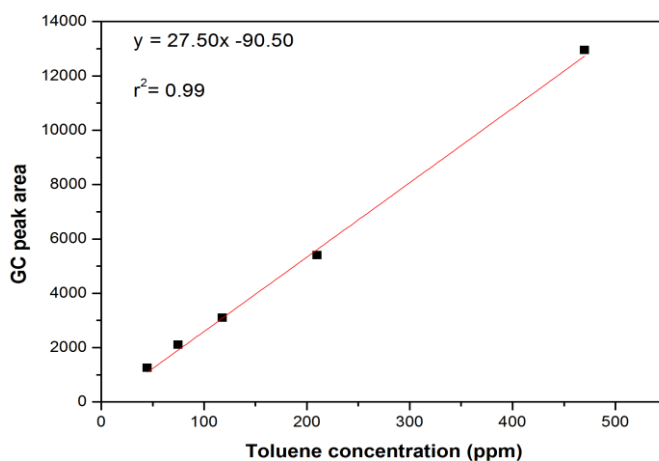
A I: CO₂ calibration curve for GMP343 sensor.

A.2 GC Calibration data

The Gas chromatography (GC) instrument (SRI-8610C,SRI Instrument) fitted with a FID detector and a MXT-15m capillary column (Restek Corporation, US). Calibration curve was generated using known volume of liquid toluene in tedlar bags (500-5L). This was used in conjunction with a standard toluene calibration cylinder (220 ppm, BOC gases, New Zealand). Calibration data is presented in Appendix. Table 2 and Curve is presented in A II

Appendix. Table 2: GC calibration curve data for toluene

ppm	Peak area	Toluene (μ L)	ml air
470	12950	2	500
210	5400	1	1000
118	3100	1	2000
75	2100	1	3000
45	1250	1	5000



A II : Calibration curve generated for toluene.

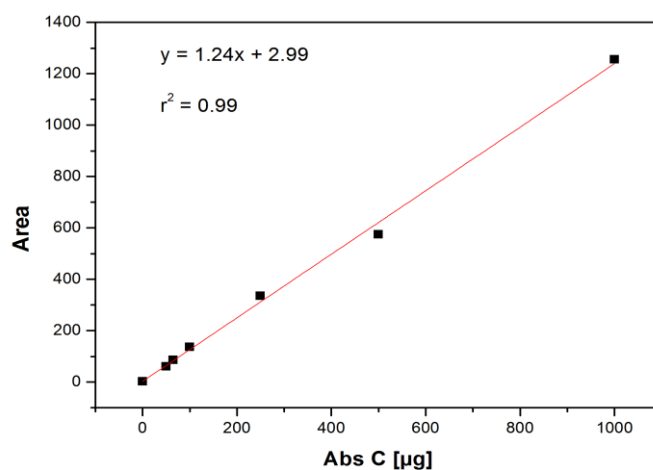
A.3 Carbon content analysis for the liquid and solid phase

A.3.1 Shimadzu TOC-L unit Calibration data for total carbon (TC)

The Shimadzu TOC-L series with auto sampler ASI-L unit was used for carbon content analysis in the liquid samples. The total carbon (TC) standard solution was prepared by accurately weighing 2.125 g of reagent grade potassium hydrogen phthalate. The standard was dried in the oven at 105°C for 1 hour and was kept in a desiccator prior to use. 1L of stock solution (1000mgC/L) was prepared using RO water (Appendix. Table 3). This was subsequently used to prepare diluted solutions as per requirement. Calibration curve is presented in A III.

Appendix. Table 3 : Calibration data for TC of the liquid sample analysis.

TC (mgC/L)	Area
0	2.2
50	60.14
75	85.73
100	136.9
250	334.7
500	574.9
1000	1256



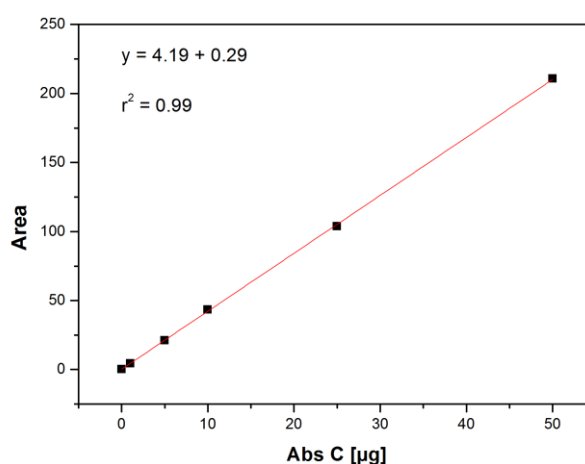
A III : Calibration curve for TC content analysis for liquid sample with TOC-L

A.3.2 Shimadzu TOC-L unit Calibration data for inorganic carbon (IC)

The total carbon (TC) standard solution was prepared by accurately weighing 3.50 g of reagent grade sodium hydrogen carbonate and 4.41 g of sodium carbonate previously dried 1 hour at 105 °C prior . The stand was dried in the oven at 105°C for 1 hour and was kept in a desiccator prior to use. 1L of stock solution (1000mgC/L) was prepared using RO water to give a final concentration of (1000 mgC/L) (Appendix. Table 4). Dilutions were similarly made as discussed before for calibration. The calibration curve is presented in

Appendix. Table 4 : Calibration data for TC of the liquid sample analysis.

IC (mgC/L)	Area
0	0.329
1	4.56
5	21.02
10	43.38
25	103.7
50	210.7



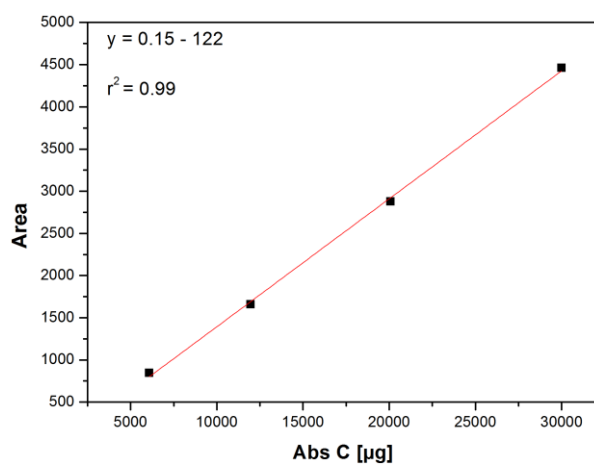
A IV: Calibration curve for IC content analysis for liquid sample with TOC-L

A.3.2: Shimadzu SSM-5000A unit calibration data for total carbon (TC)

The shimadzu solid sample combustion unit was used for soil/biofilm carbon content analysis. It can measure up to 1g sample containing 30 mgC. Standard d-Glucose anhydrous Pronalys AR ACS (Labserv) was used for calibration the SSM. Ceramic boats were thoroughly cleaned and run as blank to get rid of any residual carbon from the boats. Glucose (40% C) was used in varying weight to generate a calibration curve.

Appendix. Table 5 : Calibration data for TC of the solid sample analysis.

Glucose standard (mg)	Area
75	4461
50	2877
29.4	1657
15.2	844.4



A V: Calibration curve for TC content analysis for solid sample with SSM 5000A.

A.4 Supplementary data for ANOVA analysis

A.4.1: 3X3 factorial analysis for temperature and substrate concentration influencing CO₂ (Chapter 5. Table 5-2)

Linear model calculated from R.

A.4.1.1 ANOVA table of summary and linear model for temperature and substrate (toluene).

	Df	Sum Sq	Mean Sq	F value	Pr(>F)	
Temperature	2	1578	789	33.76	3.52e-12	***
Substrate	2	9068	4534	194.09	< 2e-16	***
Temperature:Substrate	4	1182	296	12.65	1.62e-08	***
Residuals	111	2593	23			

Signif. codes: 0 '***' 0.001 '**' 0.01 '*' 0.05 '.' 0.1 ' ' 1

Call:

```
aov(formula = CO2 ~ Temperature * Substrate)
```

Residuals:

Min	1Q	Median	3Q	Max
-10.8854	-2.9984	0.0123	2.4628	13.8002

Coefficients:

	Estimate	Std. Error	t value	Pr(> t)
(Intercept)	71.170	1.081	65.851	< 2e-16

Temperature30	-4.302	1.872	-2.298	0.023417
*				
Temperature40	12.555	1.528	8.214	4.33e-13

Substrate193	-14.021	1.872	-7.490	1.77e-11

Substrate75	5.687	1.872	3.038	0.002969
**				
Temperature30:Substrate193	12.335	2.859	4.314	3.50e-05

Temperature40:Substrate193	-5.759	2.417	-2.383	0.018879
*				
Temperature30:Substrate75	10.184	2.859	3.562	0.000544

Temperature40:Substrate75	1.547	2.647	0.584	0.560136

Signif. codes: 0 '***' 0.001 '**' 0.01 '*' 0.05 '.' 0.1 ' ' 1

Residual standard error: 4.833 on 111 degrees of freedom

Multiple R-squared: 0.8202, Adjusted R-squared: 0.8072

F-statistic: 63.29 on 8 and 111 DF, p-value: < 2.2e-16

A.4.1.2 Tukey HSD table

Simultaneous Tests for General Linear Hypotheses

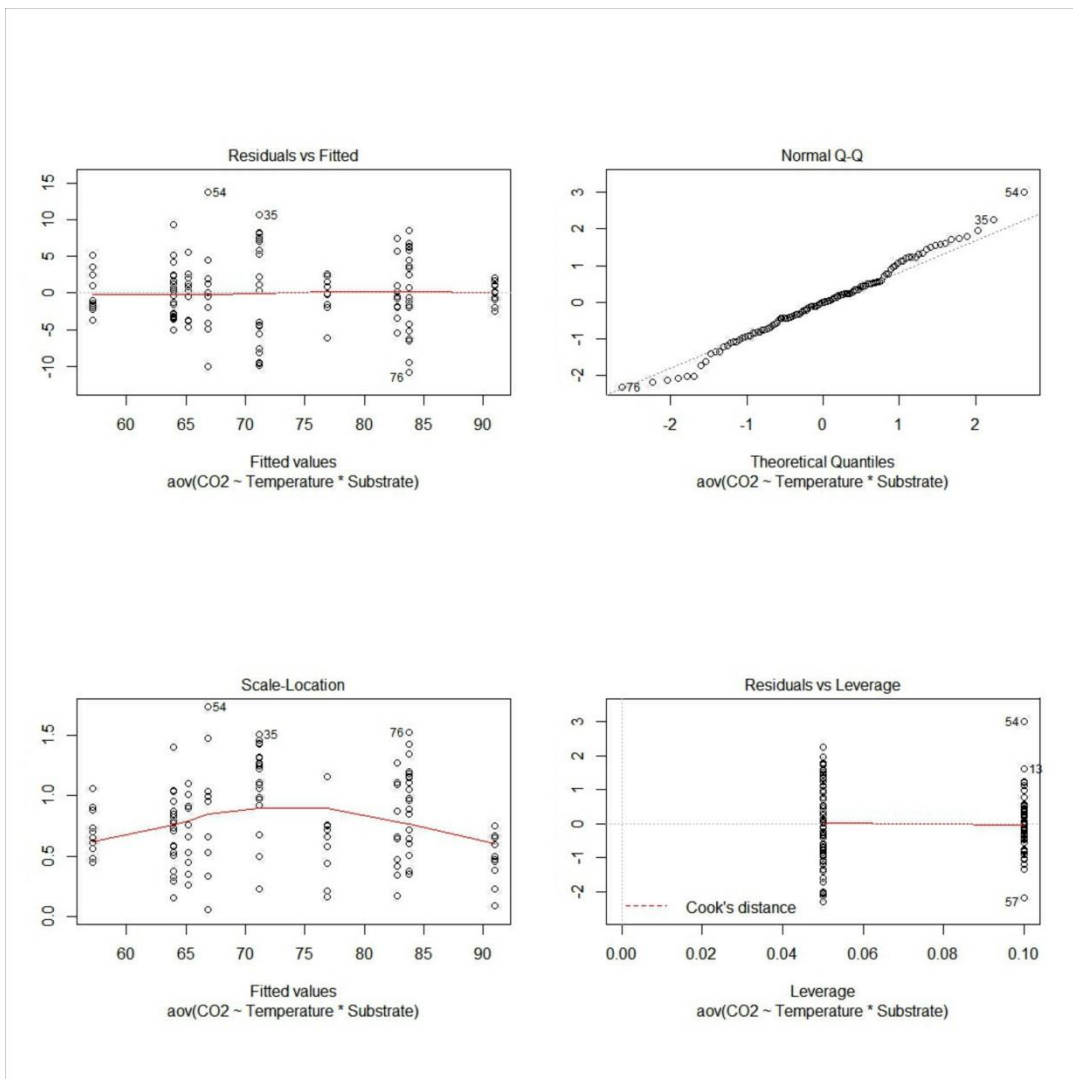
Multiple Comparisons of Means: Tukey Contrasts

Fit: aov(formula = CO2 ~ PairwiseComparison)

Linear Hypotheses:

	Estimate	Std. Error	t value	Pr(> t)	
30.120 - 20.120 == 0	-4.302	1.872	-2.298	0.34627	
40.120 - 20.120 == 0	12.555	1.528	8.214	< 0.001	***
20.193 - 20.120 == 0	-14.021	1.872	-7.490	< 0.001	***
30.193 - 20.120 == 0	-5.988	1.872	-3.199	0.04416	*
40.193 - 20.120 == 0	-7.224	1.528	-4.726	< 0.001	***
20.75 - 20.120 == 0	5.687	1.872	3.038	0.06888	.
30.75 - 20.120 == 0	11.569	1.872	6.180	< 0.001	***
40.75 - 20.120 == 0	19.790	1.872	10.572	< 0.001	***
40.120 - 30.120 == 0	16.858	1.872	9.005	< 0.001	***
20.193 - 30.120 == 0	-9.719	2.162	-4.496	< 0.001	***
30.193 - 30.120 == 0	-1.686	2.162	-0.780	0.99710	
40.193 - 30.120 == 0	-2.922	1.872	-1.561	0.81956	
20.75 - 30.120 == 0	9.990	2.162	4.621	< 0.001	***
30.75 - 30.120 == 0	15.872	2.162	7.343	< 0.001	***
40.75 - 30.120 == 0	24.092	2.162	11.146	< 0.001	***
20.193 - 40.120 == 0	-26.576	1.872	-14.197	< 0.001	***
30.193 - 40.120 == 0	-18.543	1.872	-9.906	< 0.001	***
40.193 - 40.120 == 0	-19.779	1.528	-12.941	< 0.001	***
20.75 - 40.120 == 0	-6.868	1.872	-3.669	0.01073	*
30.75 - 40.120 == 0	-0.986	1.872	-0.527	0.99983	
40.75 - 40.120 == 0	7.234	1.872	3.865	0.00568	**
30.193 - 20.193 == 0	8.033	2.162	3.716	0.00902	**
40.193 - 20.193 == 0	6.797	1.872	3.631	0.01195	*
20.75 - 20.193 == 0	19.708	2.162	9.118	< 0.001	***
30.75 - 20.193 == 0	25.590	2.162	11.839	< 0.001	***
40.75 - 20.193 == 0	33.810	2.162	15.642	< 0.001	***
40.193 - 30.193 == 0	-1.236	1.872	-0.660	0.99911	
20.75 - 30.193 == 0	11.675	2.162	5.401	< 0.001	***
30.75 - 30.193 == 0	17.558	2.162	8.123	< 0.001	***
40.75 - 30.193 == 0	25.778	2.162	11.926	< 0.001	***
20.75 - 40.193 == 0	12.911	1.872	6.897	< 0.001	***
30.75 - 40.193 == 0	18.793	1.872	10.039	< 0.001	***
40.75 - 40.193 == 0	27.014	1.872	14.431	< 0.001	***
30.75 - 20.75 == 0	5.882	2.162	2.721	0.14933	
40.75 - 20.75 == 0	14.102	2.162	6.524	< 0.001	***
40.75 - 30.75 == 0	8.220	2.162	3.803	0.00698	**

 Signif. codes: 0 '***' 0.001 '**' 0.01 '*' 0.05 '.' 0.1 ' ' 1
 (Adjusted p values reported -- single-step method)



A VI : Graphical representation of the residuals for the model fit for temperature and substrate impacting CO_2 .

A.4.2: 2X3 factorial analysis for temperature and matric potential influencing CO₂ (Chapter 5. Table 5-2)

A.4.2.1: ANOVA table of summary and linear model for temperature and matric potential.

Df	Sum Sq	Mean Sq	F value	Pr(>F)
Temperature	1	5923	236.383	<2e-16 ***
MatricP	2	26370	526.180	<2e-16 ***
Temperature:MatricP	2	39	0.785	0.459
Residuals	104	2606	25	

 Signif. codes: 0 '***' 0.001 '**' 0.01 '*' 0.05 '.' 0.1 ' ' 1

Tukey

Simultaneous Tests for General Linear Hypotheses

Multiple Comparisons of Means: Tukey Contrasts

Fit: aov(formula = CO2 ~ PairwiseComparison)

Linear Hypotheses:

	Estimate	Std. Error	t value	Pr(> t)
40.10 - 20.10 == 0	12.555	1.583	7.931	<0.001 ***
20.100 - 20.10 == 0	-35.509	1.583	-22.432	<0.001 ***
40.100 - 20.10 == 0	-22.105	1.939	-11.402	<0.001 ***
20.20 - 20.10 == 0	-28.377	1.583	-17.927	<0.001 ***
40.20 - 20.10 == 0	-17.898	1.583	-11.307	<0.001 ***
20.100 - 40.10 == 0	-48.064	1.583	-30.364	<0.001 ***
40.100 - 40.10 == 0	-34.660	1.939	-17.878	<0.001 ***
20.20 - 40.10 == 0	-40.933	1.583	-25.858	<0.001 ***
40.20 - 40.10 == 0	-30.454	1.583	-19.238	<0.001 ***
40.100 - 20.100 == 0	13.404	1.939	6.914	<0.001 ***
20.20 - 20.100 == 0	7.132	1.583	4.505	<0.001 ***
40.20 - 20.100 == 0	17.611	1.583	11.125	<0.001 ***
20.20 - 40.100 == 0	-6.272	1.939	-3.235	0.0195 *
40.20 - 40.100 == 0	4.207	1.939	2.170	0.2583
40.20 - 20.20 == 0	10.479	1.583	6.620	<0.001 ***

 Signif. codes: 0 '***' 0.001 '**' 0.01 '*' 0.05 '.' 0.1 ' ' 1
 (Adjusted p values reported -- single-step method)

A.4.2.2: Tukey HSD table

Simultaneous Tests for General Linear Hypotheses

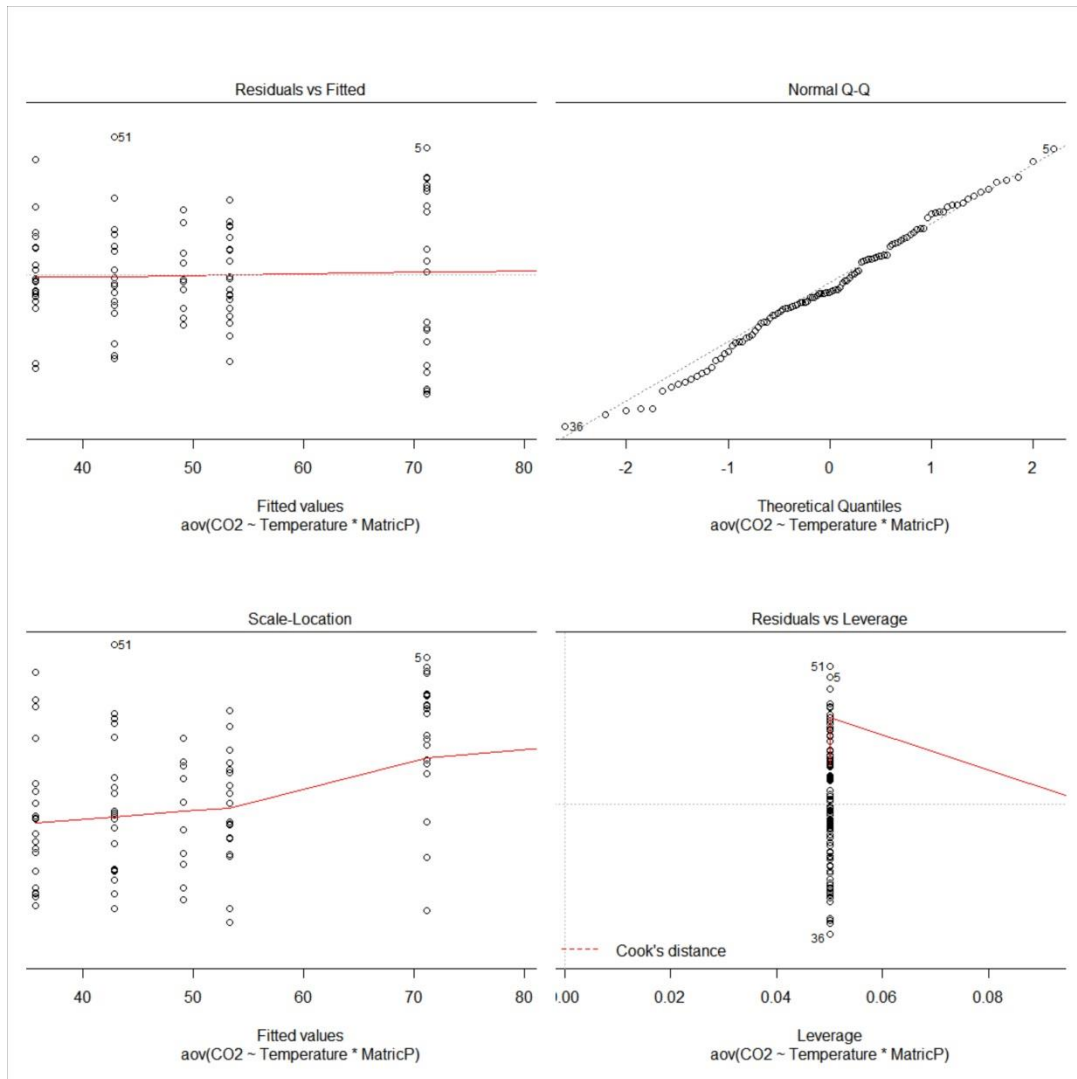
Multiple Comparisons of Means: Tukey Contrasts

Fit: aov(formula = CO2 ~ PairwiseComparison)

Linear Hypotheses:

	Estimate	Std. Error	t value	Pr(> t)	
40.10 - 20.10 == 0	12.555	1.583	7.931	<0.001	***
20.100 - 20.10 == 0	-35.509	1.583	-22.432	<0.001	***
40.100 - 20.10 == 0	-22.105	1.939	-11.402	<0.001	***
20.20 - 20.10 == 0	-28.377	1.583	-17.927	<0.001	***
40.20 - 20.10 == 0	-17.898	1.583	-11.307	<0.001	***
20.100 - 40.10 == 0	-48.064	1.583	-30.364	<0.001	***
40.100 - 40.10 == 0	-34.660	1.939	-17.878	<0.001	***
20.20 - 40.10 == 0	-40.933	1.583	-25.858	<0.001	***
40.20 - 40.10 == 0	-30.454	1.583	-19.238	<0.001	***
40.100 - 20.100 == 0	13.404	1.939	6.914	<0.001	***
20.20 - 20.100 == 0	7.132	1.583	4.505	<0.001	***
40.20 - 20.100 == 0	17.611	1.583	11.125	<0.001	***
20.20 - 40.100 == 0	-6.272	1.939	-3.235	0.0195	*
40.20 - 40.100 == 0	4.207	1.939	2.170	0.2587	
40.20 - 20.20 == 0	10.479	1.583	6.620	<0.001	***

Signif. codes: 0 '***' 0.001 '**' 0.01 '*' 0.05 '.' 0.1 ' ' 1
(Adjusted p values reported -- single-step method)



A VII : Graphical representation of the residuals for the model fit for temperature and matric potential impacting CO_2 .

A.4.3: 3X3 factorial analysis for temperature and substrate concentration influencing *EC* (Chapter 6.Table 6-2)

A.4.3.1 ANOVA table of summary and linear model for temperature and matric potential.

	Df	Sum Sq	Mean Sq	F value	Pr(>F)	
Temperature	2	25238	12619	1431.92	< 2e-16	***
Substrate	2	447	223	25.35	8.55e-10	***
Temperature:Substrate	4	1412	353	40.04	< 2e-16	***
Residuals	111	978	9			

Signif. codes: 0 '***' 0.001 '**' 0.01 '*' 0.05 '.' 0.1 ' ' 1

Call:

aov(formula = EC ~ Temperature * Substrate)

Residuals:

Min	1Q	Median	3Q	Max
-9.9350	-1.5550	-0.1844	1.4359	7.7355

Coefficients:

	Estimate	Std. Error	t value	Pr(> t)
(Intercept)	16.8759	0.6638	25.423	< 2e-16

Temperature30	5.1925	1.1497	4.516	1.58e-05

Temperature40	36.8599	0.9388	39.265	< 2e-16

Substrate193	3.7139	1.1497	3.230	0.001628
**				
Substrate75	-4.0208	1.1497	-3.497	0.000677

Temperature30:Substrate193	-4.5839	1.7563	-2.610	0.010302
*				
Temperature40:Substrate193	-14.4279	1.4843	-9.720	< 2e-16

Temperature30:Substrate75	11.0342	1.7563	6.283	6.68e-09

Temperature40:Substrate75	0.8257	1.6260	0.508	0.612571

Signif. codes: 0 '***' 0.001 '**' 0.01 '*' 0.05 '.' 0.1 ' ' 1

Residual standard error: 2.969 on 111 degrees of freedom

Multiple R-squared: 0.9652, Adjusted R-squared: 0.9626

F-statistic: 384.3 on 8 and 111 DF, p-value: < 2.2e-16

A.4.3.2 Tukey HSD table

Simultaneous Tests for General Linear Hypotheses

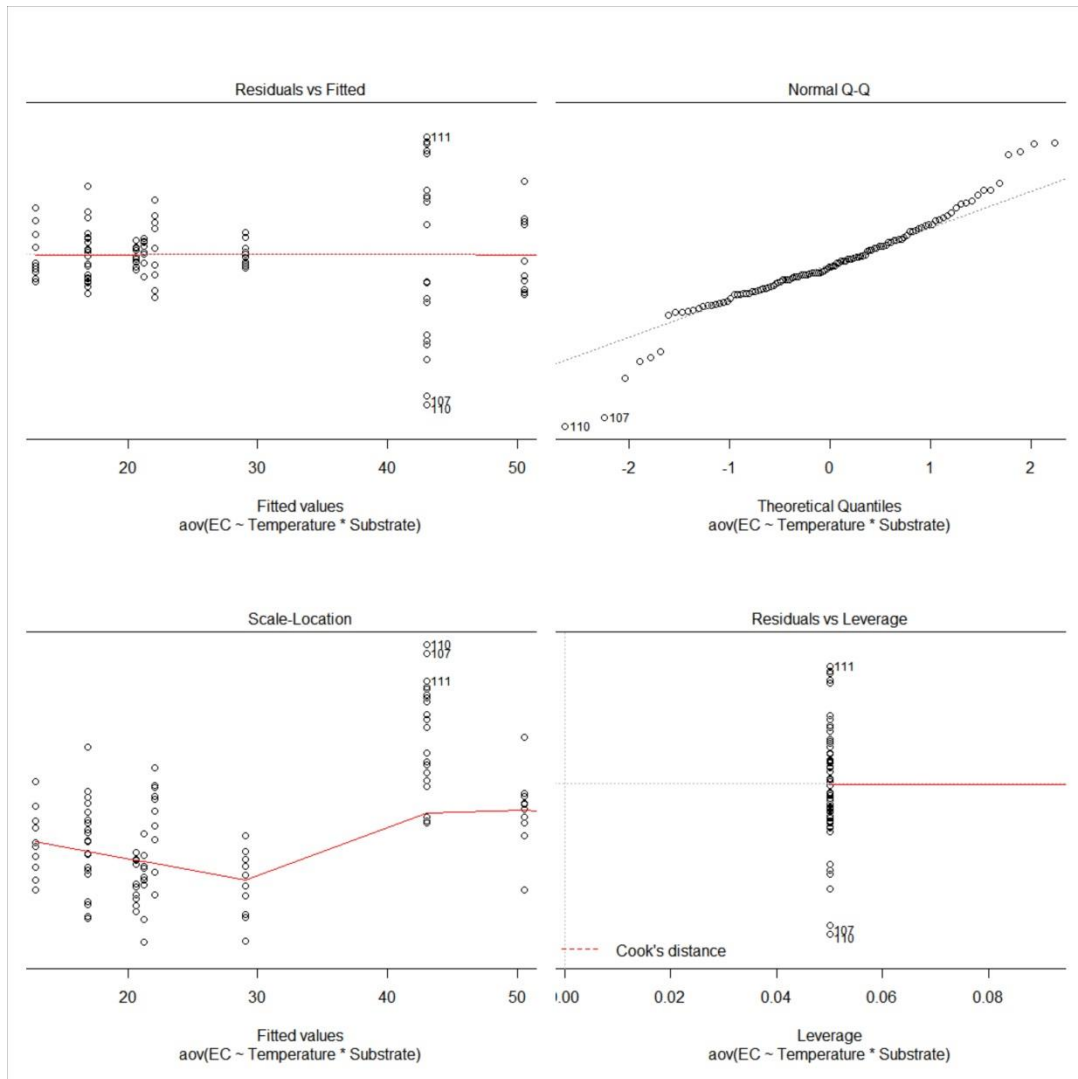
Multiple Comparisons of Means: Tukey Contrasts

Fit: aov(formula = EC ~ PairwiseComparison)

Linear Hypotheses:

	Estimate	Std. Error	t value	Pr(> t)	
30.120 - 20.120 == 0	5.1925	1.1497	4.516	<0.001	***
40.120 - 20.120 == 0	36.8599	0.9388	39.265	<0.001	***
20.193 - 20.120 == 0	3.7139	1.1497	3.230	0.0401	*
30.193 - 20.120 == 0	4.3224	1.1497	3.759	0.0078	**
40.193 - 20.120 == 0	26.1460	0.9388	27.852	<0.001	***
20.75 - 20.120 == 0	-4.0208	1.1497	-3.497	0.0186	*
30.75 - 20.120 == 0	12.2059	1.1497	10.616	<0.001	***
40.75 - 20.120 == 0	33.6649	1.1497	29.280	<0.001	***
40.120 - 30.120 == 0	31.6674	1.1497	27.543	<0.001	***
20.193 - 30.120 == 0	-1.4786	1.3276	-1.114	0.9700	
30.193 - 30.120 == 0	-0.8700	1.3276	-0.655	0.9992	
40.193 - 30.120 == 0	20.9535	1.1497	18.225	<0.001	***
20.75 - 30.120 == 0	-9.2132	1.3276	-6.940	<0.001	***
30.75 - 30.120 == 0	7.0134	1.3276	5.283	<0.001	***
40.75 - 30.120 == 0	28.4724	1.3276	21.446	<0.001	***
20.193 - 40.120 == 0	-33.1460	1.1497	-28.829	<0.001	***
30.193 - 40.120 == 0	-32.5375	1.1497	-28.300	<0.001	***
40.193 - 40.120 == 0	-10.7140	0.9388	-11.413	<0.001	***
20.75 - 40.120 == 0	-40.8807	1.1497	-35.556	<0.001	***
30.75 - 40.120 == 0	-24.6540	1.1497	-21.443	<0.001	***
40.75 - 40.120 == 0	-3.1950	1.1497	-2.779	0.1306	
30.193 - 20.193 == 0	0.6085	1.3276	0.458	0.9999	
40.193 - 20.193 == 0	22.4321	1.1497	19.511	<0.001	***
20.75 - 20.193 == 0	-7.7346	1.3276	-5.826	<0.001	***
30.75 - 20.193 == 0	8.4920	1.3276	6.397	<0.001	***
40.75 - 20.193 == 0	29.9510	1.3276	22.560	<0.001	***
40.193 - 30.193 == 0	21.8235	1.1497	18.981	<0.001	***
20.75 - 30.193 == 0	-8.3432	1.3276	-6.284	<0.001	***
30.75 - 30.193 == 0	7.8835	1.3276	5.938	<0.001	***
40.75 - 30.193 == 0	29.3425	1.3276	22.102	<0.001	***
20.75 - 40.193 == 0	-30.1667	1.1497	-26.238	<0.001	***
30.75 - 40.193 == 0	-13.9400	1.1497	-12.125	<0.001	***
40.75 - 40.193 == 0	7.5190	1.1497	6.540	<0.001	***
30.75 - 20.75 == 0	16.2267	1.3276	12.223	<0.001	***
40.75 - 20.75 == 0	37.6857	1.3276	28.386	<0.001	***
40.75 - 30.75 == 0	21.4590	1.3276	16.164	<0.001	***

 Signif. codes: 0 '***' 0.001 '**' 0.01 '*' 0.05 '.' 0.1 ' ' 1
 (Adjusted p values reported -- single-step method)



A VIII: Graphical representation of the residuals for the model fit for temperature and substrate impacting EC.

A.4.4: 2X3 factorial analysis for temperature and matric potential influencing *EC* (Chapter 6. Table 6-5)

A.4.4.1 ANOVA table of summary and linear model for temperature and matric potential.

CH6_TT_EC_ANOVA_TUKEY

	Df	Sum Sq	Mean Sq	F value	Pr(>F)
Temperature	1	9557	9557	414.26	<2e-16 ***
MatricP	2	3264	1632	70.75	<2e-16 ***
Temperature:MatricP	2	5855	2928	126.89	<2e-16 ***
Residuals	104	2399	23		

 Signif. codes: 0 '***' 0.001 '**' 0.01 '*' 0.05 '.' 0.1 ' ' 1

Call:
 aov(formula = EC ~ Temperature * MatricP)

Residuals:

Min	1Q	Median	3Q	Max
-8.8731	-2.5844	-0.3751	2.4555	18.8341

Coefficients:

	Estimate	Std. Error	t value	Pr(> t)
(Intercept)	16.876	1.074	15.713	< 2e-16 ***
Temperature40	36.860	1.519	24.267	< 2e-16 ***
MatricP100	1.514	1.519	0.997	0.32128
MatricP20	4.330	1.519	2.851	0.00526 **
Temperature40:MatricP100	-32.029	2.402	-13.337	< 2e-16 ***
Temperature40:MatricP20	-29.552	2.148	-13.758	< 2e-16 ***

 Signif. codes: 0 '***' 0.001 '**' 0.01 '*' 0.05 '.' 0.1 ' ' 1

Residual standard error: 4.803 on 104 degrees of freedom
 Multiple R-squared: 0.8862, Adjusted R-squared: 0.8807
 F-statistic: 161.9 on 5 and 104 DF, p-value: < 2.2e-16

A.4.4.2 Tukey HSD table

Simultaneous Tests for General Linear Hypotheses

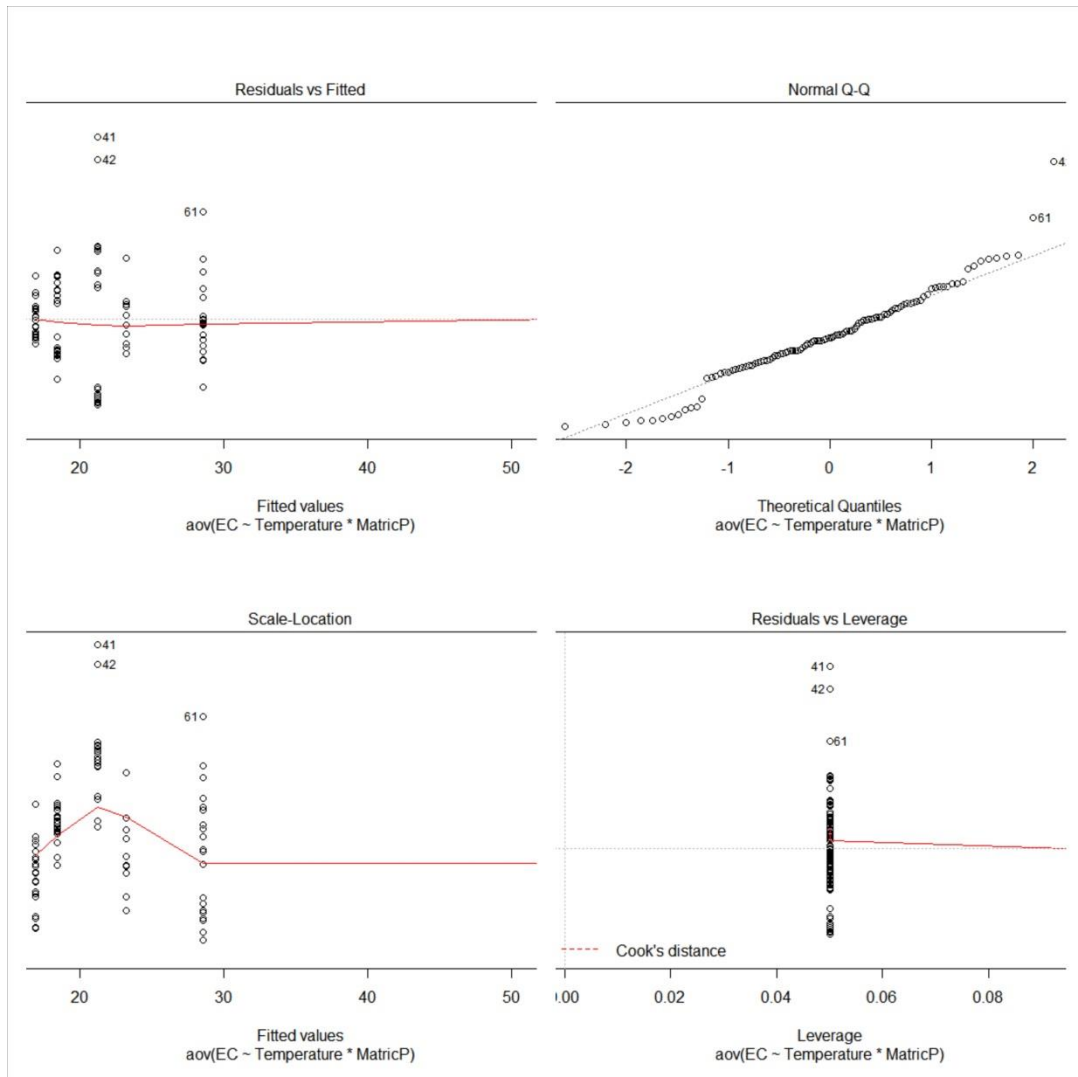
Multiple Comparisons of Means: Tukey Contrasts

Fit: aov(formula = EC ~ PairwiseComparison)

Linear Hypotheses:

	Estimate	Std. Error	t value	Pr(> t)	
40.10 - 20.10 == 0	36.860	1.519	24.267	<0.001	***
20.100 - 20.10 == 0	1.514	1.519	0.997	0.9172	
40.100 - 20.10 == 0	6.344	1.860	3.410	0.0115	*
20.20 - 20.10 == 0	4.330	1.519	2.851	0.0566	.
40.20 - 20.10 == 0	11.638	1.519	7.662	<0.001	***
20.100 - 40.10 == 0	-35.346	1.519	-23.271	<0.001	***
40.100 - 40.10 == 0	-30.516	1.860	-16.404	<0.001	***
20.20 - 40.10 == 0	-32.530	1.519	-21.417	<0.001	***
40.20 - 40.10 == 0	-25.222	1.519	-16.606	<0.001	***
40.100 - 20.100 == 0	4.831	1.860	2.597	0.1060	
20.20 - 20.100 == 0	2.816	1.519	1.854	0.4333	
40.20 - 20.100 == 0	10.124	1.519	6.665	<0.001	***
20.20 - 40.100 == 0	-2.015	1.860	-1.083	0.8859	
40.20 - 40.100 == 0	5.293	1.860	2.845	0.0575	.
40.20 - 20.20 == 0	7.308	1.519	4.811	<0.001	***

Signif. codes: 0 '***' 0.001 '**' 0.01 '*' 0.05 '.' 0.1 ' ' 1
(Adjusted p values reported -- single-step method)



A IX: Graphical representation of the residuals for the model fit for temperature and substrate impacting EC.